

Use of Hyperspectral Remote Sensing to Examine Immature Blow Fly Development

by

Jodie-Ann Warren

M.A., Simon Fraser University, 2007

B.Sc., Simon Fraser University, 1999

Thesis Submitted in Partial Fulfillment of the
Requirements for the Degree of
Doctor of Philosophy

in the
School of Criminology
Faculty of Arts and Social Sciences

© Jodie-Ann Warren 2017

SIMON FRASER UNIVERSITY

Fall 2017

All rights reserved.

However, in accordance with the *Copyright Act of Canada*, this work may be reproduced, without authorization, under the conditions for "Fair Dealing." Therefore, limited reproduction of this work for the purposes of private study, research, criticism, review and news reporting is likely to be in accordance with the law, particularly if cited appropriately.

Approval

Name: Jodie-Ann Warren
Degree: Doctor of Philosophy
Title: *Use of Hyperspectral Remote Sensing to Examine Immature Blow Fly Development*
Examining Committee: **Chair:** Sheri Fabian
Senior Lecturer

Gail S. Anderson
Senior Supervisor
Professor

Lynne S. Bell
Supervisor
Professor

Lisa M. Poirier
Supervisor
Assistant Professor
Ecosystem Science and Management
University of Northern BC

Dongya Yang
Internal Examiner
Professor
Department of Archaeology

Jeffery K. Tomberlin
External Examiner
Associate Professor
Department of Entomology
Texas A&M University

Date Defended/Approved:

November 01, 2017

Abstract

Medico-legal entomology, the study and application of insect science to criminal investigations, is most notably used to estimate a minimum post-mortem interval ($_{\min}$ PMI). Examining blow fly development to make this estimation provides the minimum time it takes to reach the oldest stage associated with the remains. Unfortunately, providing the time it takes to reach a stage may underestimate the age of the insects during the lengthier post feeding stage and intra-puparial period. Hyperspectral remote sensing is introduced as a means to solve this issue and to examine the potential for narrowing these lengthier stages into days within the stages. Hyperspectral remote sensing involves sensing, recording and processing reflected and emitted energy to produce point source measurements.

Spectral measurements of both immature *Protophormia terraenovae* and *Lucilia sericata* were completed from second instar to adult emergence from the mid-section, anterior and posterior ends of developing immature blow flies. Functional regressions and coefficient functions were examined for model prediction and generalization to identify demarcations within stadia to age the immature blow flies. Aging *P. terraenovae* larvae was successful at wavelengths ranging from 400-1000nm, however, at that wavelength range, only the last day of the intra-puparial period could be distinguished from the first five days. Immature *Lucilia sericata* were examined at a wider range of wavelengths (350-2500nm) and model prediction and generalization for both pupae and larvae was possible.

Similarities and differences were found between species and potential contributing factors were considered such as range of wavelengths analyzed, food substrate, significance of washing away surface contaminants before measuring, contributions of cuticular hydrocarbons, and potential surface bacteria, best region to measure the immature blow fly and replication experiments.

Hyperspectral remote sensing not only allows an entomologist to incorporate more precision in their estimate but error rates are also introduced which is required of a forensic science according to the National Academy of Sciences.

Keywords: immature development; *Lucilia sericata*; *Protophormia terraenovae*; hyperspectral; cuticular hydrocarbon; reflectance; functional regression

*For those that want a copy on their bookshelf
but have no intentions of ever reading it.*

Acknowledgements

This dissertation evolved from the joint efforts of many people and so there are so many to thank and acknowledge in its emergence.

I would first like to thank Dr. David Campbell for contributing significantly to this project remarkably so that he performed as a supervisor but without all the glory of being a supervisor. This project would not have transpired without the expertise and brilliant mind of Dr. Campbell who has taught me much about functional data analysis.

I would also like to offer an enormous thank you to Pulindu Ratnasekera for his continuous labor and exceptional abilities with Matlab. Pulindu's statistical mindset guided me through this process.

I am indebted to Dr. Lisa Poirier for being the authority when entomological questions arose in this long process and for taking the time to edit several versions of this dissertation. Dr. Poirier went to great lengths to get me to this point. All of Dr. Poirier's suggestions were carefully followed and genuinely appreciated.

I would like to thank Dr. Lynne Bell for her considerable effort to drive me through this process. Dr. Bell urged me to stay strong and continues to help with next steps. I am grateful that Dr. Bell's guidance will not end with the completion of this dissertation.

I would like to thank ASD Inc. for the Goetz Instrument support program which included the use of a Labspec 4 spectrometer and I would like to thank the Applied Remote Sensing Laboratory at McGill University for the use of the Fieldspec spectrometer. I would

like to express my gratitude to Dr. Barbara Winter with Simon Fraser University Museum of Archaeology and Ethnology for funding a portion of the research.

I would like to offer the sincerest gratitude to those who assisted in this research: Jennifer Mead, Aliesha Stensaker, Julie De Gea, Lawrence Wong, Dr. Gail Chmura, Vienna ChiChi Lam, Mark Romer, Kate Trincsi, Jason Wong, Emilie Roy-Dufresne, Joseph Ariwi, Bekka Brodie, Billi-Jo Cavanaugh, Saadia Uraizee, Robert Wilburn, Alexis Ohman, Kelsey Dubiel, Gary Warren, Elaine Rasmussen, Jeffrey Yung, and Jeremy Pearce for their volunteer services. The research would not have come to realization had it not been for their joint efforts.

I would like to thank Dr. Suzanne De Castel, Radina Droumeva and Dr. Rachel Altman for generously offering their services to make sure this project was completed.

I would like to offer the sincerest gratitude to Drs. Jeffrey Tomberlin and Dongya Yang for taking the time out of their busy schedules and agreeing to be examiners of my dissertation.

I have saved this acknowledgement towards the end because there is so much to say about my mentor, Dr. Gail Anderson. I need to thank Gail for being an incredible supervisor and taking on a student that was still recovering from the aftermath of a massive stroke. It took a long time to get through that chapter of my life but Gail was willing to take it on. I never had a choice but Gail did. Also, I want to show my deepest gratitude to Gail for opening up to this innovative research project. It is very new research and I was

pretty set on this project. Gail has taught me vast amounts about forensic entomology. I hope that one day I can do the same for my students. Not only have you been an incredible supervisor but you have been a wonderful friend.

Lastly, I would like to thank my husband, George, for his enduring patience of my completion of this dissertation and his unending support for my studies.

Table of Contents

Approval.....	ii
Abstract	iii
Dedication	iv
Acknowledgements	v
Table of Contents	viii
List of Tables.....	xi
List of Figures	xii
Glossary.....	xxi
Chapter 1. Introduction.....	1
1.1. Preface	1
1.2. Overview	1
Objectives:.....	3
Chapter 2. Literature Review	5
2.1 Preface	5
2.2 Overview	5
2.2.1 Immature Development and the Blow Fly Life cycle.....	6
Using Blow Fly Development to Estimate Time of Colonization	9
2.3 Estimating Time within Stadia	10
2.4 Remote Sensing	12
2.5 Applications of Remote Sensing to Forensic Science	17
2.6 Hyperspectral Remote Sensing and Forensic Entomology.....	24
Chapter 3. Initial investigations of spectral measurements to estimate the time within stages of <i>Protophormia terraenovae</i> (Robineau-Desvoidy) (Diptera: Calliphoridae).....	26
3.1 Preface	26
3.2 Abstract.....	26
3.3 Introduction	27
3.4 Materials and Methods	31
Insect colony.....	31
Experimental Protocol	31
3.5 Functional Linear Model	35
Preprocessing.....	35
Functional Linear Regression Model Fitting	36
3.6 Results	37
3.7 Discussion.....	51
3.8 Conclusion.....	54
3.9 Acknowledgements	55
3.10 Reference List.....	55

Chapter 4.	Spectral Signature of Immature <i>Lucilia sericata</i> (Meigen) (Diptera: Calliphoridae).....	62
4.1	Preface	62
4.2	Abstract.....	63
4.3	Introduction	63
4.4	Materials and Methods	67
	Insect Rearing.....	67
	Experimental Protocol	67
	Pre-processing	72
	Functional Linear Model to Estimate Day of Development	72
	Smoothing individual reflectance measurements	72
	Functional Linear model with Scalar Response	73
	Model fitting to Compare Washed to Unwashed Insects.....	74
4.5	Results	74
	Spectral Analysis	74
	Washed versus Unwashed	85
4.6	Discussion.....	91
4.7	Conclusion.....	94
4.8	Acknowledgements	95
4.9	Reference List.....	95
Chapter 5.	A Comparison of Development Times for <i>Protophormia terraenovae</i> (Robineau-Desvoidy) (Diptera: Calliphoridae) reared on different food substrates.....	102
5.1	Preface	102
5.2	Abstract.....	103
5.3	Introduction	103
5.4	Materials and Methods	107
5.5	Results	109
5.6	Discussion.....	115
5.7	Conclusion.....	118
5.8	Acknowledgements	118
5.9	Reference List.....	119
Chapter 6.	Hyperspectral measurements of <i>Lucilia sericata</i> (Meigen) (Diptera: Calliphoridae) raised on different food substrates	123
6.1	Preface	123
6.2	Abstract.....	123
6.3	Introduction	124
6.4	Materials and Methods	126
	Insect Rearing.....	126
	Spectral Measuring.....	127
	Functional model.....	128
6.5	Results	129
6.6	Discussion.....	142
6.7	Acknowledgements	147
6.8	Reference List.....	148

Chapter 7.	Hyperspectral measurements of the larval cuticular hydrocarbons of <i>Lucilia sericata</i> (Meigen) (Diptera: Calliphoridae)	153
7.1	Preface	153
7.2	Abstract.....	153
7.3	Introduction	154
7.4	Materials and Methods	156
	Insect Rearing.....	156
	Hyperspectral Remote Sensing.....	157
	Functional Regression Model.....	158
	Gas Chromatography/Mass Spectrometry	159
7.5	Results and Discussion	160
	Hyperspectral Remote Sensing.....	160
	Gas Chromatography/Mass Spectrometry	169
7.6	Conclusion.....	177
7.7	Acknowledgements	178
7.8	Reference List.....	178
Chapter 8.	Overall Discussion.....	184
8.1	Preface	184
8.2	Overview	184
8.3	Future Work and Considerations	191
8.4	Conclusions	193
	Reference List	195

List of Tables

Table 5-1	Survival rates for each of the <i>P. terraenovae</i> replicates and the mean for each rearing substrate (whole, wounded rat, beef brain, heart, muscle or liver).	113
Table 5-2	The mean weights (+/-SD) of <i>P. terraenovae</i> pupae on day 2 and the adults two weeks following death .The <i>P. terraenovae</i> were raised on whole wounded rat, beef brain, heart, muscle or liver.	114
Table 5-3	The mean lengths and widths (+/-SD) of the <i>P. terraenovae</i> pupae measured on Day 2 of the intra-puparial period. The <i>P. terraenovae</i> were raised on whole wounded rat, beef brain, heart, muscle or liver.	115
Table 6-1	The minimum development stage and accumulated degree days (ADD) of <i>Lucilia sericata</i> raised at a mean temperature of 20.6°C on each of the food substrates for each day of development is presented with the day of spectral measuring	130
Table 6-2	The fixed effect models for the hyperspectral measurements of the anterior end, midsection and posterior end of post feeding <i>Lucilia sericata</i> raised on beef heart, (BH), beef liver (BL), pork heart (PH), and pork liver (PL).	135
Table 6-3	Nutritional value per 100g of meat substrate	144
Table 7-1	An examination of the alkane cuticular hydrocarbons from three replicates of <i>Lucilia sericata</i> raised at 25°C over seven days and of the fresh thawed and spoilt beef liver substrate. Each √ or X represents presence or absence, respectively, in each replicate. Only a single replicate of each of the fresh thawed and spoilt beef liver was examined for hydrocarbons and the findings were similar.	174

List of Figures

Figure 2-1	Blow fly lifecycle (illustrator V. C. Lam) (not to scale)	8
Figure 2-2	The electromagnetic spectrum with area of significance noted for the current research. (illustrator V.C. Lam)	14
Figure 2-3	Electromagnetic radiation and its direction of propagation due to the magnetic and electric forces acting on it (Holz, 1985).....	16
Figure 2-4	The combined exhaustive details of the hundreds of narrow bands form a hyperspectral signature (illustrator V.C. Lam).....	17
Figure 3-1	Taking a reflectance measurement of <i>Protophormia terraenovae</i> with the ASD spectrometer	33
Figure 3-2	Mean plots of daily standardized spectral reflectance at wavelengths ranging from 400- 1000 nm for all days of development of <i>Protophormia terraenovae</i> raised at a mean temperature of 24.6°C from second instar to the day before adult emergence. The second instar spectral measurements are from the midsection but the larval and puparial measurements are from the posterior end. (Pupa in the figure is shortened from puparium (Martin-Vega et al., 2016)).....	38
Figure 3-3	An examination of the functional regression model based on spectral reflectance measurements from the posterior end of 3 rd instar (days 1 and 2), post feeding wandering larvae (days 3 and 4) and the first day of pupariation (day 5) for <i>Protophormia terraenovae</i> . The green dotted lines represent the pointwise 95% prediction intervals upper and lower limits of the predicted days (blue thin solid line) and the red thick solid line indicates the actual day.....	40
Figure 3-4	A functional regression analysis with 95% pointwise prediction intervals (dotted green) of the spectral measurements collected from the anterior end and midsection of <i>Protophormia terraenovae</i> third instar feeding (days 1 and 2) and post feeding larvae (days 3 and 4) indicate that the actual measurements (thin blue solid line) do not clearly differentiate all days (thick red solid line) when predicting days from 3 rd instar to the first day of pupariation.....	41
Figure 3-5	The grouped spectral measurements from the anterior end, midsection and posterior end of <i>Protophormia terraenovae</i> larvae. Measurements range from the first day of the third instar to the first day of pupariation.	42
Figure 3-6	The 95% coefficient function indicates a significant difference between the daily spectral measurements at the contributing wavelengths where the red dotted zero line is visible using posterior end spectral measurements of <i>Protophormia terraenovae</i> . Daily measurements range from third instar to the first day of pupariation.	43

Figure 3-7	The functional regressions based on collected reflectance spectra (400-1000 nm) from each of anterior/midsection/posterior regions of <i>Protophormia terraenovae</i> puparia. The upper and lower 95% prediction intervals are presented in green. The blue line indicates the predicted day and the red line indicates the actual day (Pupal Day refers to the day of the intra-puparial period (Martin-Vega et al., 2016))......	45
Figure 3-8	The visible spectrum of smoothed and preprocessed (standardized) plots of <i>Protophormia terraenovae</i> puparia spectral measurements from the anterior end, midsection and posterior end. The distinctly different black solid line plots represent the last day of the intra-puparial period and the indistinguishable remaining colours represent the earlier days of the intra-puparial period.	46
Figure 3-9	Mean standardized spectral reflectance plots of <i>Protophormia terraenovae</i> anterior end/midsection/posterior end puparia ranging from 400-1000 nm (Pupal in the figure is referring to puparium (Martin-Vega et al., 2016)).	47
Figure 3-10	Functional regression model separates the last day (class 2) from the earlier five days of the intra-puparial period (class 1) of <i>Protophormia terraenovae</i> raised at a mean temperature of 24.6 °C based on the spectral measures from puparia (anterior end, midsection and posterior end). The dotted green lines represent the 95% prediction interval upper and lower limits of the predicted days in blue and the red line distinguishes the class of day (Pupae in the figure is referring to puparium (Martin-Vega et al., 2016)).	48
Figure 3-11	The 95% coefficient function plots of spectral measurements from days one to five of the intra-puparial period compared with day six of the last day of intra-puparial period of <i>Protophormia terraenovae</i> raised at a mean temperature of 24.6°C (Pupa in the figure is short for puparium (Martin-Vega et al., 2016)). They also indicate the contributing wavelengths (red dotted line) to the model from each of the spectral reflectance measured regions (anterior, midsection, and posterior).	49
Figure 3-12	The standardized preprocessed smoothed spectral measurements of the midsection of second instar <i>Protophormia terraenovae</i> raised at a mean temperature of 24.6°C, along with the contributing wavelengths to the $\beta(w)$ coefficient (red dotted line in lower plot). Day 1 is represented by the red solid plots and Day 2 by the blue dashed plots. Each line represents a measurement from one larva. The approximate contributing wavelengths that help distinguish the days include: 400-540, 565-704, and 743-855 nm.	50
Figure 3-13	Functional regression model of predicted days (blue thin line) within second instar of <i>Protophormia terraenovae</i> raised at a mean temperature of 24.6°C based on spectral reflectance measurements. The green dotted lines represent the pointwise 95% prediction interval upper and lower limits and the red thick line was the actual day.	51
Figure 4-1	Spectrometer set up in the blackened laboratory and calibration using a Spectralon panel.	70

Figure 4-2	Demonstration of measuring reflectance from an insect with the Analytical Spectral Devices (ASD) Labspec 4 Spectrometer.	71
Figure 4-3	The actual (red) versus predicted days (blue) for <i>Lucilia sericata</i> post feeding larvae (raised at a mean temperature of 23.9°C) spectral measurements from 350-2500nm of the anterior end. The pointwise 95% prediction interval upper and lower limits appear in green.	75
Figure 4-4	The actual (red) versus predicted days (blue) for <i>Lucilia sericata</i> post feeding larvae (raised at a mean temperature of 23.9°C) spectral measurements from 350-2500nm of the midsection. The pointwise 95% prediction interval upper and lower limits appear in green.	76
Figure 4-5	The actual (red) versus predicted days (blue) for <i>Lucilia sericata</i> post feeding larvae (raised at a mean temperature of 23.9°C) spectral measurements from 350-2500nm of the posterior end. The pointwise 95% prediction interval upper and lower limits appear in green.	77
Figure 4-6	The contributing $\beta(w)_{washed}$ coefficients of the spectral measurements for each of the measured regions ((A) anterior, (B) midsection, and (C) posterior) of <i>Lucilia sericata</i> post feeding larvae raised at a mean temperature of 23.9°C.	78
Figure 4-7	The functional regression with 95% upper and lower limit pointwise prediction intervals (green) for spectral measurements from 350-2500nm of the anterior end of <i>Lucilia sericata</i> pupae raised at a mean temperature of 23.9°C. The predicted days appear in blue and the red line is the actual day.	79
Figure 4-8	The functional regression with 95% upper and lower limit pointwise prediction intervals (green) for spectral measurements from 350-2500nm of the midsection of <i>Lucilia sericata</i> pupae raised at a mean temperature of 23.9°C. The predicted days appear in blue and the red line is the actual day.	80
Figure 4-9	The functional regression with 95% upper and lower limit pointwise prediction intervals (green) for spectral measurements from 350-2500nm of the posterior end of <i>Lucilia sericata</i> pupae raised at a mean temperature of 23.9°C. The predicted days appear in blue and the red line is the actual day.	81
Figure 4-10	The contributing coefficients, $\beta(w)_{washed}$ of the spectral measurements for each of the measured regions ((A) anterior, (B) midsection, and (C) posterior) of <i>Lucilia sericata</i> puparia raised at a mean temperature of 23.9°C.	82
Figure 4-11	The coefficients with their 95% confidence bands contributing to the model that compares spectral measurements from the one day of second instar with the one day of third instar <i>Lucilia sericata</i> raised at a mean temperature of 23.9°C. It also indicates the wavelengths that contribute to the daily prediction.	83

Figure 4-12	The actual (red) versus predicted days (blue) for <i>Lucilia sericata</i> second and third instar larvae (raised at a mean temperature of 23.9°C) spectral measurements of the midsection. The pointwise 95% prediction interval upper and lower limits appear in green.	84
Figure 4-13	The mean preprocessed smoothed spectral measurement plots for each day of each stage of <i>Lucilia sericata</i> raised at a mean temperature of 23.9°C.....	85
Figure 4-14	The functional regression models of unwashed and the same washed post feeding <i>Lucilia sericata</i> (raised at a mean temperature of 23.9°C) larval anterior end spectral measurements. The red line indicates the actual day and the blue indicates the predicted day.....	86
Figure 4-15	The functional regression models of unwashed and the same washed post feeding <i>Lucilia sericata</i> (raised at a mean temperature of 23.9°C) larval midsection spectral measurements. The red line indicates the actual day and the blue indicates the predicted day.....	87
Figure 4-16	The functional regression models of unwashed and the same washed post feeding <i>Lucilia sericata</i> (raised at a mean temperature of 23.9°C) larval posterior end spectral measurements. The red line indicates the actual day and the blue indicates the predicted day.	88
Figure 4-17	The 95% confidence interval of the coefficients for post-feeding <i>Lucilia sericata</i> raised at a mean temperature of 23.9 °C in a model predicting the effect of lack of washing before taking spectral measurements (350–2500 nm) from the anterior end/midsection/posterior end of the post-feeding larvae.	89
Figure 4-18	The second and third instar <i>Lucilia sericata</i> (raised at a mean temperature of 23.9°C) function of the unwashed coefficients with 95% confidence bands for the midsection spectral measurements (350-2500nm). The contributing wavelengths are indicated by the dotted red zero line.	90
Figure 4-19	The functional regression for predicting second and third instar <i>Lucilia sericata</i> (raised at a mean temperature of 23.9°C) from unwashed larvae based on spectral measurements. The red line is the actual day, the blue is the prediction and the green lines are the upper and lower 95% pointwise prediction intervals.	91
Figure 5-1	Mean minimum development times for <i>P. terraenovae</i> to reach each stage at ~17°C in days on whole, wounded rats, and on beef brain, heart, muscle and liver.	110
Figure 5-2	Mean maximum development times for <i>P. terraenovae</i> to reach each stage at ~17°C in days on whole, wounded rats, and on beef brain, heart, muscle and liver.	111
Figure 5-3	Mean of mode development for <i>P. terraenovae</i> to reach each stage at ~17°C in days on whole, wounded rats, and on beef brain, heart, muscle and liver.....	112

Figure 6-1	The functional regression prediction for day of development in the post feeding stage of <i>Lucilia sericata</i> raised at a mean temperature of 20.6°C on beef liver, pork liver, beef heart and pork heart for the anterior end spectral measurements with 95% prediction intervals (green lines are the upper and lower limits). The red line is the actual day and the blue is the predicted day.	132
Figure 6-2	The functional regression prediction for day of development in the post feeding stage of <i>Lucilia sericata</i> raised at a mean temperature of 20.6°C on beef liver, pork liver, beef heart and pork heart for the midsection spectral measurements with 95% prediction intervals (green lines are the upper and lower limits). The red line is the actual day and the blue is the predicted day.	133
Figure 6-3	The functional regression prediction for day of development in the post feeding stage of <i>Lucilia sericata</i> raised at a mean temperature of 20.6°C on beef liver, pork liver, beef heart and pork heart for the posterior end spectral measurements with 95% prediction intervals (green lines are the upper and lower limits). The red line is the actual day and the blue is the predicted day.	134
Figure 6-4	Box plots presenting the anterior end hyperspectral measurement prediction of day compared with the observed or actual day of <i>Lucilia sericata</i> post feeding larval development on beef heart and liver and pork heart and liver.....	137
Figure 6-5	Box plots presenting the midsection hyperspectral measurement prediction of day compared with the observed or actual day of <i>Lucilia sericata</i> post feeding larval development on beef heart and liver and pork heart and liver.....	138
Figure 6-6	Box plots presenting the posterior end hyperspectral measurement prediction of day compared with the observed or actual day of <i>Lucilia sericata</i> post feeding larval development on beef heart and liver and pork heart and liver.....	139
Figure 6-7	The $\beta(w)$ coefficients (y-axis) and contributing wavelengths to the coefficients of the linear regression covariate model for the spectral measurements of the anterior end of post feeding <i>Lucilia sericata</i> . The blue area represents the 95% confidence interval and the green bands indicate wavelengths where $\beta(w)$ coefficients are significant. $\beta(w)$ is the contributing β coefficient for spectral measurements from insects raised on beef liver alone. $\beta_{Pork}(w)$ is the contributing β coefficient due to changing from beef to pork measurements regardless of organ. $\beta_{Heart}(w)$ is the contributing β coefficient due to changing from liver to heart measurements regardless of meat type. $\beta_{Pork\ Heart}(w)$ is the contributing β coefficient due to changing from beef liver to pork heart.	140

Figure 6-8	<p>The $\beta(w)$ coefficients (y-axis) and contributing wavelengths to the coefficients of the linear regression covariate model for the spectral measurements of the midsection of post feeding <i>Lucilia sericata</i>. The blue area represents the 95% confidence interval and the green bands indicate wavelengths where $\beta(w)$ coefficients are significant. $\beta(w)$ is the contributing β coefficient for spectral measurements from insects raised on beef liver alone. $\beta_{Pork}(w)$ is the contributing β coefficient due to changing from beef to pork measurements regardless of organ. $\beta_{Heart}(w)$ is the contributing β coefficient due to changing from liver to heart measurements regardless of meat type. $\beta_{Pork\ Heart}(w)$ is the contributing β coefficient due to changing from beef liver to pork heart. 141</p>	141
Figure 6-9	<p>The $\beta(w)$ coefficients (y-axis) and contributing wavelengths to the coefficients of the linear regression covariate model for the spectral measurements of the posterior end of post feeding <i>Lucilia sericata</i>. The blue area represents the 95% confidence interval and the green bands indicate wavelengths where $\beta(w)$ coefficients are significant. $\beta(w)$ is the contributing β coefficient for spectral measurements from insects raised on beef liver alone. $\beta_{Pork}(w)$ is the contributing β coefficient due to changing from beef to pork measurements regardless of organ. $\beta_{Heart}(w)$ is the contributing β coefficient due to changing from liver to heart measurements regardless of meat type. $\beta_{Pork\ Heart}(w)$ is the contributing β coefficient due to changing from beef liver to pork heart. 142</p>	142
Figure 7-1	<p>Functional regression of prediction of day of development from three replicates of posterior end spectral reflectance measurements of <i>Lucilia sericata</i> larvae raised at 25°C. The red line is the actual day of development and the blue represents the predicted day. The pointwise 95% prediction interval upper and lower limits are presented in green. 161</p>	161
Figure 7-2	<p>Functional regression of prediction of day of development from three replicates of anterior end spectral reflectance measurements of <i>Lucilia sericata</i> larvae raised at 25°C. The red line is the actual day of development and the blue represents the predicted day. The pointwise 95% prediction interval upper and lower limits are presented in green. 162</p>	162
Figure 7-3	<p>Functional regression of prediction of day of development from three replicates of midsection spectral reflectance measurements of <i>Lucilia sericata</i> larvae raised at 25°C. The red line is the actual day of development and the blue represents the predicted day. The pointwise 95% prediction interval upper and lower limits are presented in green. 163</p>	163
Figure 7-4	<p>The coefficient functions of posterior end spectral measurements for each of three replicates of developing <i>Lucilia sericata</i> larvae at 25°C indicate that the functional regressions are significant. The $\beta(w)$ coefficients are not zero at the wavelengths where the zero line is visible and it is these wavelengths that are contributing to the model. 164</p>	164

Figure 7-5	The coefficient functions of anterior end spectral measurements for each of three replicates of developing <i>Lucilia sericata</i> larvae at 25°C indicate that the functional regressions are significant. The $\beta(w)$ coefficients are not zero at the wavelengths where the zero line is visible and it is these wavelengths that are contributing to the model.....	165
Figure 7-6	The coefficient functions of midsection spectral measurements for each of three replicates of developing <i>Lucilia sericata</i> larvae at 25°C indicate that the functional regressions are significant. The $\beta(w)$ coefficients are not zero at the wavelengths where the zero line is visible and it is these wavelengths that are contributing to the model.....	166
Figure 7-7	An examination of scenario #5 that $\beta_{jar1or2}(w) \neq -\beta_{jar1}(w)$ and $\beta_{jar}(w) \neq 0$ from the posterior end spectral measurements of <i>Lucilia sericata</i> . At four separate wavelength regions the mean (blue line) falls outside of the 95% prediction interval. The red line is the prediction and the green lines are the upper and lower limits.	167
Figure 7-8	An examination of scenario #5 that $\beta_{jar1or2}(w) \neq -\beta_{jar1}(w)$ and $\beta_{jar}(w) \neq 0$ from the anterior end spectral measurements of <i>Lucilia sericata</i> . At three separate wavelength regions the mean (blue line) falls outside of the 95% prediction interval. The red line is the prediction and the green lines are the upper and lower limits.	168
Figure 7-9	An examination of scenario #5 that $\beta_{jar1or2}(w) \neq -\beta_{jar1}(w)$ and $\beta_{jar}(w) \neq 0$ from the midsection spectral measurements of <i>Lucilia sericata</i> . At six separate wavelength regions the mean (blue line) falls outside of the 95% prediction interval. The red line is the prediction and the green lines are the upper and lower limits.	169
Figure 7-10	Replicate #1 GC chromatograms of six consecutive days (ranging from 3 rd instar to the first day of the intra-pupal period) from the cuticular hydrocarbons of <i>L. sericata</i> raised at 25°C. The numbers at the top of the chromatogram represent the number of carbons and the red circles indicate similar trends to Moore et al. (2013)	170
Figure 7-11	Replicate #2 GC chromatograms of six consecutive days (ranging from 3 rd instar to the first day of the intra-pupal period) from the cuticular hydrocarbons of <i>L. sericata</i> raised at 25°C. The numbers at the top of the chromatogram represent the number of carbons and the red circles indicate similar trends to Moore et al. (2013)	171
Figure 7-12	Replicate #3 GC chromatograms of six consecutive days (ranging from 3 rd instar to the first day of the intra-pupal period) from the cuticular hydrocarbons of <i>L. sericata</i> raised at 25°C. The numbers at the top of the chromatogram represent the number of carbons and the red circles indicate similar trends to Moore et al. (2013)	172

Figure 8-1 Mean daily posterior end and midsection spectral measurements separated into stages from *Protophormia terraenovae* and *Lucilia sericata*. Similar troughs are observed at 550 and 975nm (black circles). The 550nm trough was gone once the intra-puparial period was reached and the 975nm trough was no longer visible just before adult emergence. The red circle indicates the difference observed on the last day of intra-puparial period between *P. terraenovae* and *L. sericata*.....189

List of Abbreviations

ADD/H	Accumulated degree days/hours
ASD	Analytical Spectral Devices™
ATR-FTIR	Attenuated Total Reflectance- Fourier Transform Infrared
AVHRR	Advanced Very High Resolution Radiometer
DNA	Deoxyribonucleic acid
EMR	Electromagnetic radiation
EO-1	Earth Observing-1
fdam	Functional data analysis Matlab
FLIR	Forward Looking Infrared Radiometer
GC/MS	Gas chromatography/mass spectrometry
GPR	Ground penetrating radar
L:D	Light:dark
_{min} PMI	Minimum post-mortem interval
NAS	National Academies of Science
NIR	Near infrared
PUFA	Polyunsaturated Fatty Acids
PVC	Polyvinyl chloride, (IUPAC Polychloroethene)
R-D	Robineau- Desvoidy
SPOT	Satellite Pour L' Observation de la Terre
SWIR	Shortwave infrared
TM	Thematic Mapper
TOC	Time of colonization
VIS	Visible

Glossary

Anautogenous	Insects that require a protein meal as an adult to produce mature gonads
Electromagnetic spectrum	Range of wavelengths or frequencies and the particles of energy associated with each
Excipient	Inactive ingredient that stabilizes the constituents of a drug
Gravid	Carrying eggs
Haemolymph	Fluid equivalent to blood in insects and other invertebrates
Holarctic	A region including both the Nearctic (North America) and the Palearctic (Eurasia) land regions
Holometabolous	Complete metamorphosis
Hydrocarbons (insects)	Long chains of carbon and hydrogen atoms that waterproof the insect cuticle and are involved in chemical signalling as, for example, sex pheromones or kairomones
Hyperspectral	Combining the exhaustive details within hundreds of narrow bands to achieve a spectral response or spectral signature of the element
Instar	A development stage between each moult in arthropods
Intra-puparial period	Combined prepupal, pupal and pharate adult stages (Martin-Vega, Hall, & Simonsen, 2016)
Kairomones	Chemical signals emitted by an organism and detected by another organism that benefits from the signal. It is usually not beneficial to the organism emitting the signal
Lipophorin	A mechanism of transporting lipids in insects in the haemolymph
Medico-legal entomology	The study and application of insect science to criminal investigations
Multispectral	Combined details in a few wider bands to achieve a spectral response or spectral signature
Oenocytes	Insect cells located in the epidermis that produce cuticular hydrocarbons
Oviposit	To lay eggs
Pharate adult	A confined newly forming/formed adult in the puparium of the intra-puparial period
Radiometric resolution	A measure of brightness of an image
Remote sensing	The science of obtaining information without being in physical contact, often in an electronic form, about the structures of a particular target
Spatial resolution	A measure of clarity of minute details

Spectral resolution	A measure of detail in relation to wavelength demarcation
Spiracles	External openings to the tracheal system
Stadium (stadia)	Development stage used when referring to duration
Temporal resolution	A measure of sequential documentation over time
Teneral	Newly emerged adult fly that has un-inflated wet wings
Thermoperiods	Daily temperature cycles

Chapter 1. Introduction

1.1. Preface

This chapter is an introduction to forensic entomology

1.2. Overview

Medico-legal entomology, most often referred to as forensic entomology, is the study and application of insect science to criminal investigations. Medico-legal entomology is predominantly used in death investigations but can also be used in cases of neglect and abuse (Amendt, Richards, Campobasso, Zehner, & Hall, 2011; Gennard, 2012; Rivers & Dahlem, 2014). Medico-legal entomology is a sub discipline of forensic entomology along with stored product and urban entomology. Stored product entomology involves insect counts in stored products exceeding permissible thresholds and urban entomology includes legal cases involving nuisance pests (Rivers & Dahlem, 2014).

Medico-legal entomology is primarily used to estimate the minimum period of insect colonization and thereby infer the minimum elapsed time since death. It can also be used to determine whether a body has been relocated or disturbed if there is evidence of unexpected activity of species that are not indigenous to the area or expected species that are not present (Amendt et al., 2011). Forensic entomology can also be used to estimate if and where there are wound sites (Amendt et al., 2011), by the presence of necrophagous insects in regions of the remains that are not usually colonized so prematurely. Insects can also be used as toxicological specimens since the drug or poison bio-accumulates in the larvae as they feed (Amendt et al., 2011). In questionable circumstances such as when a body is no longer present at a scene but the presence of necrophagous insects suggests one

once having been there, gut contents of the remaining insects can be examined for DNA to reveal a link with a victim (Campobasso, Linville, Wells, & Introna, 2005).

Although it has several applications, the primary use of medico-legal entomology is to provide an estimated minimum post-mortem interval ($_{\min}$ PMI) in death investigations (Amendt et al., 2011; Anderson, 2001). Following death, necrophagous insects are attracted to the remains in a predictable sequence and the first insects to colonize, the blow flies, **oviposit** eggs which hatch into larvae and develop on the cadaver in a predictable manner. Based on peer-reviewed development and succession data, forensic entomologists can estimate the minimum period of colonization.

The first documented applications of entomology to death investigations began in China in the 10th century, published by Cheng in 1890, when entomological evidence was used to identify a wound site, disputing spousal testament of death by fire (cited in Greenberg & Kunich, 2002). A much more famous case was reported in the 13th century in China by Sung T'zu in his treatise "The Washing away of Wrongs" (translated by McKnight, 1981) in which a murder weapon was identified by flies attracted to the remaining traces of blood. Forensic entomological evidence has advanced considerably since its origins in 10th and 13th century China. It no longer relies on such simplistic methods as observing fly behaviour to identify incriminating evidence, but instead applies known development rates and known successional ecology to the stage of development and the successional arrival of insects recovered from the remains.

Applications of forensic entomology were not seen until much later in Europe, and the first use of insects to estimate $_{\min}$ PMI in a courtroom did not occur until 1850 in France (Amendt, Krettek, & Zehner, 2004; Rivers & Dahlem, 2014). The remains of a human baby were discovered behind a chimney by hired workmen and the insect evidence was used to show that the current occupants of the house were not the occupants at the time of death. Although these conclusions were based on poor science, which incorrectly indicated that the species present required 8-10 months to complete a life cycle, there was no harm done as the entomological evidence was not a key element in the case and supported

prevailing minPMI evidence (Rivers & Dahlem, 2014). It was, however, the first modern usage of forensic entomology.

In Canada, the first applications of forensic entomology began in late nineteenth century Quebec with two medical doctors publishing their work, which was inspired by the pioneer successional ecology researcher, M \acute{e} gnin (Wallace, Byrd, LeBlanc, & Cervenka, 2015). Johnston and Villeneuve concentrated their labours on studying insect succession on human corpses (Anderson, 2001). Case work in Canada did not arise until the 1960s and 70s with Peter Zuk of Agriculture and Agrifoods Canada (Anderson, 2001). He was most probably the first to present evidence in a Canadian court (Anderson, 2001). Finlayson, Borden and Syed handled the case work from 1970s until current Canadian Forensic Entomologist, Anderson, seized the opportunity in the late 1980s (Anderson, 2001), later accompanied by VanLaerhoven and LeBlanc.

Forensic entomology has come a long way since its earliest applications. It has evolved into the cutting-edge science that it is today. Recent research is concentrated on improving estimation of insect ages to improve minPMI estimates. The current research was performed to determine whether **hyperspectral** imaging could improve precision in estimates of larval age.

Objectives:

The objectives of this research were to:

- 1) Develop a change detection assessment in immature blow flies by identifying daily surface changes within each of the immature stages using hyperspectral **remote sensing**
- 2) Compare unwashed to washed *Lucilia sericata* (Meigen) (Diptera: Calliphoridae) immature spectral measurements to determine whether washing was a necessary step prior to performing hyperspectral measurements

- 3) Compare spectral measurements of two forensically important blow flies, *Protophormia terraenovae* (R.-D.) and *Lucilia sericata* (Diptera: Calliphoridae) to determine whether interspecific differences occur in hyperspectral measurements
- 4) Determine which food substrate is most appropriate for raising blow fly larvae to develop data valid for whole animal minPMI estimations
- 5) Examine whether food substrate affects the spectral measurements of *L. sericata*
- 6) Examine whether cuticular **hydrocarbon** and probable surface bacterial hydrocarbon spectral measurements change on a daily basis

Chapter 2. Literature Review

2.1 Preface

This chapter highlights the uses of forensic entomology, particularly as they relate to the development of immature blow flies (Diptera: Calliphoridae) and elaborates on the drawbacks of present methods of aging within **stadia**. The innovative but long-standing science of hyperspectral remote sensing is explained and is proposed as a potential solution to the present obstacles. Finally, the chapter will conclude with a discussion of the potential value that the addition of hyperspectral remote sensing provides to entomology in its forensic framework.

2.2 Overview

First wave insects are swift to locate decomposing remains, frequently arriving within minutes of death assuming that conditions are suitable (Amendt et al., 2011; Anderson & VanLaerhoven, 1996; Erzinçlioğlu, 1996; Smith, 1986), and beginning the sequence of insect arrival. Within 72 hours of death, the forensic pathologist may be able to use medical parameters to estimate minPMI , but after this time, forensic entomology is the most accurate and often the only method available to estimate minPMI (Henssge, Madea, Knight, Nokes, & Krompecher, 1995; Kashyap & Pillai, 1989). However, even in the first few hours following death, forensic entomology can be useful in estimating minPMI .

There are two main approaches that entomologists use to estimate minPMI : blow fly development and insect succession. Of these two approaches used to estimate minPMI , the first method based on the development of the first colonizers, the blow flies, will be discussed in greater detail later since it is the focal area of this research.

Blow flies (Diptera: Calliphoridae) are true flies, therefore, the adult has only one pair of functioning wings while the hind pair is modified as halteres or balancing organs (Erzinçlioğlu, 1996). There are 17 genera and 54 species of Calliphoridae described in

North America with many divergent life histories; for example, more than half of the species belong to the genus *Protocalliphora*, which are bird blow flies, and feed by sucking the blood of nestling birds (Whitworth, 2006). Only approximately 15 species feed on carrion, making them forensically significant (T.L. Whitworth pers comm July 2007).

Forensically important blow flies are attracted to wounds or the moist natural orifices of the body as adults in order to oviposit their eggs. If there are exposed body fluids then these areas are most attractive to **gravid** blow flies. Eggs hatch and develop through their life cycle at a rate dependent on temperature. Once an entire blow fly life cycle has been completed, then the second method of estimating the minPMI is utilized. This method involves examining the successional waves of insects which are attracted to the body in sequence. Insects appear on the body in a predictable sequence as different species are attracted to the different stages of decomposition over time and this succession is used to estimate a minPMI (J. A. Payne, 1965; Smith, 1986). This sequence was first described as early as the 19th century by M \acute{e} gnin, a pioneer of the science (M \acute{e} gnin, 1894; Rivers & Dahlem, 2014). These stages include a variation of fresh, bloat, active decay, advanced decay and dry remains (skeletal) (M \acute{e} gnin, 1894; J. A. Payne, 1965; Smith, 1986; Tabor Kreitlow, 2010). It is the biological, physical and chemical changes of the body during this time that are attractive to different species and this contributes to the estimated minPMI (Amendt et al., 2011; Smith, 1986). Many parameters must be considered such as season, geographical differences, sun versus shade, larval aggregate formation and confinement scenarios as they all impact this sequence (Anderson, 2010; Greenberg & Kunich, 2002; Smith, 1986).

2.2.1 Immature Development and the Blow Fly Life cycle

The first general method of minPMI estimation based on insect development is useful for the earlier post mortem interval as it requires the examination of the stage of the early colonizers of the remains, the blow flies developing on the body. The gravid female blow fly oviposits her eggs on the body at wound sites where there is liquid protein, such as blood, or on the mucosal layer of orifices. These eggs hatch into first **instar** larvae and

follow a predictable lifecycle (Figure 2-1). The insects develop through the immature stages at a predictable rate based on temperature and species (Chapman, 1980). The first instar larvae then moult to second and then third instar larvae. The instar is identified by the number of spiracular slits observed on the posterior spiracles. With each moult, their mouth parts are shed together with the entire cuticle, including the cuticle lining the trachea, the foregut and the hindgut, and replaced by larger and further developed mouthparts and so feeding becomes much more voracious. After a period of time, the third instar changes behaviourally and physiologically, although it does not moult, and enters the post-feeding or wandering phase of the third instar stage. At this point, the larva reaches its maximum size and no longer feeds. The post feeding larva wanders to find a drier and more suitable location to enter pupariation (Greenberg & Kunich, 2002). During this dispersing stage, the post feeding larva depletes the food stored in the crop. Once a suitable site has been located, the larva stops moving, shrinks in length and develops an opaque appearance. The opaqueness is a result of forming fat bodies or food stores for the following stage (Greenberg & Kunich, 2002).

The **intra-puparial period**, one of the longest combined stages of prepupal, pupal and **pharate adult**, often incorrectly referred to as the pupal stage (Martin-Vega et al., 2016), consists of pupariation and pupation (Greenberg & Kunich, 2002). Pupariation is the tanning and hardening of the casing. Pupation is the metamorphosing of the adult and includes histolysis where tissues dissolve and reform (Goff, 2000) as the pharate adult within the puparium.

Once the adult fly forms, it inflates its ptilinum, an expandable **haemolymph**-filled bladder on the top of the head, and severs the anterior end of the casing, releasing the ecdysial caps and allowing the adult to escape the puparium (Erzinçlioğlu, 1996; Greenberg & Kunich, 2002). These ecdysial caps and puparium are often the only evidence left behind at a scene indicating that at least one complete lifecycle has concluded. The **teneral** adult fly is not fully developed at this point and must harden, or tan, its cuticle. It exits the puparium with uninflated wings. Using the haemolymph, it expands its wings and body

before the cuticle tans. Finally, the **anauto**genous fly requires a protein meal to develop its gonads and complete the lifecycle (Erzinçlioğlu, 1996).

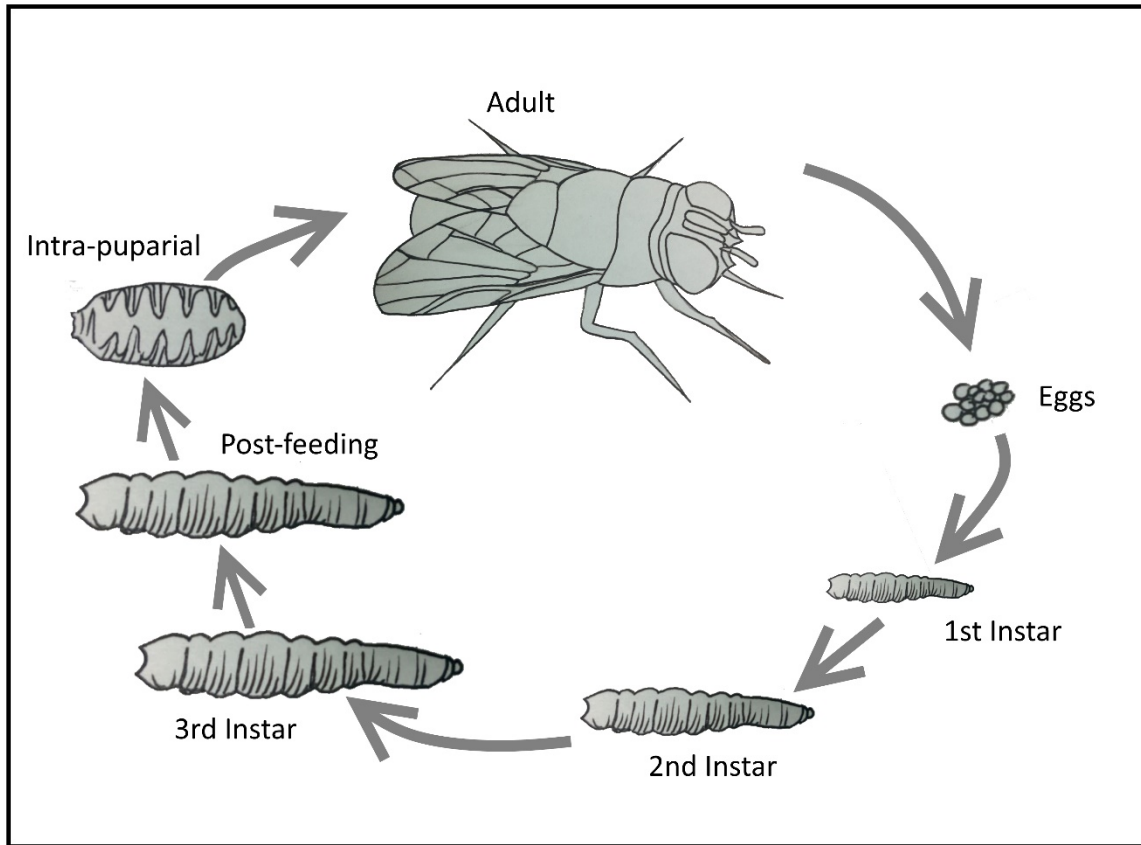


Figure 2-1 Blow fly lifecycle (illustrator V. C. Lam) (not to scale)

Forensic entomologists study this lifecycle in order to estimate the age of the oldest first colonizers on the body. In order to do this, they need four main pieces of information:

- The oldest developmental stage of insect on the body. This is determined by examining the remains and surrounding areas and identifying how far through this lifecycle the oldest insects have progressed.
- The species of insects on the body. This is primarily determined using morphological features described in dichotomous keys. In some cases, such as cold cases, when only insect parts may remain, or when very young instars are present, DNA may be of value.

- The temperature to which the insects have been exposed. Temperature data are normally obtained from the nearest and most suitable government weather station and are often complemented by using data loggers to determine whether the weather station data are appropriate for the scene. Micro-climatic factors, such as the presence of larval aggregations of maggot masses, must also be considered.
- Published, peer reviewed developmental data for the insect species. There are many published databases for most species, although local databases are most representative (Rivers & Dahlem, 2014).

Once all these data are known, the forensic entomologist can estimate the minimum age of the oldest insects on the body, and thereby infer the minimum length of colonization and hence minimum elapsed time since death or minPMI . For example, if larvae on the remains are identified as feeding 3rd instar of a particular species, the entomologist will be able to use species-specific developmental data, together with temperature records to estimate that the minimum published length of time taken to reach the beginning of this stage is seven days. Thus, insects have been colonizing the remains for at least seven days, so the decedent has been dead for at least seven days. They could have died earlier as this is a minimum on several fronts. Firstly, it is the minimum published time for this species to reach this stage and; secondly, it provides an estimate to the beginning of the instar, but the insects are already further developed within the instar.

Using Blow Fly Development to Estimate Time of Colonization

The development data for the species of interest can be based on stage of development, such as the start of the stadia, and/or growth measurements, such as length, width or weight. This is possible as immature development is consistent and, as a result, predictable (Wells & Lamotte, 2010). Presently the minimum time it takes to reach each of the stages of development is used as an estimate for time of colonization (TOC) which is then presented as a minPMI . The issue however, is that some of these stages can be quite lengthy and, therefore, offer a very general minPMI . Aging a larval insect WITHIN an instar

would allow the estimation of a much more precise minPMI , which could assist death investigators by focussing the time-frame more specifically.

Recently, other sciences such as toxicology (Kharbouche et al., 2008), molecular biology (Boehme, Amendt, & Zehner, 2009 ; Boehme, Spahn, Amendt, & Zehner, 2013; de Lourdes Chávez-Briones et al., 2013; X. Li et al., 2011; Tarone & Foran, 2011; Tarone, Jennings, & Foran, 2007; Zehner et al., 2004) and cuticular hydrocarbon analysis using GC/MS (Butcher, Moore, Day, Adam, & Drijfhout, 2013; Moore, 2013; Moore, Adam, & Drijfhout, 2013, 2014) are being applied to this long and well-established science, and subsequently highlight advances in forensic entomology. Advances in DNA and microbial sciences have recently contributed a great deal to forensic entomology (Benbow, Lewis, Tomberlin, & Pechal, 2013; Ma et al., 2012; Pechal, Benbow, Crippen, Tarone, & Tomberlin, 2014; Pechal, Crippen, et al., 2014; Pechal et al., 2013; Tomberlin et al., 2012). Additional techniques such as hyperspectral remote sensing may be equally valuable to forensic entomology.

2.3 Estimating Time within Stadia

Forensic entomology is a well-established science but that does not prevent scientists from improving upon present techniques. There are several caveats to aging based on immature development and these include larval aggregates forming and increasing development temperature well above ambient temperature, geographical development differences in the same blow fly species, and fluctuating temperature changing rate of development (Tarone, Picard, Spiegelman, & Foran, 2011; Warren, 2006; Warren & Anderson, 2013b). Also, a major shortcoming in the assessment of blow fly immature development that forensic entomologists would like to overcome is estimating age within stadia. Current methods of immature development include providing the time it takes to reach a current stage of development of the oldest blow flies associated with the remains to investigators as an estimated minPMI (Catts & Goff, 1992). Although an accurate minPMI , the precision is lacking due to an underestimate, particularly, in the longer

stadia. To be able to age within stadia rather than to stadia of blow fly would be a remarkable development in forensic entomology case analysis and would improve the precision in the estimated minPMI (Tarone & Foran, 2008).

Many efforts have been made to solve this dilemma and are being examined by forensic entomologists. Unfortunately, there are a number of issues with these efforts. The most conservative method, applying the minimum tenure of the oldest stage of development of blow fly on the remains as the minPMI , is limited by aging to a stage rather than aging within a stage. Aging using thermal summation and examining the accumulated degree days or hours (ADD/H) is another frequently used method which is constrained by the same limitation. Further limitations include the fact that this method should only be used when the ADD/Hs were generated from data at temperature close to that of the scene (Anderson, 2000; Reibe, Doetinchem, & Madea, 2010) and there is the possibility of inaccurate lower temperature thresholds being applied to thermal units.

A controversial method used to estimate the minPMI is measurements of weight, length, and width (Amendt et al., 2004; Day & Wallman, 2006b; Wells & Lamotte, 2010). Carrion is an ephemeral resource and, as anyone working in a forensic entomology lab is aware, if the food source is depleted the insects are much smaller in size compared with those with an abundance of food. This may make the insect appear much younger than they are and affect the minPMI estimate (Anderson, 2000).

A combination of gas chromatography and mass spectrometry (GC/MS) is being used to analyze volatile organic compounds recovered from the headspace of immature *Calliphora vicina* (Robineau-Desvoidy) (Frederickx et al., 2012) and cuticular **hydrocarbons** (Butcher et al., 2013; Moore, 2013; Moore et al., 2013, 2014; Pechal, Moore, Drijfhout, & Benbow, 2014; Xu, Ye, Xu, Hu, & Zhu, 2014; Zhu, Xu, Yu, Zhang, & Wang, 2007) to age immature Calliphoridae. There is considerable promise in applying these methods to case work. Their biggest drawback, however, is that GC/MS is not a rapid technique and is destructive to the insect sample. It would be preferable to allow the examined insects to develop to the adult stage in order to determine species of the exact specimens that are being aged.

Similarly, gene expression has been introduced as a means to age eggs, larvae and pupae and so offers demarcations within stages based on gene transcript levels (Tarone & Foran, 2011; Tarone et al., 2007). The limitations to using gene expression are threefold: it involves extensive equipment, requires a trained molecular biologist, and the insect sample is destroyed in the analysis.

Noted morphological changes can also be used to delineate changes within the intra-puparial period (K. Brown, Thorne, & Harvey, 2015; Davies & Harvey, 2013; Defilippo, Bonilauri, & Dottori, 2013). These methods are very effective but can be time consuming and sample preparation is damaging. Finally, micro-computed tomography has been used to view the morphological changes in metamorphosing blow flies. In addition to the benefits and costs of morphological changes, there are the added costs of equipment and the exposure of the sample to X-rays. Ideally, if many of these limitations are avoided in the methods used to age within stadia, a promising improvement to the science will evolve. As other scientists have already discovered, remote sensing has few drawbacks and is neither invasive nor damaging and may improve the precision considerably when aging immature blow flies.

2.4 Remote Sensing

Although often considered a new science, remote sensing has had a long history. Its use originated predominately with the military and is only recently being considered as a leading edge civilian tool. The term remote sensing was first devised in the 1960s but its actual use began well before this time (Cracknell & Hayes, 2007). The earliest remote sensing began with the implementation of a simple air balloon and aerial photographs but, with the discovery of different wavelength regions of the **electromagnetic spectrum** and the implementation of multi- and hyperspectral sensors, it has since surpassed early expectations and has emerged as a leading science. Remote sensing is defined as the science of obtaining information often in an electronic form, without being in physical contact, about the structures of a particular target (Canada, 2001; Cracknell & Hayes, 2007;

Schowengerdt, 2007). Reflected and emitted energy are sensed, recorded and processed to produce the sensed data in the form of an image or as point source measurements (Canada, 2001). Continuous and repetitive images are often produced by the sensor and provide a tool for change detection studies (Schowengerdt, 2007). Remotely sensed data are valuable in many fields. Remote sensing is commonly used in agriculture, environmental monitoring, military strategy, meteorological monitoring, mapping, and medical assessments (Canada, 2001; Schowengerdt, 2007). Not only does its use fall within a broad array of fields but within these fields, remote sensing exists on different scales. Remote sensing can range from the microscopic level, with very detailed spatial scales on the order of microns in medical research, to extensive levels such as Earth-wide coverage with broader application for military strategizing, forest health management, and effects of pollution on the environment (Ustin, Smith, & Adams, 1993). On a larger scale, SPOT 5, Landsat, and Earth Observing (EO-1) Hyperion hyperspectral satellite imagery is being used environmentally to measure sustainability and evaluate the ecological effects endured over time (Hais et al., 2016; Kalacska, Sanchez-Azofeifa, et al., 2007; Meng et al., 2016). Another use for remote sensing is identifying and quantifying photosynthetic pigments such as chlorophylls a and b and carotenoids in plant leaves and canopy (Blackburn, 1998). A familiar application is the use of remote sensing by police officers and the ominous radar gun (Baker, 2002).

Use of hyperspectral remote sensing at the microscopic level is a relatively recent development and incorporates the same science as the larger scale sensors but on a much smaller level. These sensors are applied to sciences involving cell fusion, histologies, cytogenetics and other material sciences (R. A. Schultz et al., 2001). An intriguing example of hyperspectral remote sensing is the use of one of its forms in the early detection of cancer. Cancerous tissue can be distinguished successfully from healthy tissue at the wavelength ranges of 1226-1251 nm and 1288-1370 nm, avoiding invasive and unnecessary biopsy treatments and assisting in successfully excising the margins of the tumour for complete removal (Akbari, Uto, Kosugi, Kojima, & Tanaka, 2010).

All objects emit electromagnetic radiation (EMR) (Figure 2-2) and this radiation is recorded by sensors as it approaches, strikes and leaves the target's surface. The radiation that is absorbed, reflected, emitted and transmitted can be measured and then recorded either in a datum format (e.g. spectrometry) or through photographic means (e.g. imaging analysis) (Canada, 2001; Holz, 1985). Under Earth observation, the radiation that is scattered or absorbed by the atmosphere is not measured. The measured radiation however, is determined by the wavelength of the EMR and the target surface (Canada, 2001). The reflected and absorbed radiation incident from the sun or a laboratory based light source is often of most importance in remote sensing as opposed to the emitted radiation from the target itself (Canada, 2001).

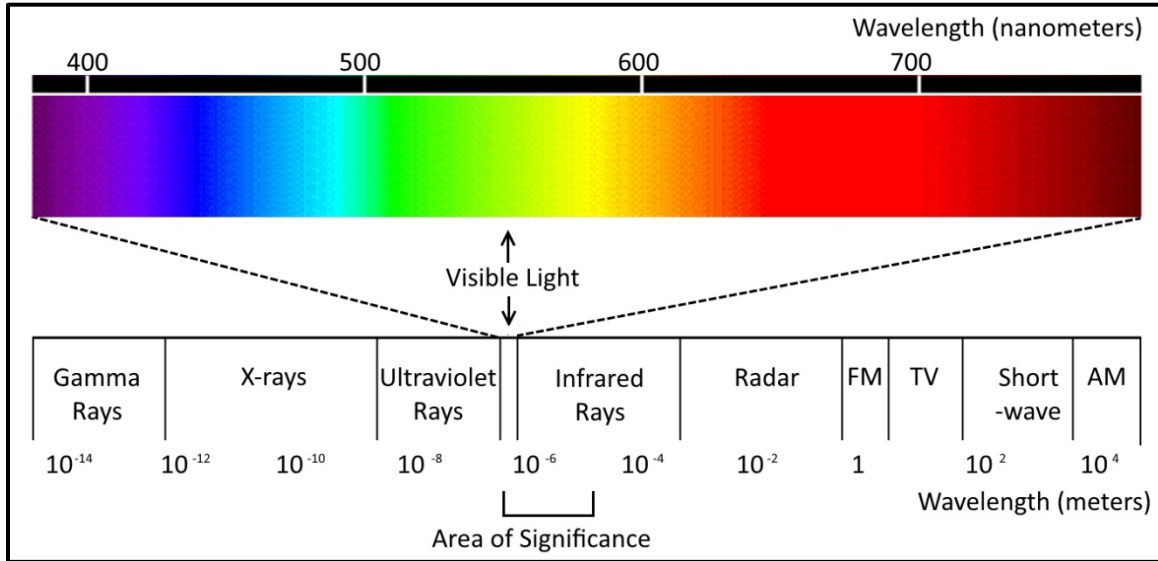


Figure 2-2 The electromagnetic spectrum with area of significance noted for the current research. (illustrator V.C. Lam)

There are four types of resolution that apply to remote sensing. The first of these is **Spatial** resolution. When referring to image resolution, spatial resolution is the resolution that is most often referenced. This resolution is specific to the clarity of the minute details in an image (Campbell, 2007). A second type is **Radiometric** resolution. This includes the capability of the sensor to document the features associated with brightness (Campbell, 2007). The higher the resolution is, the better the documentation of the different levels of brightness. A third resolution is **Temporal**. Temporal resolution is

sequential documentation over periods of time (Campbell, 2007). The time component is fundamental because the changes that are recorded are indicative of those differences created in relation to the time variable. The final resolution is **Spectral** resolution, which is most relevant here. Spectral resolution refers to the capacity to provide details in relation to wavelength demarcations which include the number and width of the intermittent bands within the electromagnetic spectrum. The sensor needs to be sensitive enough to successfully identify the detailed information that may be averaged within the bands (Campbell, 2007). The intermittent bands can be examined by either **Multispectral** or Hyperspectral imaging, which differentiate the two sets of grouping of the multiple layers of the electromagnetic spectrum (Borengasser, Hungate, & Watkins, 2008). With multispectral remote sensing, the layers are grouped for imaging purposes and only examined for wider bands and as few as three to six spectral bands (Govender, 2007). Hyperspectral remote sensing, however, involves the examination of radiation at much narrower and more numerous bands of the electromagnetic spectrum (Govender, 2007). This leads to a much finer resolution and, therefore, a more complete image (Canada, 2001; Govender, 2007). The crude imaging abilities of the multispectral sensors, although completely adequate for some applications, have evolved into the finer imaging abilities of the hyperspectral sensors. High resolution spectral imaging, as provided by hyperspectral sensors, permits the distinction of finer detailed elements through both spectroscopy and imaging processes (Govender, 2007; Servakaranpalayam, 2006).

Before a complete understanding of hyperspectral sensing can be met, further comprehension of the electromagnetic spectrum must be satisfied. Particles of EMR or photons (also quanta) are released and the energy associated with each particle determines its wavelength and, therefore, where on the electromagnetic spectrum it is located (Borengasser et al., 2008).

A combination of the wave theory, which suggests that energy travels in wave form at the speed of light as a result of both an electrical and magnetic force field (Figure 2-3), and Planck's quantum theory apply (Holz, 1985). Photons travel at the speed of light, c

(3.0×10^8 m/s) and, therefore, the relationship between frequency, ν and wavelength, λ is represented.

The wave theory indicates that the forces interact with the wave at vertical and horizontal right angle directions from the direction of the wave of photons (Holz, 1985). The quantum theory component explains the emission of photon energy at distinct predictable spectral bands. The photons do not form a smooth wave but instead propagate in assemblages (Holz, 1985). The wavelengths associated with the various particles of energy compose the electromagnetic spectrum (Holz, 1985).

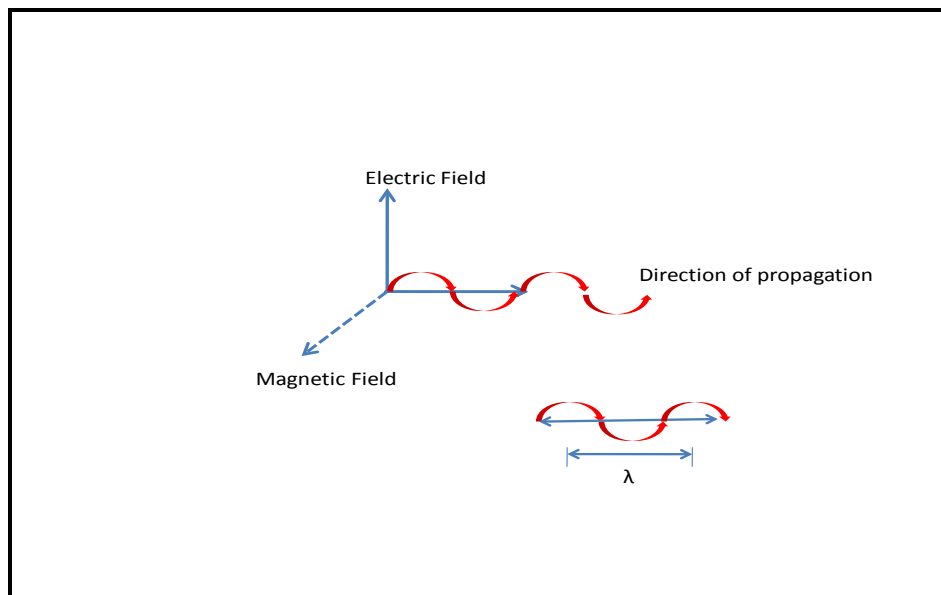


Figure 2-3 Electromagnetic radiation and its direction of propagation due to the magnetic and electric forces acting on it (Holz, 1985)

Hyperspectral sensing can be applied to the longer wavelengths of the spectrum including the visible, near, mid and thermal infrared sections, which, in fact, range from 0.4 to as much as 100 microns (Govender, 2007). At longer wavelengths, emissivity, chemical absorption and thermal changes can be monitored. Hyperspectral sensing involves combining the exhaustive details within hundreds of narrow bands to achieve a spectral response or spectral signature of the element (Figure 2-4). A combination of both spectral and two-dimensional spatial information is collected and accumulated in each pixel or unit (Servakaranpalayam, 2006). The data stored in each pixel remain as a separate unit of information and these pixels are arranged in sequences of stored information

according to the band and line (Campbell, 2007). The spectral response then is composed of this organized and stored material.

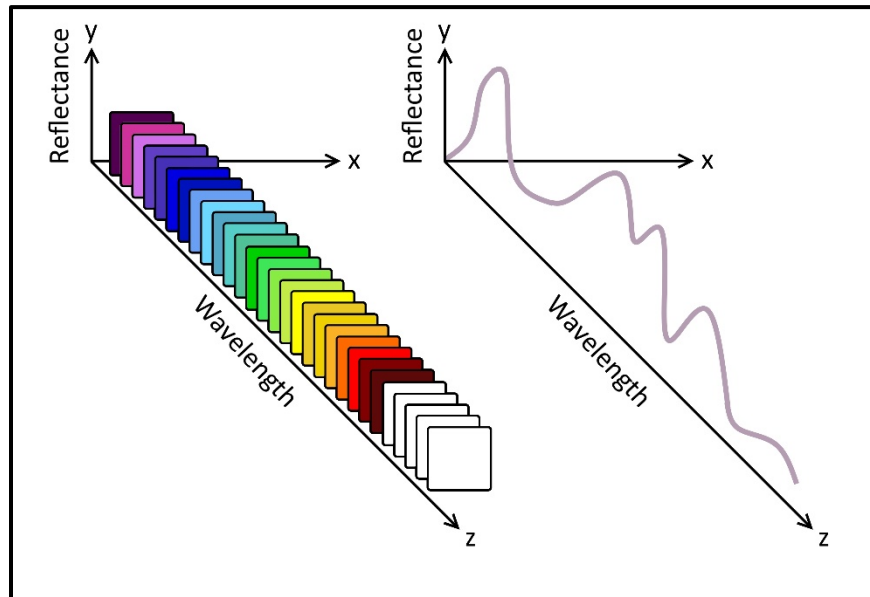


Figure 2-4 The combined exhaustive details of the hundreds of narrow bands form a hyperspectral signature (illustrator V.C. Lam)

2.5 Applications of Remote Sensing to Forensic Science

Diverse techniques using different means of remote sensing are being applied to the forensic sciences. In fact, hyperspectral imaging, one such form, is being adapted for countless forensic sciences. Persistent attempts to age bruises on human tissue with the use of a combination of spectrophotometry, histology, colour gradient and observation have finally been successful with the use of hyperspectral remote sensing (Hughes & Langlois, 2011; Langlois, 2007; Mimasaka, Ohtani, Kuroda, & Tsunenari, 2010). Hyperspectral imaging has been shown to further the science of age determination in cases of bruising due to its ability to provide both spectral, and spatial information (Randeberg, Baarstad, Loke, Kaspersen, & Svaasand, 2006). Hyperspectral imaging recognizes the area of impact and illustrates it as a white area within the bruised region (Randeberg et al., 2006). This white area resembles the object that created the bruise so, even if time cannot be determined from the bruise, perhaps the object that caused the bruise can be deciphered.

Not only is hyperspectral remote sensing being used to age a contusion but it is being applied to crime scenes to estimate the age of bloodstains (Bremmer, de Bruin, et al., 2011; Bremmer, Nadort, van Leeuwen, van Gemert, & Aalders, 2011; Edelman, Manti, van Ruth, van Leeuwen, & Aalders, 2012; Edelman, van Leeuwen, & Aalders, 2012; Li, Beveridge, O'Hare, & Islam, 2011, 2013, 2014).

Chemical imaging methods in the ultraviolet, visible and near infrared regions have been investigated in the use of analyzing forensic samples such as paint, adhesives and firearm propellants (G. Payne, Wallace, et al., 2005). They have been demonstrated to be beneficial over traditional methods by offering a more discerning and non-destructive means of examining the samples as well as by reducing risks of contamination (G. Payne, Wallace, et al., 2005). Because these means of analysis are so much less destructive, forensic chemists are able to apply these to their case exhibits and avoid having to explain to the courts any changes that have been made to exhibits when they are testifying. It also allows a second individual to confirm or disprove any results if a second expert is brought in to testify.

Fibre examination, also completed by forensic chemists, can be improved upon by the use of infrared chemical imaging or hyperspectral imaging (Flynn, O'Leary, Roux, & Reedy, 2006). This technique is rapid in comparison with traditional methods of fibre examination and determines the spectral signatures of the components of bi-component fibres. It not only provides the signature but where in the sample the components are located (Flynn et al., 2006). Unfortunately, for samples whose components were very similar, only the spectral response could be determined and not the spatial configuration. Impressively, however, the infrared chemical imaging could distinguish the components and provide signatures without having any prior knowledge of the fibre constituents (Flynn et al., 2006).

Similarly, infrared chemical imaging of automobile multi-layer paint chips can be used to compare two separate paint chips (Flynn, O'Leary, Lennard, Roux, & Reedy, 2005). All of the collected spectral information is congregated in a hyperspectral image and samples are compared (Flynn et al., 2005). There are several advantages to using this

comparison method and these include time and spatial distribution. The collection of the infrared spectral response is extremely rapid and can be completed within minutes. The spatial distribution that can be identified from the hyperspectral imaging can also offer a key characteristic to the sample for comparison (Flynn et al., 2005). A final advantage expressed by the researchers is that this science is applicable to other parts of the electromagnetic spectrum rather than simply that of the infrared (Flynn et al., 2005).

There is no quality control in the street production of illicit drugs such as N-methyl-3,4-methylenedioxyamphetamine (ecstasy) and contamination of this drug, whether purposeful or not, is a common and dangerous occurrence. Near-infrared spectroscopy has been applied to screen the quality of these street produced drugs to determine which contaminants may appear in the tablets (Schneider & Kovar, 2003; Sondermann & Kovar, 1999). Examination of the drug also involves examination of the spectral responses of the constituents or **excipients** that make up the base of the tablet (Baer, Gurny, & Margot, 2007). Common excipients are cellulose and lactose because they are easily acquired (Baer et al., 2007).

Quality control of pharmaceutical drugs and detection of counterfeit drugs is often quite an involved process for packaged products and, until recently, has involved sub-sampling (MacLeod & Matousek, 2008). Raman spectroscopy offers a means to detect counterfeit or tainted drugs through packaging such as blister packs and opaque plastic bottles. Raman spectroscopy examines and records the scattered light of a target due to molecular vibrations when a laser is shone on the target. It presents a molecular fingerprint of the examined target and provides both a qualitative and quantitative analysis (Bumrah & Sharma, 2015). By using Raman spectroscopy over older methods, a non-invasive examination of the drugs can be done to authenticate drugs much faster than previous destructive sampling practices.

Raman spectroscopy can also be applied to fibre evidence collected at a scene or on a suspect's clothing in order to detect and link illicit drugs to a person (West & Went, 2009). The detection of these drugs can be done on fibres that have been collected at crime scenes or on suspects with the use of adhesive lifters, and can also be performed through

evidence bags (West & Went, 2009). The benefits to this are twofold. First, the evidence is not contaminated by opening the evidence bag and second, the fibre can be tested multiple times without destroying the drug sample (West & Went, 2009).

The fibres themselves can also be distinguished from one another based on dyes using Raman spectroscopy (Thomas, Buzzini, Massonnet, Reedy, & Roux, 2005). This can be done for the difficult blues and black-grey dyes (Thomas et al., 2005). Fluorescence conflicts with spectral reading but the problem can be avoided altogether by adjusting the laser wavelength and, therefore, the near infrared wavelength (Thomas et al., 2005). Based on this technology, a reference library of fibres and their dyes can be created and used in criminal investigations, even if it is a reference library that is created on a case by case basis.

Also, chemical signatures of simulated bio agents have been identified using hyperspectral imaging along with microanalysis and have revealed its possible use in forensic investigations of unknown suspicious substances (Brewer, Ohlhausen, Kotula, & Michael, 2008). The hyperspectral methods produce a great deal of data to identify chemical signatures and are extremely sensitive to trace elements, unlike traditional methods where trace elements may have gone unnoticed. Traditional methods of collecting large amounts of data are susceptible to human bias or error, whereas hyperspectral imaging avoids this by collecting and combining the bands of data in a matter of moments so there is less need for human manipulation.

Fingerprint examiners can also find a non-destructive use for hyperspectral imaging of latent prints. Fingerprint powders are damaging to trace evidence, but their use to perceive latent fingerprints can be avoided by using Fourier transform infrared (FTIR) spectroscopic imaging. FTIR involves sending a controlled amount of IR radiation through a sample and recording absorption and transmittance. Details become evident without the powder and without inhibiting the investigation of the material in question for discovery of further types of physical evidence (Crane, Bartick, Perlman, & Huffman, 2007). Exploration of recovering difficult-to-retrieve children's latent fingerprints was initiated successfully as early as 2002, with the introduction of hyperspectral techniques (Bartick et

al., 2002). Prepubescent fingerprints do not have the same chemical composition as those prints left by adults since children do not have the esters in the sebaceous glands that adults do (Bartick et al., 2002; Buchanan, Asano, & Bohanon, 1997). With the growing use of hyperspectral techniques, improvements above conventional methods are more and more evident. Surfaces that contain text or pictures can be rather “difficult” on which to identify ridge characteristics due to their obscuring features (Tahtouh, Despland, Shimmon, Kalman, & Reedy, 2007). However, FTIR can be used to produce superior ridge detailing and completely eliminate any unwanted background obscurities (Tahtouh et al., 2007). Chemical imaging using the recommended Condor macroscope (Chem Image Inc.) can reveal faint prints or those that would otherwise go undetected using standard methods (Exline, Schuler, Treado, & Corporation, 2003; G. Payne, Reedy, et al., 2005). Chemical imaging offers increased contrast between the print and the background as well as decreasing the effects of luminescent surfaces (Exline et al., 2003; Maynard et al., 2009).

Not only is identifying the ridge characteristics of a print with an obscure background an important scientific advancement, but so is identifying illicit substances in the fingerprint (Ng, Walker, Tahtouh, & Reedy, 2009). This has been made possible with hyperspectral imaging. Illicit substances such as drugs, gunshot residues, and trace explosives can be linked directly to a person if they are found deposited within that person’s fingerprints. A spectral angle mapper and correlation algorithms combined with second-derivative image and reference spectra when tested offered the best performance (Ng et al., 2009).

Hyperspectral technology, using Raman dispersive spectroscopy and chemical imaging, has also been used to explore the possibility of identifying condom lubricants that may have been used in the commission of a sexual assault. There is the prospect for this science to become routine in sexual assault investigations and to provide further corroboration when compiling evidence in a case (Wolfe & Exline, 2003).

Hyperspectral remote sensing is being used to detect environmental crimes in police investigations and the hyperspectral science speeds up the detection time, which assists immensely in the investigation (Lega, Ferrara, Persechino, & Bishop, 2014). Drones

carrying sensors overhead are just one of the means that can be used to detect sites of pollution and waste run off as well as identify the pollutant (Lega et al., 2014).

Further, visible and NIR hyperspectral imaging are being used by questioned documents examiners as a non-destructive way to examine fraudulent documents (Brauns & Dyer, 2006; Khan, Shafait, & Mian, 2015; Silva et al., 2014). Common black ballpoint pens are being distinguished using Raman microscopy (Claybourn & Ansell, 2000). Gel pen ink analysis, similarly, is being examined by Raman spectroscopy in a non-destructive manner (Mazella & Buzzini, 2005) and is more recently being examined using multiple incident light sources and a hyperspectral spectrometer ranging from 400-1000 nm (Reed, Savage, Edwards, & Daeid, 2014). In addition, authenticity and aging of inks as well as enhancement and improved legibility of historical documents is being done with quantitative hyperspectral imaging broadening approaches in the field of questioned documents (Padoan, Steemers, Klein, Aalderink, & de Bruin, 2008).

Not only are questioned documents examiners using Raman spectroscopy on pen inks, but they also are applying the chemical analysis to colour printer toner (Udristioiu, Bunaciu, Aboul-Enein, & Tanase, 2009). Conventional examination is destructive and does not offer the favourable feature of profiling the target surface and examining the depth spectral measurements as Raman spectroscopy does (Udristioiu et al., 2009).

Non-invasive ground penetrating radar (GPR) can be applied to the forensic sciences in the search for and identification of even the smallest of illicit graves (J. J. Schultz, 2008). Complexity in identifying smaller graves increases with less disturbed soil surrounding the cadaver as the contrast is not as abundant (J. J. Schultz, 2008). On a larger scale, mass graves from human rights violations can be identified using airborne or satellite recorders that collect the hyperspectral data (Kalacska & Bell, 2006; Kalacska, Bell, Sanchez-Azofeifa, & Caelli, 2009; Kalacska, Bell, & Thiessen, 2007). The subtlest of changes can be identified from the hundreds of bands of collected data (Kalacska & Bell, 2006; Kalacska et al., 2009; Kalacska, Bell, et al., 2007). The reflected spectra can detect any environmental changes and, therefore, discriminate between a grave and its adjacent surroundings (Kalacska & Bell, 2006; Kalacska et al., 2009; Kalacska, Bell, et al., 2007;

Snirer, 2013). This same airborne hyperspectral science is being assessed as a tool to identify single graves (Leblanc, Kalacska, & Soffer, 2014; Snirer, 2013).

As early as 1996, studies were performed comparing visible means to infrared means of facial recognition scenarios (Wilder, Philips, Jiang, & Wiener, 1996). The discrimination against infrared means is argued to be based on its higher cost, poorer image resolution, greater image noise, and deficiency in datasets (Socolinsky, Selinger, & Neuheisel, 2003). Wilder et al. (1996) argue, based on their findings, that visible and infrared imaging perform similarly in most cases and would only act to better enhance each other if used simultaneously, whereas Socolinsky et al. (2003) argue that thermal infrared imagery performs better in most cases and is equivalent in performance in all other cases. Eye glasses obscure much of the thermal image unlike that of visible images and facial expression can create clear differences in visible images of the same person, unlike that of thermal images; together, the two image types can clearly identify the contender as the suspected person.

The social science of archaeology has found many ways to apply near infrared photography to its field which would be useful forensically in theft or destruction of property cases. For example it can be used to decipher documents that are deteriorated from charring, aging, obliteration and fading (Verhoeven, 2008). Also, near-infrared photography is being used on tapestry and paintings for inspection and extensive examination (Verhoeven, 2008). Further, forms of tattooing are being identified on mummified human remains and near infrared photography can be used to reveal pigments on pottery artefacts (Verhoeven, 2008). As well, near infrared photography is being applied to aerial photography and excavation. Differences in vegetation are reflected and, for those times when visibility is distorted, the near infrared portion of the spectrum permits clarity (Verhoeven, 2008). During the process of excavation, stratifications and features are discernible from other components using near infrared photography as opposed to visible photography (Verhoeven, 2008).

Forensically, the application of hyperspectral imaging can be quite innovative with its application to credit card verification (Sumriddetchkajorn & Intaravanne, 2008). Visual

identification is no longer enough to recognize counterfeit cards as technology improves. The hologram can be verified using hyperspectral imaging measures which will identify those features that are not visible to the naked eye.

Finally, hyperspectral imaging in the mid and long wave infrared regions is increasingly being applied to forensic medicine in the areas of diagnosis and detection, monitoring and investigating diseases, determining the circumstances of a death, injury patterns and aging, and so forth (Malkoff & Oliver, 2000).

2.6 Hyperspectral Remote Sensing and Forensic Entomology

Researchers in the forensic sciences have begun applying forms of remote sensing to their disciplines and continue to find new benefits. Forensic entomology could derive further benefits from the addition of this technology and science to its field (Pickering, Hands, Fullwood, Smith, & Baker, 2015). The main practice of forensic entomology is to provide an estimated time of colonization. A minPMI can be inferred from this estimate based on the stage of the developing insects on the corpse and the successional arrival of insects to the corpse (Anderson, 2001). Insects develop and arrive at a predictable rate and, as long as the temperature and species are known, a minPMI can be estimated by comparing with known development and arrival sequences (Anderson & VanLaerhoven, 1996; Chapman, 1980). Estimating time of colonization of a corpse using known development data involves aging immature Calliphoridae collected from a corpse. Assigning an instar to a blow fly larva is very simple, but aging an insect within stages is much more problematic. Hyperspectral remote sensing has tremendous potential to expand the ability to age immature blow flies within stages and reduce the subjectivity by including error rates, as recommended by the National Academies of Science analysis of forensic science in 2009 (Council, 2009).

Because remote sensing has such a wide array of applications, the aim of this research was to explore its application in forensic entomology, in order to improve current

methods of estimating immature development, and the potential to apply this to estimate post-mortem intervals.

Chapter 3. Initial investigations of spectral measurements to estimate the time within stages of *Protophormia terraenovae* (Robineau-Desvoidy) (Diptera: Calliphoridae)

WARREN, J.-A., RATNASEKERA, T.D.P., CAMPBELL, D.A., and ANDERSON, G.S.

Published in Forensic Science International (with minor updates):

Warren, J.-A., Ratnasekera, T.D.P., Campbell, D.A., and Anderson, G.S. (2017). Initial investigations of spectral measurements to estimate the time within stages of *Protophormia terraenovae* (Robineau-Desvoidy) (Diptera: Calliphoridae). *Forensic Science International* 278: 205-216.

3.1 Preface

This chapter covers the initial explorations of hyperspectral remote sensing to identify the potential to estimate the time within stadia of *Protophormia terraenovae*. The wavelengths used in this research range from 400-1000 nm and include the visible and a large component of the near-infrared spectrum.

3.2 Abstract

Current applications of forensic entomology to post-mortem interval estimations involve aging the insects colonizing the remains based on minimum time to reach the oldest stage of development. Immature species of blow fly develop at a predictable rate to each stage of development in their lifecycle. Unfortunately, the minimum time to reach a stage of development can be a rather unrefined estimate of tenure on the body in the sometimes lengthy time frame of the later stages. In a successful attempt to narrow this time frame, daily spectral measurements of the immature stages of *Protophormia terraenovae*

(Robineau-Desvoidy) raised at a mean temperature of 24.6°C were collected and the functional data analysis was completed. Functional regressions and coefficient functions were examined for model prediction and generalization. *Protophormia terraenovae* is a **Holarctic** species as well as an early colonizer of human remains and is, therefore, an excellent indicator species in North American death investigations.

Spectral measurements can be used successfully to estimate the day of development in the third instar including post feeding stage. In the intra-puparial period, however, only the last day of development could be distinguished from the earlier days of the intra-puparial period. Distinguishing day within second instar is also possible for *P. terraenovae* raised at a mean temperature of 24.6°C and, although not fully within the pointwise 95% confidence interval, it still accurately predicts the day.

The results of this proof of concept research are promising and show a potential method for narrowing the original death estimates and offering a better overall estimate of age of *P. terraenovae* larvae and, therefore, estimated time since death.

Keywords: *Protophormia terraenovae*; larval development; hyperspectral; remote sensing; functional regression

3.3 Introduction

Remote sensing is the science of obtaining information, without being in physical contact, about the structures of the Earth's surface or a particular target (2001; Cracknell & Hayes, 2007; Schowengerdt, 2007). Reflected, transmitted, absorbed and emitted energy are sensed, recorded and processed to produce the sensed data in the form of an image or point source measurements (2001). Remote sensing is not new to the field of entomology; in fact, radar is a very common form of remote sensing applied to insect behaviour patterns (Riley, 1989). Radar is used to monitor insect flight behaviour and migration (Riley, 1989). Sonic detection and ranging (sodar) has been used to count the number of insects that are attracted to sex pheromone dispensers (Hendricks, 1980). Remote sensing is also used in monitoring population densities and mortality rates of the

tsetse fly (*Glossina* spp. Wiedemann) (Rogers & Randolph, 1991) as well as monitoring insect migration as in the corn earworm moth (*Helicoverpa zea* (Boddie)) (Westbrook, Eyster, & Wolf, 2014). Vectors carrying diseases such as chikungunya, Lyme disease, malaria, West Nile and schistosomiasis are mapped using remote sensors ranging from Landsat Thematic Mapper (TM) to Advanced Very High Resolution Radiometer (AVHRR) and France's Satellite Pour L'Observation de la Terre (SPOT) technologies (L. R. Beck, Lobitz, & Wood, 2000; H. E. Brown, Diuk-Wasser, Guan, Caskey, & Fish, 2008; Fuller et al., 2011; Ruiz-Moreno, 2016). The search for crop damaging insects is made possible using hyperspectral imaging (Carroll et al., 2008; Lawrence & Labus, 2003; Mirik et al., 2014; Mirik, Michels jr., Kassymzhanova-Mirik, Elliot, & Bowling, 2006; Williams, Bartels, Sawyer, & Mastro, 2004; Xing, Guyer, Ariana, & Lu, 2008) and can be used to follow insect movement in order to predict and avoid damaged crops (Reynolds & Riley, 2002). Not only are the insects themselves observed using remote sensing but damage to crops for example, created by the insects, is also observed (Hart et al., 1971; Mirik, Michels jr., Kassymzhanova-Mirik, Elliot, Catana, et al., 2006; Moran, Inoue, & Barnes, 1997; Riley, 1989; Singh, Jayas, Paliwal, & White, 2009; Solberg et al., 2007). Aerial infrared colour photography has been used to identify crop pests, which can reduce costs to growers as they can concentrate their actions on the areas of infestation rather than on the entire growing area. Furthermore, disruption to beneficial species of insects can be better avoided if only the infested areas are treated (Hart et al., 1971). As well, the application of spectral transmission analysis of blowfly puparia to examine the development of visual receptor cell formation of pharate adults has also been demonstrated (Järvilehto & Finell, 1983).

Recent applications of remote sensing include using reflectance data to identify insect stress and response to mortality factors in *Trichogramma* spp.(Riley) (Nansen, Coelho Jr, Viera, & Parra, 2014) and mapping forest disturbance history by overlaying Landsat time series data of harvesting and insect mortality (Neigh, Bolton, Diabate, Williams, & Carvalhais, 2014).

Forensic entomologists estimate the minimum tenure of immature species of blow flies colonizing remains based on the time to reach the oldest stage of development. Since

immature species of blow fly develop at a predictable rate, forensic entomologists estimate the minimum tenure of the insects on a body by comparing the stage of the oldest species associated with the body with previously collected development data for the ambient temperature. The length of time the insects have been associated with the body indicates a minimum elapsed time since death. Remote sensing has the potential to further refine these methods.

Forensic entomologists have been using remote sensing by applying Forward Looking Infrared Radiometer (FLIR[®]) to explore the use of thermal imaging in response to heat increases caused by larval aggregations (Hall & Brandt, 2006a, 2006b; Johnson & Wallman, 2014). Larval aggregates form on carrion and increase development temperatures above the ambient temperature. Unless the maggot mass temperature is recorded, the temperature at which the larvae are developing can only be estimated thereby providing a poor estimate for the post-mortem interval.

Other forms of remote sensing in forensic entomology include the use of hyperspectral sensing to discriminate blow fly species using Attenuated Total Reflectance-Fourier Transform Infrared (ATR-FTIR) (Pickering et al., 2015). Pickering *et al.* pulverized insect epidermis and internal matter and firmly pressed the sample against a crystal solid to discriminate species by absorption of radiation (Pickering et al., 2015). Another form of hyperspectral remote sensing examining reflectance was used by Voss *et al.* to age *Calliphora dubia* Macquart and *Chrysomya rufifacies* Macquart puparia based on morphological changes of the pharate adult within the puparium (Voss, Magni, Dadour, & Nansen, 2016).

Hyperspectral sensing involves combining the exhaustive details within hundreds of narrow bands of the electromagnetic spectrum to achieve a spectral response or spectral signature of the measured source (Campbell, 2007). Hyperspectral sensing technology has great promise for future forensic entomology investigations, based on its value in other sciences and forensic science. Its technology can offer promising assistance in maggot mass research at the mid- and long wave infrared regions of the spectrum due to the thermal infrared features at longer wavelengths. Furthermore, it can offer additional capabilities at

the visible, NIR and shortwave infrared (SWIR) regions of the spectrum, where physiological changes can be identified to narrow the estimate of age of insect stages and provide an even narrower minimum post-mortem interval (minPMI) estimate. Current methods of forensic entomology rely on identifying stage changes through immature development and successional arrival of insects. The intra-puparial period of *Calliphora vicina* (= *erythrocephala*) Robineau-Desvoidy can be divided into several shorter stages based on morphological changes in the insect inside the puparium (Finell & Järvillehto, 1983; Järvillehto & Finell, 1983; Martin-Vega et al., 2016) and it has been shown that light progressively penetrates the puparium with increasing wavelength beginning at 500 nm (Järvillehto & Finell, 1983). This can offer a much more precise insect age without being destructive to the pupa or pharate adult. The infrared bands can potentially provide consistent differences at each of the wavelengths that occur within the identified stages of the intra-puparial period. This may offer a shorter window of age estimation based on constant physiological changes and, therefore, a more precise estimate of the minPMI . Improvements to current methods have been investigated to estimate age of immature insects and these methods include the examination of volatile organic compounds (Frederickx et al., 2012), integrating gene expression (Boehme et al., 2013; Tarone & Foran, 2011; Tarone et al., 2007; Zajac, Amendt, Horres, Verhoff, & Zehner, 2015), examining cuticular hydrocarbons (Butcher et al., 2013; Moore, 2013; Moore et al., 2013, 2014; Pechal, Moore, et al., 2014; Xu et al., 2014; Zhu et al., 2007) and using 3D micro-computed tomography (Martin-Vega, Simonsen, & Hall, 2017; Martin-Vega, Simonsen, Wicklein, & Hall, 2017; Richards et al., 2012), however, these methods are destructive and very costly.

The objectives of this research were to examine spectral measurements taken from developing *Protophormia terraenovae* (Robineau-Desvoidy) (Diptera: Calliphoridae) on different days of development to see if reflectance differs within stages of development, particularly the lengthier stages of third instar, post feeding and the intra-puparial period. The recent uses of remote sensing in forensic entomology focus on temperature of development in blow fly larvae masses, species discrimination and comparing hyperspectral measurements to morphological changes of the developing pharate adult

blow fly within the puparium. The current focus is spectral measurements from the individual immature blow fly in order to identify the potential for using hyperspectral remote sensing to estimate age within several lengthier immature stages, from second instar to adult emergence, of the forensically relevant Holarctic species *Protophormia terraenovae*, a frequent colonizer of remains in Northern Europe and Canada (Warren & Anderson, 2013a).

3.4 Materials and Methods

Insect colony

The three year old *Protophormia terraenovae* colonies were established with blow flies wild-caught in Maple Ridge, British Columbia. The blow flies were trapped using beef liver and inverted cone traps made from coffee cans (Martin, 1977) and were replenished each insect season. The insects were identified at the adult stage (Whitworth, 2006) and separated into species. One of the generated colonies of *P. terraenovae* was shipped to McGill University, Montreal, Quebec where the research was conducted.

The colony was maintained in the Phytotron facility in the Stewart biology building in a CMP 4030 Conviron[®] envirochamber (#105). The colony and the experimental insects were maintained at 25°C and 75% relative humidity. The photoperiod cycled from 14:10 (L:D) and approximately 1480 lux. The adult colony was raised on milk powder/sugar/water *ad libitum*.

Experimental Protocol

Milk fed veal liver was used as the oviposition medium and also as the larval rearing source. A thumb sized piece of veal liver was placed into a black film canister which was positioned on its side inside the colony cage to facilitate oviposition (Byrd, J. pers. comm.). After eight hours had passed, once enough eggs were laid, approximately 200 eggs were removed and placed on fresh veal liver in a wide mouthed plastic ~1.5L container. The bottom of the container was lined with an estimated 6 cm of dampened straw and a piece of industrial paper towel to soak up any excess fluid released from the liver. The container

was covered with industrial paper towel secured by an elastic band. Veal liver was added daily to ensure the availability of a food source.

The immature larvae were raised to second instar at which point they were transported daily to Burnside Hall, the geography building where the ASD Fieldspec[®] handheld spectrometer (Analytical Spectral Devices, Inc., Boulder CO) was situated. An ACR Systems Inc. Smart Button[®] data logger (Surrey, BC, Canada) travelled with the specimens and including the travel (*c.*20 minutes each way) and measuring time outside the environment chamber (*c.*1.5 to 2 hours); the data logger indicated an average temperature of 24.6°C (ranging from 18.5-26.5°C) for development. All specimens used in the experiment followed the same temperature regime.

The ASD Fieldspec[®] spectrometer measures radiation at wavelengths ranging from 325-1075 nm. The spectrometer, although typically used in the field and handheld, was set up in a laboratory painted matte black with light source at 90 degrees to the insect platform in a measured and equivalent position for every measurement taken to ensure that reflectance measurements were consistent, equidistant and strictly from the specimen of interest. All equipment was painted black, including forceps used to hold the live larvae still for measuring and the dish where the measurements took place, to further ensure measurements were that of the insect alone. Measurements were completed with no lights on in the laboratory and, therefore, there was minimal light from external sources. The computer screen was turned away from the insect platform and light source to minimize any effect on the reflectance measures. The spectrometer measured the insect in milliseconds and measurements were taken at *c.*30 degrees from the insect platform by the fibre optic cable which was held approximately two millimetres from the insect (Figure 3-1).



Figure 3-1 Taking a reflectance measurement of *Protophormia terraenovae* with the ASD spectrometer

Due to time constraints, the research was completed as two separate components: second instar to pupariation, and the intra-puparial period which begins at pupariation and continues to adult emergence (Martin-Vega et al., 2016). Daily measurements of larvae and puparia occurred back to back. Measurements were completed on each of the larvae and puparia such that a minimum of 12 insects (three measurements each except second instar) of each stadium were measured in a single day. If time was not a factor then measurements of more insects were completed. Measurements were taken every 24 hours beginning at approximately 1300 h. The three measurements taken from each specimen were from anterior, mid, and posterior sections, except for second instar. First instar larvae were too small to measure; second instar larvae were too small to distinguish between body regions when measuring, so instead were measured only at the mid-section to be confident that a measurement was from light reflecting from the larva and not surrounding surfaces. Insects were not washed prior to measuring; however, I examined this in the upcoming chapter.

Calibration was completed using a Spectralon™ diffuse reflectance panel and was conducted at the start of measuring each day and then again following every 5-6 measurements. The Spectralon panel is 99% reflective and provides a baseline measure with which every measurement is compared. This ratio is then presented as the reflectance.

A dark current adjustment of the raw data was also completed with each calibration to filter noise from the measurements.

The compatible software with the spectrometer is RS³TM (Analytical Spectral Devices, Boulder, CO, USA). The collected data were stored as RS³ files and then Viewspec proTM (Analytical Spectral Devices, Boulder, CO, USA) was used to convert the files to text files which were then moved to more user friendly Microsoft[®] Excel files (Microsoft[®], Redmond, WA, USA). By visual inspection, the spectra that were obviously of the blackened surroundings (most probably due to insect movement) were removed from the data sets. The spectra were trimmed on either end due to the substantial noise found in these areas such that only the wavelengths ranging from 400-1000 nm were examined. These files were then stored in the Microsoft Excel template used by the Applied Remote Sensing Laboratory at McGill University. At this point, the files could be manipulated using Matlab R2015b (MathworksTM, Natick, MA, USA) and fdaM (functional data analysis Matlab) tools (<http://www.psych.mcgill.ca/misc/fda/downloads/FDAfuns/>).

The pre-processed raw data were rescaled and noise reduction was performed, and then the multivariate linear regression analysis was completed. A leave- one- out cross-validation analysis was performed to train/ test the data (Ramsay & Silverman, 2005). It was then possible to see how well the data could be generalized in order to predict an insect's day of development. Functional regressions were examined for model prediction for two days of second instar, five days of third instar including post feeding and the first day of intra-puparial period, and for the entire six days of the intra-puparial period. They were plotted for each body region that was measured (anterior/mid-section/posterior). Finally, the coefficient functions were examined for each and confidence intervals determined for those that were significant.

3.5 Functional Linear Model

Preprocessing

Preprocessing of all of the curves was carried out for each body section measured for each day. Vertical rescaling followed to make all spectral signatures fit within a reflectance of minimum zero and maximum one.

Reflectance curves tend to be very smooth and should be because near-infrared spectra are (Foley et al., 1998) but, to correct any lingering artefacts a basis of 100 6th order B-spline functions $\phi(w)$ with evenly spaced knots was fitted to the spectra to remove the noise from the data (Ramsay & Silverman, 2005). The reflectance functions $X(w)$ were approximated using the coefficients $C=[C_1\dots,C_J]$ for the basis expansion:

$$X(w) \approx X_{smooth}(w) = \sum_{j=1}^J C_j \Phi_j(w).$$

Overfitting was controlled using a curvature penalty (Ramsay & Silverman, 2005):

$$PEN_x = \int_{400}^{1000} \left(\frac{d^2}{dw^2} X_{smooth}(w) \right)^2 dw,$$

where the bounds of integration are the bounds of the wavelengths for which reflectance was measured (400-1000 nm). Using a smoothing/ tuning parameter λ , the basis coefficients are chosen by minimizing the smoothing criterion (Ramsay & Silverman, 2005):

$$\operatorname{argmin}_C \left[\sum_{400}^{1000} (X_{smooth}(w) - X(w))^2 + \lambda \int_{400}^{1000} \left(\frac{d^2}{dw^2} X_{smooth}(w) \right)^2 dw \right]. \quad (1)$$

The summation in the first term was over the measured wavelengths. A single smoothing parameter, λ was used for all data from all the days within a single body region (either anterior, mid-section or posterior). Generalized Cross Validation was used to tune λ in order to avoid noise found in the original pre-processed data (Ramsay & Silverman, 2005).

Functional Linear Regression Model Fitting

The functional linear model with scalar response models the day of development Y_i , for the i^{th} individual insect based on the functional predictor $X_{i,smooth}(w)$ over wavelength (w) with $X_{i,smooth}(w)$ held fixed and estimated from (1). The model:

$$Y_i = \int_{400}^{1000} X_{i,smooth}(w)\beta(w)dw, \quad (2)$$

estimates the functional covariate $\beta(w)$ which best predicts the response. The process is similar to estimating the smoothed covariate $X_{i,smooth}(w)$, where the regression covariate was made from 100 6th order B-Spline basis functions, except this time rather than being penalized by PEN_x , a 3rd order derivative penalty function applies,

$$PEN_\beta = \int_{400}^{1000} \left(\frac{d^3}{dw^3} \beta(w) \right)^2 dw.$$

PEN_β has its own smoothing parameter λ_β , which was obtained through a leave-one-out cross-validation. For a given value of λ_β , the regression was performed N times when there are N individuals (Ramsay & Silverman, 2005): The i^{th} regression was performed by omitting the i^{th} individual Y_i and $X_{i,smooth}(w)$. The value of $\beta_{-i}(w)$ obtained from leaving out the i^{th} observation was used in (2) using PEN_β and the current given value of λ_β to estimate \hat{Y}_i . The Sum of Squares Cross-Validation for the fixed value of λ_β :

$$\sum_i (\hat{Y}_i - Y_i)^2 = \sum_i \left(\int_{400}^{1000} X_{i,smooth}(w)\beta_{-i}(w)dw - Y_i \right)^2, \quad (3)$$

is minimized with respect to λ_β (Ramsay & Silverman, 2005). The resulting estimate of $\hat{\lambda}_\beta$ was best able to predict new observations when the model was fitted using this smoothing

parameter. This value of $\hat{\lambda}_\beta$ was used to obtain fit of the regression by minimizing the equation:

$$\operatorname{argmin}_{\beta} \left[\sum_{400}^{1000} (Y_i(w) - \hat{Y}(w))^2 + \hat{\lambda}_\beta \int_{400}^{1000} \left(\frac{d^3}{dw^3} \beta(w) \right)^2 dw \right]. \quad (4)$$

3.6 Results

Protophormia terraenovae raised at an average temperature of 24.6°C (ranging from 18.5-26.5°C) spent two days as second instar, another two days as third instar and then two days as post feeding third instar larvae before entering the intra-puparial period. The intra-puparial period lasted six days at this temperature. The mean spectral measurements for the posterior end of the larvae and intra-puparial period and midsection for second instar from each day beginning with second instar can be found in Figure 3-2.

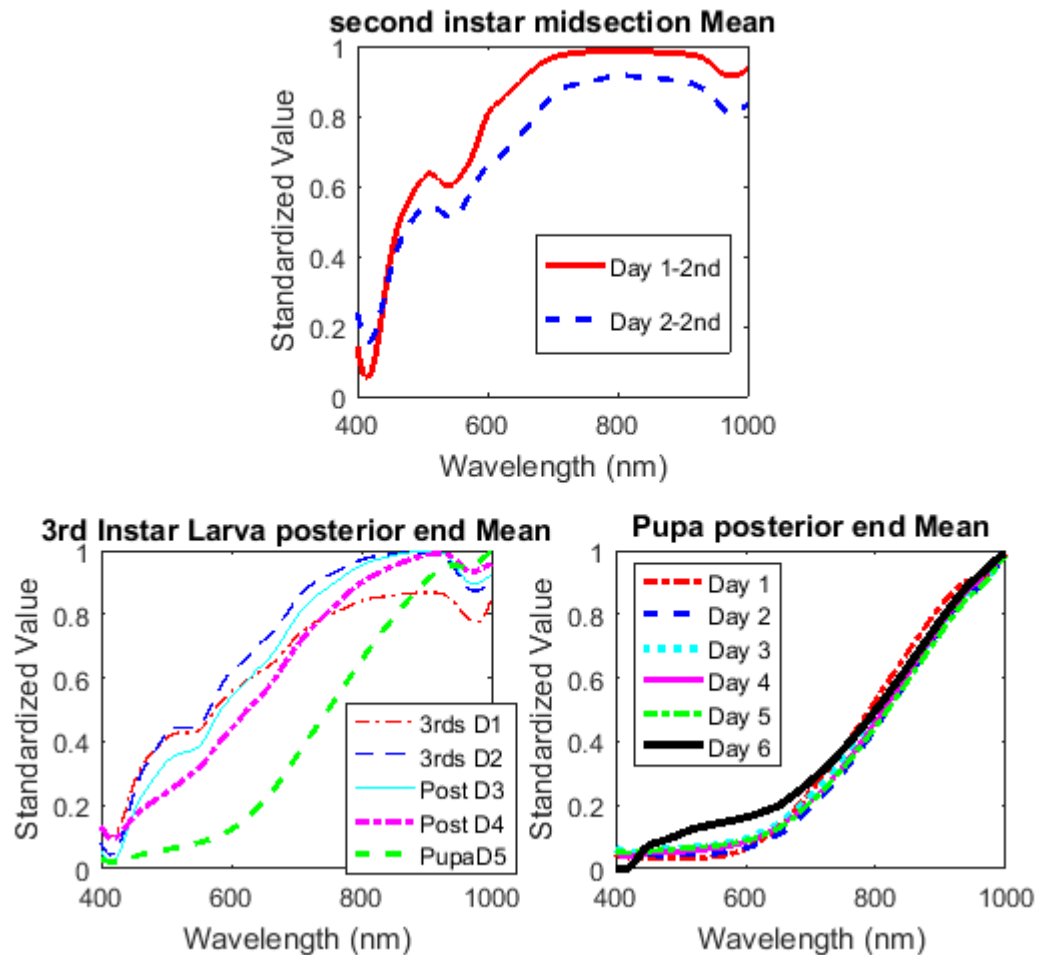


Figure 3-2 Mean plots of daily standardized spectral reflectance at wavelengths ranging from 400- 1000 nm for all days of development of *Protophormia terraenovae* raised at a mean temperature of 24.6°C from second instar to the day before adult emergence. The second instar spectral measurements are from the midsection but the larval and puparial measurements are from the posterior end. (Pupa in the figure is shortened from puparium (Martin-Vega et al., 2016))

The *P. terraenovae* spectral signatures were separated into three arrays, larval second instar, larval third instar (including post feeding and the first day of intra-puparial period), and intra-puparial signatures. These were further subdivided into body region (anterior, midsection or posterior) from which the measurements were collected. Following spectral curve cleaning, standardization and model fitting of the pre-processed raw data, significant differences were found between days of the later larval stages. The functional

regressions indicate a strong distinction between the different days when measuring the posterior of the larvae (Figure 3-3) but spectral reflectance was weaker at predicting day when using the anterior or midsection of the larvae (Figure 3-4). Based on the anterior and midsection functional regressions, it is difficult to distinguish between days one, two and three. Day one is most difficult to distinguish from the other days in the functional regression analyses of the anterior and midsection measures, but day one is clearly distinguished using the posterior measurements. The posterior region was the best area for distinguishing day of development, and this was very obvious even in the preprocessed smoothed tight-fitting data for all three measured body regions (Figure 3-5). The coefficient function indicates that wavelengths 550-575 nm contribute to distinguishing between the days of the later larval stages when examining the posterior of the *P. terraenovae* larvae, but also, when examining the spectral measurements of strictly the posterior region, there are several wavelengths of the NIR that contribute to the model (Figure 3-6). The reflectance that is contributing to the model was identified to a series of wavelengths. The contributing wavelengths are 550-575, 600-604, 693-718, 730-760, 775-789, 815-830, 860-870, 940-960, 970-990 and 994-1000+nm. This was evident in the coefficient function because the slope of β was significantly different from zero at each of these wavelengths.

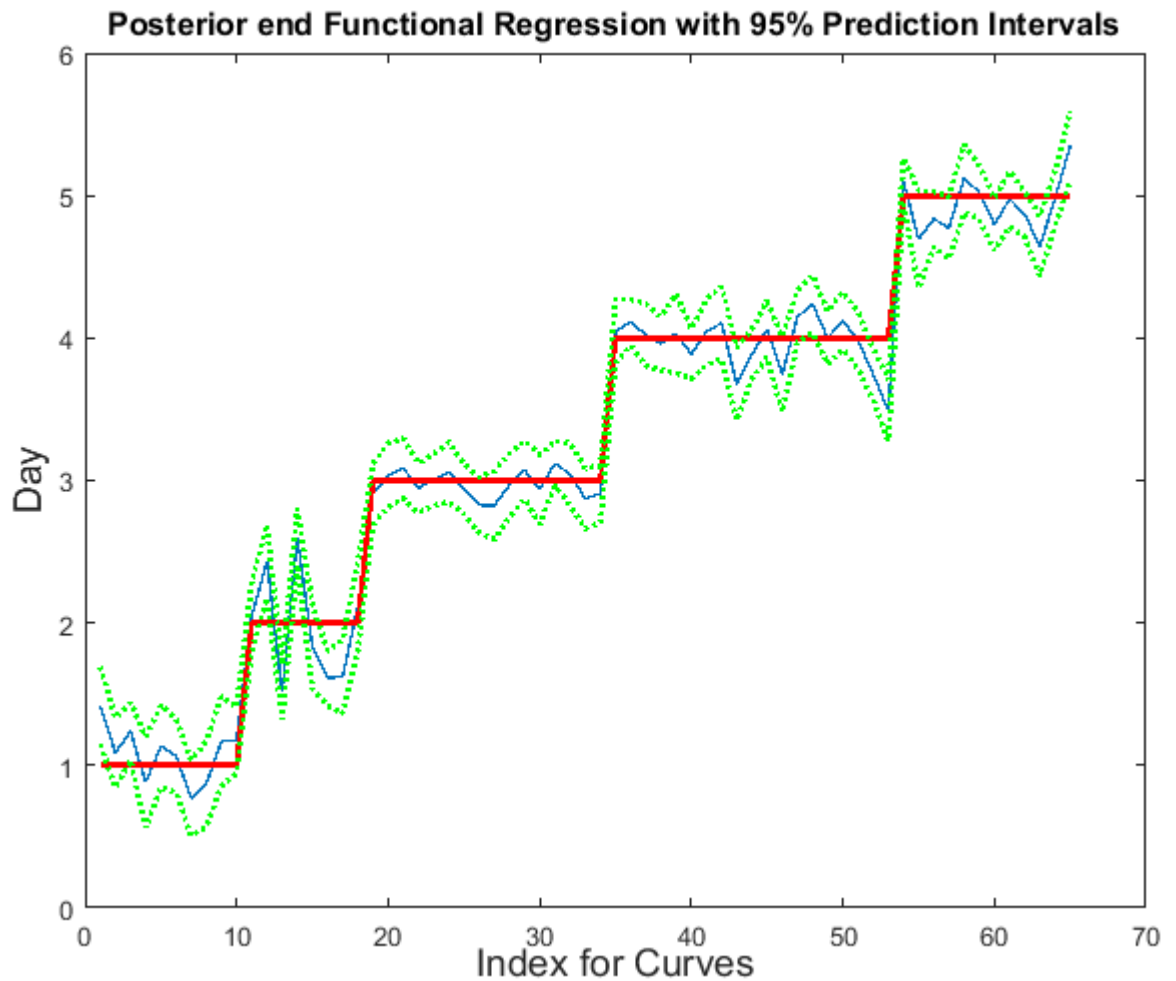


Figure 3-3 An examination of the functional regression model based on spectral reflectance measurements from the posterior end of 3rd instar (days 1 and 2), post feeding wandering larvae (days 3 and 4) and the first day of pupariation (day 5) for *Protophormia terraenovae*. The green dotted lines represent the pointwise 95% prediction intervals upper and lower limits of the predicted days (blue thin solid line) and the red thick solid line indicates the actual day.

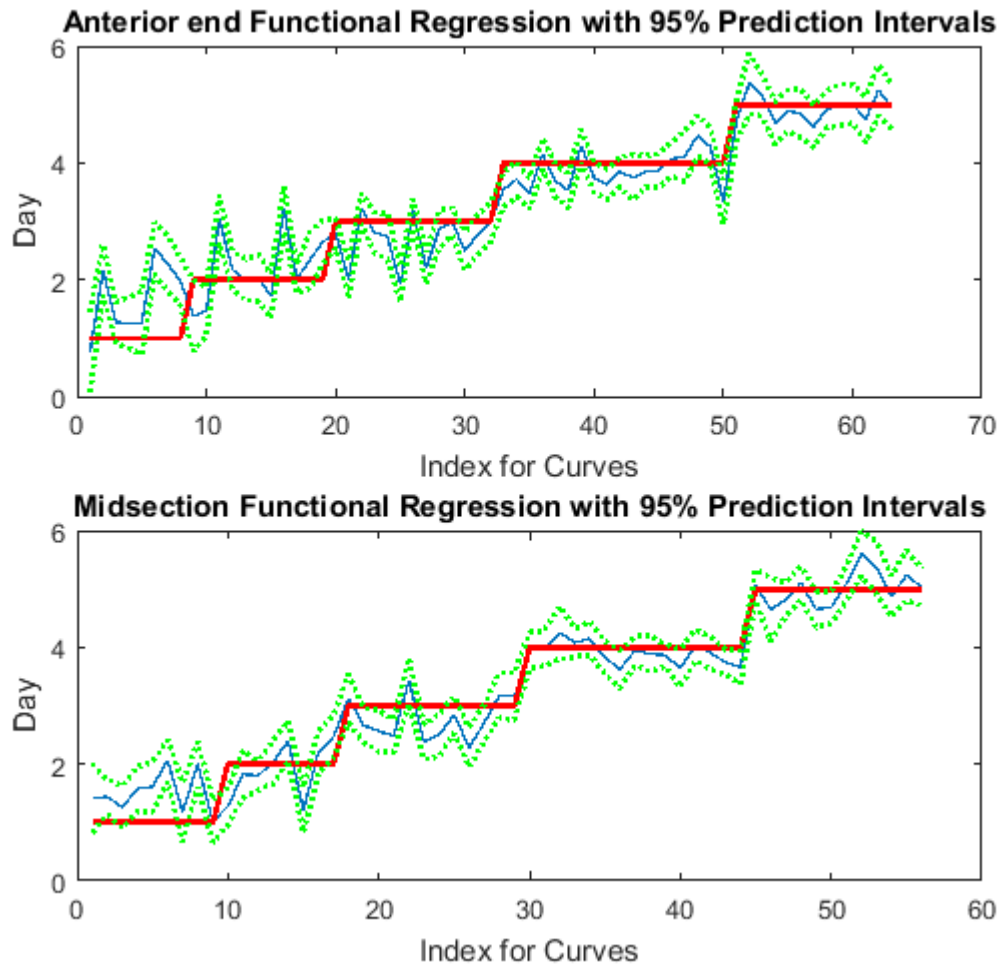


Figure 3-4 A functional regression analysis with 95% pointwise prediction intervals (dotted green) of the spectral measurements collected from the anterior end and midsection of *Protophormia terraenovae* third instar feeding (days 1 and 2) and post feeding larvae (days 3 and 4) indicate that the actual measurements (thin blue solid line) do not clearly differentiate all days (thick red solid line) when predicting days from 3rd instar to the first day of pupariation.

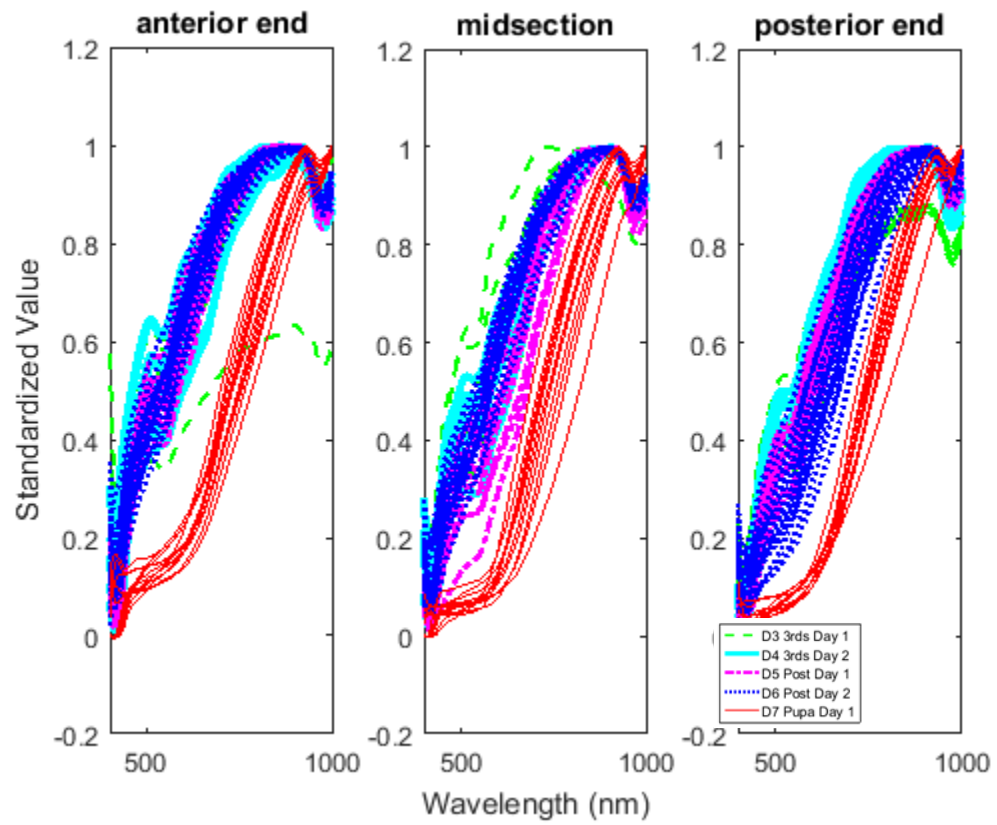


Figure 3-5 The grouped spectral measurements from the anterior end, midsection and posterior end of *Protophormia terraenovae* larvae. Measurements range from the first day of the third instar to the first day of pupariation.

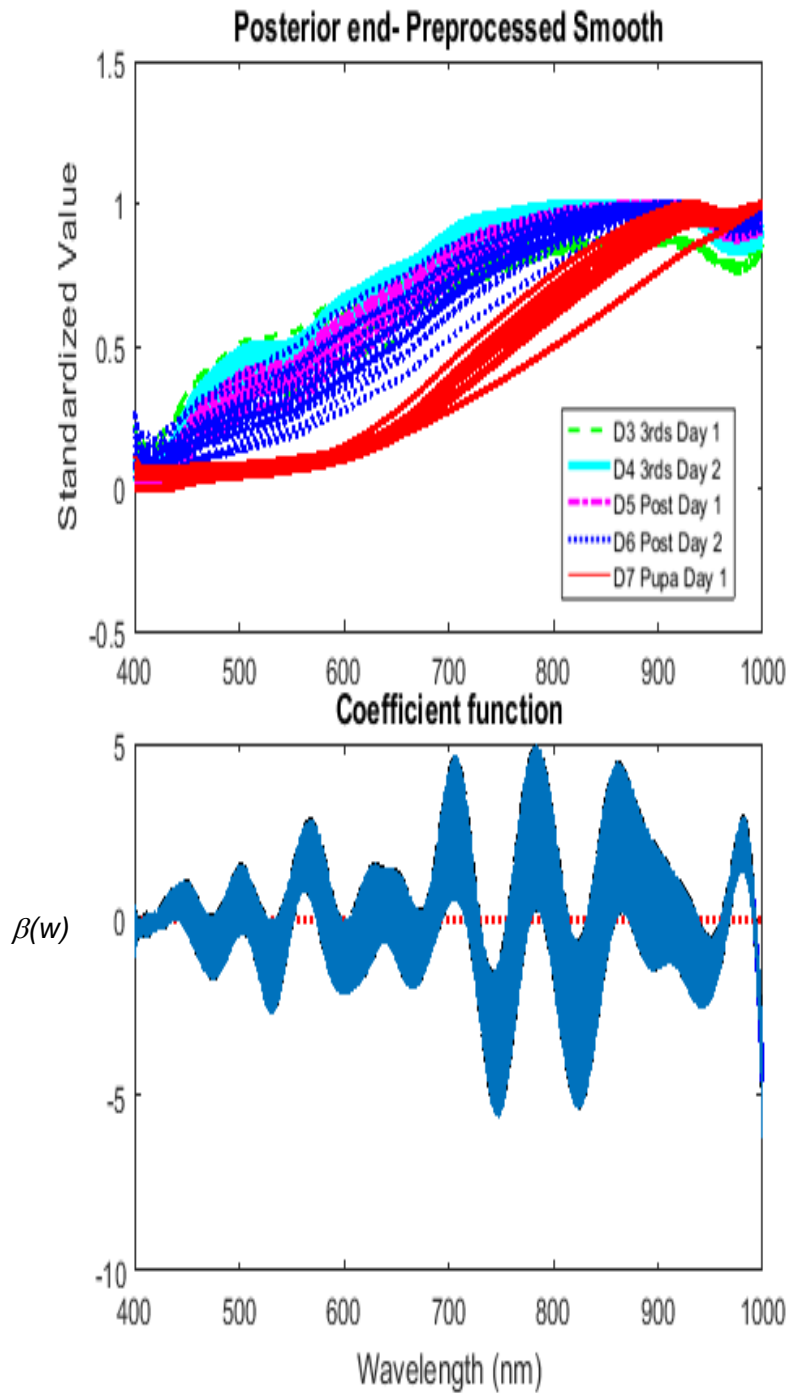


Figure 3-6 The 95% coefficient function indicates a significant difference between the daily spectral measurements at the contributing wavelengths where the red dotted zero line is visible using posterior end spectral measurements of *Protophormia terraenovae*. Daily measurements range from third instar to the first day of pupariation.

There was no significant difference identified between the days of development for *P. terraenovae* in the intra-puparial period at wavelengths ranging from 400 to 1000 nm, and so a predictive model should not be used based on these datasets to estimate the day within the intra-puparial period (Figure 3-7). The disarray of the smoothed pre-processed raw data support this (Figure 3-8). The last day of the intra-puparial period however was very clearly distinguished from the remaining days, and can be distinguished quite clearly in the preprocessed smoothed mean plots from each of the three measured regions (Figure 3-9). A model was created to distinguish the last day from the earlier days of the intra-puparial period (Figure 3-10). Class one included days one to five and class two included day six of the intra-puparial period. The β coefficients and the contributing wavelengths that distinguish between the two sets of days in the intra-puparial period are each presented in Figure 3-11 for each body region.

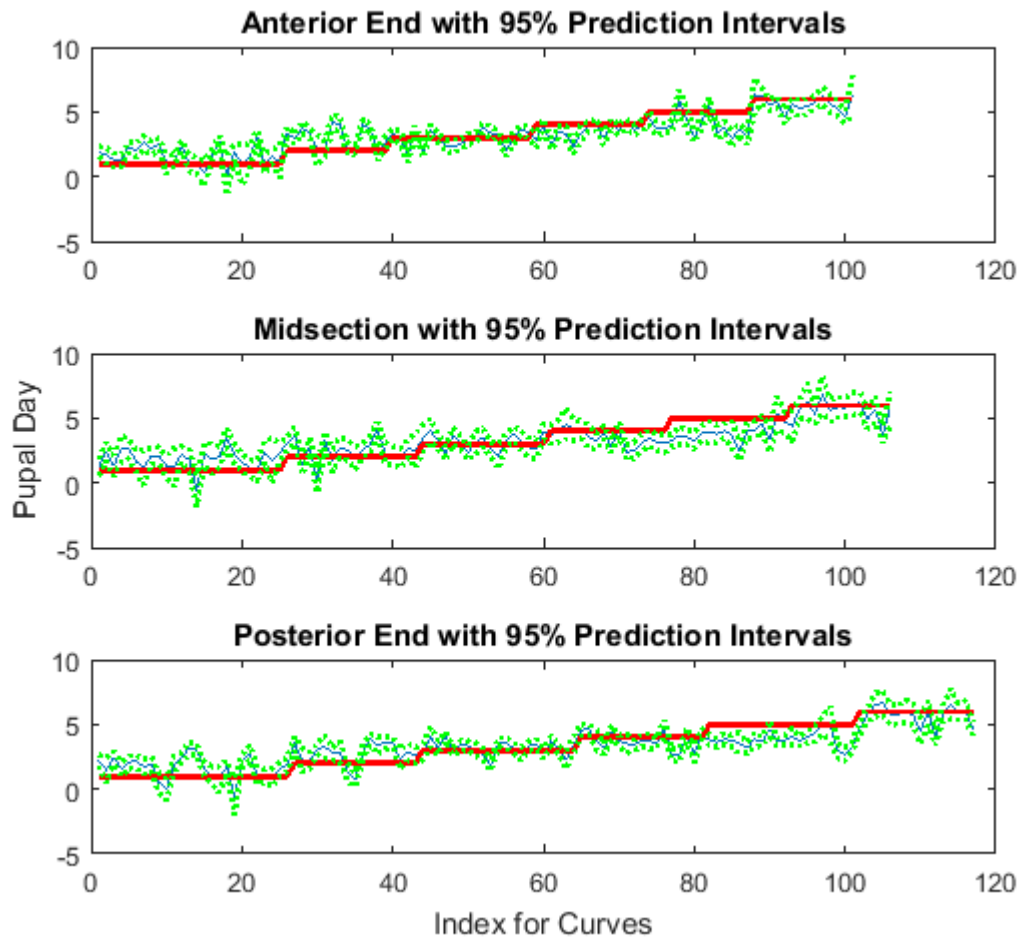


Figure 3-7 The functional regressions based on collected reflectance spectra (400-1000 nm) from each of anterior/midsection/posterior regions of *Protophormia terraenovae* puparia. The upper and lower 95% prediction intervals are presented in green. The blue line indicates the predicted day and the red line indicates the actual day (Pupal Day refers to the day of the intra-puparial period (Martin-Vega et al., 2016)).

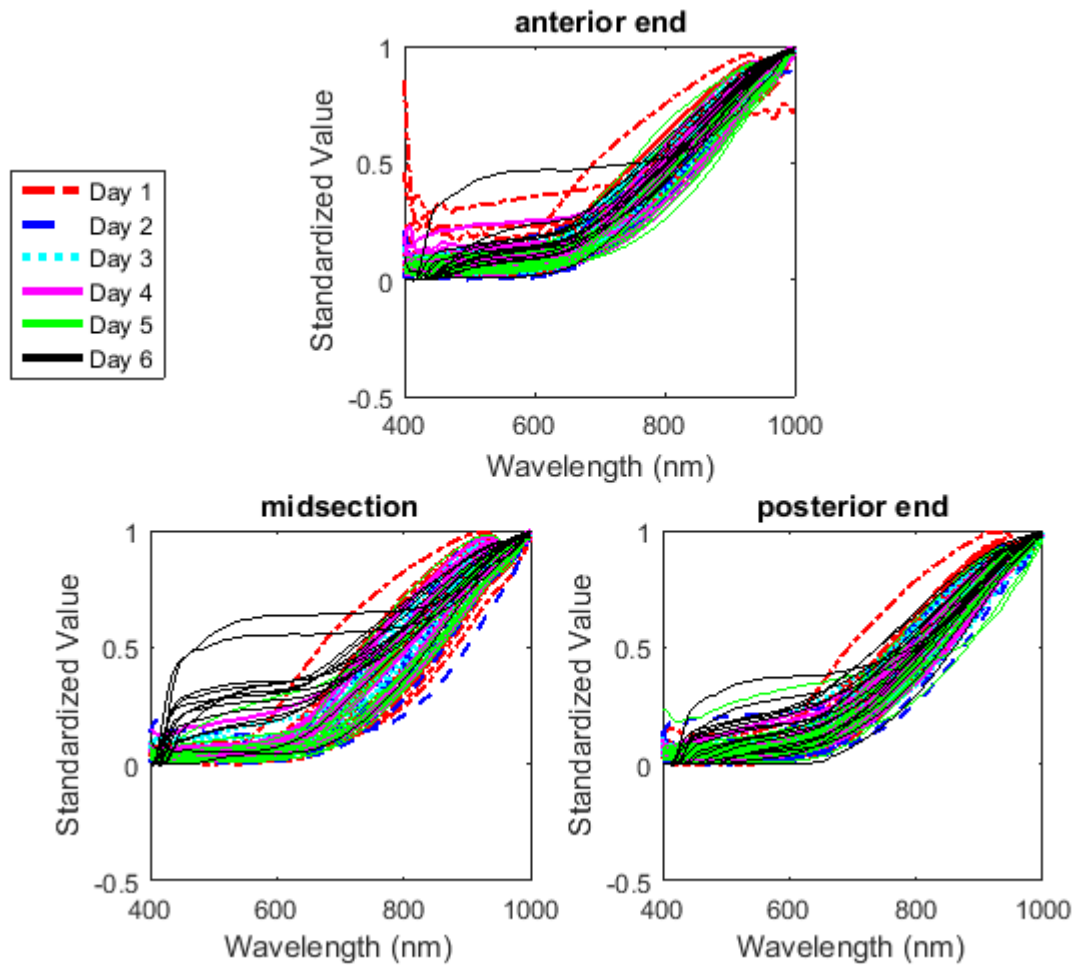


Figure 3-8 The visible spectrum of smoothed and preprocessed (standardized) plots of *Protophormia terraenovae* puparia spectral measurements from the anterior end, midsection and posterior end. The distinctly different black solid line plots represent the last day of the intra-puparial period and the indistinguishable remaining colours represent the earlier days of the intra-puparial period.

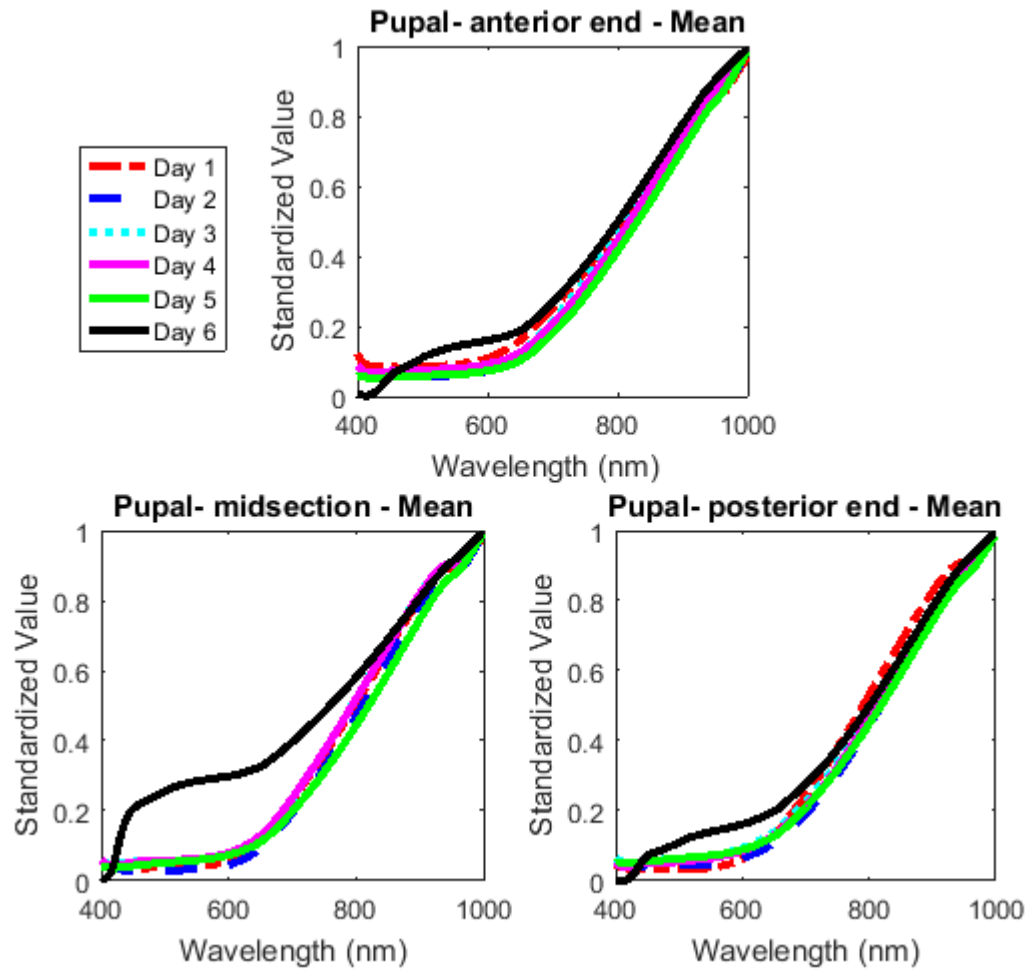


Figure 3-9 Mean standardized spectral reflectance plots of *Protophormia terraenovae* anterior end/midsection/posterior end puparia ranging from 400-1000 nm (Pupal in the figure is referring to puparium (Martin-Vega et al., 2016)).

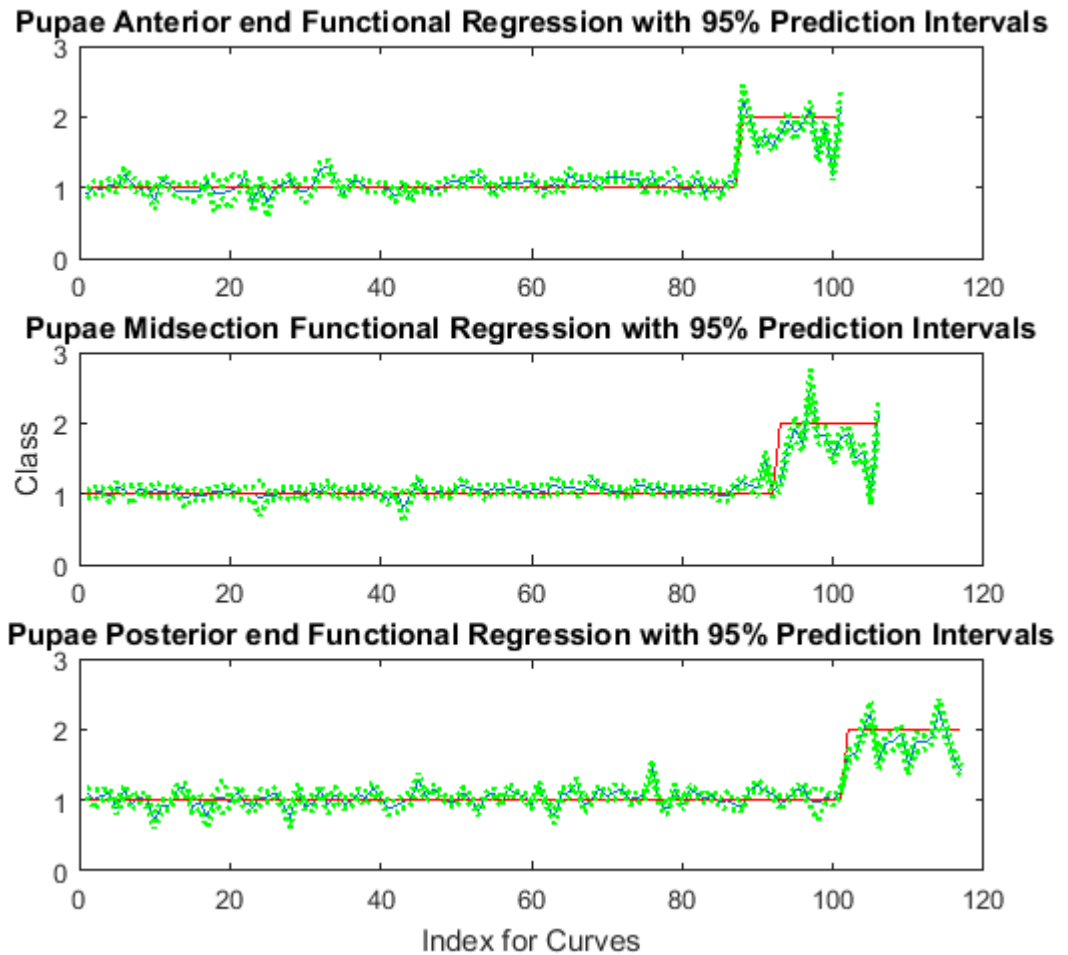


Figure 3-10 Functional regression model separates the last day (class 2) from the earlier five days of the intra-pupal period (class 1) of *Protophormia terraenovae* raised at a mean temperature of 24.6 °C based on the spectral measures from puparia (anterior end, midsection and posterior end). The dotted green lines represent the 95% prediction interval upper and lower limits of the predicted days in blue and the red line distinguishes the class of day (Pupae in the figure is referring to puparium (Martin-Vega et al., 2016)).

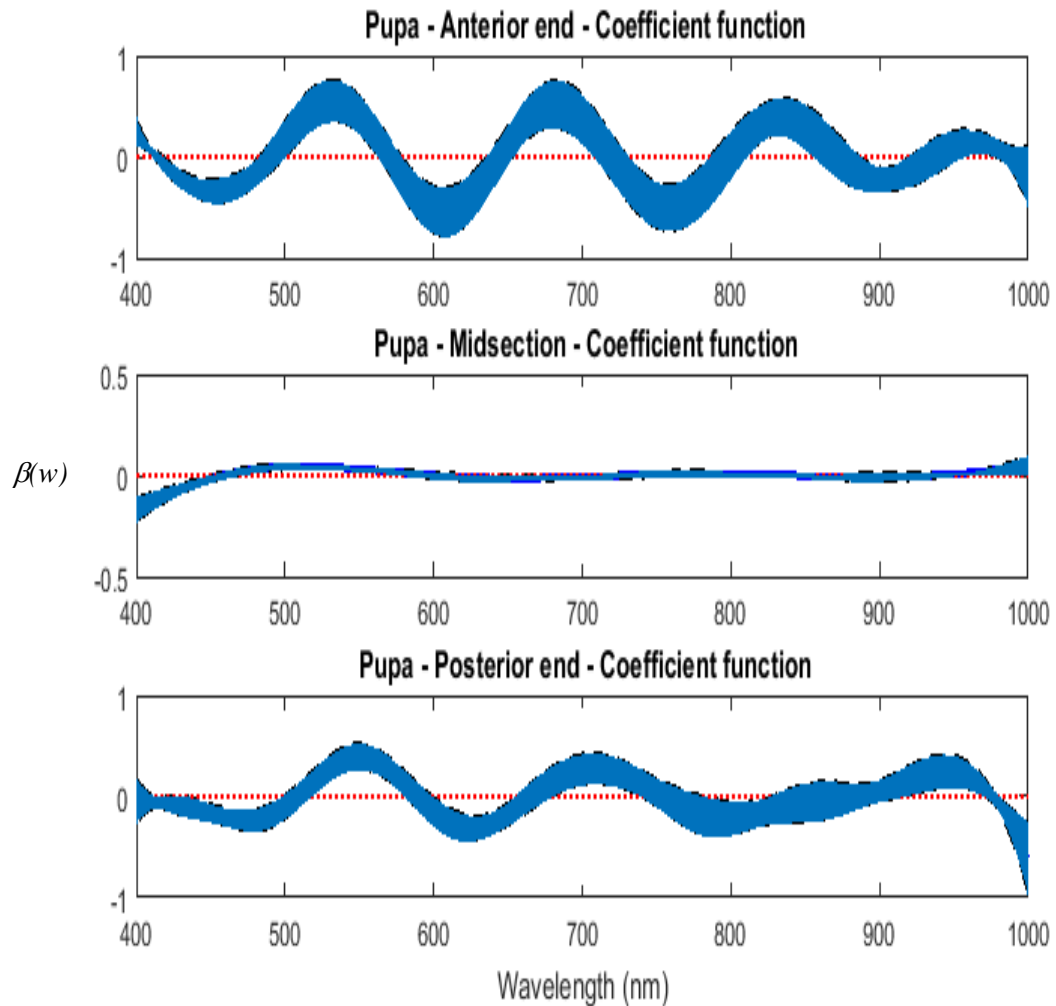


Figure 3-11 The 95% coefficient function plots of spectral measurements from days one to five of the intra-puparial period compared with day six of the last day of intra-puparial period of *Protophormia terraenovae* raised at a mean temperature of 24.6°C (Pupa in the figure is short for puparium (Martin-Vega et al., 2016)). They also indicate the contributing wavelengths (red dotted line) to the model from each of the spectral reflectance measured regions (anterior, midsection, and posterior).

The spectral measurements of the two days of second instar from the midsection of *P. terraenovae* raised at mean 24.6°C were compared with each other and there are several wavelengths which contribute to the influencing β coefficient (Figure 3-12). Although some areas of the prediction fall outside the interval, the functional regression with 95%

confidence interval indicates that it is still a good predictor of day between the two days of second instar (Figure 3-13).

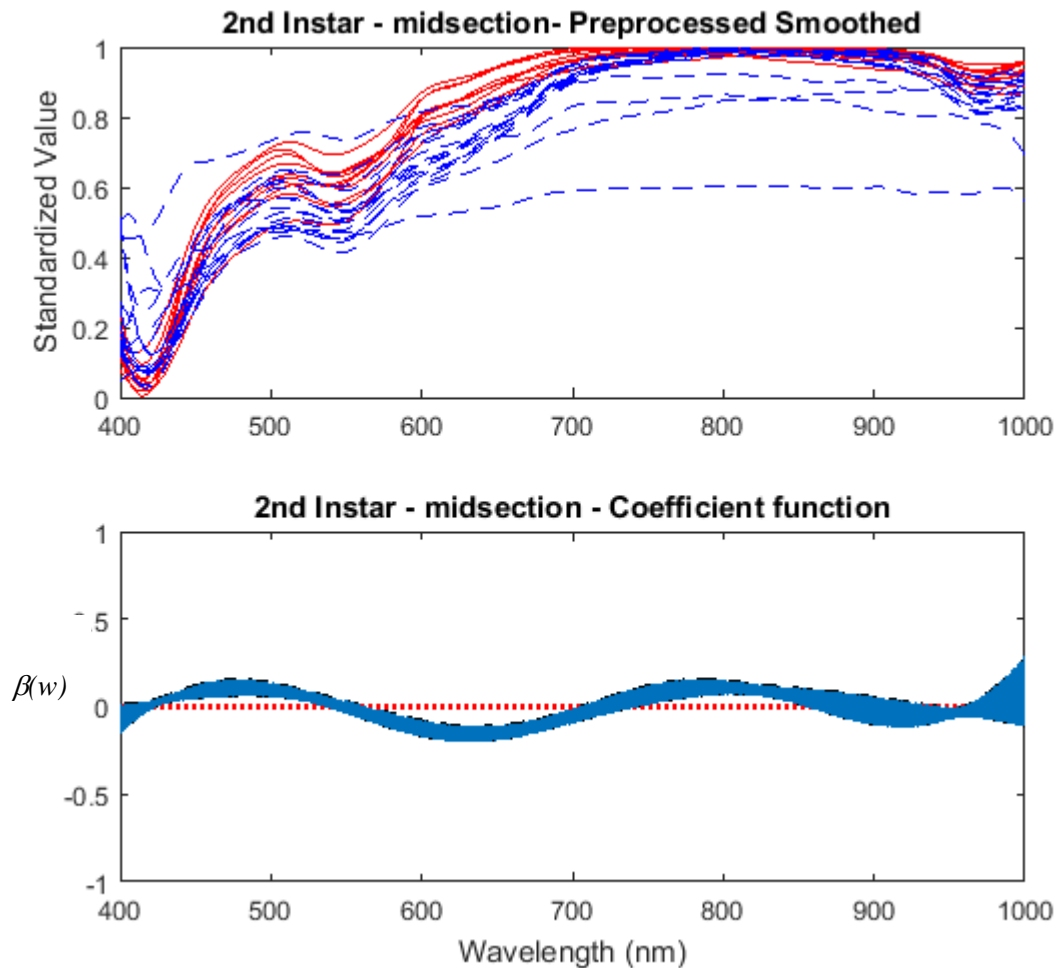


Figure 3-12 The standardized preprocessed smoothed spectral measurements of the midsection of second instar *Protophormia terraenovae* raised at a mean temperature of 24.6°C, along with the contributing wavelengths to the $\beta(w)$ coefficient (red dotted line in lower plot). Day 1 is represented by the red solid plots and Day 2 by the blue dashed plots. Each line represents a measurement from one larva. The approximate contributing wavelengths that help distinguish the days include: 400-540, 565-704, and 743-855 nm.

2nd Instar midsection- Functional Regression with 95% Prediction Intervals

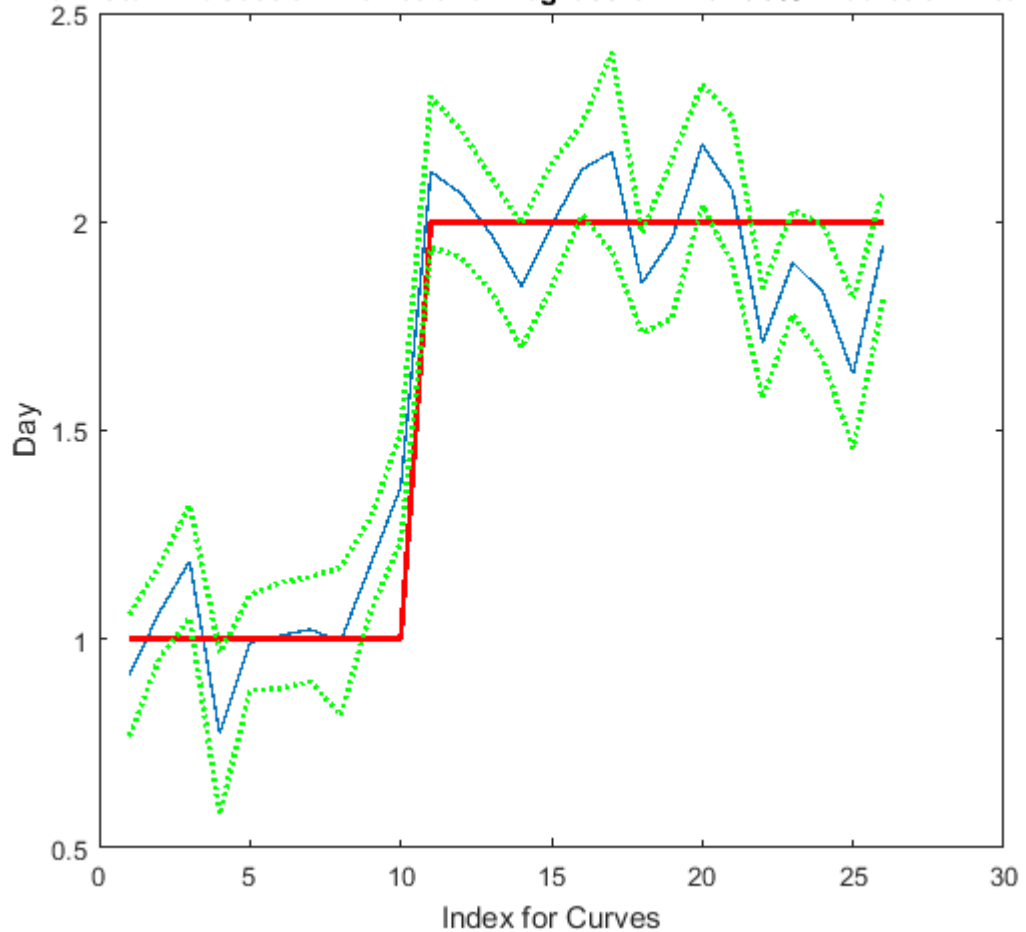


Figure 3-13 Functional regression model of predicted days (blue thin line) within second instar of *Protophormia terraenovae* raised at a mean temperature of 24.6°C based on spectral reflectance measurements. The green dotted lines represent the pointwise 95% prediction interval upper and lower limits and the red thick line was the actual day.

3.7 Discussion

The functional regression model has identified very clear day demarcations which are seen in the spectral signatures from posterior measurements of *P. terraenovae* larvae raised at a mean temperature of 24.6°C (ranging from 18.5-26.5°C). The daily mean plots of the smoothed preprocessed spectral measurements in Figure 3-2 show a loss of a trough that was clearly evident in second instar at ~550 nm and completely gone by the intra-

puparial period. This trough was probably due to water absorption from the cuticle and was no longer visible once the puparium had formed. A dramatic water loss occurs in the cuticle with the formation of the puparium (Zdarek & Fraenkel, 1972).

Clear differences are identified within 550-575 nm of the visible spectrum for third instar larvae including post feeding and are evident at all of the measured areas, the anterior/midsection/posterior regions of the larvae. From 570-585 nm, yellow is reflected and is bookmarked by reflections of green (490-570 nm) and orange (585- 620 nm). There are also contributing wavelengths in the near infrared region. The posterior region offers the best model for distinguishing between the days of development. This may be because cuticular hydrocarbons are contributing more to this region, or because the posterior spiracles are dynamic. The addition of waterproofing lipids modifies posterior spiracles even when a moult is not imminent (Makki, Cinnamon, & Gould, 2014). In addition to colour and surface texture, hydrocarbons are considered a top contributor to the spectral measurements of the insect surface particularly in the near infrared (NIR) and short wave infrared (SWIR) (Blomquist, 2010b). Cuticular hydrocarbons are produced by the **oenocytes** and the position of the oenocytes in the ectoderm are species (Fan, Zurek, Dykstra, & Schal, 2003; Makki et al., 2014; Martins & Ramalho-Ortigão, 2012) and development stage (Fan et al., 2003) dependent. The oenocytes develop in areas proximal to the spiracles (Makki et al., 2014) and if the oenocytes are located in the abdominal integument, as they are in, for example, the German cockroach (*Blatella germanicus* L.) (Fan et al., 2003), this may explain the stronger spectral signature prediction at the posterior end of the larvae. The cuticular hydrocarbons travel by **lipophorins** in the haemolymph to the rest of the cuticle and the fat body (Fan et al., 2003).

The day to day distinguishing separations of the larval stages were not seen in the intra-puparial period with any significance and so the model cannot be used to distinguish between days of *P. terraenovae* intra-puparial development at a mean temperature of 24.6°C from 400-1000 nm. The day to day demarcations may not have been distinguished during the intra-puparial period because changes to the cuticle are too slight to recognize at wavelengths 400-1000 nm. There are definite colour changes from the fat body

formation in the post feeding stage to the darkening of the cuticle over the span of the intra-puparial period. Additionally, it is probable that there are no cuticular hydrocarbons being delivered to the puparium following puparial formation since the cuticle of the puparium has lifted from the pupa following apolysis (Martin-Vega et al., 2016). In the larval stages there are continuous changes to the cuticular hydrocarbons. Throughout the larval stage, hydrocarbons are transported to the cuticle but there is no likely means in the intra-puparial period once apolysis has occurred and instead they are applied to the pupa or pharate adult (Blomquist, 2010b).

The last day of the intra-puparial period is distinguishable from the earlier days and this is most evident in the midsection. This was probably because a fully formed pharate adult blow fly has formed within the puparium. The adult fly was visible to the human eye through the puparium under the direct light source when measuring on the last day and so the spectrometer identified this and it was revealed in the measurements between 400 and 500 nm (Figure 3-9).

For the days within the intra-puparial period that were not distinguishable by spectral measurements, days of development potentially may be distinguished if experiments are conducted at a lower temperature to slow development and thereby extend it over more days, or at a higher temperature to shorten the development over fewer days, and make any daily changes more obvious. More probable, however, is that differences in the daily spectral signature may be identified in the short wave infrared (SWIR) region of the electromagnetic spectrum rather than just the visible (VIS) and near infrared (NIR) regions as were examined here (Warren, Ratnasekera, Campbell, & Anderson, 2017b).

Based on these data, it was also very possible to distinguish between days of the short second instar larval stage for *P. terraenovae*. This was probably due to the hydrocarbon changes that occur with insect moult forming cuticular changes that are readily distinguished between days of this short stage. The hydrocarbons being deposited to the cuticle following moult are probably very specific in such short stages. These daily predictions were completed using developing *P. terraenovae* at a mean temperature of

24.6°C and could potentially be applied to *P. terraenovae* raised at any other temperature if converted to accumulated degree days (ADD).

Many sciences have been explored to improve estimates of aging immature insects (Boehme et al., 2013; Butcher et al., 2013; Martin-Vega, Simonsen, & Hall, 2017; Martin-Vega, Simonsen, Wicklein, et al., 2017; Moore, 2013; Moore et al., 2013, 2014; Pechal, Moore, et al., 2014; Richards et al., 2012; Tarone & Foran, 2011; Tarone et al., 2007; Xu et al., 2014; Zajac et al., 2015; Zhu et al., 2007) but these methods are destructive to the specimens and involve costly equipment. One of the advantages of being a non-destructive and non-invasive method is that remote sensing can be applied to the insect specimens and then another ageing method can be performed if corroboration is needed or if the age estimation needs to be refined (particularly in the case of the intra-puparial period). The hyperspectral methods used here and those by Voss *et al* (Voss et al., 2016) are not destructive, and non-invasive. However, measuring each insect using the current methods is preferred due to rapid measuring since there is minimal preparation of the specimens and these methods can be completed with larvae as well as puparia. They can also easily be modified to perform in the field with the field spectrometer. In the near future, once the most discriminating wavelengths are identified, a reasonably inexpensive spectrometer specific to those wavelengths can be used by forensic entomology practitioners to age live immature blow flies in the field.

3.8 Conclusion

This research was completed to initiate an investigation into whether hyperspectral measurements can be used to identify changes within stages of development which can be used as a further reference for insect age estimation. The promising initial findings of this proof of concept research indicate that day of development within the lengthy third instar, including post feeding stage, of *P. terraenovae* can be distinguished from the other days within the stage extremely well from posterior spectral measurements. These spectral measurements range from 400-1000 nm. The day of development can then be used to

further infer a post mortem interval in death investigations. The intra-puparial period needs to be examined further into the SWIR region of the electromagnetic spectrum, beyond 1000 nm and potentially at different temperatures to see if it too can be delineated into days or groups to further classify the stage of *P. terraenovae*.

3.9 Acknowledgements

The authors would like to offer the sincerest gratitude to those who assisted in this research: Jennifer Mead, Julie De Gea, Lawrence Wong, Dr. Gail Chmura, ChiChi Lam, Mark Romer, Kate Trincsi, Jason Wong, Emilie Roy-Dufresne, Joseph Ariwi, and Dr. Barbara Winter with Simon Fraser University Museum of Archaeology and Ethnology for funding the research.

3.10 Reference List

- Beck, L. R., Lobitz, B. M., & Wood, B. L. (2000). Remote Sensing and Human Health: New sensors and new opportunities. *Emerging Infectious Diseases*, 6(3), 217-226.
- Blomquist, G. J. (2010). Structure and analysis of insect hydrocarbons. In G. J. Blomquist & A.-G. Bagnères (Eds.), *Insect Hydrocarbons Biology, Biochemistry and Chemical Ecology* (pp. 19-34). New York: Cambridge University Press.
- Boehme, P., Spahn, P., Amendt, J., & Zehner, R. (2013). Differential gene expression during metamorphosis: a promising approach for age estimation of forensically important *Calliphora vicina* pupae (Diptera: Calliphoridae). *International Journal of Legal Medicine*, 127, 243-249.
- Brown, H. E., Diuk-Wasser, M. A., Guan, Y., Caskey, S., & Fish, D. (2008). Comparison of three satellite sensors at three spatial scales to predict larval mosquito presence in connecticut wetlands. *Remote Sensing of Environment*, 112, 2301-2308.
- Butcher, J. B., Moore, H. E., Day, C. R., Adam, C. D., & Drijfhout, F. P. (2013). Artificial neural network analysis of hydrocarbon profiles for the ageing of *Lucilia sericata* for post mortem interval estimation. *Forensic Science International*, 232, 25-31.

- Campbell, J. B. (2007). *Introduction to Remote Sensing* (Fourth ed.). New York: The Guilford Press.
- Canada, N. R. (2001). Fundamentals of Remote sensing, A Canada Centre for Remote Sensing Remote Sensing Tutorial. Retrieved from http://ccrs.nrcan.gc.ca/resource/tutor/fundam/pdf/fundamentals_e.pdf
- Carroll, M. W., Glaser, J. A., Hellmich, R. L., Hunt, T. E., Sappington, T. W., Calvin, D., . . . Fridgen, J. (2008). Use of spectral vegetation indices derived from airborne hyperspectral imagery for detection of European corn borer infestation in Iowa corn plots. *Journal of Economic Entomology*, *101*(5), 1614-1623.
- Cracknell, A. P., & Hayes, L. (2007). *Introduction to remote sensing*. Boca Raton: CRC Press.
- Fan, Y., Zurek, L., Dykstra, M. J., & Schal, C. (2003). Hydrocarbon synthesis by enzymatically dissociated oenocytes of the abdominal integument of the German Cockroach, *Blattella germanica*. *Naturwissenschaften*, *90*, 121-126.
- Finell, N., & Järvilehto, M. (1983). Development of the compound eyes of the blow fly *Calliphora erythrocephala*: changes in morphology and function during metamorphosis. *Annales Zoologici Fennici*, *20*, 223-234.
- Foley, W. J., McIlwee, A., Lawler, I., Aragonés, L., Woolnough, A. P., & Berding, N. (1998). Ecological applications of near infrared reflectance spectroscopy - a tool for rapid, cost-effective prediction of the composition of plant and animal tissues and aspects of animal performance. *Oecologia*, *116*, 293-305.
- Frederickx, C., Dekeirsschieter, J., Brostaux, Y., Wathelet, J.-P., Verheggen, F. J., & Haubruge, E. (2012). Volatile organic compounds released by blowfly larvae and pupae: New perspectives in forensic entomology. *Forensic Science International*, *219*, 215-220.
- Fuller, T., Thomasson, H. A., Mulembakani, P. M., Johnston, S. C., Lloyd-Smith, J. O., Kivalu, N. K., . . . Rimoin, A. W. (2011). Using remote sensing to map the risk of human Monkeypox virus in the Congo Basin. *EcoHealth*, *8*, 14-25. doi:DOI: 10.1007/s10393-010-0355-5
- Hall, M. J. R., & Brandt, A. P. (2006a). Forensic entomology. *Science in School The European journal for science teachers*. Retrieved from www.scienceinschool.org

- Hall, M. J. R., & Brandt, A. P. (2006b, 26-29th April). *The use of thermal imaging to study the effect of larval masses on the development of blow fly larvae*. Paper presented at the Page 33 in Programs and Abstracts of European Association of Forensic Entomology, Bari, Italy.
- Hart, W. G., Ingle, S. J., Davis, M. R., Mangum, C., Higgins, A., & Boling, J. C. (1971, 2-4 March). *Some uses of infrared aerial color photography in entomology*. Paper presented at the Proceedings of the third Biennial workshop on Aerial Color in the Plant Sciences.
- Hendricks, D. E. (1980). Low frequency sodar device that counts flying insects attracted to sex pheremone dispensers. *Environmental Entomology*, 9, 452-457.
- Järvilehto, M., & Finell, N. (1983). Development of the function of visual receptor cells during the pupal life of the fly *Calliphora*. *Journal of Comparative Physiology*, 150, 529-536.
- Johnson, A. P., & Wallman, J. F. (2014). Infrared imaging as a non-invasive tool for documenting maggot mass temperatures. *Australian Journal of Forensic Science*, 46(1), 73-79.
- Lawrence, R., & Labus, M. (2003). Early detection of Douglas -fir beetle infestation with subcanopy resolution hyperspectral imagery. *Western Journal of Applied Forestry*, 18(3), 1-5.
- Makki, R., Cinnamon, E., & Gould, A. P. (2014). The development and functions of oenocytes. *Annual Review of entomology*, 59, 405-425. doi:10.1146/annurev-ento-011613-162056
- Martin-Vega, D., Hall, M. J. R., & Simonsen, T. J. (2016). Resolving confusion in the use of concepts and terminology in intrapuparial development studies of cyclorrhaphous diptera *Journal of Medical Entomology*, 53(6), 1249-1251. doi:doi:10.1093/jme/tjw081
- Martin-Vega, D., Simonsen, T. J., & Hall, M. J. R. (2017). Looking into the puparium: Micro-CT visualization of the internal morphological changes during metamorphosis of the blow fly, *Calliphora vicina*, with the first quantitative analysis of organ development in cyclorrhaphous dipterans. *Journal of Morphology*, 278, 629-651. doi:10.1002/jmor.20660
- Martin-Vega, D., Simonsen, T. J., Wicklein, M., & Hall, M. J. R. (2017). Age estimation during the blow fly intra-puparial period: a qualitative and quantitative approach using micro-computed tomography. *International Journal of Legal Medicine*. doi:10.1007/s00414-017-1598-2

- Martin, J. E. H. (1977). *The Insect and Arachnids of Canada. Part I. Collecting, preparing and preserving insects, mites and spiders*, Biosystematics Research Institute. Ottawa, Ontario, Research Branch, Canada Department of Agriculture.
- Martins, G. F., & Ramalho-Ortigão, J. M. (2012). Oenocytes in insects. *Invertebrate Survival Journal*, 9(2).
- Mirik, M., Ansley, R. J., Steddom, K., Rush, C. M., Michels, G. J., Workneh, F., . . . Elliott, N. C. (2014). High spectral and spatial resolution hyperspectral imagery for quantifying Russian wheat aphid infestation in wheat using the constrained energy minimization classifier. *Journal of Applied Remote Sensing*, 8, 083661-083661-083661-083614.
- Mirik, M., Michels jr., G. J., Kassymzhanova-Mirik, S., Elliot, N. C., & Bowling, R. (2006). Hyperspectral spectrometry as a means to differentiate uninfested and infested winter wheat by greenbug (Hemiptera: Aphididae). *Journal of Economic Entomology*, 99(5), 1682-1690.
- Mirik, M., Michels jr., G. J., Kassymzhanova-Mirik, S., Elliot, N. C., Catana, V., Jones, D. B., & Bowling, R. (2006). Using digital image analysis and spectral reflectance data to quantify damage by greenbug (Hemiptera: Aphididae) in winter wheat. *Computers and Electronics in Agriculture*, 51, 86-98.
- Moore, H. E. (2013). *Analysis of cuticular hydrocarbons in forensically important blowflies using mass spectrometry and its application in Post Mortem Interval estimations*. (Doctor of Philosophy), Keele University, Keele Staffordshire University.
- Moore, H. E., Adam, C. D., & Drijfhout, F. P. (2013). Potential Use of Hydrocarbons for Aging *Lucilia sericata* Blowfly Larvae to Establish the Postmortem Interval. *Journal of Forensic Science*, 58(2), 404-412.
- Moore, H. E., Adam, C. D., & Drijfhout, F. P. (2014). Identifying 1st instar larvae for three forensically important blowfly species using “fingerprint” cuticular hydrocarbon analysis. *Forensic Science International*, 240, 48-53.
- Moran, M. S., Inoue, Y., & Barnes, E. M. (1997). Opportunities and limitations for image-based remote sensing in precision crop management. *Remote Sensing Environment*, 61, 319-346.
- Nansen, C., Coelho Jr, A., Viera, J. M., & Parra, J. R. P. (2014). Reflectance-based identification of parasitized host eggs and adult *Trichogramma* specimens. *Journal of Experimental Biology*, 217, 1187-1192. doi:10.1242/jeb.095661

- Neigh, C. S. R., Bolton, D. K., Diabate, M., Williams, J. J., & Carvalhais, N. (2014). An Automated Approach to Map the History of Forest Disturbance from Insect Mortality and Harvest with Landsat Time-Series Data. *Remote Sensing*, 6, 2782-2808.
- Pechal, J. L., Moore, H. E., Drijfhout, F., & Benbow, M. E. (2014). Hydrocarbon profiles throughout adult Calliphoridae aging: A promising tool for forensic entomology. *Forensic Science International*, 245, 65-71.
- Pickering, C. L., Hands, J. R., Fullwood, L. M., Smith, J. A., & Baker, M. J. (2015). Rapid discrimination of maggots utilising ATR-FTIR spectroscopy. *Forensic Science International*, 249, 189-196.
- Ramsay, J. O., & Silverman, B. W. (2005). *Functional Data Analysis*. New York: Springer.
- Reynolds, D. R., & Riley, J. R. (2002). Remote-sensing, telemetric and computer-based technologies for investigating insect movement: A survey of existing and potential techniques. *Computers and Electronics in Agriculture*, 35, 271-307.
- Richards, C. S., Simonsen, T. J., Abel, R. L., Hall, M. J. R., Schwyn, D. A., & Wicklein, M. (2012). Virtual forensic entomology: Improving estimates of minimum post-mortem interval with 3D micro-computed tomography. *Forensic Science International*, 220, 251-264.
- Riley, J. R. (1989). Remote Sensing in Entomology. *Annual Review of entomology*, 34, 247-271.
- Rogers, D. J., & Randolph, S. E. (1991). Mortality rates and population density of tsetse flies correlated with satellite imagery. *Nature*, 351, 739-741.
- Ruiz-Moreno, D. (2016). Assessing Chikungunya risk in a metropolitan area of Argentina through satellite images and mathematical models. *BMC Infectious diseases*, 16(49), 1-12. doi:DOI 10.1186/s12879-016-1348-y
- Schowengerdt, R. A. (2007). *Remote Sensing Models and Methods for Image Processing*. London: Elsevier.
- Singh, C. B., Jayas, D. S., Paliwal, J., & White, N. D. G. (2009). Detection of insect-damaged wheat kernels using near-infrared hyperspectral imaging. *Journal of Stored Products Research*, 45, 151-158.
- Solberg, S., Eklundh, L., Gjertsen, A. K., Johansson, T., Joyce, S., Lange, H., . . . Solberg, A. (2007). Testing remote sensing techniques for monitoring large scale insect defoliation. *Remote Sensing of Environment*, 99(3), 295-303.

- Tarone, A. M., & Foran, D. R. (2011). Gene expression during blow fly development: Improving the precision of age estimates in forensic entomology. *Journal of Forensic Science*, 56(S1), S112-S122.
- Tarone, A. M., Jennings, K. C., & Foran, D. R. (2007). Aging blow fly eggs using gene expression: A feasibility study. *Journal of Forensic Science*, 52(6), 1350-1354.
- Voss, S. C., Magni, P., Dadour, I., & Nansen, C. (2016). Reflectance-based determination of age and species of blowfly puparia. *International Journal of Legal Medicine*. doi:doi:10.1007/s00414-016-1458-5
- Warren, J.-A., Ratnasekera, T. D. P., Campbell, D. A., & Anderson, G. S. (2017). Spectral Signature of Immature *Lucilia sericata* (Meigen) (Diptera: Calliphoridae). *Insects*, 8(2). doi:10.3390/insects8020034
- Warren, J. A., & Anderson, G. S. (2013). The development of *Protophormia terraenovae* (R-D) at constant temperatures and its minimum temperature threshold *Forensic Science International*, 233, 374-379.
- Westbrook, J. K., Eyster, R. S., & Wolf, W. W. (2014). WSR-88D doppler radar detection of corn earworm moth migration. *International Journal of Biometeorology*, 58, 931-940.
- Whitworth, T. L. (2006). Keys to the genera and species of blow flies (Diptera: Calliphoridae) of America north of Mexico. *Proceedings of the Entomological Society of Washington*, pp. 689-725.
- Williams, D. W., Bartels, D. W., Sawyer, A. J., & Mastro, V. (2004). *Application of hyperspectral imaging to survey for emerald ash borer* Paper presented at the Proceedings of XV U.S. Department of Agriculture Interagency Research Forum on Gypsy Moth and other invasive species Annapolis Maryland.
- Xing, J., Guyer, D., Ariana, D., & Lu, R. (2008). Determining optimal wavebands using genetic algorithm for detection of internal insect infestation in tart cherry. *Sensing and Instrumentation for food quality*, 2, 161-167.
- Xu, H., Ye, G.-Y., Xu, Y., Hu, C., & Zhu, G.-H. (2014). Age-dependent changes in cuticular hydrocarbons of larvae in *Aldrichina grahami* (Aldrich) (Diptera: Calliphoridae). *Forensic Science International*, 242, 236-241.
- Zajac, B. K., Amendt, J., Horres, R., Verhoff, M. A., & Zehner, R. (2015). De novo transcriptome analysis and highly sensitive digital gene expression profiling of *Calliphora vicina* (Diptera: Calliphoridae) pupae using MACE (Massive Analysis of cDNA Ends). *Forensic Science International: Genetics*, 15, 137-146.

Zdarek, J., & Fraenkel, G. (1972). The mechanism of puparium formation in flies. *Journal of Experimental Zoology*, 179, 315-324.

Zhu, G. H., Xu, X. H., Yu, X. J., Zhang, Y., & Wang, J. F. (2007). Puparial case hydrocarbons of *Chrysomya megacephala* as an indicator of the postmortem interval. *Forensic Science International*, 169, 1-5.

Chapter 4. Spectral Signature of Immature *Lucilia sericata* (Meigen) (Diptera: Calliphoridae)

WARREN J.-A., RATNASEKERA, T.D.P., CAMPBELL, D.A. and ANDERSON, G.S.

Originally published in *Insects Journal* as

Warren J.-A., Ratnasekera, T.D.P., Campbell, D.A. and Anderson, G.S. (2017). Spectral Signature of Immature *Lucilia sericata* (Meigen) (Diptera: Calliphoridae). *Insects* 8(2). doi:10.3390/insects8020034. (CC BY 4.0)

And appears with minor updates.

4.1 Preface

This chapter further refines the methods of Chapter 3. A greater wavelength range (350-2500 nm) is introduced via an ASD LabSpec 4 Spectrometer, and as the insects were not washed before sampling in the previous chapter, a comparison is made between washing with deionized water and not washing. This research was carried out on a different blow fly colony, *Lucilia sericata*, as time had passed between the research in Chapter 3 and 4 and the risk of genetic bottlenecking would have been too great to continue to use the older *P. terraenovae* colony.

Several questions were considered to refine the work: Will examining the insects over more wavebands (350-2500 nm) improve the estimation of day within stadia? Is it necessary to wash the specimens before measuring, particularly the larval stages when the insects are moving through the food source? Are there species differences/similarities in spectral signatures?

4.2 Abstract

Hyperspectral remote sensing is an innovative technology with applications in many sciences and is a non-destructive method that may offer more precise aging within development stages. Hyperspectral reflectance measurements from the anterior, midsection, and posterior of *Lucilia sericata* (Meigen) larvae and pupae were conducted daily from samples of the developing insects beginning at second instar. Only midsection measurements were conducted on second instar larvae due to their size, to ensure that the measurement was not of reflective surroundings. Once measured, all insects were washed with deionized water, blotted with filter paper, and re-measured. Daily age prediction during the post-feeding stage was not impacted by the unwashed insect measurements and was best predicted based on posterior measurements. The second and third instar larvae, which move about their food source, had different contributing coefficients to the functional regression model for the hyperspectral measurements of the washed compared with unwashed specimens. Although washing did not affect the daily prediction within these stages, it is still encouraged in order to decrease the effect of food source on spectral reflectance. Days within the intra-puparial period were best predicted based on anterior measurements and were not well distinguished from one another in the first few days based on midsection and posterior measurements.

Keywords: *Lucilia sericata*; hyperspectral; remote sensing; reflectance; wavelength; functional regression; coefficient

4.3 Introduction

Hyperspectral remote sensing is an innovative geographic technique that applies the science of the electromagnetic spectrum, and has been used in many other sciences including many of the forensic sciences. Remote sensors measure reflectance, transmittance, emittance and absorbance from a target surface (Nansen, Ribeiro, Dadour, & Roberts, 2015). Hyperspectral remote sensing is not invasive, is non-destructive to the

sample and can be used to identify surface features to light penetrable depths and express them as spectral signatures (Nansen et al., 2015; B. C. Wilson & Jacques, 1990).

Hyperspectral remote sensing has been used in entomology to monitor insect damaged crops and the crop damaging species themselves (Carroll et al., 2008; Hart et al., 1971; Lawrence & Labus, 2003; Mirik et al., 2014; Mirik, Michels jr., Kassymzhanova-Mirik, Elliot, & Bowling, 2006; Mirik, Michels jr., Kassymzhanova-Mirik, Elliot, Catana, et al., 2006; Moran et al., 1997; Riley, 1989; Singh et al., 2009; Solberg et al., 2007; Williams et al., 2004; Xing et al., 2008), as well as to monitor insect vectors carrying diseases (L. R. Beck et al., 2000; H. E. Brown et al., 2008). Besides monitoring entire population clusters, the non-invasive methods have been implemented in examining stress responses in single adult beetles exposed to killing agents (Nansen et al., 2015) and used on insect eggs to identify if they have been parasitized by *Trichogramma* wasps (Nansen et al., 2014).

Forensic entomologists provide minimum post-mortem intervals ($_{\min}$ PMI) based on the stage reached by the oldest insects developing on the remains. Forensic entomologists provide accurate minimum estimates of insect age but seek more precision in these estimates (Tarone & Foran, 2011).

Although a well-established science, forensic entomology, particularly the assessment of blow fly immature development, does have one major shortcoming and that is estimating time within stadia. Current means provide the estimated time it takes to reach a stage from the time of colonization and offer that to death investigators as an estimated $_{\min}$ PMI (Catts & Goff, 1992). This estimation is far from wrong, but is an underestimate and this is compounded in longer duration stadia. Ideally precision would be improved if forensic entomologists could provide a minimum estimate within the stage itself. Development demarcations within stages, particularly the latter stages, could condense the minimum estimate of tenure on the remains and hence provide more precision to the post-mortem interval (Tarone & Foran, 2008).

There have been many efforts to solve this problem. Several methods of aging immature Calliphoridae are currently being applied by forensic entomologists but these

methods can be complicated by several limitations. As already stated, the most conservative method is to examine the stage reached and to provide an estimated age based on the length of time required to reach that stage. The estimated time to reach each stage is based on development data collected from a similar geographic area and temperature. The greatest limitation with this method is that a minPMI is provided based on the time required to reach the beginning of the stage for the oldest species at that temperature. Unfortunately, the latter stages of the life cycle can be quite lengthy and so the estimated minPMI is a cautious estimate and lacks precision.

Similarly, another common method is to apply the thermal summation required to reach each of these stages. This is done by examining the required accumulated degree days or hours (ADD/H) and applying this to the stage of the oldest insects on the remains. This method, too, provides an estimate to reach each stage and suffers the same limitation during lengthy stages. A second limitation is that this method is best used only when the ADD/H used to estimate the minPMI were generated at a nearby temperature (Anderson, 2000; Reibe et al., 2010).

Measurements of weight, length and width of developing larvae are being used to estimate the minPMI (Amendt et al., 2004; Day & Wallman, 2006b; Wells & Lamotte, 2010). The drawback to these methods is that carrion is an ephemeral food source and if the food source becomes depleted the larvae will be smaller in size compared with those that have a surplus food source and, therefore, may appear younger than they actually are (Anderson, 2000).

Volatile organic compounds and cuticular hydrocarbons are being examined by gas chromatography and mass spectrometry (GC/MS) to age immature Calliphoridae and are showing some considerable promise (Butcher et al., 2013; Frederickx et al., 2012; Moore, 2013; Moore et al., 2013, 2014; Pechal, Moore, et al., 2014; Xu et al., 2014; Zhu et al., 2007). Shortcomings do, however, arise with aging by changes in cuticular hydrocarbons and volatile organic compounds recovered from the headspace. These methods are destructive to the sample of insects and are not rapid.

Gene expression has been introduced as a viable means to age blow fly eggs, larvae and pupae (Tarone & Foran, 2011; Tarone et al., 2007). The gene transcript levels are examined and can be used as demarcations within stages to offer a more precise timeline. The analysed sample is destroyed in a lengthy process and requires a trained molecular biologist and extensive equipment to carry out the gene sequencing.

Within the intra-puparial period, there are well noted morphological changes that can be used to further demarcate the stage and provide more precision when estimating insect age during metamorphosis (K. Brown et al., 2015; Davies & Harvey, 2013; Defilippo et al., 2013). These methods are very valuable but time consuming and destructive to the insect sample. 3D micro-computed tomography has been used to assist in viewing the changes to the developing pupae and pharate adults during metamorphosis (Richards et al., 2012). However, CT technology is costly and although not normally invasive except for the X-ray exposure to the sample, in this research the sample preparation was damaging.

Caveats such as larval aggregate formation increasing development temperature, inaccurate lower temperature thresholds applied to calculate the ADD/Hs, geographical developmental differences and fluctuating temperatures changing rate of development already exist in estimating the age of immature Calliphoridae (Tarone et al., 2011; Warren, 2006; Warren & Anderson, 2013b). Hence, if further limitations in the methods used to estimate age can be reduced then compounded errors can be avoided. Remote sensing is a promising science with few shortcomings and is being utilized in many sciences. Remote sensing is well known for being neither invasive nor damaging and can considerably improve precision of most techniques.

Very recently, hyperspectral remote sensing has shown beneficial impact on forensic entomology by rapidly discriminating blow fly species at the larval stage (Pickering et al., 2015). Also, first attempts at navigating hyperspectral measurements to further age within stadia were made using *Protophormia terraenovae* (Robineau-Desvoidy) and have shown tremendous promise with aging the larval stages. Conservative pointwise prediction intervals were presented with the in stadia aging (Warren, Ratnasekera, Campbell, & Anderson, 2017a). Also, pushbroom hyperspectral imaging to

age *Calliphora dubia* Macquart and *Chrysomya rufifacies* Macquart puparia measured dorsally and ventrally has now also been completed to refine the puparial stage based on development of adult morphological characteristics (Voss et al., 2016).

Since much of the immature stages of necrophagous blow flies is spent moving on the food substrate, food contaminants may cover the surface which can pose an issue with measuring reflectance because reflectance measurements may not be of the developing larvae but instead of the decomposing tissue.

The objectives of this research were to examine hyperspectral point source measurements of developing *Lucilia sericata* (Meigen) at wavelengths that extend from 350-2500 nm, to identify the optimal location on the insect for applying hyperspectral measurements, and to compare measurements from washed specimens to the same unwashed specimens.

4.4 Materials and Methods

Insect Rearing

Lucilia sericata colonies were established with blow flies provided by the Simon Fraser University Department of Biological Sciences Insectary. These recent colonies originated from wild caught flies collected from Burnaby, Langley, and Vancouver British Columbia. The blow flies were trapped using dimethyl trisulfide lures in combination with dead rats. The *L. sericata* species were confirmed using Whitworth's key (Whitworth, 2006) and were separated into two colonies. These colonies were maintained at room temperature (23-25°C) in the Centre for Forensic Research's Forensic Entomology Laboratory at Simon Fraser University. These adult colonies were maintained in 75 cm³ cages and raised on milk powder, sugar cubes and water *ad libitum*. Beef liver was added to the cages frequently to encourage reproductive development and to maintain the colony.

Experimental Protocol

Beef liver was used as the oviposition medium and was placed inside black film canisters positioned on their sides in each colony (Byrd, 2016). To ensure that enough eggs

were collected for the experiment, eggs were collected two hours after placing the canisters into the cages. The eggs from the two colonies were divided amongst four “treatments” so that each treatment received an estimated 240 combined number of eggs from both colonies. Each treatment consisted of a one gallon/four litre wide mouthed glass jar of moistened sawdust (~5cm deep) and on top of that was placed ~250g of freshly thawed beef liver as the larval rearing medium, positioned on a folded industrial paper towel to soak up any excess fluids. The jars were secured with two pieces of paper towel and fastened by elastic bands to prevent escape.

The treatments were maintained in a Conviron[®] E/7 (Controlled Environments Ltd., Winnipeg, MB, Canada) environmental chamber set for 75% relative humidity and a 14:10(L:D) photoperiod. The chamber maintained a constant mean temperature of 23.9°C and the jars were rotated daily within the chamber to account for any temperature differences. Temperature was recorded by Smartbutton[®] data loggers (ACR Systems Inc., Surrey, BC, Canada) and confirmed daily with Fisherbrand[™] thermometers (Thermo Fisher Scientific, Ottawa, ON, Canada).

Once the insects reached second stadium, each treatment was removed once daily, beginning at approximately noon, from the chamber for measuring with an ASD (Analytical Spectral Devices[™], Boulder CO, USA) LabSpec 4 Spectrometer. The stage of development was noted daily based on the number of spiracular slits and crop size, (Smith, 1986) and spectral measurements of 10 insects from each of the four treatments were completed daily until adult emergence. Those same larvae/pupae were measured again after washing with deionized water and filter paper and then blotting dry with filter paper in order to ensure that the measurements taken were of the insect and not from the feeding media on the insect surface. In order to keep the insects alive and not to affect reflectance measures, this is modified slightly from the suggested washing techniques of deionized water (tap water)/filter paper/freezing (Kharbouche et al., 2008) (Sadler, Fuke, Court, & Pounder, 1995), deionized water/ 0.9% NaCl solution (Gosselin et al., 2011; Kharbouche et al., 2008) and distilled water/methanol (Bourel et al., 2001; Gosselin et al., 2011). Excess water was removed with dry filter paper from the insect surface because water

exhibits specular reflections and could be misleading to the spectral signature (Fleming, Torralba, & Adelson, 2004).

All reflectance measurements were performed in a blackened laboratory. The light source used was an ASD lower intensity Welch Allyn plant probe bulb (lux = 968 at 0.9 mm and 4.25 v but used at a distance of 8.5 cm and a reduced voltage of 3.825 v) in a contact probe. Negligible extraneous light did enter the room from the computer screen which was turned away from the measuring area and from under the door; this was consistent in all measurements. The walls were draped with black fabric and the insect platform on which the measurements were carried out was painted flat black (General Paint fast drying spray enamel) as was all the equipment including petri dishes and forceps (Figure 4-1, & 4-2). This was done to ensure that measurements were strictly of the insect and not of any reflecting surrounding surfaces and was verified with the spectrometer. For each measurement taken, the reflectance was recorded from wavelengths ranging from 350-2500 nm. All measurements were equidistant (8.5 cm) from the 90 degree light source and taken at approximately a 30 degree angle from the insect platform. There was more saturated light within the central 3cm diameter of the field of light and so that was where the measurements were consistently taken. The light source was originally tested at a height of 5.5 cm above the insects but the larvae were dying under the light following washing so the height was extended to 8.5 cm to avoid this.

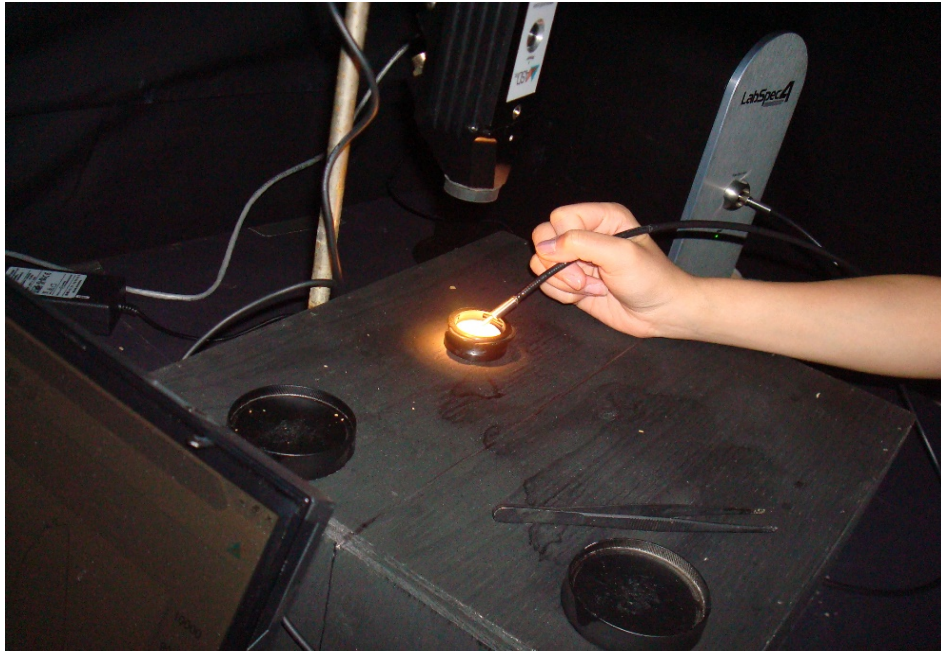


Figure 4-1 Spectrometer set up in the blackened laboratory and calibration using a Spectralon panel.

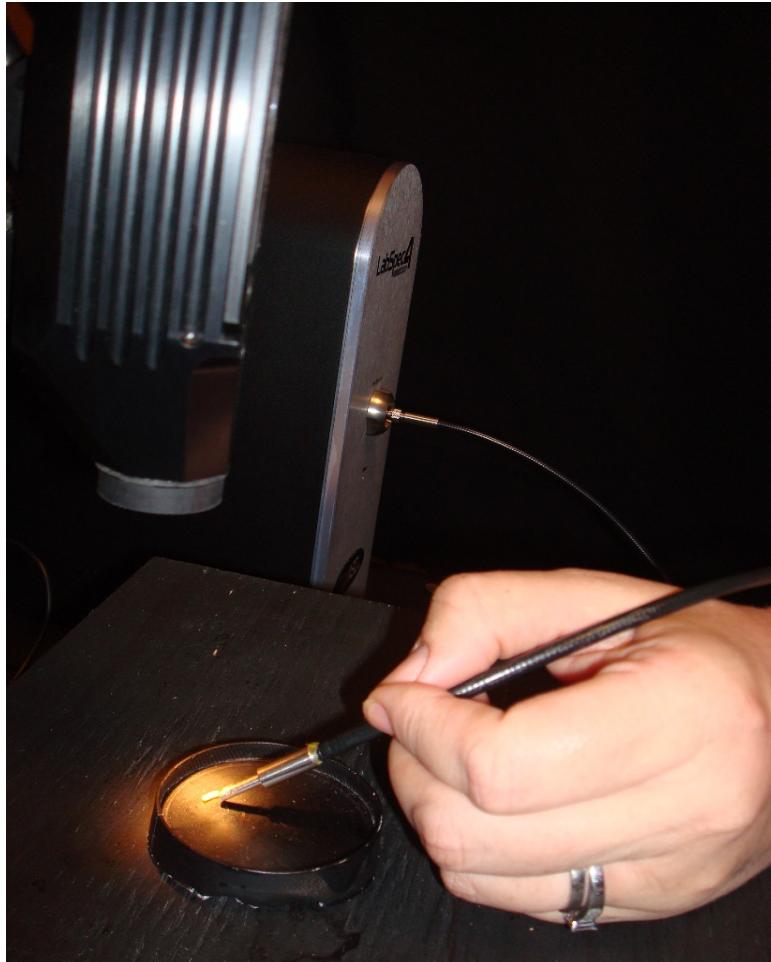


Figure 4-2 Demonstration of measuring reflectance from an insect with the Analytical Spectral Devices (ASD) Labspec 4 Spectrometer.

Three point measurements were taken from each unwashed and then washed insect, from the anterior, middle and posterior regions of the insect. Before insect measurements were taken, and following every five to seven measurements, calibration with a pure diffuse reflectance standard was completed to provide a baseline. In this case, a Spectralon™ panel was used to calibrate the spectrometer (Figure 4-1). Optimization of the spectrometer is necessary to accommodate the integration time and counterbalance the short wave infrared. During the process of optimization, a black reference was also completed.

These data were stored as files specific to the RS³™ software (Analytical Spectral Devices, Boulder, CO, USA) and so Viewspec pro™ (Analytical Spectral Devices, Boulder, CO, USA) was used to convert them to usable text files. These text files were then

organized into a Microsoft Office™ Excel (Microsoft, Redmond, WA, USA) template to organize them by day and body region before transferring them into Matlab (Mathworks™, Natick, MA, USA) for statistical analysis along with fdaM (functional data analysis Matlab) tools (<http://www.psych.mcgill.ca/misc/fda/downloads/FDAfuns/>).

Pre-processing

The original data had a particular artefact. Specifically, reflectance curves tended to be very smooth with the exception of a few abrupt vertical shifts. These vertical shifts were not unique to each individual insect but were unique to a given day of measuring. For a set of reflectance curves $X(w)$, over wavelength, w , the first differences: $X(w+1) - X(w)$, were scanned and the wavelength with the largest maximum absolute difference over all individuals was flagged as a jump point or vertical shift. At the jump point, all individuals were processed based on the amount of their individual shift such that:

$$X(w+1: \text{end}) = X(w+1: \text{end}) - (X(w+1) - X(w)) \quad (1)$$

In general, two such jump points were present in the data from each measurement. These jump points were not in any particular direction and consisted of different amplitudes for different individuals. It is probable that there may have been a crimp in the PVC (a synthetic polymer of poly vinyl chloride) fiber optic cable that went unnoticed while measuring, which caused the jump point.

The reflectance levels were internally calibrated for each reflectance curve for each measured insect. In order to calibrate the baseline measurement, the reflectance curves were first smoothed and then the smooth curves were vertically shifted so that they take an average value of 0 reflectance over the wavelength interval (400, 550 nm). The curves were then rescaled by setting the maximum value of reflectance to 1.

Functional Linear Model to Estimate Day of Development

Smoothing individual reflectance measurements

Individual reflectance functions were smoothed using 6th order B-Spline basis functions, $\Phi(w)$, with 100 evenly spaced knots (Ramsay & Silverman, 2005). The coefficients, $C=[C_1, \dots, C_J]$ were acquired in order to approximate the reflectance functions

$X(w)$ for the basis expansion: $X(w) \approx X_{smooth}(w) = \sum_{j=1}^J C_j \Phi_j(w)$ (Ramsay & Silverman, 2005). A curvature penalty was generated to avoid bias from over-fitting the functions (Ramsay & Silverman, 2005):

$$PEN_x = \int_{350}^{2500} \left(\frac{d^2}{dw^2} X_{smooth}(w) \right)^2 dw. \quad (2)$$

For all days at each body region, (anterior, mid-section, and posterior) a tuning parameter λ was applied (Ramsay & Silverman, 2005):

$$\underset{C}{\operatorname{argmin}} \left[\sum_{350}^{2500} (X_{smooth}(w) - X(w))^2 + \lambda \int_{350}^{2500} \left(\frac{d^3}{dw^3} X_{smooth}(w) \right)^2 dw \right], \quad (3)$$

where $\underset{C}{\operatorname{argmin}}$ is argument of the minimum coefficient. Generalized Cross Validation was used to tune λ uniquely for each body region to avoid overfitting while reducing the noise found within the original spectra (Ramsay & Silverman, 2005).

Functional Linear model with Scalar Response

The multivariate functional linear model (similar to (Warren et al., 2017a)):

$$Y_i = \int_{350}^{2500} X_{i,smooth}(w) \beta(w) dw \quad (4)$$

estimates the functional covariate $\beta(w)$ which best predicts the age of insect (Y_i) for each body region. In this case a third order derivative penalty, PEN_β was used to penalize the function (Ramsay & Silverman, 2005)

$$PEN_\beta = \int_{350}^{2500} \left(\frac{d^2}{dw^2} \beta(w) \right)^2 dw, \quad (5)$$

with its own smoothing parameter, λ_β to prevent overfitting the regression model for the data. Leave-one-out cross validation was used to estimate λ_β (Ramsay & Silverman, 2005).

The Sum of Squares Cross Validation for the fixed value of λ_β :

$$\sum_i (\hat{Y}_i - Y_i)^2 = \sum_i \left(\int_{350}^{2500} X_{i,smooth}(w) \beta_{-i}(w) dw - Y_i \right)^2 \quad (6)$$

is minimized to choose the optimal λ_β that avoids overfitting the data (Ramsay & Silverman, 2005). The resulting estimate of $\beta(w)$ and λ_β can then be used to predict new insect ages, Y , based on new wavelength reflectance, $X(w)$. The bootstrap 95% confidence intervals with upper and lower limits were applied to each functional regression using Matlab R2015b.

Model fitting to Compare Washed to Unwashed Insects

To compare the spectral measurements of the unwashed insects to the spectral measurements of the washed insects an extension of the previous model was used:

$$Y_i = \int_{350}^{2500} X_{i,smooth}(w) [\beta(w)_{was} + I_{unw} \beta(w)_{unw}] dw. \quad (7)$$

This extension allows the examination of the functional regression coefficients of the washed insects $\beta(w)_{was}$,

$$Y_i = \int_{350}^{2500} X_{i,smooth}(w) \beta(w)_{was} dw, \quad (8)$$

and the impact of coefficients of the unwashed insects, $\beta(w)_{unw}$,

$$Y_i = \int_{350}^{2500} X_{i,smooth}(w) [\beta(w)_{was} + \beta(w)_{unw}] dw. \quad (9)$$

An examination of the coefficients was used to test the null hypothesis $\beta(w)_{unw}=0$ to see if there is an advantage to washing the insects before collecting spectral measurements.

4.5 Results

Spectral Analysis

At an average temperature of 23.9°C, *L. sericata* spent one day as second instar, one day as third instar and then 6 days as a post feeding third instar larvae before entering the intra-puparial period. The intra-puparial period lasted 5 days and on day 6 the adults began emerging. Spectral measurements were collected for *L. sericata* from each of these days of development for each of the anterior end, midsection and posterior end of the insects.

At each of the anterior end, midsection and posterior end, the daily spectral signatures were examined for the lengthy post feeding stage, the intra-puparial period and then, as there was only a single day each of second and feeding third instar, a comparison was made between those two stages from the midsection measurements.

The functional regressions for each model based on the post feeding stage of the washed larvae indicate that each of the models from all three measured regions are a good predictor of day within the post feeding stage (Figures 4-3, 4-4, & 4-5). The spectral measurements from the posterior region of the larvae provide a superior prediction, compared with the anterior and midsection measurements.

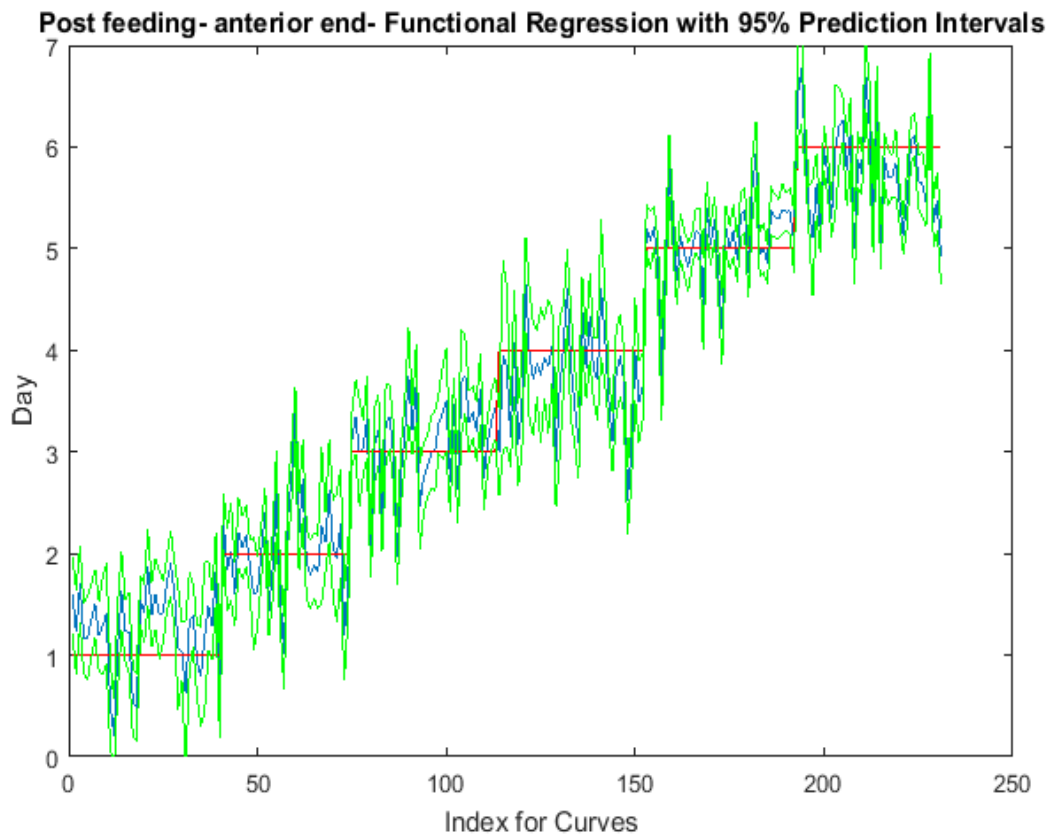


Figure 4-3 The actual (red) versus predicted days (blue) for *Lucilia sericata* post feeding larvae (raised at a mean temperature of 23.9°C) spectral measurements from 350-2500nm of the anterior end. The pointwise 95% prediction interval upper and lower limits appear in green.

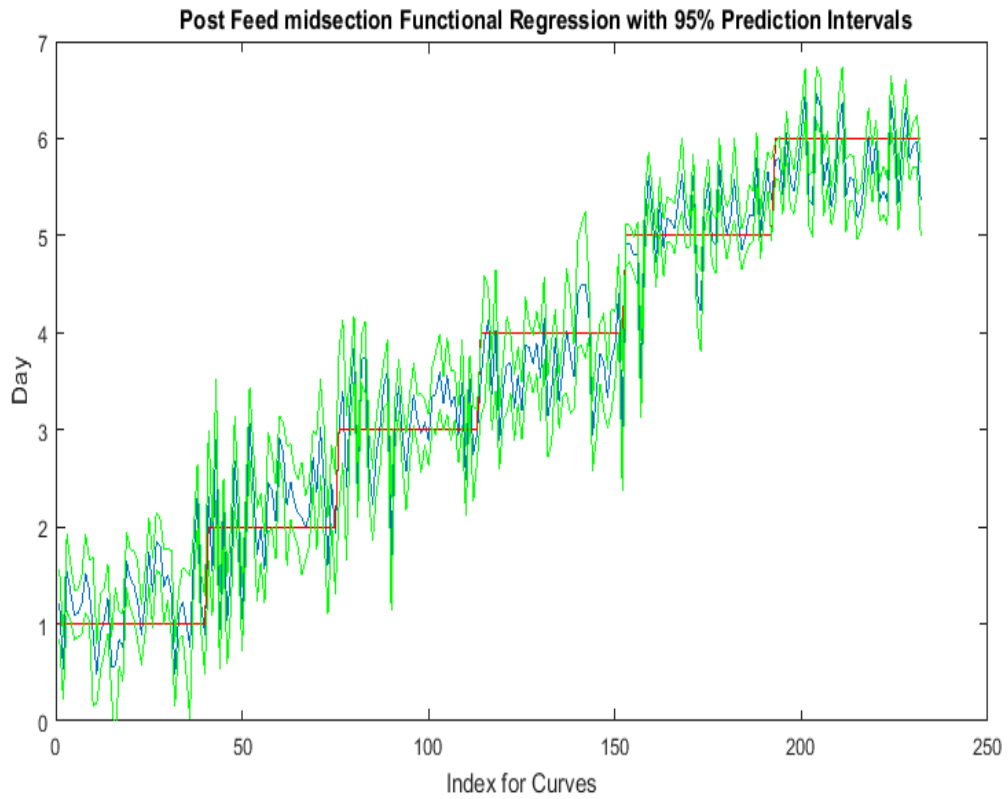


Figure 4-4 The actual (red) versus predicted days (blue) for *Lucilia sericata* post feeding larvae (raised at a mean temperature of 23.9°C) spectral measurements from 350-2500nm of the midsection. The pointwise 95% prediction interval upper and lower limits appear in green.

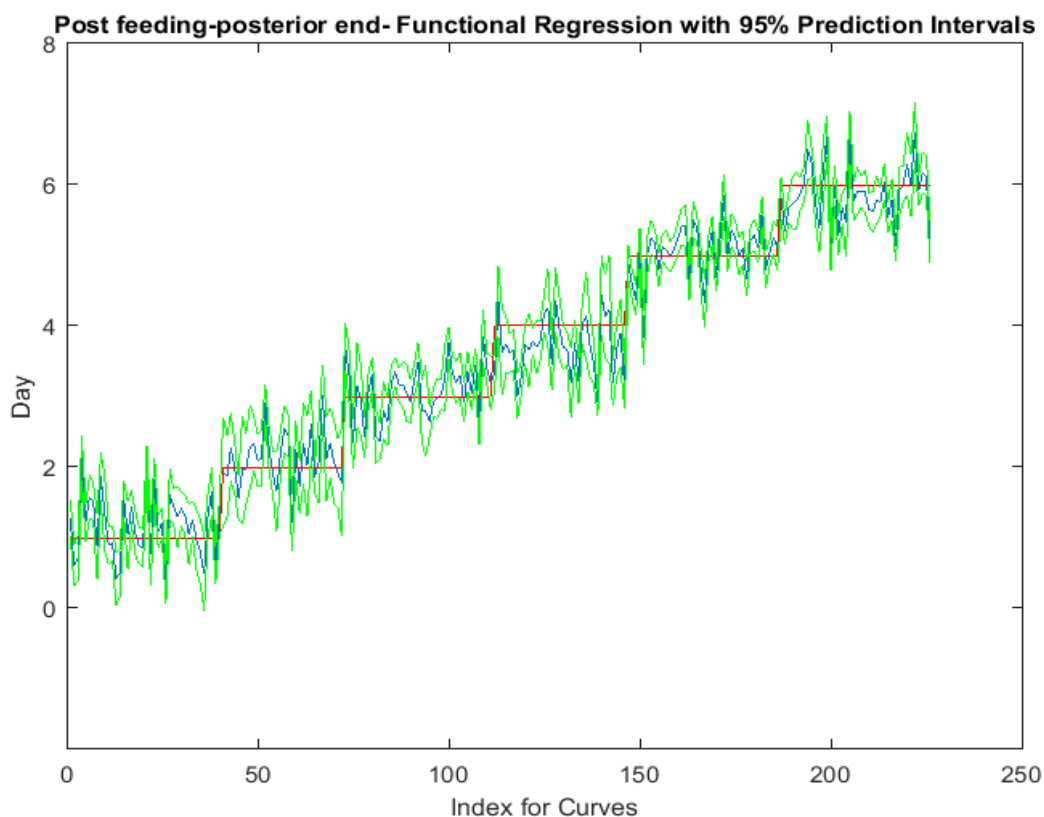


Figure 4-5 The actual (red) versus predicted days (blue) for *Lucilia sericata* post feeding larvae (raised at a mean temperature of 23.9°C) spectral measurements from 350-2500nm of the posterior end. The pointwise 95% prediction interval upper and lower limits appear in green.

The coefficient functions are presented in Figure 4-6 and indicate that the model is strong for predicting age because the $\beta(w)$ coefficient did not overlap with zero over all wavelength regions. This is evident because the red zero line is visible, which indicates that there is a slope. Not only do the coefficient functions indicate that the slope of the linear function is not zero, but they also indicate the contributing wavelengths of the electromagnetic spectrum to the model for each measured body region.

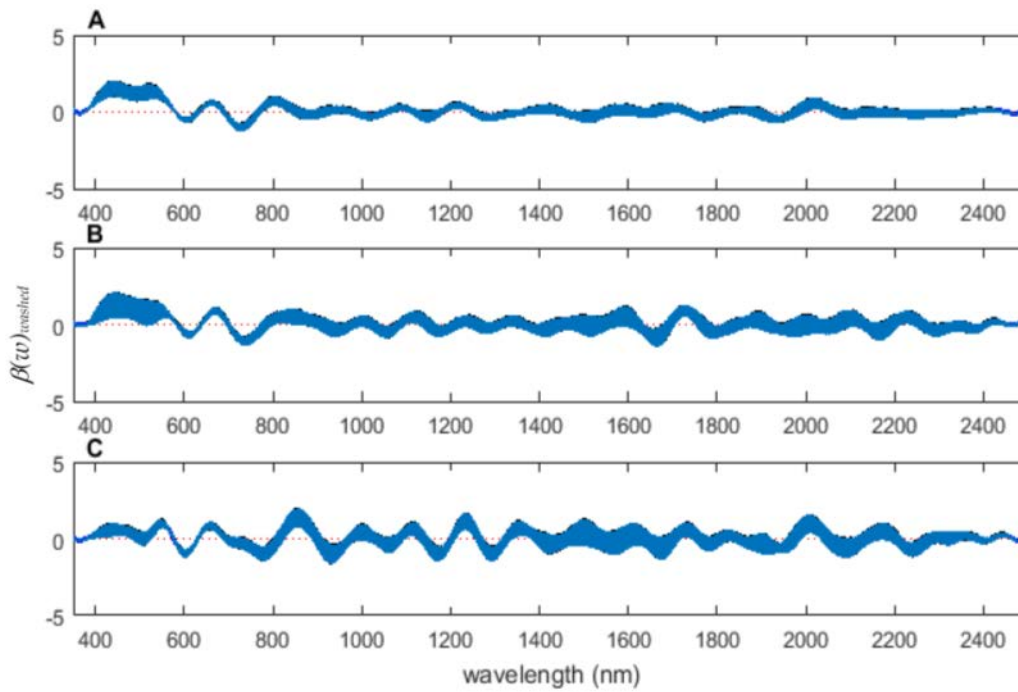


Figure 4-6 The contributing $\beta(w)_{washed}$ coefficients of the spectral measurements for each of the measured regions ((A) anterior, (B) midsection, and (C) posterior) of *Lucilia sericata* post feeding larvae raised at a mean temperature of 23.9°C.

Examining the intra-puparial functional regressions from spectral signatures that range from 350-2500 nm does show some distinction between the days (Figure 4-7, 4-8, & 4-9). The anterior measurements of the puparia offer the best prediction of day in the intra-puparial period. The first three days of the intra-puparial period are not clearly predicted from the spectral measures of the midsection and posterior regions.

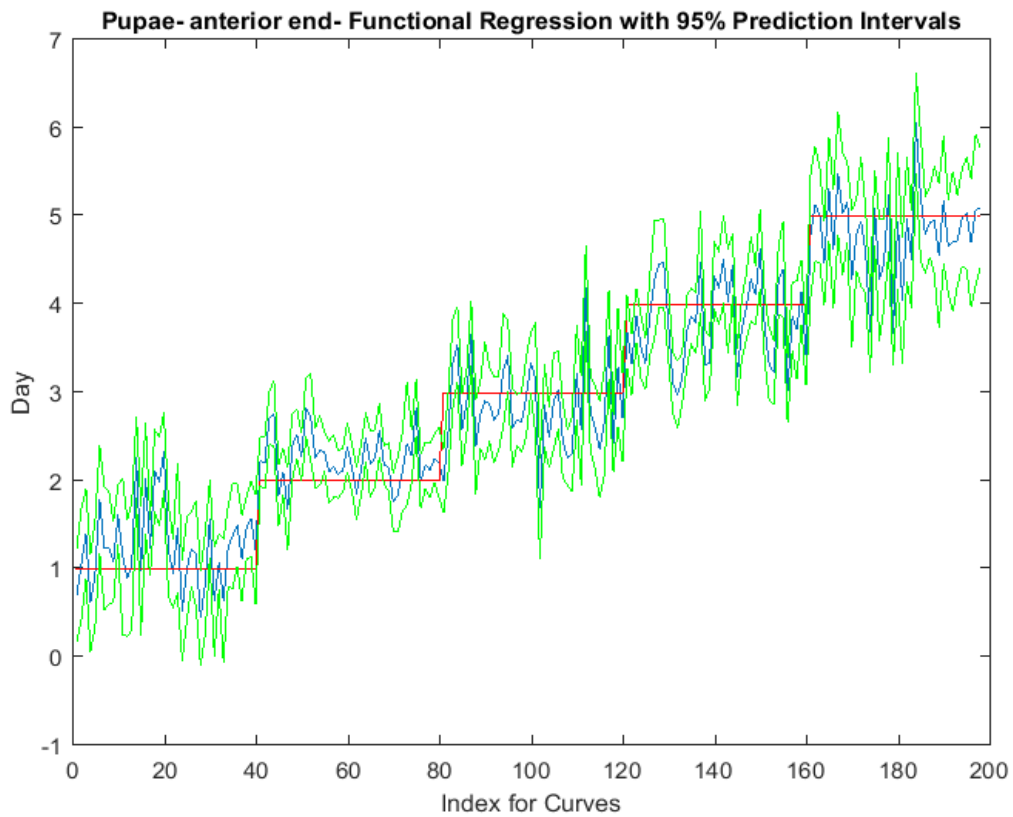


Figure 4-7 The functional regression with 95% upper and lower limit pointwise prediction intervals (green) for spectral measurements from 350-2500nm of the anterior end of *Lucilia sericata* pupae raised at a mean temperature of 23.9°C. The predicted days appear in blue and the red line is the actual day.

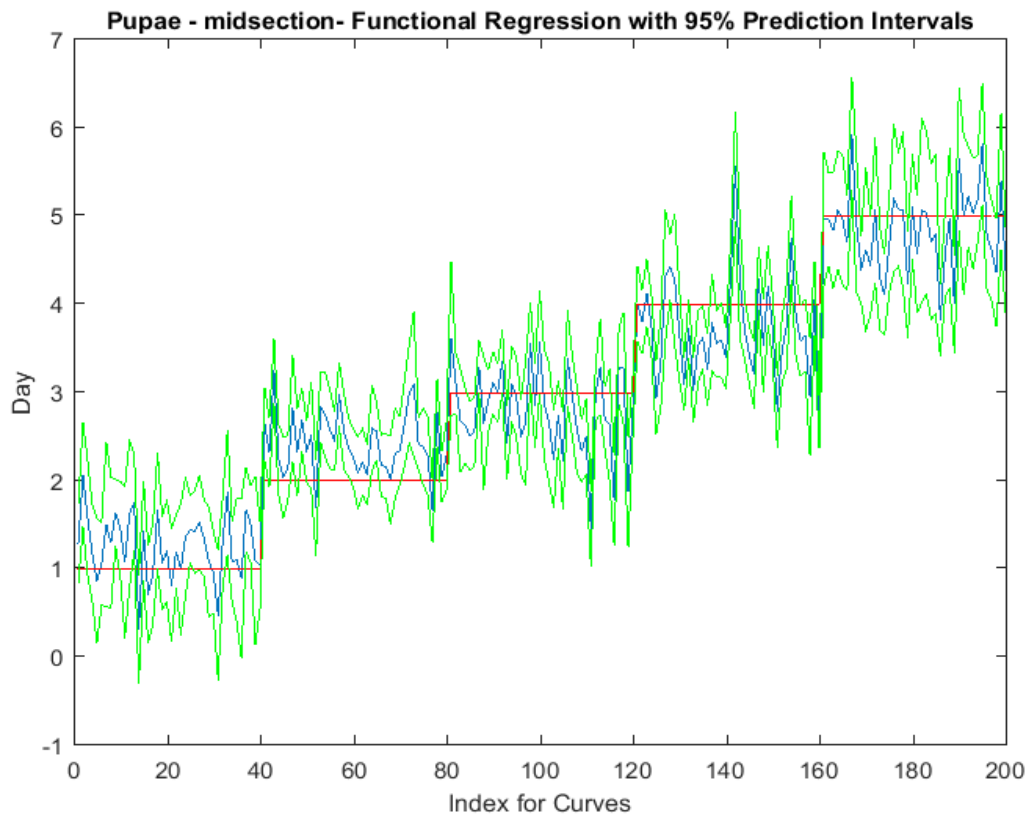


Figure 4-8 The functional regression with 95% upper and lower limit pointwise prediction intervals (green) for spectral measurements from 350-2500nm of the midsection of *Lucilia sericata* pupae raised at a mean temperature of 23.9°C. The predicted days appear in blue and the red line is the actual day.

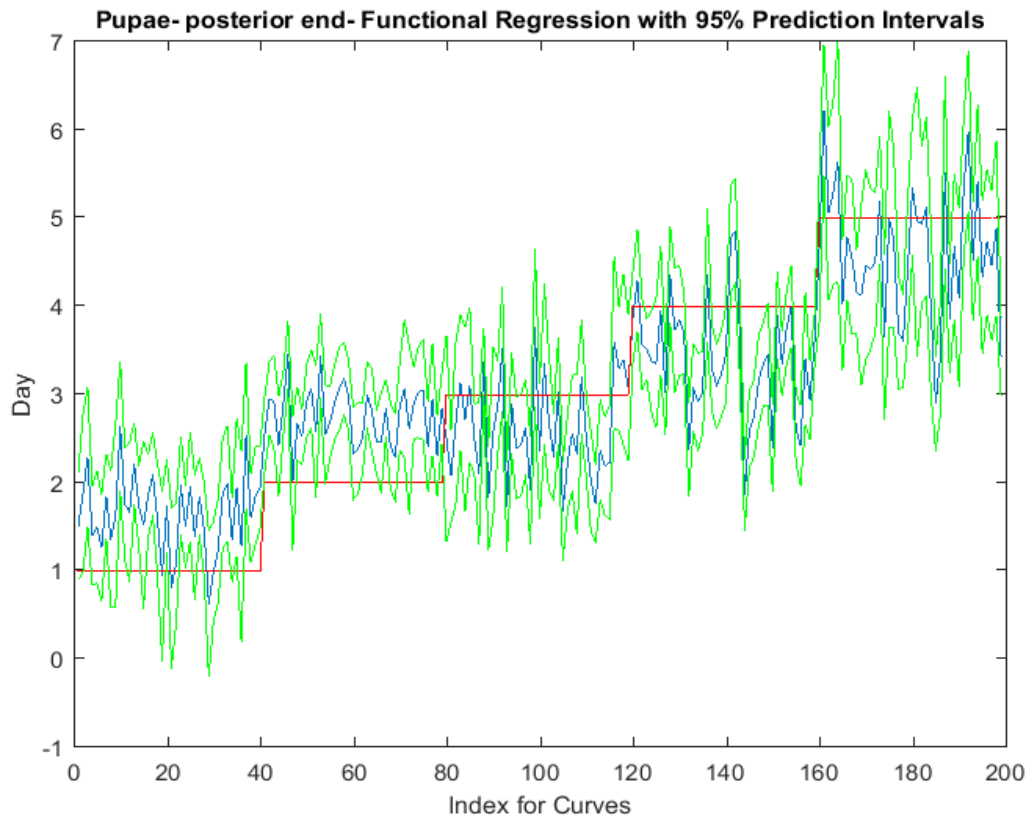


Figure 4-9 The functional regression with 95% upper and lower limit pointwise prediction intervals (green) for spectral measurements from 350-2500nm of the posterior end of *Lucilia sericata* pupae raised at a mean temperature of 23.9°C. The predicted days appear in blue and the red line is the actual day.

The coefficient functions indicate that there is a contributing $\beta(w)$ coefficient to the function for each measured body region, and also indicate that there are different contributing wavelengths to the spectral signatures for each of the body regions (Figure 4-10).

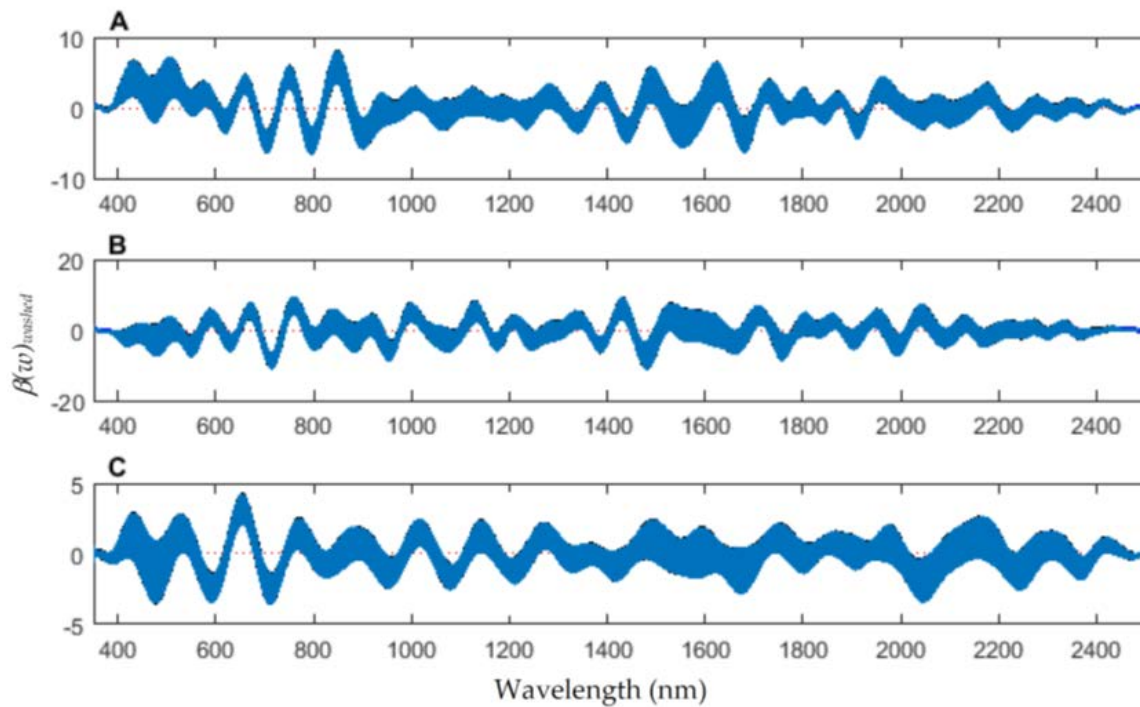


Figure 4-10 The contributing coefficients, $\beta(w)_{washed}$ of the spectral measurements for each of the measured regions ((A) anterior, (B) midsection, and (C) posterior) of *Lucilia sericata* puparia raised at a mean temperature of 23.9°C.

The contributing wavelengths and coefficients for distinguishing second instar from third instar are presented in Figure 4-11. The functional regression based on midsection spectral measurements easily predicts day one (second instar) from day two (third instar) (Figure 4-12). The predicted days hover over the actual day and fall within the 95% prediction upper and lower limits.

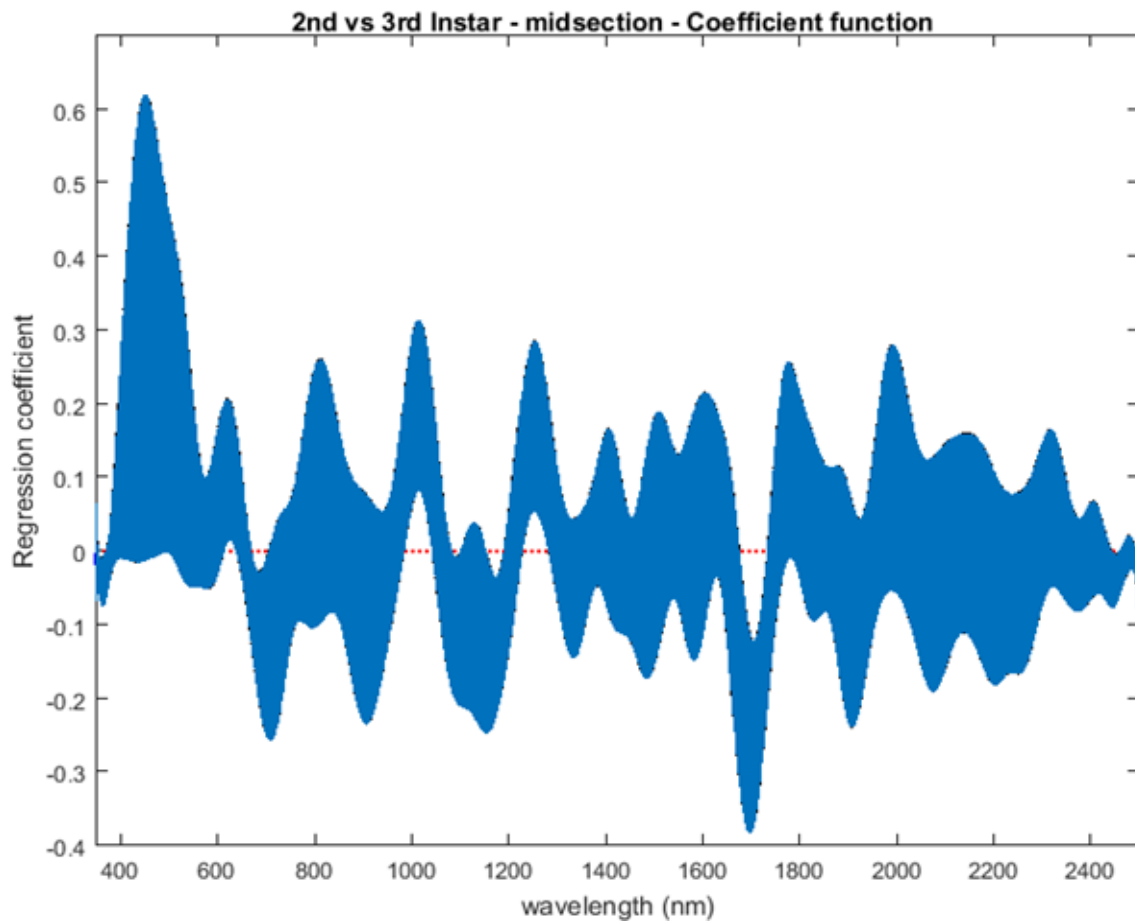


Figure 4-11 The coefficients with their 95% confidence bands contributing to the model that compares spectral measurements from the one day of second instar with the one day of third instar *Lucilia sericata* raised at a mean temperature of 23.9°C. It also indicates the wavelengths that contribute to the daily prediction.

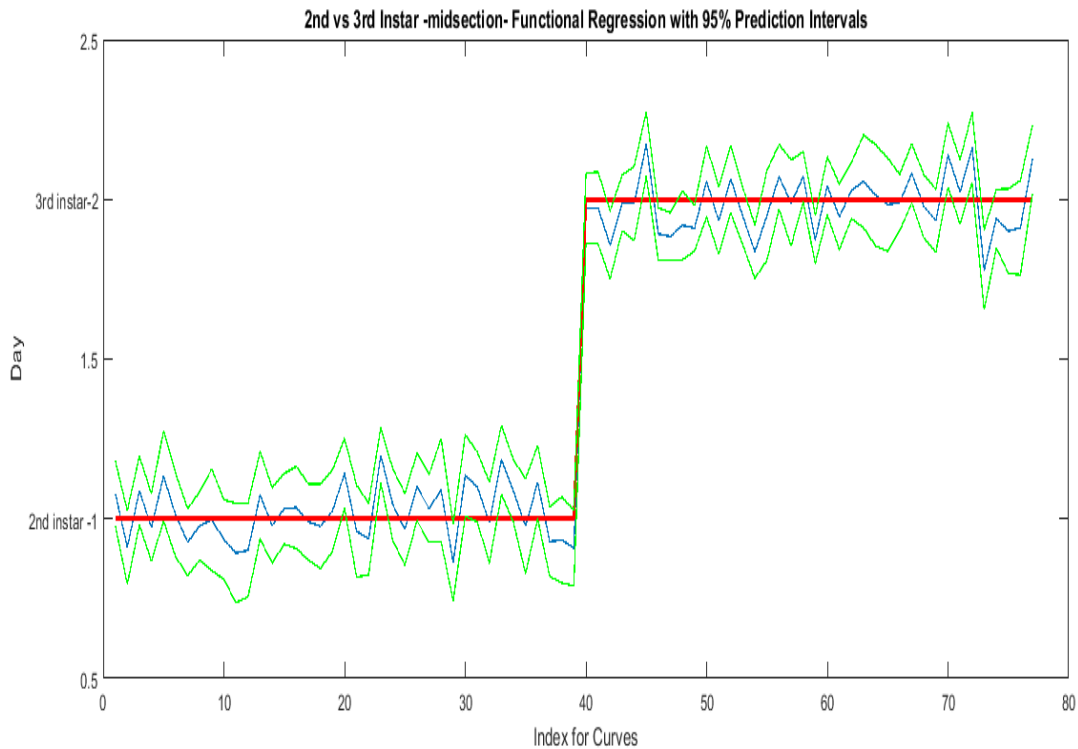


Figure 4-12 The actual (red) versus predicted days (blue) for *Lucilia sericata* second and third instar larvae (raised at a mean temperature of 23.9°C) spectral measurements of the midsection. The pointwise 95% prediction interval upper and lower limits appear in green.

The mean preprocessed smoothed plots for each day within the stages from second instar until adult emergence from *L. sericata* raised at a mean temperature of 23.9°C (Figure 4-13) show the daily differences in spectral measurements. Troughs that are observed at ~550 and 950 nm in the second instar both disappear before intra-puparial development and adult emergence are reached, respectively.

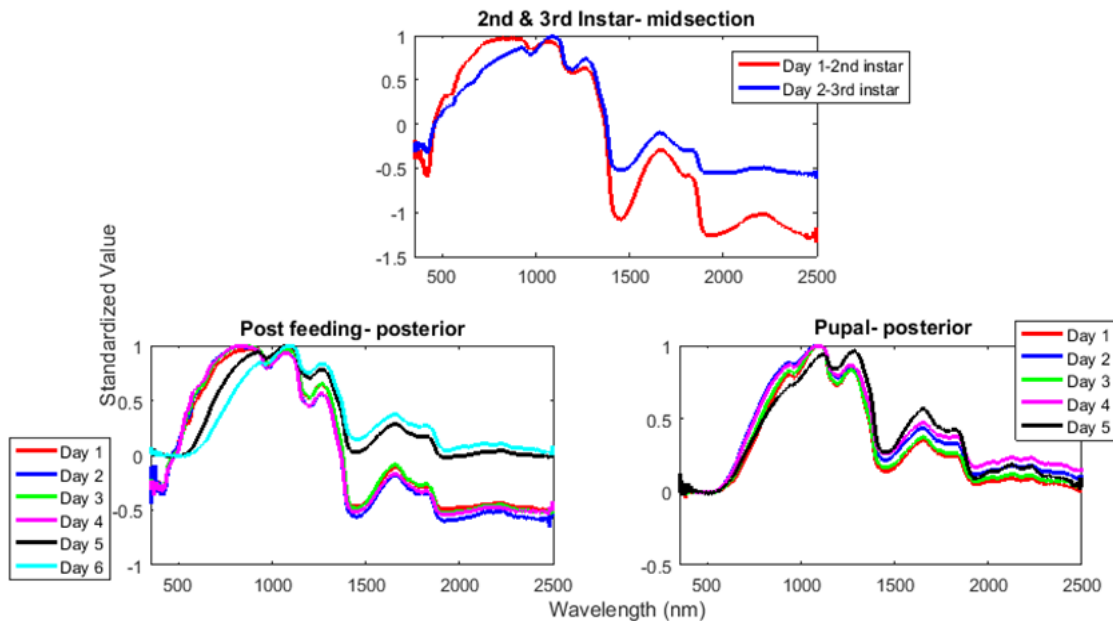


Figure 4-13 The mean preprocessed smoothed spectral measurement plots for each day of each stage of *Lucilia sericata* raised at a mean temperature of 23.9°C.

Washed versus Unwashed

To examine the necessity to wash the larvae for the spectral measurements, an analysis of the impact of the unwashed larvae spectral measurements on the washed larvae measurements was completed for each of the stages. Applying the unwashed post feeding larvae spectral measurements to each of the three models has no significant effect on the models. This was evident when examining the functional regressions based on all measured regions (Figures 4-14, 4-15 & 4-16). At no wavelength does the addition of unwashed measurements change the prediction. The slopes of the coefficients are almost zero and do not contribute to the model (Figure 4-17). Thus, this implies that there is no significant difference when including the unwashed data when it comes to predicting the day within the post feeding stage.

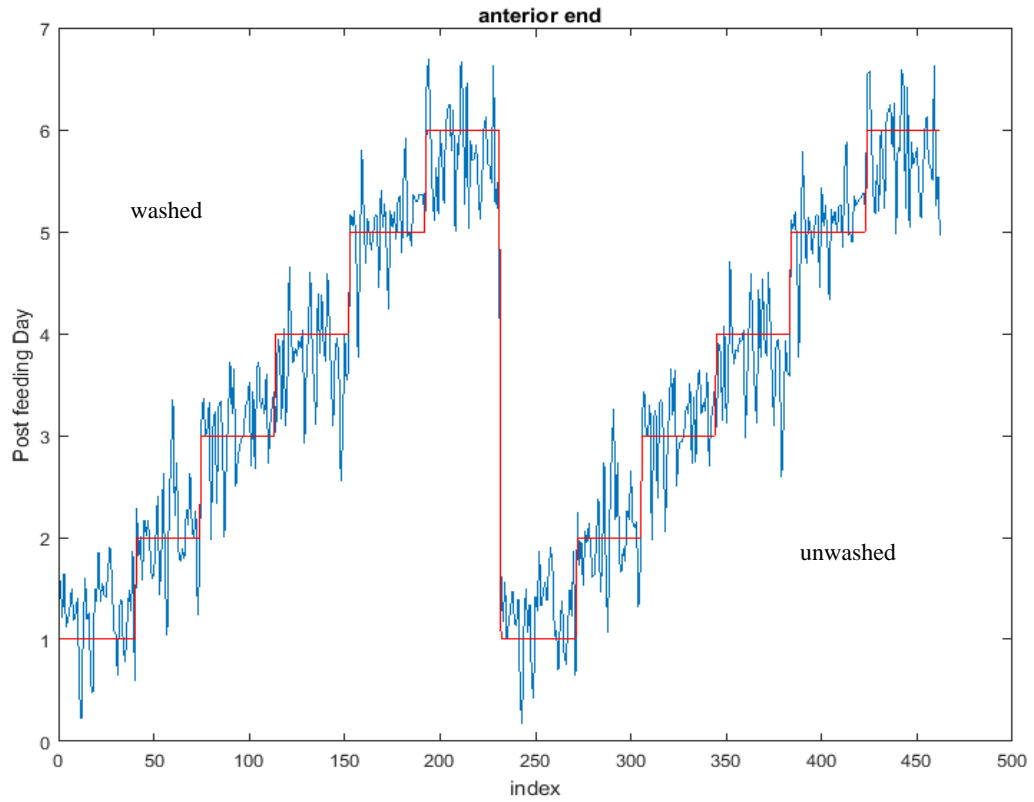


Figure 4-14 The functional regression models of unwashed and the same washed post feeding *Lucilia sericata* (raised at a mean temperature of 23.9°C) larval anterior end spectral measurements. The red line indicates the actual day and the blue indicates the predicted day.

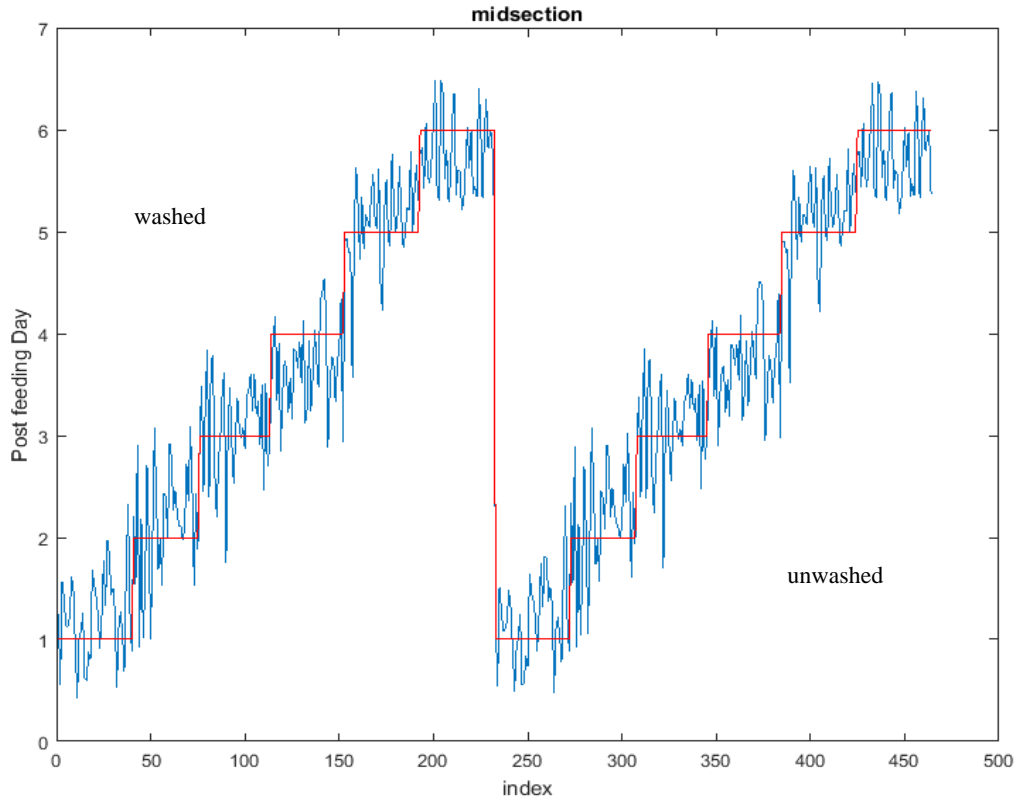


Figure 4-15 The functional regression models of unwashed and the same washed post feeding *Lucilia sericata* (raised at a mean temperature of 23.9°C) larval midsection spectral measurements. The red line indicates the actual day and the blue indicates the predicted day.

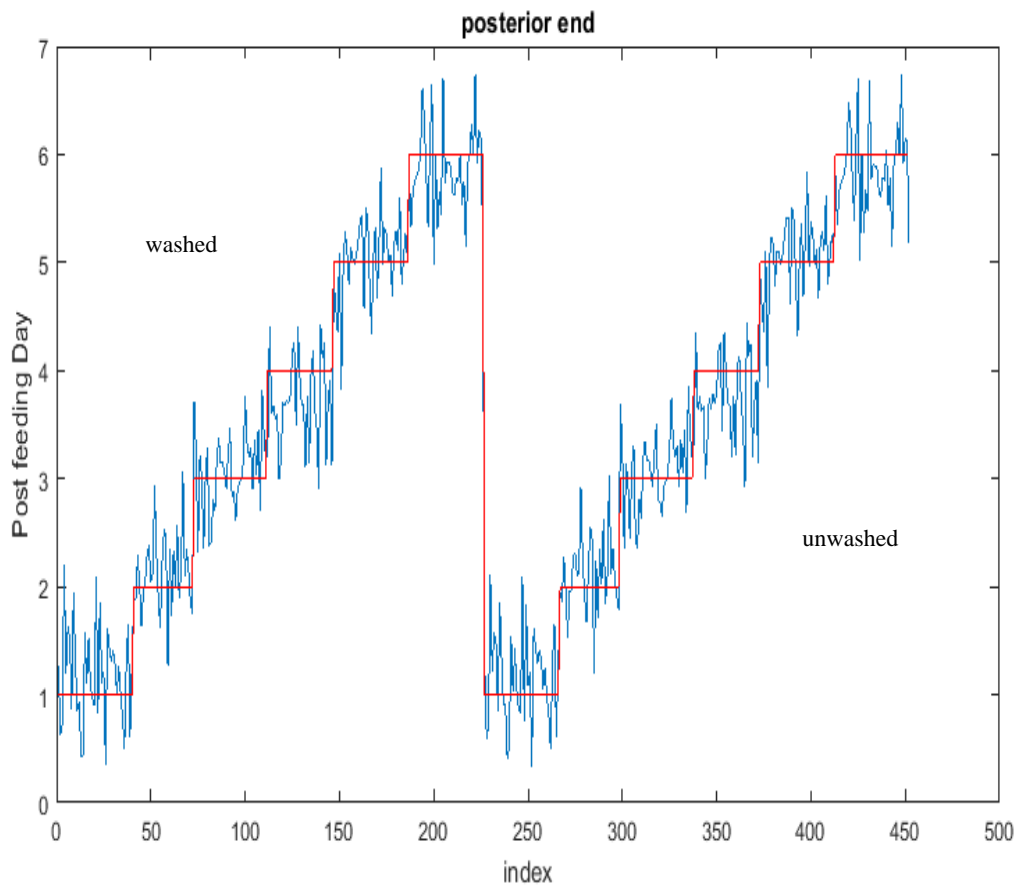


Figure 4-16 The functional regression models of unwashed and the same washed post feeding *Lucilia sericata* (raised at a mean temperature of 23.9°C) larval posterior end spectral measurements. The red line indicates the actual day and the blue indicates the predicted day.

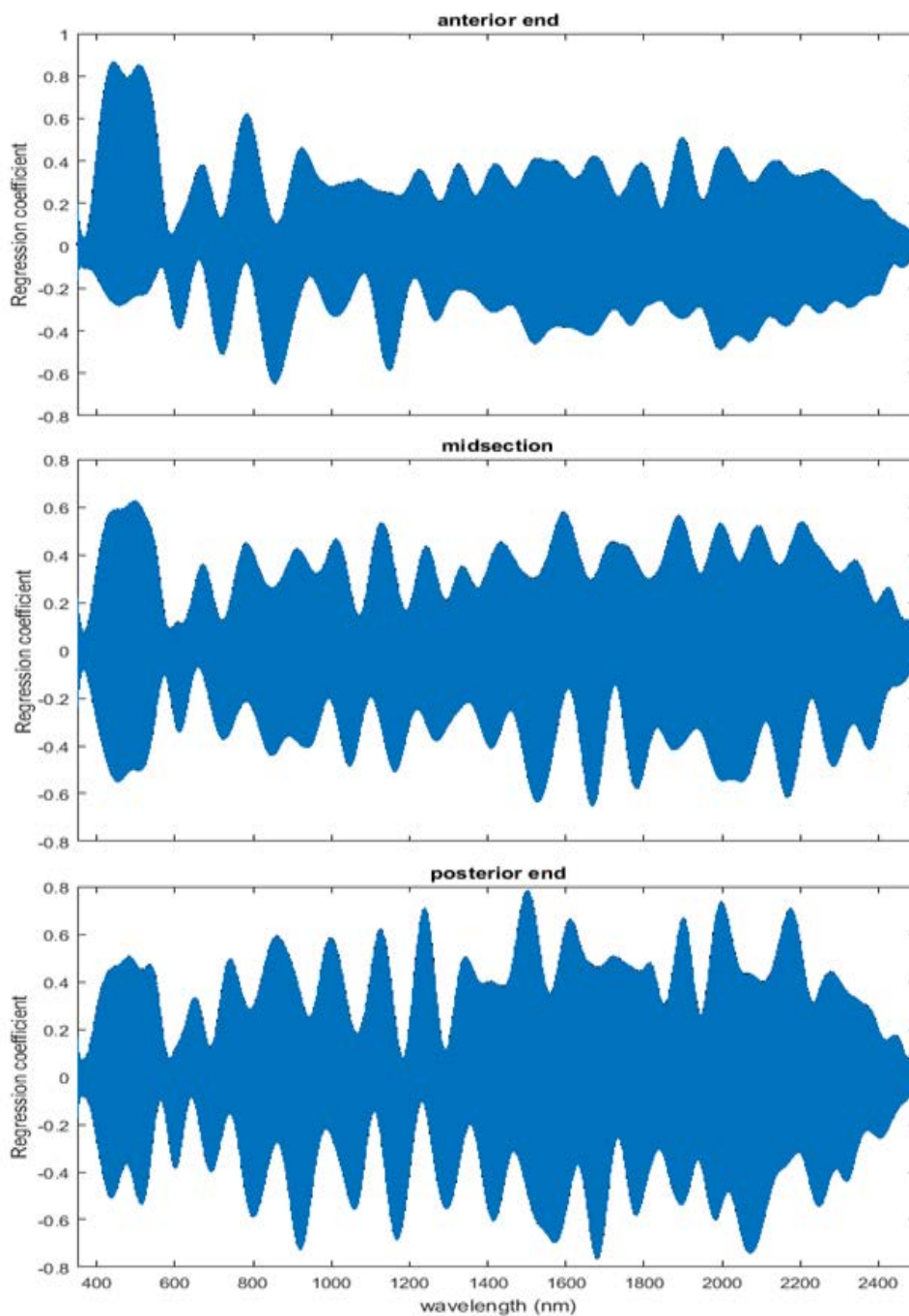


Figure 4-17 The 95% confidence interval of the coefficients for post-feeding *Lucilia sericata* raised at a mean temperature of 23.9 °C in a model predicting the effect of lack of washing before taking spectral measurements (350–2500 nm) from the anterior end/midsection/posterior end of the post-feeding larvae.

An examination of whether washing is necessary in the feeding larval stages was also completed as this would presumably affect the spectral measurements since the larvae are moving through the food source. The contributing coefficients of the washed specimens in Figure 4-11 differ from those of the unwashed specimens in Figure 4-18. There are more contributing wavelengths in the unwashed specimens and at those wavelengths the $\beta(w)$ coefficients are significant ($p < 0.05$). However, the functional regression of the unwashed specimens (Figure 4-19) predicts the different days just as consistently within 95% confidence intervals as the functional regression of the washed specimens (Figure 4-12). Including unwashed specimens in the analysis does affect the analysis but the findings are the same.

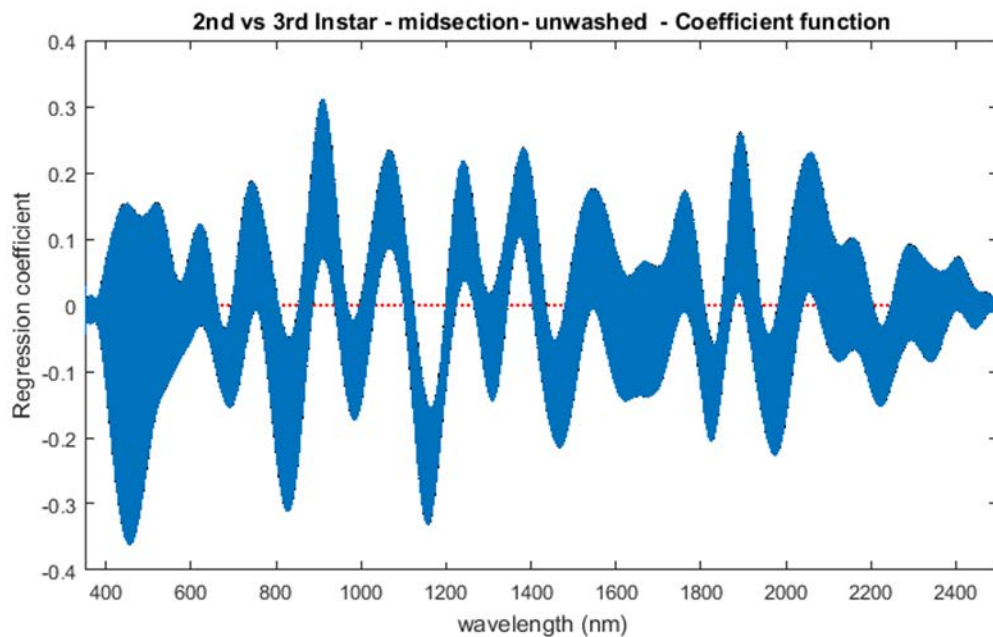


Figure 4-18 The second and third instar *Lucilia sericata* (raised at a mean temperature of 23.9°C) function of the unwashed coefficients with 95% confidence bands for the midsection spectral measurements (350-2500nm). The contributing wavelengths are indicated by the dotted red zero line.

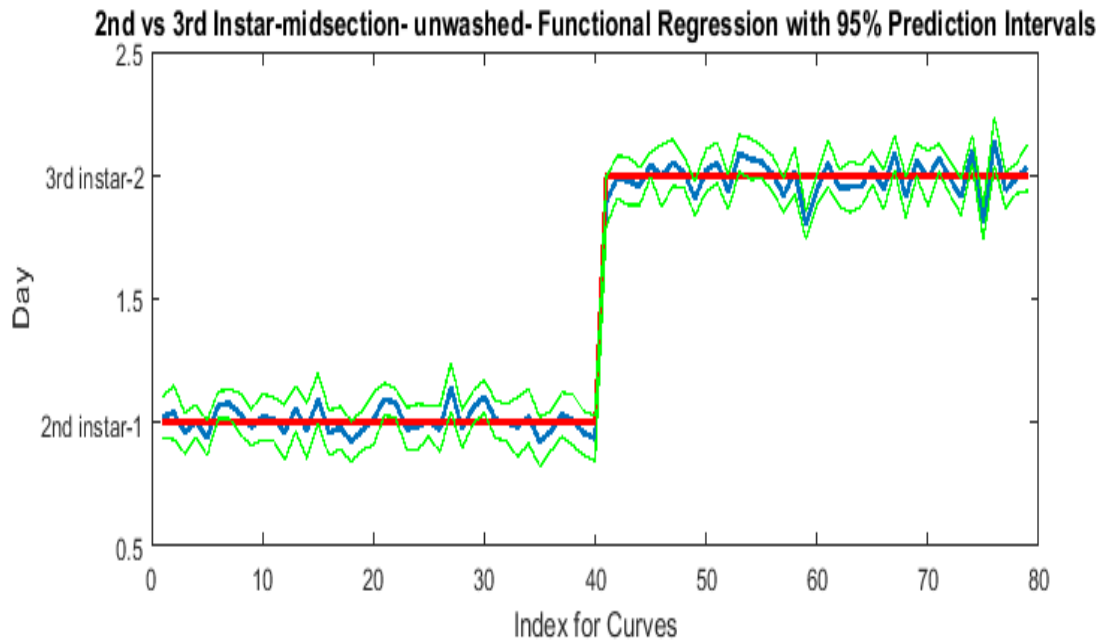


Figure 4-19 The functional regression for predicting second and third instar *Lucilia sericata* (raised at a mean temperature of 23.9°C) from unwashed larvae based on spectral measurements. The red line is the actual day, the blue is the prediction and the green lines are the upper and lower 95% pointwise prediction intervals.

4.6 Discussion

Differences were found in the daily spectral signatures of the post feeding stage of *L. sericata*. The posterior spectral measurements surpassed the anterior and midsection measurements for prediction of day in the post feeding stage. There were different contributing wavelengths and coefficients for the different regions of the insect (Figure 4-6). The posterior end had the most contributing wavelengths to the model. In fact, while measuring, it was noted that daily changes were visible in the posterior spectral measurements before they were in the midsection and anterior measurements. The position of oenocytes probably indirectly explains these findings. They are regularly found in the insect abdominal integument proximal to the spiracles (Makki et al., 2014). Oenocytes produce cuticular hydrocarbons, which are then transported to the remainder of the cuticle and fat body by lipophorin in the hemolymph (Fan et al., 2003). Cuticular hydrocarbons

waterproof the insect and contribute to the near infrared (NIR) and shortwave infrared (SWIR) spectral measurements of the insect surface (Blomquist, 2010b). Since the oenocytes are most probably located in the abdomen, cuticular hydrocarbons are probably identified earlier and at a stronger concentration than they are at the further away body regions of the anterior end and midsection. Besides hydrocarbons, colour or opaqueness, surface texture, tracheal changes near to the light penetrable surface, mouthpart and spiracular changes all may contribute in some form to the spectral measurements.

In the intra-puparial period, the best daily prediction was provided by the anterior measurements. This was probably due to the changes that occur to the brain and blow fly ommatidia appearance, which are much more immediate in metamorphosis than those changes that occur in the remaining insect body, which remains obscured longer by the fat body (Davies & Harvey, 2013). It was very probable that light was able to penetrate the puparium through the chitinous pore canals that extend along the endocuticle from which the puparium has formed. The outer portion of the very thick endocuticle is formed by secretion during the larval stages and it is the outer endocuticle which is perforated by the pore canals. This outer endocuticle with pore canals is then predetermined to form the puparium in the intra-puparial period (Dennell, 1946). The pore canals form a vertical striation in the puparium (Dennell, 1947) and it potentially may be these striations that allow light to penetrate the puparium to detect these changes. Unlike this research, previous researchers examined spectral imaging of the dorsal and ventral surfaces of blow fly puparia ranging from 389 to 892 nm in relation to morphological changes and found that both surfaces were well within 80% accurate (Voss et al., 2016).

In a few pointwise 95% confidence interval daily predictions the actual day did not fully fall within the upper and lower limits but was very close. These outlier measurements may be explained by slight development differences within replicates. These slight variations may be explained by time differences outside of the environmental chamber or temperature variations due to placement of replicate within the chamber. To avoid temperature variations within the chamber, replicates were rotated but replicates may still have been exposed to slight differences.

Simpler methods already exist to distinguish between second and third instar larvae, such as examining the number of spiracular slits. Examining the earlier stadia with spectral measurements, although accurate, is not necessary at higher temperatures, but may be useful at lower temperatures when the second and third instar stages extend over multiple days. Figure 4-13 presents the daily mean preprocessed spectral signatures for each day of development at a mean of 23.9°C. The figure shows the loss of a trough at 550 nm in the second and third instar measurements and the loss of a second trough during the intra-pupal period. The first trough is completely gone by the intra-pupal period (550 nm) and the second is almost missing by the last day of intra-pupal development before the adult emerges (950 nm). The disappearance of both troughs is probably due to water loss or absorption from the cuticle. In the intra-pupal period, a substantial water loss occurs in the cuticle, in order to reinforce the puparium as it forms (Zdarek & Fraenkel, 1972).

Unusual vertical jump points were found in some of the raw collected spectral data in a few of the collected days of data. They were not found consistently and were not a component of a regular measurement as there are smooth transitions from wavelength to wavelength in reflectance (Foley et al., 1998). Hence the only explanation can be human or machine error. There may have been a crimp within the fiber optic cable that went unnoticed. Even with this vertical jump that appeared in one day of measuring, correction was easily managed.

A noteworthy detail was that the spectral signature from the last day of one stage was basically the same as the spectral signature from the first day of the next stage. By examining the spiracular slits and combining this with the knowledge of what the insects' spectral reflectance signature is in the following stage, conclusions can be made that the insect is at the end of a stage rather than the beginning. Rather than using the minimum time it takes to reach a stage it would be more appropriate to examine the time spent in a stage at that developing temperature.

Washing the newly moulted third instar larvae with deionized water and filter paper, patting dry with clean dry filter paper, and then placing under the light source before taking the spectral measurements was distressing to the larvae at this stage only. At first it

was thought that it was the heat of the light source so the light source was moved from 5.5 cm height to 8.5 cm but this did not seem to correct this issue. It was later believed that the washing following the third instar moult was in fact the issue. By being very gentle with the third instar larvae, it was possible to keep the larvae alive for measurement.

Washing the post feeding larvae made no difference to the contributing coefficients. There was no advantage to washing the insects in the wandering post feeding stage. However, the β coefficients of the unwashed second and third instar larvae did differ from the washed. Nevertheless, the predictions of the washed and unwashed were both excellent and within 95% prediction interval upper and lower limits and so suggest that washing the specimens does not affect prediction of day of development. Washing did however affect the recent feeding third instar larvae. High mortality rates were experienced when washing the newly moulted third instar *L. sericata* larvae. It is probable that because they were newly moulted, the third instar larvae were more susceptible to washing.

4.7 Conclusion

Hyperspectral measurements of the surface of *L. sericata* larvae can be used to distinguish day within the lengthy post feeding stage quite readily and a satisfactory estimate from the intra-puparial period can also be estimated using:

$$Y = \int_{350}^{2500} X(w) * \beta(w)dw, \quad (10)$$

Where Y is the predicted day in the stage, X is the spectral measurement from 350 to 2500nm and $\beta(w)$ is the contributing coefficients of the function.

It is recommended to use posterior measurements for post feeding larvae and anterior measurements for pupae. Washing the post feeding larvae before taking spectral measurements does not seem to offer any benefit, which is not surprising since the larvae have moved away from the food source. Washing does make a difference to the coefficients for the feeding second and third instar larval spectral measurements but the predictions are not changed by the lack of washing and closely fit the upper and lower limits of the 95%

confidence intervals. Nevertheless, it is recommended that surface contaminants be gently washed from the insect cuticle if possible, so that the spectral daily signatures can best be individualized.

4.8 Acknowledgements

The authors would like to thank ASD Inc. and their Alexander Goetz instrument support program for providing the LabSpec 4 spectrometer. We would also like to thank Bekka Brodie for the *Lucilia sericata* and Billi-Jo Cavanaugh, Saadia Uraizee, Robert Wilburn, Alexis Ohman, Kelsey Dubiel, Gary Warren, and Jeremy Pearce for their volunteer services. The research would not have come to realization had it not been for their joint forces.

4.9 Reference List

- Amendt, J., Krettek, R., & Zehner, R. (2004). Forensic Entomology. *Naturwissenschaften*, *91*, 51-65.
- Anderson, G. S. (2000). Minimum and maximum development rates of some forensically important Calliphoridae (Diptera). *Journal of Forensic Science*, *45*(4), 824-832.
- Beck, L. R., Lobitz, B. M., & Wood, B. L. (2000). Remote Sensing and Human Health: New sensors and new opportunities. *Emerging Infectious Diseases*, *6*(3), 217-226.
- Blomquist, G. J. (2010). Structure and analysis of insect hydrocarbons. In G. J. Blomquist & A.-G. Bagnères (Eds.), *Insect Hydrocarbons Biology, Biochemistry and Chemical Ecology* (pp. 19-34). New York: Cambridge University Press.
- Bourel, B., Tournel, G., Hedouin, V., Deveaux, M., Goff, M. L., & Gosset, D. (2001). Morphine extraction in necrophagous insects remains for determining ante-mortem opiate intoxication. *Forensic Science International*, *120*, 127-131.

- Brown, H. E., Diuk-Wasser, M. A., Guan, Y., Caskey, S., & Fish, D. (2008). Comparison of three satellite sensors at three spatial scales to predict larval mosquito presence in connecticut wetlands. *Remote Sensing of Environment*, *112*, 2301-2308.
- Brown, K., Thorne, A., & Harvey, M. (2015). *Calliphora vicina* (Diptera: Calliphoridae) pupae: a timeline of external morphological development and a new age and PMI estimation tool. *International Journal of Legal Medicine*, *129*, 835-850.
- Butcher, J. B., Moore, H. E., Day, C. R., Adam, C. D., & Drijfhout, F. P. (2013). Artificial neural network analysis of hydrocarbon profiles for the ageing of *Lucilia sericata* for post mortem interval estimation. *Forensic Science International*, *232*, 25-31.
- Byrd, J. H. (2016). [Department of Pathology, Immunology and Laboratory Medicine, University of Florida College of Medicine].
- Carroll, M. W., Glaser, J. A., Hellmich, R. L., Hunt, T. E., Sappington, T. W., Calvin, D., . . . Fridgen, J. (2008). Use of spectral vegetation indices derived from airborne hyperspectral imagery for detection of European corn borer infestation in Iowa corn plots. *Journal of Economic Entomology*, *101*(5), 1614-1623.
- Catts, E. P., & Goff, M. L. (1992). Forensic entomology in criminal investigations. *Annual Review of entomology*, *37*, 253-272.
- Davies, K., & Harvey, M. L. (2013). Internal Morphological Analysis for Age Estimation of Blow Fly Pupae (Diptera: Calliphoridae) in Postmortem Interval Estimation. *Journal of Forensic Science*, *58*(1), 79-84. doi:doi: 10.1111/j.1556-4029.2012.02196.x
- Day, D. M., & Wallman, J. F. (2006). Width as an alternative measurement to length for post-mortem interval estimations using *Calliphora augur* (Diptera: Calliphoridae) larvae. *Forensic Science International*, *159*, 158-167.
- Defilippo, F., Bonilauri, P., & Dottori, M. (2013). Effect of Temperature on Six Different Developmental Landmarks within the Pupal Stage of the Forensically Important Blowfly *Calliphora vicina* (Robineau-Desvoidy) (Diptera: Calliphoridae). *Journal of Forensic sciences*, *58*(6), 1554-1557.
- Dennell, R. (1946). *A Study of an Insect Cuticle: The Larval Cuticle of Sarcophaga falculata* Pand. (Diptera). Paper presented at the Proceedings of the Royal Society of London. Series B, Biological Sciences.
- Dennell, R. (1947). A Study of an Insect Cuticle: The Formation of the Puparium of *Sarcophaga falculata* Pand.(Diptera). *Proceedings of the Royal Society of London. Series B, Biological Sciences*, *134*(874), 79-110.

- Fan, Y., Zurek, L., Dykstra, M. J., & Schal, C. (2003). Hydrocarbon synthesis by enzymatically dissociated oenocytes of the abdominal integument of the German Cockroach, *Blattella germanica*. *Naturwissenschaften*, *90*, 121-126.
- Fleming, R. W., Torralba, A., & Adelson, E. H. (2004). Specular reflections and the perception of shape. *Journal of Vision*, *4*, 798-820.
- Foley, W. J., McIlwee, A., Lawler, I., Aragones, L., Woolnough, A. P., & Berding, N. (1998). Ecological applications of near infrared reflectance spectroscopy - a tool for rapid, cost-effective prediction of the composition of plant and animal tissues and aspects of animal performance. *Oecologia*, *116*, 293-305.
- Frederickx, C., Dekeirsschieter, J., Brostaux, Y., Wathelet, J.-P., Verheggen, F. J., & Haubruge, E. (2012). Volatile organic compounds released by blowfly larvae and pupae: New perspectives in forensic entomology. *Forensic Science International*, *219*, 215-220.
- Gosselin, M., Wille, S. M. R., del Mar Ramirez Fernandez, M., Di Fazio, V., Samyn, N., De Boeck, G., & Bourel, B. (2011). Entomotoxicology, experimental set-up and interpretation for forensic toxicologists. *Forensic Science International*, *208*, 1-9.
- Hart, W. G., Ingle, S. J., Davis, M. R., Mangum, C., Higgins, A., & Boling, J. C. (1971, 2-4 March). *Some uses of infrared aerial color photography in entomology*. Paper presented at the Proceedings of the third Biennial workshop on Aerial Color in the Plant Sciences.
- Kharbouche, H., Augsburger, M., Cherix, D., Sporkert, F., Giroud, D., Wyss, C., . . . Mangin, P. (2008). Codeine accumulation and elimination in larvae, pupae, and imago of the blowfly *Lucilia sericata* and effects on its development. *International Journal of Legal Medicine*, *122*, 205-211. doi:DOI 10.1007/s00414-007-0217-z
- Lawrence, R., & Labus, M. (2003). Early detection of Douglas -fir beetle infestation with subcanopy resolution hyperspectral imagery. *Western Journal of Applied Forestry*, *18*(3), 1-5.
- Makki, R., Cinnamon, E., & Gould, A. P. (2014). The development and functions of oenocytes. *Annual Review of entomology*, *59*, 405-425. doi:10.1146/annurev-ento-011613-162056
- Mirik, M., Ansley, R. J., Steddom, K., Rush, C. M., Michels, G. J., Workneh, F., . . . Elliott, N. C. (2014). High spectral and spatial resolution hyperspectral imagery for quantifying Russian wheat aphid infestation in wheat using the constrained energy minimization classifier. *Journal of Applied Remote Sensing*, *8*, 083661-083661-083661-083614.

- Mirik, M., Michels jr., G. J., Kassymzhanova-Mirik, S., Elliot, N. C., & Bowling, R. (2006). Hyperspectral spectrometry as a means to differentiate uninfested and infested winter wheat by greenbug (Hemiptera: Aphididae). *Journal of Economic Entomology*, *99*(5), 1682-1690.
- Mirik, M., Michels jr., G. J., Kassymzhanova-Mirik, S., Elliot, N. C., Catana, V., Jones, D. B., & Bowling, R. (2006). Using digital image analysis and spectral reflectance data to quantify damage by greenbug (Hemiptera: Aphididae) in winter wheat. *Computers and Electronics in Agriculture*, *51*, 86-98.
- Moore, H. E. (2013). *Analysis of cuticular hydrocarbons in forensically important blowflies using mass spectrometry and its application in Post Mortem Interval estimations*. (Doctor of Philosophy), Keele University, Keele Staffordshire University.
- Moore, H. E., Adam, C. D., & Drijfhout, F. P. (2013). Potential Use of Hydrocarbons for Aging *Lucilia sericata* Blowfly Larvae to Establish the Postmortem Interval. *Journal of Forensic Science*, *58*(2), 404-412.
- Moore, H. E., Adam, C. D., & Drijfhout, F. P. (2014). Identifying 1st instar larvae for three forensically important blowfly species using “fingerprint” cuticular hydrocarbon analysis. *Forensic Science International*, *240*, 48-53.
- Moran, M. S., Inoue, Y., & Barnes, E. M. (1997). Opportunities and limitations for image-based remote sensing in precision crop management. *Remote Sensing Environment*, *61*, 319-346.
- Nansen, C., Coelho Jr, A., Viera, J. M., & Parra, J. R. P. (2014). Reflectance-based identification of parasitized host eggs and adult *Trichogramma* specimens. *Journal of Experimental Biology*, *217*, 1187-1192. doi:10.1242/jeb.095661
- Nansen, C., Ribeiro, L. P., Dadour, I., & Roberts, J. D. (2015). Detection of temporal changes in insect body reflectance in response to killing agents. *PlosONE*, *10*(4), 1-15. doi:10.1371/journal.pone.0124866
- Pechal, J. L., Moore, H. E., Drijfhout, F., & Benbow, M. E. (2014). Hydrocarbon profiles throughout adult Calliphoridae aging: A promising tool for forensic entomology. *Forensic Science International*, *245*, 65-71.
- Pickering, C. L., Hands, J. R., Fullwood, L. M., Smith, J. A., & Baker, M. J. (2015). Rapid discrimination of maggots utilising ATR-FTIR spectroscopy. *Forensic Science International*, *249*, 189-196.
- Ramsay, J. O., & Silverman, B. W. (2005). *Functional Data Analysis*. New York: Springer.

- Reibe, S., Doetinchem, P. v., & Madea, B. (2010). A new simulation-based model for calculating post-mortem intervals using developmental data for *Lucilia sericata* (Dipt.: Calliphoridae). *Parasitology Research*, *107*, 9-16.
- Richards, C. S., Simonsen, T. J., Abel, R. L., Hall, M. J. R., Schwyn, D. A., & Wicklein, M. (2012). Virtual forensic entomology: Improving estimates of minimum post-mortem interval with 3D micro-computed tomography. *Forensic Science International*, *220*, 251-264.
- Riley, J. R. (1989). Remote Sensing in Entomology. *Annual Review of entomology*, *34*, 247-271.
- Sadler, D. W., Fuke, C., Court, F., & Pounder, D. J. (1995). Drug accumulation and elimination in *Calliphora vicina* larvae. *Forensic Science International*, *71*, 191-197.
- Singh, C. B., Jayas, D. S., Paliwal, J., & White, N. D. G. (2009). Detection of insect-damaged wheat kernels using near-infrared hyperspectral imaging. *Journal of Stored Products Research*, *45*, 151-158.
- Smith, K. G. V. (1986). *A Manual of Forensic Entomology*. London: British Museum (Natural History).
- Solberg, S., Eklundh, L., Gjertsen, A. K., Johansson, T., Joyce, S., Lange, H., . . . Solberg, A. (2007). Testing remote sensing techniques for monitoring large scale insect defoliation. *Remote Sensing of Environment*, *99*(3), 295-303.
- Tarone, A. M., & Foran, D. R. (2008). Generalized additive models and *Lucilia sericata* growth: Assessing Confidence intervals and error rates in forensic entomology. *Journal of Forensic Science*, *53*(4), 942-948.
- Tarone, A. M., & Foran, D. R. (2011). Gene expression during blow fly development: Improving the precision of age estimates in forensic entomology. *Journal of Forensic Science*, *56*(S1), S112-S122.
- Tarone, A. M., Jennings, K. C., & Foran, D. R. (2007). Aging blow fly eggs using gene expression: A feasibility study. *Journal of Forensic Science*, *52*(6), 1350-1354.
- Tarone, A. M., Picard, C. J., Spiegelman, C., & Foran, D. R. (2011). Population and temperature effects on *Lucilia sericata* (Diptera: Calliphoridae) body size and minimum development time. *Journal of Medical Entomology*, *48*(5), 1062-1068. doi:10.1603/me11004

- Voss, S. C., Magni, P., Dadour, I., & Nansen, C. (2016). Reflectance-based determination of age and species of blowfly puparia. *International Journal of Legal Medicine*. doi:doi:10.1007/s00414-016-1458-5
- Warren, J.-A., Ratnasekera, T. D. P., Campbell, D. A., & Anderson, G. S. (2017). Initial investigations of spectral measurements to estimate the time within stages of *Protophormia terraenovae* (Robineau-Desvoidy) (Diptera: Calliphoridae). *Forensic Science International*, 278, 205-216. doi:10.1016/j.forsciint.2017.06.027
- Warren, J. A. (2006). *The development of Protophormia terraenovae (Robineau-Desvoidy) (Diptera:Calliphoridae) at constant and fluctuating temperatures*. (Master of Arts), Simon Fraser University, Burnaby.
- Warren, J. A., & Anderson, G. S. (2013). Effect of fluctuating temperatures on the development of a forensically important blow fly, *Protophormia terraenovae* (Diptera: Calliphoridae). *Environmental Entomology*, 42(1), 167-172.
- Wells, J. D., & Lamotte, L. R. (2010). *Estimating the postmortem interval* (second ed.). Ch 9 of *The Utility of Arthropods in Legal investigations* edited by Byrd, J.H.and Castner, J.L: CRC Press.
- Whitworth, T. L. (2006). Keys to the genera and species of blow flies (Diptera: Calliphoridae) of America north of Mexico. *Proceedings of the Entomological Society of Washington*, pp. 689-725.
- Williams, D. W., Bartels, D. W., Sawyer, A. J., & Mastro, V. (2004). *Application of hyperspectral imaging to survey for emerald ash borer* Paper presented at the Proceedings of XV U.S. Department of Agriculture Interagency Research Forum on Gypsy Moth and other invasive species Annapolis Maryland.
- Wilson, B. C., & Jacques, S. L. (1990). Optical Reflectance and Transmittance of Tissues: Principles and Applications. *IEEE Journal of Quantum Electronics*, 26(12), 2186-2199.
- Xing, J., Guyer, D., Ariana, D., & Lu, R. (2008). Determining optimal wavebands using genetic algorithm for detection of internal insect infestation in tart cherry. *Sensing and Instrumentation for food quality*, 2, 161-167.
- Xu, H., Ye, G.-Y., Xu, Y., Hu, C., & Zhu, G.-H. (2014). Age-dependent changes in cuticular hydrocarbons of larvae in *Aldrichina grahami* (Aldrich) (Diptera: Calliphoridae). *Forensic Science International*, 242, 236-241.
- Zdarek, J., & Fraenkel, G. (1972). The mechanism of puparium formation in flies. *Journal of Experimental Zoology*, 179, 315-324.

Zhu, G. H., Xu, X. H., Yu, X. J., Zhang, Y., & Wang, J. F. (2007). Puparial case hydrocarbons of *Chrysomya megacephala* as an indicator of the postmortem interval. *Forensic Science International*, 169, 1-5.

Chapter 5. A Comparison of Development Times for *Protophormia terraenovae* (Robineau-Desvoidy) (Diptera: Calliphoridae) reared on different food substrates

WARREN, J.-A.

Published in Canadian Society of Forensic Science:

Warren, J.-A. and Anderson, G.S. (2009) A comparison of development times for *Protophormia terraenovae* (R-D) reared on different food substrates Can. Soc. Forensic Sci. J. 42(3) pp. 161–171.
<http://dx.doi.org/10.1080/00085030.2009.10757604>

With the addition of these references to update the publication:

Bernhardt et al. 2016
Beuter & Mendes, 2013
Boatwright and Tomberlin 2010
El-Moaty 2013
Flores et al. 2014
Harnden & Tomberlin 2016
Niederegger et al. 2013
Richards et al. 2013
Thyssen et al. 2014
Wilson et al. 2014

5.1 Preface

This chapter is different from the others in that there is no remote sensing but instead it is an examination of the effect of food type on the development of *Protophormia terraenovae*. This research was published in 2009 and so I have added the newer references examining this science to this chapter. Beef liver along with other organs is most often used in research due to its economical value. This chapter examines whether beef liver should be the food of choice. This research is the only comparison of development on laboratory rearing substrates to development on whole animal remains. Research has shown that food substrate does affect development rate of many species. Thus, before

determining if food substrate affects spectral measurements, it was necessary to determine if *P. terraenovae* development is affected by food substrate.

5.2 Abstract

Experiments were conducted to determine whether a specific larval substrate impacted immature development rates. *Protophormia terraenovae* (R-D) was raised on beef organs and compared with whole carcasses (rat), to determine if development times differed. The minimum development time on beef liver was the most consistent with the rat carcass but a significant difference between all substrates was found after the third instar. These differences can be explained by the differences between heart and muscle, and the other substrates. Often, length of the larvae is used to estimate insect age and so, on Day 2, weight, length, and width of the pupae were measured. Significant differences were found for all parameters measured on each of the substrates. These measurements should not be used to estimate the age of *P. terraenovae* due to differences between rearing substrates. Significant differences within substrates were only found for weight of insects developing on heart and length of insects developing on muscle.

There was no significant difference in survival from first instar to the adult stage on any of the substrates but personal observation suggested that mortality was higher in insects developing on the brain tissue.

5.3 Introduction

Forensically important insect species, including blow flies (Diptera: Calliphoridae), are ubiquitous and are vital to the decomposition of remains. A decaying corpse provides an ephemeral yet adequate resource for insect development. While feeding on the decaying organism, blow flies progress through their immature stages. This progression is completed at a temperature-dependent and predictable rate, which can be applied by forensic entomologists to estimate a minimum post-mortem interval (minPMI) in death

investigations. Conflicting findings for these rates have been found (Anderson, 2000; Ash & Greenberg, 1974; Greenberg, 1991; Kamal, 1958; Nuorteva, 1977). A multitude of factors can result in variation in developmental rates. There is a lower temperature limit below which development does not occur and this, as well as rates for insect development, have been found to differ for insects of the same species from different geographical areas.

Furthermore, the heat generated from maggot mass formation can increase development rates substantially (Grassberger & Reiter, 2001; Greenberg & Kunich, 2002; Reiter & Grassberger, 2002; Warren, 2006). Ambient temperature may be consistent with the recorded temperature but this temperature may vary from that at which the insects are developing (Greenberg & Kunich, 2002; Warren, 2006). If the maggots aggregate, they can create a micro- environment with much higher temperatures that can influence development rates (Anderson & VanLaerhoven, 1996; Catts, 1992; Early & Goff, 1986; J. A. Payne, 1965; Shean, Messinger, & Papworth, 1993; Wells & Lamotte, 2001). Temperature fluctuations can also create varying development rates as compared with that at the mean temperature (Clark, Evans, & Wall, 2006; Greenberg & Kunich, 2002; Warren, 2006; Warren & Anderson, 2013b).

Variables related to insect nutrition may also contribute to the differences in development rates (Ireland & Turner, 2006). The larvae feed on semi-liquefied food sources, and then further rely on their mouthparts to grind solid food into a pulp (Hobson, 1932). The liquefaction can result from a combination of bacteria creating an alkaline reaction during the decomposition process, and from the proteolytic digestion of the excreta released from the larvae themselves (Hobson, 1932). The extent to which the food source is liquefied may factor into the rate of digestion or merely the ability to digest the source.

Various meat substrates, including organs and sometimes something as inadequate as artificial diets containing cat food (Mandeville, 1988), are used to obtain the developmental data that are applied to death investigations. It is crucial to death investigations to avoid any inconsistencies in development data; particularly, based on rearing substrate differences in developmental data collection, as the consequences are too important. The research completed by forensic entomologists at the Centre for Forensic

Research at Simon Fraser University, among many other researchers, is regularly conducted with beef liver. It is important to determine whether inconsistencies in development times and rates lie within the type of substrate used, and whether application of the data generated with substrates that are different from the specimen in question should occur. Discrepancies in development times have been found among different substrates for several different blow fly species. In fact, researchers found that, of pig brain, liver, and muscle, brain was the least nourishing and most rapidly consumed by *Calliphora vomitoria* Linnaeus. *C. vomitoria* development was the most successful on liver (Ireland & Turner, 2006). This could be explained by the nutrition contribution of each tissue. In comparison to muscle and liver, brain has a higher water content and fewer proteins and carbohydrates to offer (Ireland & Turner, 2006). Larvae of *Lucilia sericata* (Meigen) when fed on both cow and pig liver, lung, and heart were found to develop faster and to a larger size on the pig tissues compared with the beef tissues (Clark et al., 2006). The authors also found that the insects developed faster and to a larger size on lung tissue than on liver tissue (Clark et al., 2006). Subsequent research on the same species found, when examining development on cow tissues, that the duration of development differed for all examined stages (El-Moaty & Kheirallah, 2013). The *L. sericata* raised on heart were smaller in size compared to those raised on the other bovine tissues (El-Moaty & Kheirallah, 2013). *Calliphora vicina* (Meigen) larvae also develop at different rates on various rearing substrates (Kaneshrajah & Turner, 2004). *C. vicina* was found to develop considerably faster on lung, brain, heart, and kidney than on pig liver (Kaneshrajah & Turner, 2004). Succeeding investigation indicated that development is significantly slower on decomposing pig liver compared to fresh pig liver and may be a factor in these findings (Richards, Rowlinson, Cuttiford, Grimsley, & Hall, 2013). *Calliphora augur* (Fabricius) and *Lucilia cuprina* (Wiedemann) were found to reach moult later and develop to a smaller size when developing on sheep's liver compared to sheep's brain and meat (Day & Wallman, 2006a). Much more recent research examining both *C. vicina* and *C. vomitoria* found that *C. vicina* showed little difference in its development on different tissue types and was classified as a 'generalist' whereas *C. vomitoria* showed better development on processed substrates and should therefore be classified as a 'specialist' (Niederegger, Wartenberg, Spiess, & Mall, 2013).

Subsequently, immature growth rates of *C. vicina* reared on several pork tissues (liver, loin, and minced) were compared with *C. vicina* raised on human muscle tissue and Bernhardt et al. (2016) found growth rates on pork loin and pork liver to be significantly slower than on human tissue. However, there were no significant differences between *C. vicina* raised on human tissue with *C. vicina* raised on any pork tissues to the post feeding stage and intra-puparial period. They recommend doing laboratory research on minced pork instead of other pork tissues since they did not find any significant difference with development on human tissue (Bernhardt, Schomerus, Verhoff, & Amendt, 2016). *Chrysomya rufifacies* (Macquart) development on canine, equine and porcine muscle tissues was compared and findings were that variation existed on each of the tissue types at each of the temperatures examined (Flores, Longnecker, & Tomberlin, 2014). Three *Chrysomya* spp. raised on bovine liver, muscle, stomach and tongue, as well as chicken heart, were all found to show slower growth on liver compared to the remaining tissues (Thyssen, de Souza, Shimamoto, Salewski, & Moretti, 2014). *Chrysomya albiceps* (Wiedemann) raised on pig fat, meat and brain tissue developed faster on the fat tissue. However, many fewer insects raised on fat tissue emerged as adults (Beuter & Mendes, 2013). A further interesting finding by Beuter and Mendes (2013) was that when *Chrysomya albiceps* was raised on the different pig tissues, males emerged as adults on average a day earlier than females. Contrary to what was found with *C. albiceps* developing faster on pig fat tissue, *Phormia regina* developed faster by as much as 6 hours on the leaner venison than it did on the fattier pork tissue (J. M. Wilson, Lafon, Kreitlow, Brewster, & Fell, 2014). This is a key detail when applying development rates of *Phormia regina* to wildlife poaching post-mortem interval estimates (J. M. Wilson et al., 2014). Dissimilar findings to the other species were made for *Cochliomyia macellaria* (Fabricius) raised on vertebrate muscle. Comparable development rates and sizes were found for the secondary screw worm fly raised on equine muscle and porcine muscle (Boatright & Tomberlin, 2010). *Hermetia illucens* (Linnaeus) required more degree hours to complete larval development when raised on pork loin muscle than beef loin muscle and the control grain based diet of alfalfa meal, corn meal and wheat bran. Larval development of *H. illucens* was considerably faster on the control diet (Harnden & Tomberlin, 2016).

Larval length is often used as an alternative for age estimation (Anderson, 2000; Day & Wallman, 2006b; Tantawi & Greenberg, 1993). However, two problems arise with its use. The first of these is that an overlap between lengths is often recognized for the successive stages (Anderson, 2000). Secondly, head curling can often be problematic (Day & Wallman, 2006b) and so fixing the insects in a preservative is often done to correct this (Tantawi & Greenberg, 1993). Under circumstances when it is necessary to keep the insect alive, or when estimation is being made from a photograph, fixing insects is not an alternative. Day and Wallman (2006) have introduced an alternative method by measuring larval width. The length and width measurements further distinguish the larval stages and perhaps can distinguish the intra-puparial period as well. Likewise, Wells and LaMotte (Wells & Lamotte, 1995) have explored the possibility of using weights to predict maggot age. A great deal of overlap of stages was found between days of development extending the ranges of days beyond clear partitions. Standardized measurements to distinguish age have not been explored at the intra-puparial period as they have been with larval stages. Measurements taken on Day 2 of the intra-puparial period considerably reduce the variability in measurements taken. Firstly, there is no need for fixing for length measurements and this prevents a reduction in sample size. Secondly, standardized measurements are possible because of the rather uncomplicated ability to distinguish Day 2 from any other day for each puparium as opposed to the difficulty of doing the same in the larval stage.

The objectives of this research were to determine if significant discrepancies occur with *Protophormia terraenovae* (Robineau-Desvoidy) development on various substrates and to determine if it is possible to use a standardized intra-puparial measurement for insect age estimation of this species.

5.4 Materials and Methods

Four separate stock colonies were established from wild caught *P. terraenovae* and have been replenished regularly each insect season from the Lower Mainland of British

Columbia. These insects were maintained in 75 cm³ cages on a diet of milk powder, sugar, and water *ad libitum*. The adult flies in each cage were provided with approximately 200 g of beef liver as an oviposition medium and, when it appeared that sufficient numbers of eggs had been laid (~4 hours), the medium was removed. The liver was placed into rearing containers and more beef liver added. Once the insects had reached first instar after ~24 hours, the larvae were divided among 15 4.5 L wide-mouthed glass rearing jars that contained approximately a 5 cm depth of dampened sawdust, folded industrial paper towel, and the larval rearing medium. Three replicates of each of the five media were conducted, and a mean of 61 with a range of 50 to 71 first instar larvae were placed into each container. A paper towel lid was secured over each jar using elastic bands to prevent the larvae from crawling out of the rearing jars. First instar larvae rather than eggs were placed onto each of the rearing substrates to be certain that the insects that were being used in the experiment were, in fact, viable. Also, only 50 to 71 insects were used in each replicate to avoid overcrowding. Overcrowding was avoided because of its ability to increase development rates. Maggot mass formation can substantially amplify development temperatures above ambient temperatures and, therefore, increase rates (Greenberg & Kunich, 2002). Also, aggregation of maggots can cause competition for resources. This, too, can increase development rates while decreasing insect size (Ireland & Turner, 2006).

Beef muscle was purchased at a butcher shop, and a local abattoir was contacted for beef organs including brain, heart, and liver. The Animal Research Care facility at Simon Fraser University provided frozen rat carcasses with abdominal incisions. The first instar larvae were placed directly on the wound and other substrates. The rearing media were all consistently previously frozen and thawed for the research with one exception. The veal brain was never frozen. The abattoir advised against freezing, as it impacts consistency of the tissue.

The glass jars were placed in a Conviron[®] E/7 environmental chamber that was set for continuous lighting and a relative humidity of 75%. The chamber maintained a mean temperature of approximately 17°C ± 1°C and, to account for any temperature differences within the chamber, the jars were rotated daily. These temperatures were recorded on ACR

Systems Inc. Smartbutton[®] data logger temperature recorders and confirmed with Fisherbrand[®] mercury thermometers. The insects were checked approximately every 12 hours for stage changes in every jar. The larval stage changes were based on the number of posterior spiracular slits and the crop size (Smith, 1986). For each stage, the minimum development times, mode development (the time when the largest number of insects changed stage), and maximum development times were determined.

On Day 2 of the intra-puparial period, the insects were weighed and their width and length measured to determine if a pattern occurs that can be used to further distinguish stages within the intra-puparial period itself. This was done in accordance with Day and Wallman's larval measurements; that is, the width measurements of the puparium were made at the intersection of abdominal segments five and six and the length measurements were made from the outlying distances of the eighth segment of the abdomen and the anterior end of the puparium (Day & Wallman, 2006b). Finally, the adult eclosed flies were weighed consistently on the same day, after they had expired. All statistical analyses to examine differences in development times of *P. terraenovae* on the different rearing substrates were completed using nonparametric Kruskal Wallis tests from the SAS statistics package JMP[®] version 7, and Microsoft Excel[®] was used to plot the graphs.

5.5 Results

The mean temperatures for each of the three replicates in the environment chamber were maintained at 17°C ± 1°C. There was no significant difference in development time between replicates except the first replicate, where all of the insects from each rearing jar reached the adult stage on the 29th and last day of experimentation ($\chi^2=5.99$, $df=2$, $p<0.0401^*$).

Significant differences ($\alpha = 0.05$) based on substrate were found for minimum development to the adult stage ($\chi^2 = 9.49$, $df = 4$, $p < 0.05^*$). The minimum development to the post-feeding stage was also found to differ significantly ($\chi^2 = 9.49$, $df = 4$, $p < 0.05^*$). A significant difference was noted for maximum development on the substrates to the post

feeding stage for all the food types ($\chi^2 = 9.49$, $df = 4$, $p < 0.03^*$). At $\alpha = 0.05$, significant differences were not identified for mode of development to any stage (second instar, $\chi^2 = 7.05$ and $p > 0.13$; third instar, $\chi^2 = 8.26$ and $p > 0.08$; post-feeding, $\chi^2 = 8.65$ and $p > 0.07$; intra-puparial period $\chi^2 = 2.99$ and $p > 0.56$; and adult stage, $\chi^2 = 7.45$ and $p > 0.11$) for any of the substrates.

Clear differences in development rates were observed for each of the different substrates, and development on no one substrate reflects the development of the insects on the whole rat carcasses. However, based on the mean minimum and maximum development, the development on beef liver most closely resembles the development on the rat carcass (Figure 5-1, & 5-2).

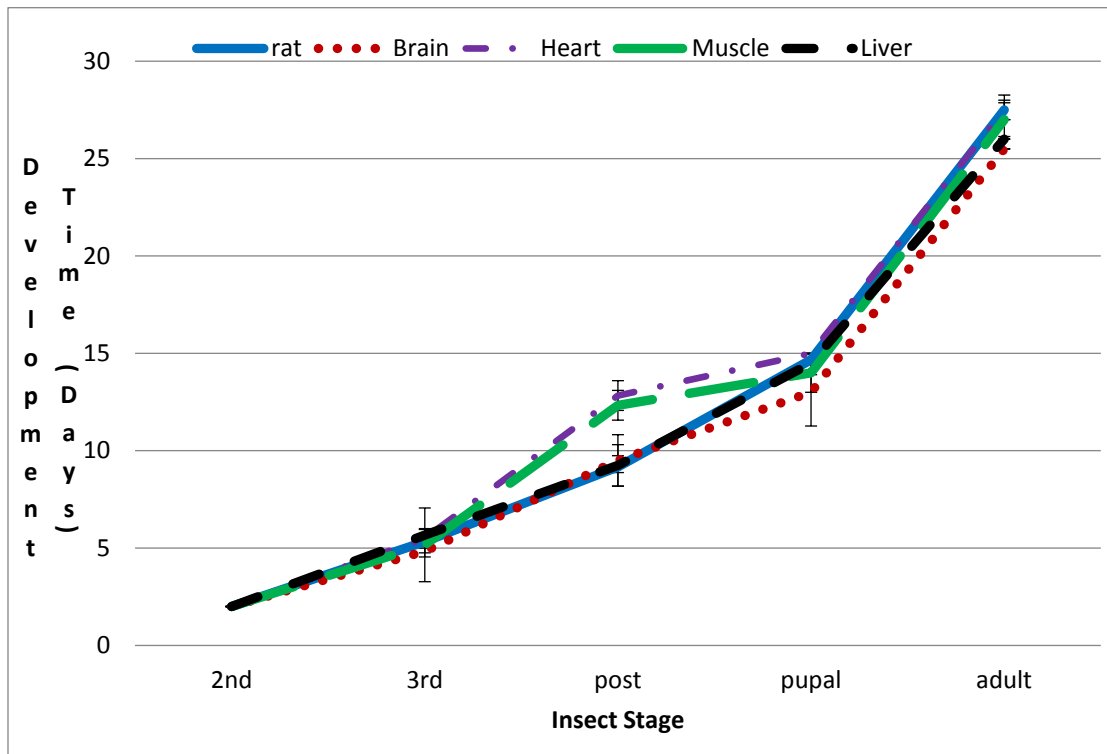


Figure 5-1 Mean minimum development times for *P. terraenovae* to reach each stage at ~17°C in days on whole, wounded rats, and on beef brain, heart, muscle and liver.

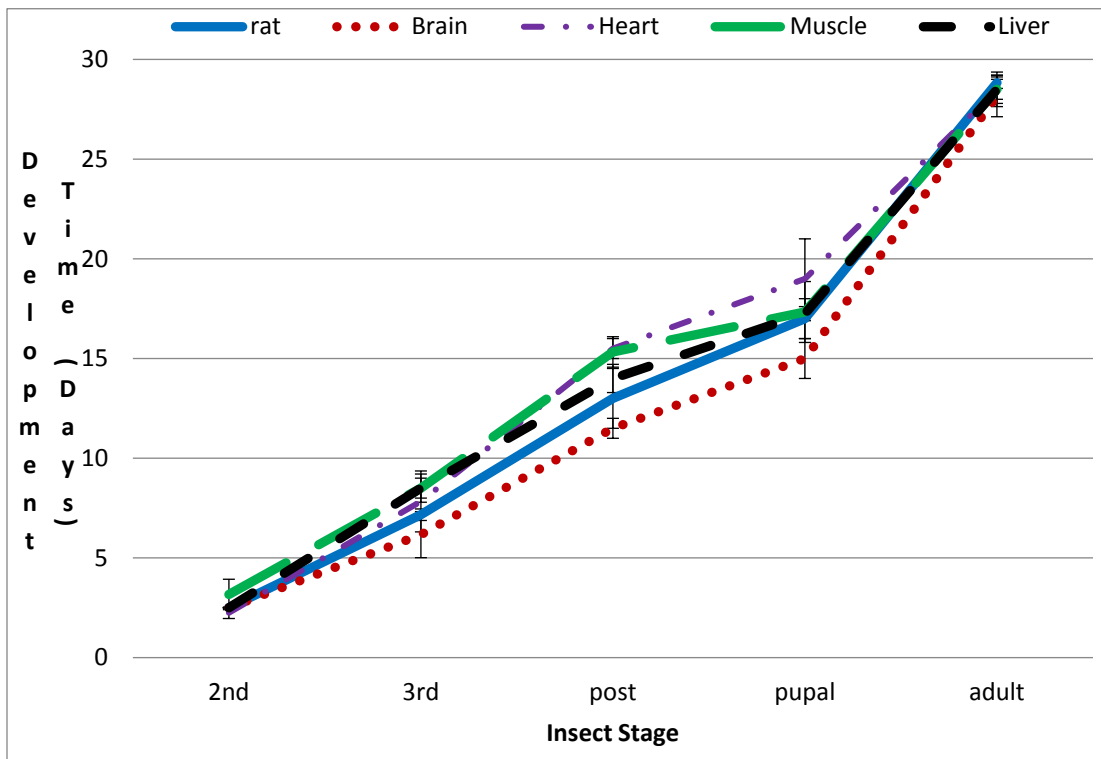


Figure 5-2 Mean maximum development times for *P. terraenovae* to reach each stage at ~17°C in days on whole, wounded rats, and on beef brain, heart, muscle and liver.

On average, insects developing in the jars that contained brain tissue were the first to reach each stage. The exceptions were maximum development time on heart to second instar, and minimum time of development and mode of development to the post-feeding stage (Figure 5-3).

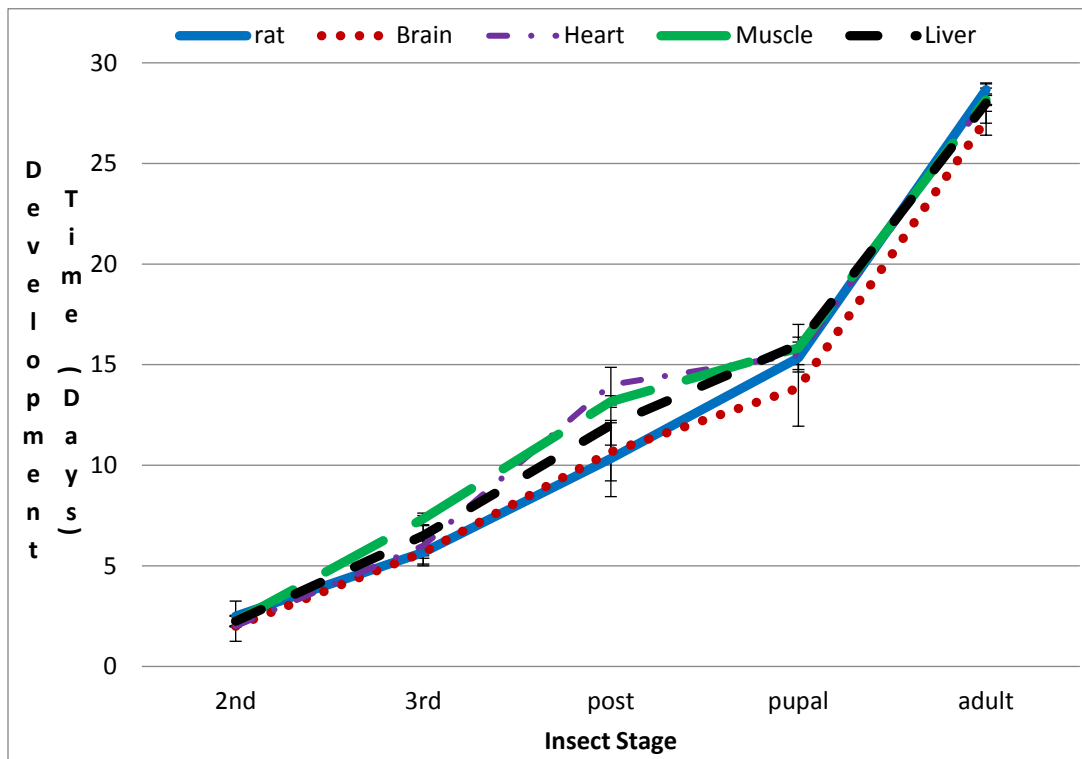


Figure 5-3 Mean of mode development for *P. terraenovae* to reach each stage at ~17°C in days on whole, wounded rats, and on beef brain, heart, muscle and liver.

No significant difference was found for the survival rates between substrates, however, the mortality of the insects developing on brain was highest in the third instar. Also, the second liver replicate died off completely during the second instar. Percent survival was greatest on muscle followed by heart, which was where the insects were the slowest to develop, and survival was lowest on brain, where the insects developed the fastest (Table 5-1). A significant difference in weight was found between substrates for Day 2 puparium measurements ($\alpha = 0.05$, $\chi^2 = 22.0382$, $df = 4$, $p < 0.0002^*$). The insects were weighed at both the adult stage following death as well as on the second day of the intra-puparial period, and the mean weights for each replicate and each substrate are presented in Table 5-2. The ratio of mean intra-puparial to adult weight range from 4.83:1 for those raised on heart to 6.88:1 for those raised on brain. A substantial difference in mean ratio of intra-puparial weight compared to adult weight exists for heart, liver, and muscle compared to a mean ratio of 6.75:1 for the rat. A consistency in size of the pupae in relation to the adult size does not appear to be a set component of the insect's development. Also on Day 2 of the intra-puparial period, length and width measurements

were taken. For a sample of 152, significant differences of the mean length and width measurements were found between substrates. For length, a significant p value of less than 0.0001 was indicated ($\alpha = 0.05$, $\chi^2 = 23.79$, $df = 4$) and for width, a significant p value of less than 0.01 was indicated ($\alpha = 0.05$, $\chi^2 = 12.74$, $df = 4$) (Table 5-3).

Table 5-1 Survival rates for each of the *P. terraenovae* replicates and the mean for each rearing substrate (whole, wounded rat, beef brain, heart, muscle or liver).

Replicate	# Larvae	Adults Emerged	% Survival	%Mean
Rat (1)	70	11	15.7	
Rat (2)	60	12	20	
Rat (3)	65	8	12.3	16.0
Brain (1)	57	5	8.7	
Brain (2)	60	4	6.67	
Brain (3)	70	21	30	15.1
Heart (1)	70	19	27.1	
Heart (2)	68	6	8.82	
Heart (3)	58	23	39.7	25.2
Muscle (1)	51	13	25.5	
Muscle (2)	50	25	50	
Muscle (3)	52	27	51.9	42.5
Liver (1)	57	12	21	
Liver (2)	54	0	0	
Liver (3)	71	23	32.4	17.8

Table 5-2 The mean weights (+/-SD) of *P. terraenovae* pupae on day 2 and the adults two weeks following death .The *P. terraenovae* were raised on whole wounded rat, beef brain, heart, muscle or liver.

Replicate	Mean weight of Pupae	Mean pupal weight for each substrate	Mean weight of Adults	Mean adult weight for each substrate
Rat (1)	0.053+/-0.006g		0.007+/-0.001g	
Rat (2)	0.055+/-0.006g		0.009+/-0.001g	
Rat (3)	0.054+/-0.008g	0.054+/-0.006g	0.007+/-0.002g	0.008+/-0.002g
Brain (1)	0.059+/-0.003g		0.008+/-0.001g	
Brain (2)	0.062+/-0.005g		0.008+/-0.001g	
Brain (3)	0.062+/-0.007g	0.062+/-0.006g	0.010+/-0.001g	0.009+/-0.001g
Heart (1)	0.057+/-0.002g		0.011+/-0.002g	
Heart (2)	0.049+/-0.002g		0.009+/-0.001g	
Heart (3)	0.060+/-0.007g	0.058+/-0.007g	0.013+/-0.001g	0.012+/-0.002g
Muscle (1)	0.057+/-0.005g		0.010+/-0.001g	
Muscle (2)	0.059+/-0.004g		0.011+/-0.002g	
Muscle (3)	0.055+/-0.006g	0.056+/-0.005g	0.009+/-0.002g	0.010+/-0.002g
Liver (1)	0.058+/-0.007g		0.014+/-0.002g	
Liver (2)	Nil		Nil	
Liver (3)	0.059+/-0.008g	0.059+/-0.008g	0.011+/-0.001g	0.012+/-0.002g

Table 5-3 The mean lengths and widths (+/-SD) of the *P. terraenovae* pupae measured on Day 2 of the intra-puparial period. The *P. terraenovae* were raised on whole wounded rat, beef brain, heart, muscle or liver.

	Trial 1		Trial 2		Trial 3	
	Length (mm)	Width (mm)	Length (mm)	Width (mm)	Length (mm)	Width (mm)
Rat	9.4+/-0.5	3.1+/-0.4	9.4+/-0.5	3.1+/-0.4	9.4+/-0.5	3.1+/-0.4
Brain	10.1+/-0.6	3.4+/-0.6	9.9+/-0.4	3.4+/-0.4	9.9+/-0.4	3.5+/-0.5
Heart	9.9+/-0.4	3.4+/-0.5	9.3+/-0.5	3.3+/-0.5	9.8+/-0.5	3.3+/-0.6
Muscle	9.3+/-0.3	3.1+/-0.6	9.7+/-0.3	3.5+/-0.5	9.4+/-0.5	3.2+/-0.5
Liver	9.8+/-0.4	3.6+/-0.4	nil	nil	9.8+/-0.5	3.4+/-0.5

5.6 Discussion

Previous experiments with blow flies have not compared development on different rearing substrates to an entire corpse. The opportunity was taken here to compare development on a wounded rat carcass to development on beef tissues, including the commonly used rearing substrate, liver. Beef liver is used extensively to determine developmental data for many blow fly species, not just *P. terraenovae*. Development rates were found to differ for *P. terraenovae* on the different rearing substrates, but in most cases not significantly. However, significant differences were found for the minimum development times to the adult and post-feeding stages. In all probability, the significant difference to the adult stage can be explained by the significant difference between brain, heart, and muscle alone ($\chi^2 = 5.99$, $df = 2$, $p < 0.05^*$). Also, to further explain the significant difference of the post-feeding stage, although not indicated as being significant, a difference is evident to the post-feeding stage with heart, liver, muscle, and rat ($\chi^2 = 7.81$, $df = 3$, $p < 0.050$). A significant difference was observed in the maximum development time on all substrates to the post-feeding stage only. This difference appears to be the result of

the different rates between development on brain as compared to development on muscle or heart ($\chi^2 = 3.84$, $df = 1$, $p < 0.05^*$). There were no significant differences observed for mode of development for any of the rearing substrates. An analysis of the mean weights of the pupae on Day 2 and the adult flies after death indicated that the mean weights of the insects raised on brain, in the intra-puparial period, were the greatest but produced flies that were some of the smallest at a mean weight of 0.009 g. It can be argued that the insects that developed on muscle and heart fed the longest and produced the greater sized adult flies, however, they still maintained some of the smaller puparia sizes. The insects that developed on liver had a noticeably large mean weight for both the intra-puparial period and the adult stage whereas those that were reared on the rat carcass developed into small pupae and small adults. Size differences of the same species are found based on which organ the insect was feeding on. If insect size were used to estimate age, a strong bias would be transferred to that age determination.

The photoperiod, which naturally fluctuates along with ambient temperature (S. D. Beck, 1983), was not set to fluctuate between light and dark because the temperature was maintained at a constant 17°C. Therefore, to maintain a consistent environment, the chambers remained in continuous light as well as at continuous temperature. The replicate experiments were run in an environment chamber set at 17°C, however, the chamber did not maintain an equivalent temperature throughout, so it was necessary to rotate the replicates in the chamber as well as rotate the jars within each replicate. A significant difference in development between replicates was only found when measuring the maximum development at the adult stage but may be explained by all of the third replicates reaching the adult stage at the same time on the 29th day or the last day. Furthermore, the data logger recordings are not representative of the jar rotations within each replicate because there was only one data logger representing all five jars at one time, so the jars may in fact have been exposed to temperatures that were more similar than alleged.

The liver development data are based predominately on two replicates since the larvae in the second liver replicate all died unexpectedly before the third instar larval stage. This unanticipated result cannot be explained since the beef liver was from the same liver

source as the other experiments and the first instar larvae were randomly selected from the four separate stock colonies and randomly placed into each of the experimental jars.

The weight, length, and width measurements of *P. terraenovae* were taken at the intra-puparial period to determine if a pattern occurs that can be used to further distinguish stages within the intra-puparial period itself. The parameters measured on Day 2 of the intra-puparial period did not indicate a pattern and the use of measured parameters including weight, length, and width is not recommended for *P. terraenovae* puparia since a significant difference was observed for the varying substrates. However, significant differences within substrates were only observed for weight with development on heart, and length with development on muscle. Therefore, the developmental substrate may determine whether these parameters can be used to predict intra-puparial age. An interesting finding that was incidentally noted was the decrease in weight of the pupae as the days passed and an examination of this occurrence may provide further indication of an accurate post-mortem interval for certain species of blow flies and would be worth exploring.

The insects that developed on brain developed the fastest but had an extremely low percent survival from first instar to adult emergence. Although not a statistically significant difference, this is an important trend to be considered for future research. This higher mortality is probably due to brain tissue having higher water content and also being the least nourishing of the experimental substrates (Ireland & Turner, 2006). The insects that developed at the slower rates on muscle and heart had the greatest survival rates. This is suggestive of an inverse relationship between survival and rate of consumption. Research completed on other insects has indicated that there is an optimal balance of dietary requirements and that, if this balance is not met, functioning decreases (Warbrick-Smith, Raubenheimer, Simpson, & Behmer, 2009). Perhaps this is also true for *P. terraenovae* and future research should explore this phenomenon. Furthermore, forthcoming research should involve comparing development rates for wounded versus non-wounded substrates. The decomposition may occur at dissimilar rates as the liquefaction of the rearing position may be affected differently from micro-organism activity increasing alkalinity and from

proteolytic digestion of the excreta from the maggots themselves (Hobson, 1932). Rates may be affected and a significant difference may be observed. It is quite probable that, since variation occurs between some rearing substrates, it may also occur within substrates, and that different development data may be required for the initial stages of non-wounded substrates.

5.7 Conclusion

The research indicated that development of *P. terraenovae* on beef liver follows most closely with that of the development on abdominal wounds of the rat carcass but it cannot be assumed that data collected on liver can be applied under all circumstances. If there are no wounds, the typical insect development occurs on the mucosal tissues of the face and genitalia. Under such circumstances, it is probable that the brain tissue and facial muscles will be consumed first and, therefore, a combination of brain tissue and muscle may best represent the tissues consumed during development. Development may be completed at a different rate than that which is presently assumed. Nevertheless, in a death investigation, it should always be noted as to where on the body the insects were collected so that the closest rearing substrate development data can be applied to the tissues in question.

5.8 Acknowledgements

The authors would like to show their gratitude to Ms. Jennifer Mead for her support and perseverance in assisting in the experiments and maintaining the stock colonies. Another thank you is due to the technical assistance of Ms. Aliasha Stensaker, who stepped into a rather uninviting volunteer position.

5.9 Reference List

- Anderson, G. S. (2000). Minimum and maximum development rates of some forensically important Calliphoridae (Diptera). *Journal of Forensic Science*, 45(4), 824-832.
- Anderson, G. S., & VanLaerhoven, S. L. (1996). Initial studies on insect succession on carrion in southwestern British Columbia. *Journal of Forensic sciences*, 41(4), 613-621.
- Ash, N., & Greenberg, B. (1974). Developmental temperature responses of the sibling species *Phaenicia sericata* and *Phaenicia pallescens*. *Annals of the Entomological Society of America*, 68(2).
- Beck, S. D. (1983). Insect thermoperiodism. *Annual Review of Entomology*, 28, 91-108.
- Bernhardt, V., Schomerus, C., Verhoff, M. A., & Amendt, J. (2016). Of pigs and men-comparing the development of *Calliphora vicina* (Diptera:Calliphoridae) on human and porcine tissue. *International Journal of Legal Medicine*. doi:DOI 10.1007/s00414-016-1487-0
- Beuter, L., & Mendes, J. (2013). Development of *Chrysomya albiceps* (Wiedemann) (Diptera: Calliphoridae) in different pig tissues. *Neotropical Entomology*, 42, 426-430.
- Boatright, S. A., & Tomberlin, J. K. (2010). Effects of temperature and tissue type on the development of *Cochliomyia macellaria* (Diptera: Calliphoridae). *Journal of Medical Entomology*, 47(5), 917-923.
- Catts, E. P. (1992). Problems in estimating the postmortem interval in death investigations. *Journal of Agricultural Entomology*, 9(4), 245-255.
- Clark, K., Evans, L., & Wall, R. (2006). Growth rates of the blowfly, *Lucilia sericata*, on different body tissues. *Forensic Science International*, 156, 145-149.
- Day, D. M., & Wallman, J. F. (2006a). Influence of substrate tissue type on larval growth in *Calliphora augur* and *Lucilia cuprina* (Diptera: Calliphoridae). *Journal of Forensic Science*, 51(3), 657-663.
- Day, D. M., & Wallman, J. F. (2006b). Width as an alternative measurement to length for post-mortem interval estimations using *Calliphora augur* (Diptera: Calliphoridae) larvae. *Forensic Science International*, 159, 158-167.

- Early, M., & Goff, M. L. (1986). Arthropod succession patterns in exposed carrion on the island of Oahu, Hawaii. *Journal of Medical Entomology*, 23(5), 520-531.
- El-Moaty, Z. A., & Kheirallah, A. E. M. (2013). Developmental variation of the blow fly *Lucilia sericata* (Meigen, 1826) (Diptera: Calliphoridae) by different substrate tissue types. *Journal of Asia-Pacific Entomology*, 16, 297-300.
- Flores, M., Longnecker, M., & Tomberlin, J. K. (2014). Effects of temperature and tissue type on *Chrysomya rufifacies* (Diptera: Calliphoridae) (Macquart) development. *Forensic Science International*, 245, 24-29.
- Grassberger, M., & Reiter, C. (2001). Effects of temperature on *Lucilia sericata* (Diptera: Calliphoridae) development with special reference to the Isomegalen- and Isomorphen -Diagram. *Forensic Science International*, 120, 32-36.
- Greenberg, B. (1991). Flies as forensic indicators. *Journal of Medical Entomology*, 28, 565-577.
- Greenberg, B., & Kunich, J. C. (2002). *Entomology and the Law, Flies as Forensic Indicators*. United Kingdom: Cambridge University Press.
- Harnden, L. M., & Tomberlin, J. K. (2016). Effects of temperature and diet on black soldier fly, *Hermetia illucens* (L.) (Diptera: Stratiomyidae), development. *Forensic Science International*, 266, 109-116.
- Hobson, R. P. (1932). Studies on the nutrition of blow fly larvae. III. The liquefaction of muscle. *Journal of Experimental Biology*, 9, 359-365.
- Ireland, S., & Turner, B. (2006). The effects of larval crowding and food type on the size and development of the blowfly, *Calliphora vomitoria*. *Forensic Science International*, 159, 175-181.
- Kamal, A. S. (1958). Comparative study of thirteen species of sarcosaprophagous Calliphoridae and Sarcophagidae (Diptera) I. Bionomics. *Annals of the Entomological Society of America*, 51, 261-270.
- Kaneshrajah, G., & Turner, B. (2004). *Calliphora vicina* larvae grow at different rates on different body tissues. *International Journal of Legal Medicine*, 118, 242-244. doi:DOI 10.1007/s00414-004-0444-5
- Mandeville, D. J. (1988). as cited in Byrd J.H. Laboratory Rearing of Forensic Insects. In J. H. Byrd & J. L. Castner (Eds.), *Forensic Entomology: The Utility of Arthropods in Legal Investigations 2001*. Boca Raton: CRC Press Ltd.

- Niederegger, S., Wartenberg, N., Spiess, R., & Mall, G. (2013). Influence of food substrates on the development of the blowflies *Calliphora vicina* and *Calliphora vomitoria* (Diptera, Calliphoridae). *Parasitology Research*, *112*, 2847-2853.
- Nuorteva, P. (1977). Sarcosaprophagous insects as forensic indicators. In C. G. Tedeschi, W. G. Eckert, & L. G. Tedeschi (Eds.), *Forensic Medicine: A study in trauma and environmental hazards* (pp. 1-680). Philadelphia: WB Saunders Co.
- Payne, J. A. (1965). A summer carrion study of the baby pig *Sus scrofa* Linnaeus. *Ecology*, *46*, 592-602.
- Reiter, C., & Grassberger, M. (2002). *Post-mortem interval estimation using insect development data*. Paper presented at the Proceedings of the First European Forensic Entomology Seminar Rosny sous Bois, France.
- Richards, C. S., Rowlinson, C. C., Cuttiford, L., Grimsley, R., & Hall, M. J. R. (2013). Decomposed liver has a significantly adverse affect on the development rate of the blowfly *Calliphora vicina*. *International Journal of Legal Medicine*, *127*, 259-262.
- Shean, B. S., Messinger, L., & Papworth, M. (1993). Observations of differential decomposition on sun exposed v. shaded pig carrion in coastal Washington State. *Journal of Forensic Science*, *38*(4), 938-949.
- Smith, K. G. V. (1986). *A Manual of Forensic Entomology*. London: British Museum (Natural History).
- Tantawi, T. I., & Greenberg, B. (1993). The effect of killing and preservative solutions on estimates of maggot age in forensic cases. *Journal of Forensic Science*, *38*(3), 702-707.
- Thyssen, P. J., de Souza, C. M., Shimamoto, P. M., Salewski, T. d. B., & Moretti, T. C. (2014). Rates of development of immatures of three species of *Chrysomya* (Diptera: Calliphoridae) reared in different types of animal tissues: implications for estimating the postmortem interval. *Parasitology Research*, *113*, 3373-3380.
- Warbrick-Smith, J., Raubenheimer, D., Simpson, S. J., & Behmer, S. T. (2009). Three hundred and fifty generations of extreme food specialisation: testing predictions of nutritional ecology. *Entomologia Experimentalis et Applicata*, *132*, 65-75.
- Warren, J. A. (2006). *The development of Protophormia terraenovae (Robineau-Desvoidy) (Diptera:Calliphoridae) at constant and fluctuating temperatures*. (Master of Arts), Simon Fraser University, Burnaby.

- Warren, J. A., & Anderson, G. S. (2013). Effect of fluctuating temperatures on the development of a forensically important blow fly, *Protophormia terraenovae* (Diptera: Calliphoridae). *Environmental Entomology*, 42(1), 167-172.
- Wells, J. D., & Lamotte, L. R. (1995). Estimating maggot age from weight using inverse prediction. *Journal of Forensic Science*, 40(4), 585-590.
- Wells, J. D., & Lamotte, L. R. (2001). Estimating the postmortem interval. In J. H. Byrd & J. L. Castner (Eds.), *Forensic Entomology: The Utility of Arthropods in Legal Investigations* (1st edition ed., pp. 263-286). Boca Raton: CRC Press.
- Wilson, J. M., Lafon, N. W., Kreitlow, K. L., Brewster, C. C., & Fell, R. D. (2014). Comparing growth of pork- and venison-reared *Phormia regina* (Diptera: Calliphoridae) for the application of forensic entomology to wildlife poaching. *Journal of Medical Entomology*, 51(5), 1067-1072.

Chapter 6. Hyperspectral measurements of *Lucilia sericata* (Meigen) (Diptera: Calliphoridae) raised on different food substrates

WARREN, J.-A., RATNASEKERA, T.D.P., CAMPBELL, D.A. and ANDERSON, G.S.

Submitted to PLOS ONE (in review and resubmit stage)
(CC BY 4.0 licence)

6.1 Preface

As seen in chapter five, food substrate has an effect on development rate of immature blow flies. This chapter investigates whether food substrate also has an effect on the hyperspectral signature of developing immature *Lucilia sericata*.

6.2 Abstract

Immature *Lucilia sericata* (Meigen) raised on beef liver, beef heart, pork liver and pork heart at a mean temperature of 20.6°C took a minimum of 20 days to complete development. Minimum development time differences within stages were observed between the meat types (pork/beef), but not the organ types (liver/heart). Daily hyperspectral measurements were conducted and a functional regression was completed to examine the main effects of meat and organ type on daily spectral measurements. The model examined post feeding larval spectral measurements of insects raised on beef liver alone, the effect of those raised on pork compared with those raised on beef, the effect of those raised on heart compared with those raised on liver and the interactional effect of those raised on pork heart compared with those raised on beef liver. The analyses indicated

that the spectral measurements of post feeding *L. sericata* raised on pork and beef organs (liver and heart) are affected by the meat and organ type.

6.3 Introduction

Blow flies are **holometabolous** insects and, in some species, most of the immature stages are associated with carrion or remains. These remains are an ephemeral resource that the larval stages depend on for their nutritional requirements. The immature blow fly develops at a predictable rate on the known food source and it is precisely that on which medico-legal entomology is based (Wells & Lamotte, 2010).

One area of medico-legal entomology or forensic entomology includes examining immature blow fly development in order to estimate the tenure of blow flies developing on decomposing corpses in death investigations. The estimated tenure or time since colonization can then be used to infer the minimum elapsed time since death occurred (Benbow et al., 2013; Catts & Goff, 1992; Tomberlin, Mohr, Benbow, Tarone, & VanLaerhoven, 2011).

Unfortunately due to many variables, the minimum time since death, although accurate, is a modest estimate (Tarone & Foran, 2008). Most methods of extrapolating time since death are estimates. Precision is lessened in the latter stages of the lifecycle as those stages are much lengthier than earlier stages (Tarone & Foran, 2008). Finding techniques with more precision in estimating the minimum time since death is of great importance. Forensic entomologists have sought ways to improve current estimation methods by using gas chromatography/mass spectrometry to identify changes in cuticular hydrocarbons commensurate with development (Butcher et al., 2013; Moore, 2013; Moore et al., 2013, 2014; Pechal, Moore, et al., 2014), Micro-Computed Tomography scanning to assist in identifying morphological changes in intra-puparial development throughout metamorphosis (Richards et al., 2012), integrating gene expression variations with conventional methods (Boehme et al., 2013; Tarone & Foran, 2011; Tarone et al., 2007) and, most recently, examining microorganisms associated with carrion (Ma et al., 2012;

Pechal, Crippen, et al., 2014; Pechal et al., 2013; Pechal, Moore, et al., 2014; Tomberlin et al., 2012), all of which improve current methods. Hyperspectral remote sensing has joined the ranks of these methods by improving current means and offering much needed confidence intervals (Tarone & Foran, 2008; Warren et al., 2017a, 2017b), thereby satisfying the United States National Research Council's criticisms of many forensic sciences (Benbow et al., 2013; Council, 2009; Tomberlin, Benbow, Tarone, & Mohr, 2011; Tomberlin, Mohr, et al., 2011).

Hyperspectral remote sensing is a non-intrusive means of sensing and recording reflected energy from a target surface (Nansen et al., 2015). Depending on the wavelengths examined, it combines exhaustive details from the visible spectrum, short wave, near and far infrared. In this case, with each measurement, it is a means to identify changes in the target surface of the immature blow fly as it develops. A spectral signature for each day for each target surface is identified and these signatures change daily (Warren et al., 2017b). These target surface changes can be used to further identify demarcations within larval stages and allow for more precision of time within larval stadia estimations (Warren et al., 2017a, 2017b).

An obstacle that potentially arises is that most laboratory experiments are not completed on entire remains but instead on beef liver or other animal tissues. Differences in development times have been found among different food substrates for several different blow fly species (Beuter & Mendes, 2013; Boatright & Tomberlin, 2010; El-Moaty & Kheirallah, 2013; Flores et al., 2014; Niederegger et al., 2013; Richards et al., 2013; Thyssen et al., 2014; Warren & Anderson, 2009; J. M. Wilson et al., 2014). *Protophormia terraenovae* (Robineau-Desvoidy) development on beef liver was shown to be representative of a whole animal (wounded rat carcass), which supports the use of beef liver in laboratory experiments (Warren & Anderson, 2009). Comparisons of the development of other species of blow fly on whole animals to animal tissue has not been done, and so cannot be commented on; only comparisons between tissues have been made (Bernhardt et al., 2016; Beuter & Mendes, 2013; Boatright & Tomberlin, 2010; El-Moaty & Kheirallah, 2013; Flores et al., 2014; Harnden & Tomberlin, 2016; Niederegger et al.,

2013; Richards et al., 2013; Thyssen et al., 2014; J. M. Wilson et al., 2014). The effects of the food substrate on hyperspectral measurements have not been examined. The objective of this research was to examine the effects of different food substrates on developing immature *Lucilia sericata* (Meigen) and, consequently, the effects on the hyperspectral measurements of the lengthy post feeding stage.

6.4 Materials and Methods

Insect Rearing

Black film canisters positioned on their sides with approximately 50 g of beef liver within were used to collect eggs from two separate colonies of *L. sericata* (Warren et al., 2017b). The colonies originated from recently wild-trapped flies and were provided by Simon Fraser University's Biological Sciences Department. The colonies were maintained on a diet of water, sugar and milk powder *ad libitum*. Also, beef liver was added to the cages regularly as an oviposition medium.

Once eggs were oviposited, they were divided among 16 treatments, four each of beef liver, beef heart, pork liver and pork heart. Each treatment consisted of a one gallon/4L wide mouth glass jar with approximately a five centimetre depth of moistened sawdust topped by a folded industrial paper towel and the appropriate meat source (approximately 250g). An estimated 200-240 eggs from the combined colonies were placed onto each meat type in each treatment. Each jar was secured with two pieces of industrial paper towel and two elastic bands to prevent escape during the post feeding stage.

All treatments were placed into a Conviron[®] E/7 environmental chamber set for 75% relative humidity and a 14:10 (L:D) photoperiod. A mean temperature of 20.6°C was maintained in the chamber and recorded by ACR Systems Inc. Smartbutton[®] data loggers and confirmed daily with Fisherbrand[™] thermometers. The treatments were rotated daily to account for temperature differences within the chamber. Development stage reached was recorded daily and was presented as thermal units, accumulated degree days (ADD). A

base temperature of 0°C was applied since the base temperature for this species is unknown for this geographic location. To calculate,

ADD=Time (days) X (Temperature (°C) –lower threshold (°C)) (Rivers & Dahlem, 2014).

Spectral Measuring

Once the developing *L. sericata* reached the second day of second instar, measurements were taken using an ASD (Analytical Spectral Devices™, Boulder CO) LabSpec 4 Spectrometer. All treatments successfully reached a large enough size by the third day of development and were washed with deionized water and patted with filter paper and finally patted with dry filter paper to dry them before measuring. Attempts were made to measure the larvae earlier but the larvae were too small to measure using the fiber optic probe and guarantee that the measurement was of the larva and not surrounding dark surfaces.

Measurements were completed in a blackened laboratory to ensure that measurements were of the larvae and pupae and not interfering reflecting surfaces. All surfaces and instruments were painted with a matte black paint and the light in the room was that of the light source only. The minimal light from the turned away computer screen and from under the door were consistent and trivial to the measurements.

Each treatment was removed from the environmental chamber once daily beginning at noon and 10 insects were measured from each treatment. Point measurements were taken from the anterior, middle and posterior regions of the washed insect. Calibration using a Spectralon™ panel was completed before starting and following every five to seven measurements. A Spectralon™ panel is a pure diffuse reflectance standard and is the baseline against which all measurements were compared. A black reference was completed each time with the process of optimization of the spectrometer.

Data files were collected by RS³™ software, the program that is specific to ASD spectrometers. Viewspec pro™ was then used to convert the files to text files. Mathworks™ Matlab formulae were then used to transfer the files and organize the Matlab files by day,

meat type and region of measurement to be manipulated for statistical analyses along with fdaM (functional data analysis Matlab) tools (<http://www.psych.mcgill.ca/misc/fda/downloads/FDAfuns/>).

Functional model

The raw spectral reflectance observations, $X_i(w)$ across wavelength (w) for insect i on day Y_i were smoothed using a 6th order B-Spline basis while controlling roughness through a 3rd derivative penalty to reduce the noise associated with the raw spectra (Ramsay & Silverman, 2005). The maximum spectral reflectance scale for each observation was set to one and data were also scaled to have an average reflectance value of zero between 400 and 550 nm wavelengths.

The functional regression equations, where $\beta(w)$ is the contributing regression coefficient for spectral measurements from insects raised on beef liver alone, is given below:

$$Y_i = \int_{350}^{2500} X_{i,smooth}(w)\beta(w)dw \quad \dots \quad (1a)$$

$$\dots \quad + \int_{350}^{2500} X_{i,smooth}(w)\beta_{Pork}(w)dw \quad (1b)$$

$$\dots \quad + \int_{350}^{2500} X_{i,smooth}(w)\beta_{Heart}(w)dw \quad (1c)$$

$$\dots \quad + \int_{350}^{2500} X_{i,smooth}(w)\beta_{Pork\ Heart}(w)dw, \quad (1d)$$

The coefficient function $\beta_{Pork}(w)$ allows for differences in the spectral measurement on the day of development due to changing from beef to pork measurements regardless of organ. The coefficient function $\beta_{Heart}(w)$ allows for differences in the spectral measurement on the day of development due to changing from liver to heart measurements regardless of meat type. The coefficient function $\beta_{Pork\ Heart}(w)$ allows for an interaction in the differences in the spectral measurement on the day of development due to changing from beef liver to pork heart. The model (1a-1d) has additive coefficients from a beef liver baseline. As such, predicting day Y_i with spectral reflectance $X(w)$ for a pork liver substrate, the model

terms used are 1a and 1b. Predicting the day from a beef heart substrate uses 1a and 1c, and predictions when a pork heart substrate is used, all terms 1a-d are applied.

The goal was to predict the development day based on the spectral reflectance curves and to see if the reflectance is affected by changes in meat type and organs used for rearing the insects. A test for the interaction effect of changing from beef liver to pork heart was performed through testing the null hypothesis that $\beta_{Pork\ Heart}(w) = 0$ for all wavelengths, w . Regardless of whether or not there was an interaction effect then the main effect of moving from beef to pork irrespective of organ type can be tested with the null hypothesis that $\beta_{Pork}(w)=0$ for all wavelengths. Similarly, the main effect of moving from liver to heart can be tested with the null hypothesis $\beta_{Heart}(w)=0$ for all wavelengths. Finally, a test of significance of the reflectance in estimating the day of development can be performed by testing the null hypothesis that $\beta(w)=0$ for all w .

All of the functional coefficients $\beta(w)$ were modelled as 6th order B-Spline functions with a roughness penalty on their 3rd derivative to prevent unrealistic fluctuations in the reflectance effect across nearby wavelengths. The roughness penalties for the $X(w)$ and $\beta(w)$ were determined via cross validation.

6.5 Results

Lucilia sericata raised at an average of 20.6 °C takes a minimum of 20 days to complete immature development on beef liver, beef heart, pork liver and pork heart. Development stage reached and accumulated degree days (ADD) with 0°C base temperature is presented for each of the meat substrates in Table 6-1. An extra day was spent in the feeding third instar on each of the pork substrates compared with the beef substrates but development to the adult stage took the same number of days. The insects raised on pork were in the intra-puparial period for nine days rather than 10. Although not measured, based on observation alone, the feeding larvae were smaller on the pork substrates compared with the beef substrates but caught up in size to those feeding on the beef substrates with the extra day of feeding.

Table 6-1 The minimum development stage and accumulated degree days (ADD) of *Lucilia sericata* raised at a mean temperature of 20.6°C on each of the food substrates for each day of development is presented with the day of spectral measuring.

Spectral Measuring	Day of Development	ADD	Beef liver	Beef heart	Pork liver	Pork Heart
--	Day 0	0	Eggs	Eggs	Eggs	Eggs
--	Day 1	21.3	1st instar	1st instar	1st instar	1st instar
--	Day 2	42.8	2nd instar	2nd instar	2nd instar	2nd instar
--	Day 3	64.1	all 2nds	all 2nds	all 2nds	all 2nds
--	Day 4	84.8	3rd instar	3rd instar	3rd instar	3rd instar
--	Day 5	105.4	¹ Postf day1	Postf day1	3rd instar	3rd instar
Day 1	Day 6	126.1	Postf day2	Postf day2	Postf day1	Postf day1
Day 2	Day 7	146.8	Postf day3	Postf day3	Postf day2	Postf day2
Day 3	Day 8	167.4	Postf day4	Postf day4	Postf day3	Postf day3
Day 4	Day 9	187.8	Postf day5	Postf day5	Postf day4	Postf day4
Day 5	Day 10	208.3	² Pupa day1	Pupa day1	Postf day5	Postf day5
--	Day 11	228.9	Pupa day2	Pupa day2	Pupa day1	Pupa day1
--	Day 12	249.7	Pupa day3	Pupa day3	Pupa day2	Pupa day 2
--	Day 13	270.2	Pupa day4	Pupa day4	Pupa day3	Pupa day3
--	Day 14	291.6	Pupa day5	Pupa day5	Pupa day4	Pupa day4
--	Day 15	313.4	Pupa day6	Pupa day6	Pupa day5	Pupa day5
--	Day 16	333.4	Pupa day7	Pupa day7	Pupa day6	Pupa day6
--	Day 17	353.4	Pupa day8	Pupa day8	Pupa day7	Pupa day7
--	Day 18	373.3	Pupa day9	Pupa day9	Pupa day8	Pupa day8
--	Day 19	393.2	Pupa day10	Pupa day10	Pupa day9	Pupa day9
--	Day 20	413.1	Adults	Adults	Adults	Adults

¹Postf = post feeding, ²Pupa = intra-puparial period

Examinations of the spectral measurements of the post feeding larvae raised on each of the substrates were made in relation to beef liver, as beef liver is a substrate that is used regularly to rear blow flies in laboratory research (Warren & Anderson, 2009).

The functional regression model fits for the post feeding stage from measurements of the posterior end, anterior end and midsection are presented in Figures 6-1, 6-2 & 6-3, respectively. The measurements from the midsection and posterior end of the post feeding larvae outweigh the spectral measurements from the anterior end for predicting day within the post feeding stage. The actual day of post feeding development falls outside of the 95% prediction interval more often in the anterior measurements (Figure 6-1) than the midsection and posterior end measurements (Figures 6-2 & 6-3) in the functional regression plots. Also, most days of development are clearly distinguished from each of the other days in the post feeding stage in the midsection and posterior measurements.

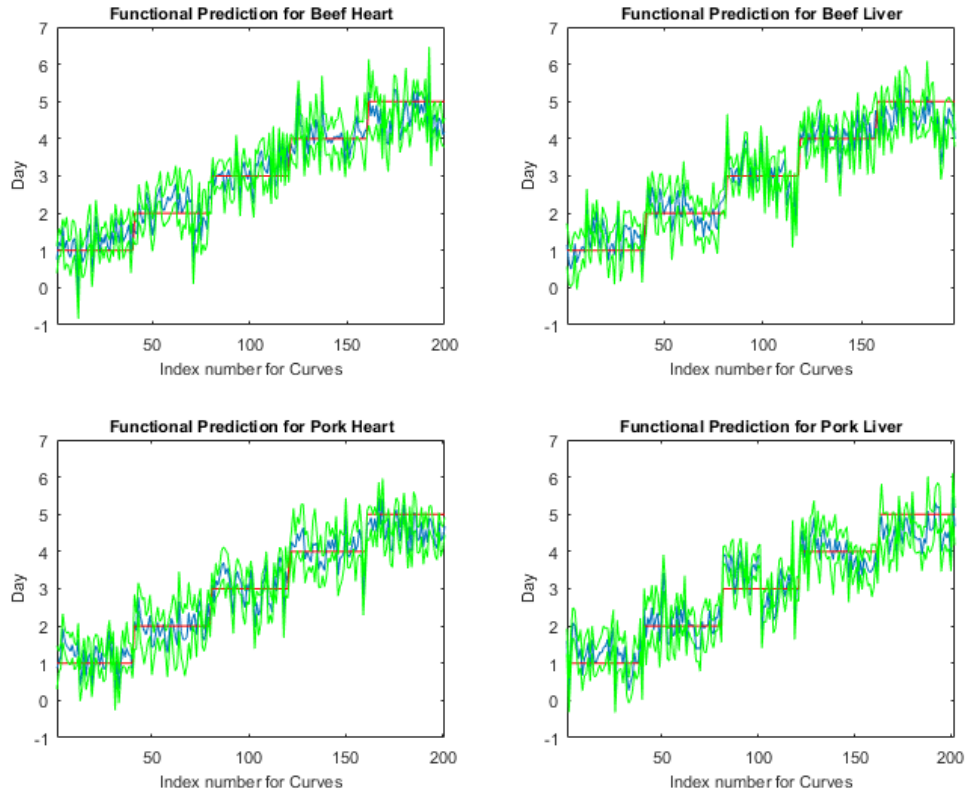


Figure 6-1 The functional regression prediction for day of development in the post feeding stage of *Lucilia sericata* raised at a mean temperature of 20.6°C on beef liver, pork liver, beef heart and pork heart for the anterior end spectral measurements with 95% prediction intervals (green lines are the upper and lower limits). The red line is the actual day and the blue is the predicted day.

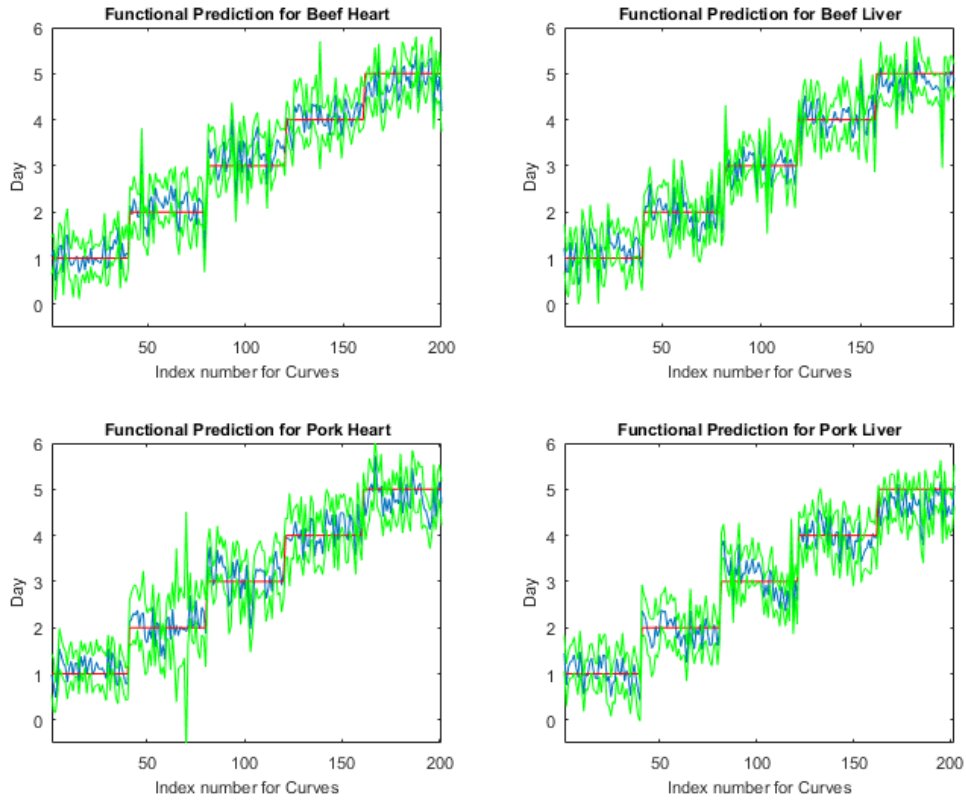


Figure 6-2 The functional regression prediction for day of development in the post feeding stage of *Lucilia sericata* raised at a mean temperature of 20.6°C on beef liver, pork liver, beef heart and pork heart for the midsection spectral measurements with 95% prediction intervals (green lines are the upper and lower limits). The red line is the actual day and the blue is the predicted day.

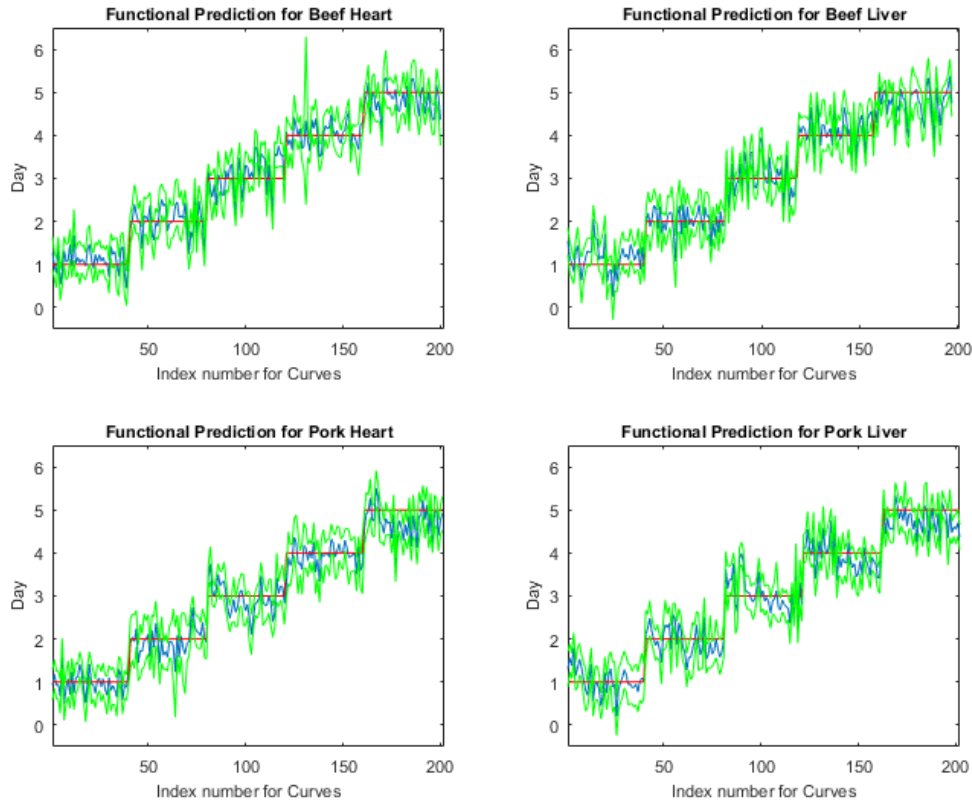


Figure 6-3 The functional regression prediction for day of development in the post feeding stage of *Lucilia sericata* raised at a mean temperature of 20.6°C on beef liver, pork liver, beef heart and pork heart for the posterior end spectral measurements with 95% prediction intervals (green lines are the upper and lower limits). The red line is the actual day and the blue is the predicted day.

As well as the functional regressions, the mean squared error (MSE) indicates that the functional prediction on the meat types have the highest error on anterior end measurements (Table 6-2). Therefore, it has the least accurate prediction capability compared with the midsection and the posterior end of the larvae. To confirm this, the overall percentage of true measurements falling outside of the 95% prediction interval for the anterior end, midsection and posterior end is 40.9%, 25.1% and 31.3%, respectively. The poor prediction capability of the anterior measurements is due to days one and five. This is evident when examining the anterior functional prediction plots in relation to the

functional prediction plots of the midsection and posterior end. Many of the true values that tend to fall outside of the 95% prediction interval are from days one and five.

In addition to the body region findings, the post feeding larvae that were raised on pork heart have the lowest MSE and the lowest number of times that the hyperspectral measurement falls outside of the 95% confidence interval for each body region. These are lowest for pork heart except with midsection measurements where with beef heart the percent of time that the true value falls outside of the 95% confidence interval is lower by a minimal difference of 0.4% than it is with post feeding larvae that were raised on pork heart.

Table 6-2 The fixed effect models for the hyperspectral measurements of the anterior end, midsection and posterior end of post feeding *Lucilia sericata* raised on beef heart, (BH), beef liver (BL), pork heart (PH), and pork liver (PL).

Fixed Effect Models						
Region measured	Meat	Mean Squared Error (MSE)	# Outside	Total #	% of time true value falls outside interval estimate	% total outside interval for region
Anterior end	BH	0.2320	77	200	38.5%	
	BL	0.2630	87	197	44.2%	
	PH	0.1973	74	201	36.8%	
	PL	0.2767	89	202	44.1%	40.9%
Midsection	BH	0.1235	44	200	22.0%	
	BL	0.1375	57	197	28.9%	
	PH	0.1093	45	201	22.4%	
	PL	0.1272	55	202	27.2%	25.1%
Posterior end	BH	0.1159	58	200	29.0%	
	BL	0.1435	68	197	34.5%	
	PH	0.1108	52	201	25.9%	
	PL	0.1286	72	202	35.6%	31.3%
MSE subtotals	Anterior	0.9690				
	Midsection	0.4975				
	Posterior	0.4988				

In a comparison between the observed day and predicted day and the uncertainty associated with the predicted day for each of the measured body regions, it is evident that days one and day five provide the weakest prediction (Figures 6-4, 6-5, & 6-6). In the anterior end measurement plots of predicted versus observed day (Figure 6-4), days two, three and four predictions are similar to the observed or actual day and days one and five predictions are least like the observed day, which is consistent with the mean squared error findings. In the midsection measurement plots of predicted versus observed day (Figure 6-5), in most days, the predicted day falls within the inter-quartile range and the median measurements predict the observed day. The predicted day based on midsection spectral measurements of post feeding larvae raised on beef heart for day three did not match the observed day within the interquartile range but did just outside in the lower whisker or 25th percentile of measurements. For post feeding larvae raised on both beef and pork liver, the predicted day from the spectral measurements for day five falls outside of the interquartile in the upper whisker and so the observed day does not fall in the middle 50% of measurements. The median prediction based on posterior spectral measurements of the post feeding larvae that were raised on beef heart and liver and pork heart and liver was accurate for days one, two, three and four but was just outside in the upper whisker of the interquartile for day five (Figure 6-6). The predicted day falls closest to the observed day in the midsection and posterior measurement compared to the anterior measurements. Prediction of development day was most accurate based on the models that examined insects raised on pork heart.

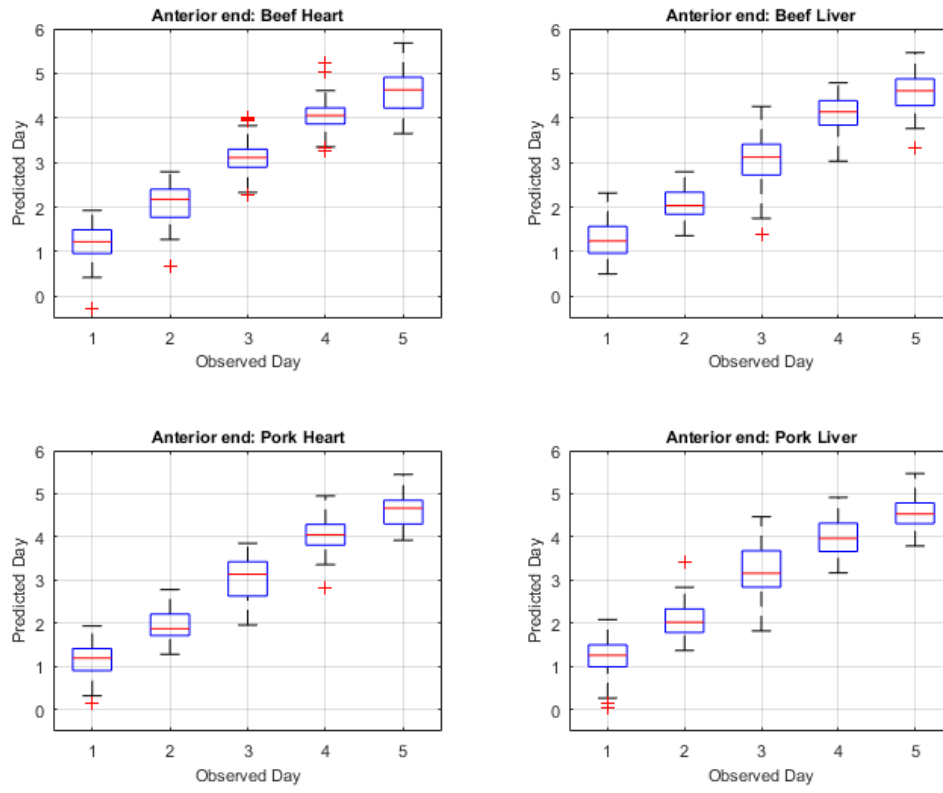


Figure 6-4 Box plots presenting the anterior end hyperspectral measurement prediction of day compared with the observed or actual day of *Lucilia sericata* post feeding larval development on beef heart and liver and pork heart and liver

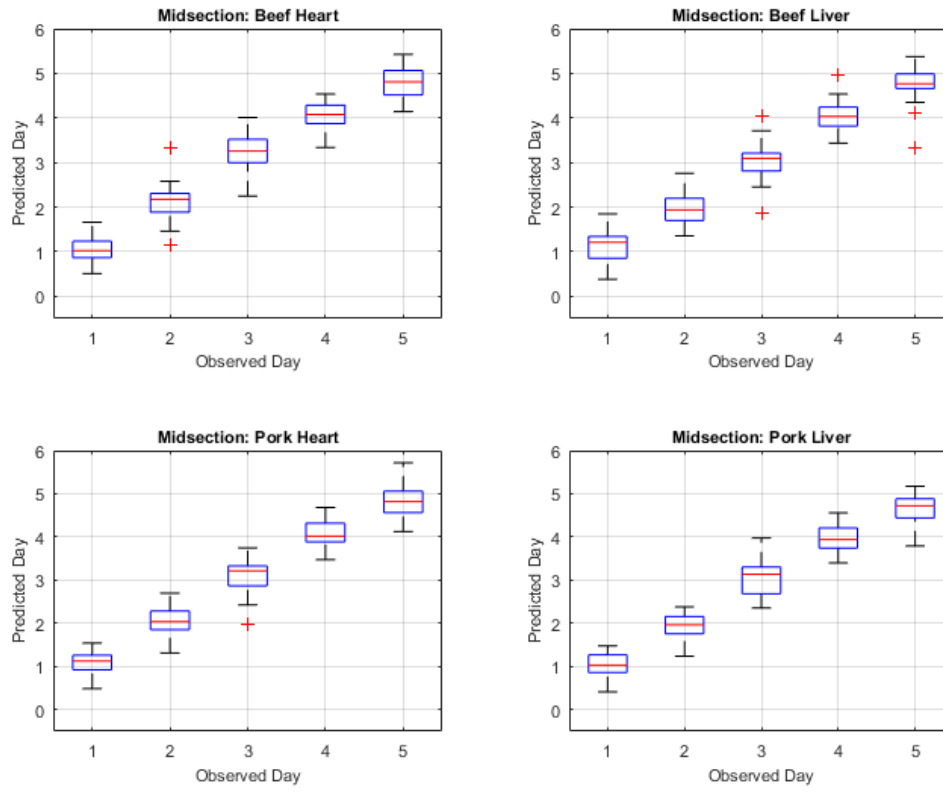


Figure 6-5 Box plots presenting the midsection hyperspectral measurement prediction of day compared with the observed or actual day of *Lucilia sericata* post feeding larval development on beef heart and liver and pork heart and liver

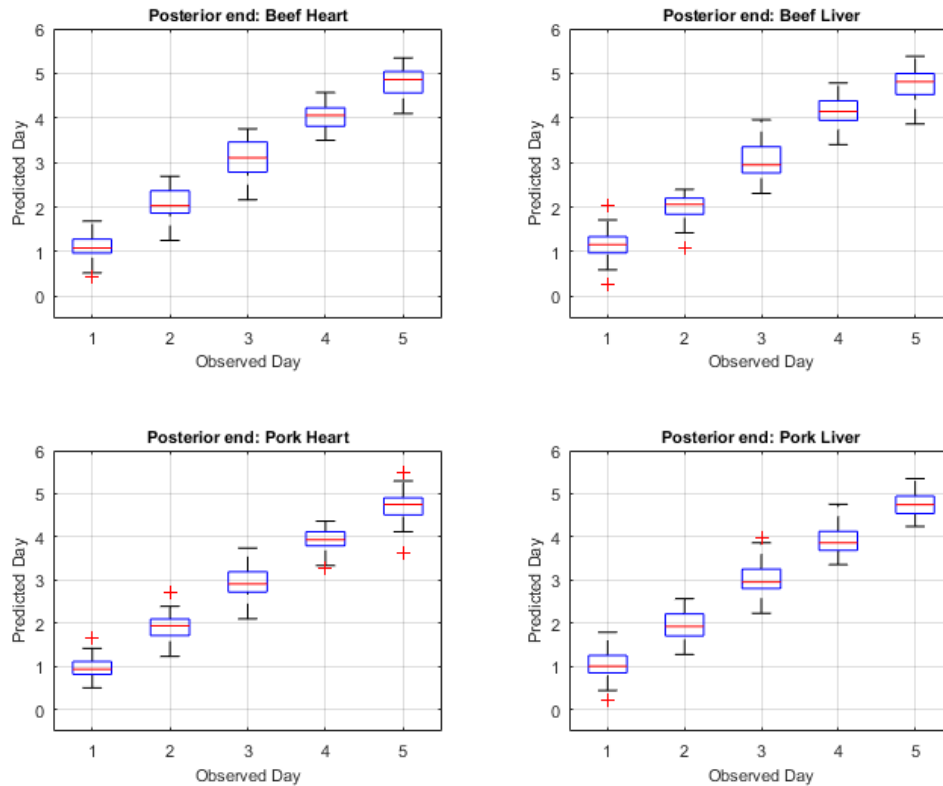


Figure 6-6 Box plots presenting the posterior end hyperspectral measurement prediction of day compared with the observed or actual day of *Lucilia sericata* post feeding larval development on beef heart and liver and pork heart and liver

Based on the coefficient functions (Figures 6-7, 6-8, & 6-9), the ranges of wavelengths that are significant and contributing to the prediction for each meat type can be identified and were highlighted with green vertical bands. The green highlighted bands are the regions of wavelengths where the null hypothesis that there is no regression effect for predicting the day of development is rejected at the 5% significance level. Equivalently, the blue bands in Figures 6-7, 6-8 & 6-9 show the confidence intervals for the regression coefficient effects across wavelengths. The regression effect is particularly evident at wavelengths 350-800nm except for the anterior measurements where the greatest contributions appear to fall between 900 and 1350nm. Each of the regression coefficient functions have significant non-zero effect regions and therefore, the null hypotheses for *L.*

sericata raised on all the meat types were rejected at $p \leq 0.05$ for at least some wavelength bands. The contributing wavelengths for each of the coefficient functions differ, in some cases only slightly, from each other when examining the effect of the organ type and meat type and the interaction effect of different organ and different meat type with pork heart.

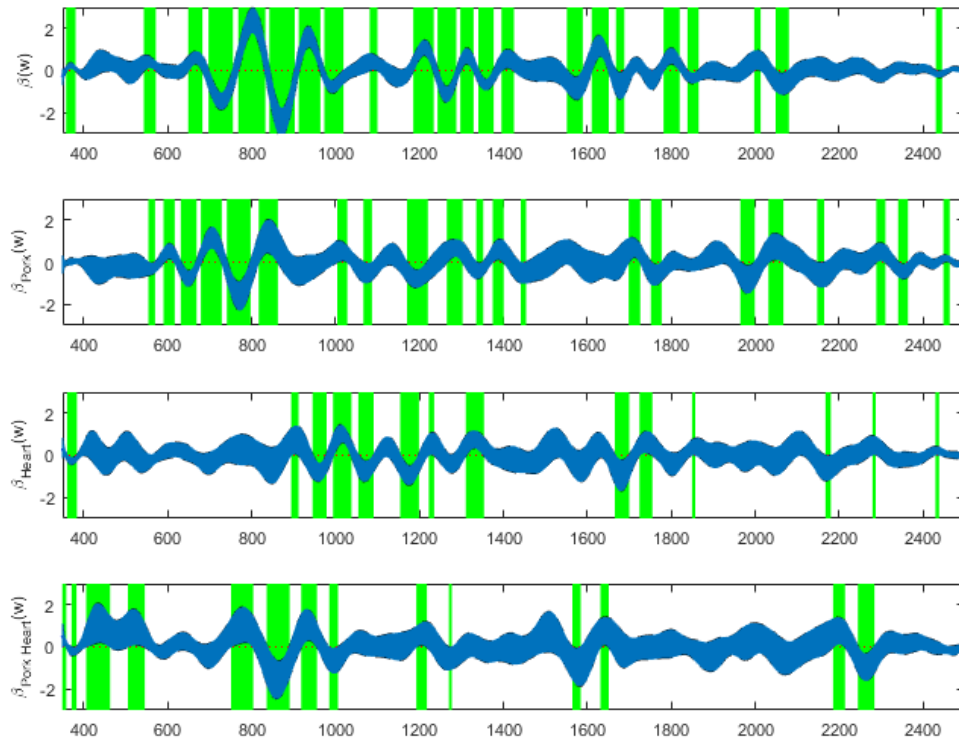


Figure 6-7 The $\beta(w)$ coefficients (y-axis) and contributing wavelengths to the coefficients of the linear regression covariate model for the spectral measurements of the anterior end of post feeding *Lucilia sericata*. The blue area represents the 95% confidence interval and the green bands indicate wavelengths where $\beta(w)$ coefficients are significant. $\beta(w)$ is the contributing β coefficient for spectral measurements from insects raised on beef liver alone. $\beta_{Pork}(w)$ is the contributing β coefficient due to changing from beef to pork measurements regardless of organ. $\beta_{Heart}(w)$ is the contributing β coefficient due to changing from liver to heart measurements regardless of meat type. $\beta_{Pork\ Heart}(w)$ is the contributing β coefficient due to changing from beef liver to pork heart.

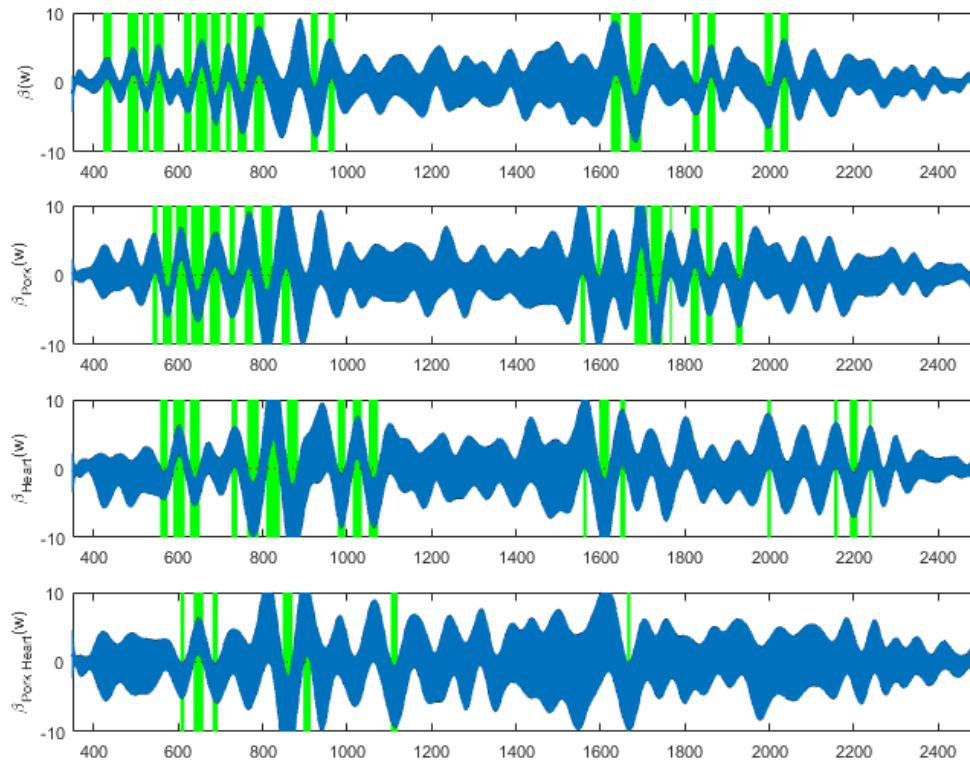


Figure 6-8 The $\beta(w)$ coefficients (y-axis) and contributing wavelengths to the coefficients of the linear regression covariate model for the spectral measurements of the midsection of post feeding *Lucilia sericata*. The blue area represents the 95% confidence interval and the green bands indicate wavelengths where $\beta(w)$ coefficients are significant. $\beta(w)$ is the contributing β coefficient for spectral measurements from insects raised on beef liver alone. $\beta_{Pork}(w)$ is the contributing β coefficient due to changing from beef to pork measurements regardless of organ. $\beta_{Heart}(w)$ is the contributing β coefficient due to changing from liver to heart measurements regardless of meat type. $\beta_{Pork\ Heart}(w)$ is the contributing β coefficient due to changing from beef liver to pork heart.

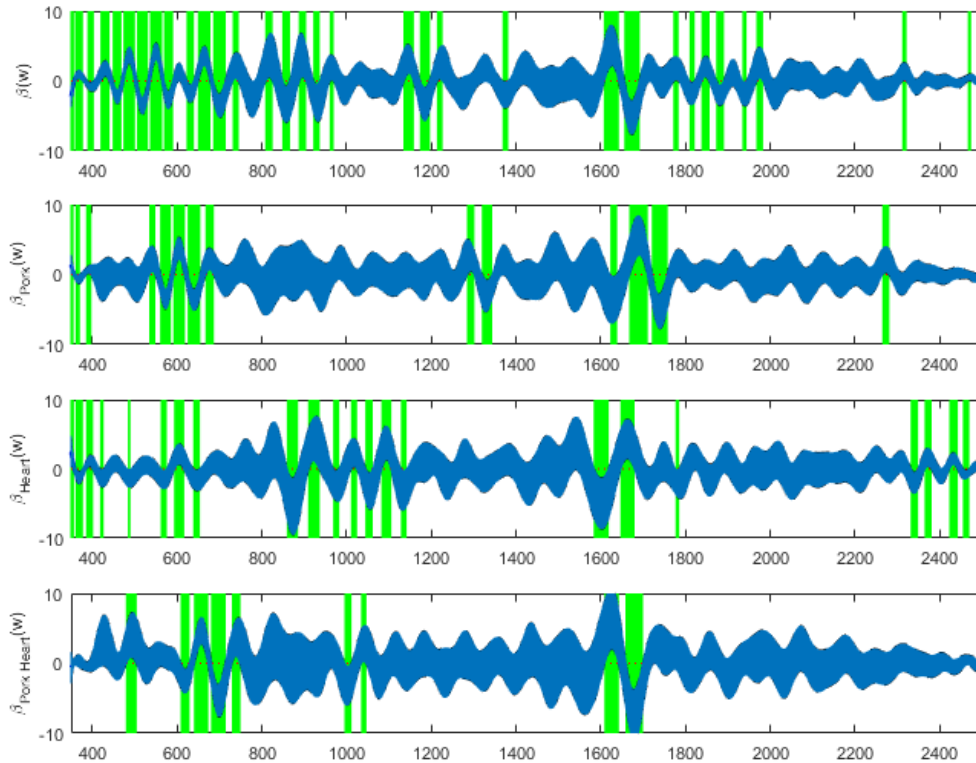


Figure 6-9 The $\beta(w)$ coefficients (y-axis) and contributing wavelengths to the coefficients of the linear regression covariate model for the spectral measurements of the posterior end of post feeding *Lucilia sericata*. The blue area represents the 95% confidence interval and the green bands indicate wavelengths where $\beta(w)$ coefficients are significant. $\beta(w)$ is the contributing β coefficient for spectral measurements from insects raised on beef liver alone. $\beta_{Pork}(w)$ is the contributing β coefficient due to changing from beef to pork measurements regardless of organ. $\beta_{Heart}(w)$ is the contributing β coefficient due to changing from liver to heart measurements regardless of meat type. $\beta_{Pork\ Heart}(w)$ is the contributing β coefficient due to changing from beef liver to pork heart.

6.6 Discussion

Lucilia sericata raised on beef liver and heart increased in size visibly faster than those raised on pork liver and heart. They fed for one day less on beef organs than they did

on pork organs. The larvae feeding on the pork organs were noticeably much smaller but increased in size with the extra day of feeding. These findings were very different from previous findings, which indicate that *L. sericata* grew faster on pork lung, liver and heart than on the same beef tissues (Clark et al., 2006). Differences between the findings for the same species could be a result of geographically separate populations, as it is probable that the earlier research was performed on *L. sericata* trapped in the United Kingdom (Gallagher, Sandhu, & Kimsey, 2010; Grassberger & Reiter, 2002). Genetic and phenotypic differences have been found in *L. sericata* from environmentally separate populations and ecological differences may be a contributor (Tarone et al., 2011). A temperature and size relationship between strains was found in the studied populations (Tarone et al., 2011).

Interestingly, adult *L. sericata* reared on beef or pork began emerging on the same day, and so the *L. sericata* raised on pork spent one less day in the intra-puparial period. The nutritional value of pork heart and liver does not explain the need for the extra day of feeding in comparison with the beef organs (Table 6-3) but fatty acids may. Fatty acids increase the oily consistency of the meat substrate (Wood et al., 2008) and the beef heart was noticeably oilier than the pork heart. The oily consistency of the beef and pork liver was not detectable because of the moist surface consistency of liver. Since beef animals primarily have a grass diet, their vitamin E intake is higher thereby increasing their polyunsaturated fatty acid (PUFA) levels at slaughter to higher than that of pork (Wood et al., 2008). Without Vitamin E in a ruminants' diet, however, oxidation of the fatty acids is faster than that of porcine following slaughter (Wood et al., 2008). Vitamin E slows the oxidation of PUFAs and causes an oily consistency (Wood et al., 2008), which may have made it easier for the third instar larvae to break the surface of the beef substrates when feeding compared with the larvae feeding on the pork substrates accounting for the extra day of feeding. There was no delay with the earlier larval stages feeding on pork and this is probably because there was enough liquid protein in those first feeding days for the less developed mouth parts of first and second instar larvae.

Table 6-3 Nutritional value per 100g of meat substrate

	Beef liver	Beef heart	Pork liver	Pork heart
Calories/ fat cal	135/32.7	112/35.5	134/32.9	118/39.3
Fat total/sat (g)	3.6/1.2	3.9/1.4	3.6/1.2	4.4/1.2
Cholesterol(mg)	275	124	301	131
Carbohydrates (g)	3.9	0.1	2.5	1.3
Protein (g)	20.4	17.7	21.4	17.3
Water content (g)	70.8	77.1	71.1	76.2

(<http://nutritiondata.self.com/> accessed Jun04 2017)

One of the four replicates for each of the pork liver and pork heart took more time (an extra day for pork heart and an extra two days for pork liver) for the adults to begin emerging. This was probably due to much greater mortality in these replicates as higher mortality was observed in these slower developing replicates.

The anterior measurement median predictions are consistent with the observed day for days two, three and four but are not for days one and five. These results support the findings of the higher mean squared error for the anterior measurements. The median prediction based on midsection spectral measurements of post feeding larvae that were raised on pork heart according to the box plots was most consistent with the observed day as compared with development on the other meat types and organs. This is consistent with the mean squared error findings. The lowest mean squared error was observed with development on pork heart and spectral measurements of the midsection. The accurate median prediction for most days but day five from the posterior measurements is consistent with the low mean squared errors from the posterior end measurements of post feeding

larvae raised on all the meat types and would explain the higher mean squared error than the midsection measurements.

Based on the coefficient functions, Figures 6-7, 6-8, & 6-9, there are fewer significant wavelengths for pork heart, particularly in the midsection and posterior measurements; this can potentially explain the lower MSE for pork heart compared with the other meat types (Table 6-2). Surprisingly the MSE is very slightly lower in the midsection measurements than the posterior end measurements for predicting day of development. Previous findings have found that prediction based on posterior measurements has outweighed those of anterior and midsection measurements for *P. terraenovae* (Warren et al., 2017a) and *L. sericata* (Warren et al., 2017b) when raised on veal liver and beef liver, respectively. The slightly lower MSE subtotal for midsection is probably a result of the lower pork heart MSE and the lower percent of times that the true value for beef heart fell outside of the 95% confidence interval (Table 6-2). The true value fell outside of the 95% confidence interval only 0.4% fewer times for the post feeding larvae that were raised on beef heart than those raised on pork heart. From an overall perspective, the majority of the wavelengths at which measurements were taken do not contribute to the prediction as their functional coefficients are not significant and focus can remain on those wavelengths identified in Figures 6-7, 6-8 & 6-9.

The spectral measurements from the midsection and posterior end of the *L. sericata* larvae were found to be superior for predicting the day within the post feeding stage as compared with anterior measurements. This is probably a result of the ectodermal oenocytes which produce cuticular hydrocarbons (Martins & Ramalho-Ortigão, 2012). They are often located in the abdomen of the larvae in close proximity to the spiracles but are species and stage dependent (Fan et al., 2003). The cuticular hydrocarbons are then transported by lipophorin in the haemolymph to the remaining cuticle and fat body (Fan et al., 2003; Makki et al., 2014). The oenocytes have been found to grow and form new variations with each moult (Klowden, 2007; Makki et al., 2014), and so it is very probable that the change in oenocytes may result in changes to the cuticular hydrocarbons.

The anterior end of the larvae was found to be particularly poor for predicting age of larvae and there may have been several causes for this. First, the anterior end was a smaller target and the larvae had a tendency to move their anterior regions away from the fiber optic probe when attempting to position them and hold them still for long enough to complete a measurement. Second, the cuticular hydrocarbons may potentially not be as abundant or were lacking precision in delivery to that region since it is farthest from the oenocytes and the hydrocarbons require transport to this region. Third, feeding has stopped upon entering the post feeding stage and so there may no longer be a release of digestive enzymes potentially laced with bacteria on the anterior end of the insect surface (Ma et al., 2012). Day five prediction was probably least convincing because the insects were transitioning from the post feeding stage to the intra-puparial period and so were reducing their transport of cuticular hydrocarbons to the surface in preparation for apolysis. This would reduce the changes to the insect cuticle and make it more difficult to distinguish from the previous day, as was seen in Figures 6-1, 6-2 & 6-3 where the blue prediction line somewhat blurs between the last two days. This is much more evident in Figure 6-1, the anterior end measurements.

The experiments showed that the food substrate on which insects are raised does have a minimal effect on the day of development prediction from spectral measurements. The functional regressions from each body region indicated that, when examining the effect of spectral measurements from insects raised on pork to those on beef, there is an effect on predicting day within the post feeding stage. Similarly, when examining the effect of *L. sericata* spectral measurements raised on heart compared with those raised on liver, there was also an effect. Day predictions within the post feeding stage were also affected when examining the interactional effect of both organ and meat type, pork heart in reference to beef liver.

It is most probable that differences in the cuticular hydrocarbons are due to differences in the food substrates. There is a strong possibility that the fatty acids in the food substrates were impacting the cuticular hydrocarbon profile since this has been reported to occur in the herbivorous mustard leaf beetle, *Phaedon cochleariae* (F.). The

mustard leaf beetle was fed artificial diets of fatty acids and this resulted in changes to the straight chain and methyl-branched cuticular hydrocarbons (Otte, Hilker, & Geiselhardt, 2015).

Based on the coefficient functions (Figures 6-7, 6-8, & 6-9), the significantly nonzero portions of the $\beta_{Pork\ Heart}(w)$ functions that are contributing to the interactional effect are not as numerous as the contributing $\beta(w)$ coefficients in the beef liver alone model. Also, for the meat and organ type effect, there are missing and extra contributing $\beta(w)$ coefficients that are not contributing to the beef liver alone model. Hence the significance of different wavelength regions within all of the coefficient functions across all of the body regions shows that there are additional wavelengths of spectral measurements contributing to differentiating the model during changes in meat type and organ choice. The β coefficients indicate whether or not a significant relationship exists between wavelength and spectral reflectance for the measured insects and also indicates at which wavelengths a significant relationship exists. Although day predictions are accurate, the differences in β coefficients and, therefore, different contributing wavelengths indicate why care must be taken when using spectral measurements to age larvae raised on different food substances. This is particularly important when applying findings from different food substrates to casework.

6.7 Acknowledgements

We would like to thank the many volunteers that assisted with the spectral measuring and maintaining the *Lucilia sericata* colonies. We would also like to thank ASD Inc, a Panalytical company for awarding J. Warren the Alexander Goetz prize so that this research could be conducted.

6.8 Reference List

- Benbow, M. E., Lewis, A. J., Tomberlin, J. K., & Pechal, J. L. (2013). Seasonal necrophagous insect community assembly during vertebrate carrion decomposition. *Journal of Medical Entomology*, *50*(2), 440-450.
- Bernhardt, V., Schomerus, C., Verhoff, M. A., & Amendt, J. (2016). Of pigs and men-comparing the development of *Calliphora vicina* (Diptera:Calliphoridae) on human and porcine tissue. *International Journal of Legal Medicine*. doi:10.1007/s00414-016-1487-0
- Beuter, L., & Mendes, J. (2013). Development of *Chrysomya albiceps* (Wiedemann) (Diptera: Calliphoridae) in different pig tissues. *Neotropical Entomology*, *42*, 426-430.
- Boatright, S. A., & Tomberlin, J. K. (2010). Effects of temperature and tissue type on the development of *Cochliomyia macellaria* (Diptera: Calliphoridae). *Journal of Medical Entomology*, *47*(5), 917-923.
- Boehme, P., Spahn, P., Amendt, J., & Zehner, R. (2013). Differential gene expression during metamorphosis: a promising approach for age estimation of forensically important *Calliphora vicina* pupae (Diptera: Calliphoridae). *International Journal of Legal Medicine*, *127*, 243-249.
- Butcher, J. B., Moore, H. E., Day, C. R., Adam, C. D., & Drijfhout, F. P. (2013). Artificial neural network analysis of hydrocarbon profiles for the ageing of *Lucilia sericata* for post mortem interval estimation. *Forensic Science International*, *232*, 25-31.
- Catts, E. P., & Goff, M. L. (1992). Forensic entomology in criminal investigations. *Annual Review of entomology*, *37*, 253-272.
- Clark, K., Evans, L., & Wall, R. (2006). Growth rates of the blowfly, *Lucilia sericata*, on different body tissues. *Forensic Science International*, *156*, 145-149.
- Council, N. R. (2009). *Strengthening Forensic Science in the United States: A Path Forward*. Washington, D.C.: The National Academies Press.
- El-Moaty, Z. A., & Kheirallah, A. E. M. (2013). Developmental variation of the blow fly *Lucilia sericata* (Meigen, 1826) (Diptera: Calliphoridae) by different substrate tissue types. *Journal of Asia-Pacific Entomology*, *16*, 297-300.

- Fan, Y., Zurek, L., Dykstra, M. J., & Schal, C. (2003). Hydrocarbon synthesis by enzymatically dissociated oenocytes of the abdominal integument of the German Cockroach, *Blattella germanica*. *Naturwissenschaften*, *90*, 121-126.
- Flores, M., Longnecker, M., & Tomberlin, J. K. (2014). Effects of temperature and tissue type on *Chrysomya rufifacies* (Diptera: Calliphoridae) (Macquart) development. *Forensic Science International*, *245*, 24-29.
- Gallagher, M. B., Sandhu, S., & Kimsey, R. (2010). Variation in developmental time for geographically distinct populations of the common Green Bottle Fly, *Lucilia sericata* (Meigen). *Journal of Forensic Science*, *55*(2), 438-442. doi:10.1111/j.1556-4029.2009.01285.x
- Grassberger, M., & Reiter, C. (2002). Effect of temperature on development of the forensically important holarctic blow fly *Protophormia terraenovae* (Robineau-Desvoidy) (Diptera:Calliphoridae). *Forensic Science International*, *128*, 177-182.
- Harnden, L. M., & Tomberlin, J. K. (2016). Effects of temperature and diet on black soldier fly, *Hermetia illucens* (L.) (Diptera: Stratiomyidae), development. *Forensic Science International*, *266*, 109-116.
- Klowden, M. J. (2007). *Physiological Systems in Insects*. Burlington MA: Elsevier Inc.
- Ma, Q., Fonseca, A., Liu, W., Fields, A. T., Pimsler, M. L., Spindola, A. F., . . . Wood, T. K. (2012). *Proteus mirabilis* interkingdom swarming signals attract blow flies. *International Society for Microbial Ecology*, *6*, 1356-1366.
- Makki, R., Cinnamon, E., & Gould, A. P. (2014). The development and functions of oenocytes. *Annual Review of entomology*, *59*, 405-425. doi:10.1146/annurev-ento-011613-162056
- Martins, G. F., & Ramalho-Ortigão, J. M. (2012). Oenocytes in insects. *Invertebrate Survival Journal*, *9*(2).
- Moore, H. E. (2013). *Analysis of cuticular hydrocarbons in forensically important blowflies using mass spectrometry and its application in Post Mortem Interval estimations*. (Doctor of Philosophy), Keele University, Keele Staffordshire University.
- Moore, H. E., Adam, C. D., & Drijfhout, F. P. (2013). Potential Use of Hydrocarbons for Aging *Lucilia sericata* Blowfly Larvae to Establish the Postmortem Interval. *Journal of Forensic Science*, *58*(2), 404-412.

- Moore, H. E., Adam, C. D., & Drijfhout, F. P. (2014). Identifying 1st instar larvae for three forensically important blowfly species using “fingerprint” cuticular hydrocarbon analysis. *Forensic Science International*, *240*, 48-53.
- Nansen, C., Ribeiro, L. P., Dadour, I., & Roberts, J. D. (2015). Detection of temporal changes in insect body reflectance in response to killing agents. *PlosONE*, *10*(4), 1-15. doi:10.1371/journal.pone.0124866
- Niederegger, S., Wartenberg, N., Spiess, R., & Mall, G. (2013). Influence of food substrates on the development of the blowflies *Calliphora vicina* and *Calliphora vomitoria* (Diptera, Calliphoridae). *Parasitology Research*, *112*, 2847-2853.
- Otte, T., Hilker, M., & Geiselhardt, S. (2015). The effect of dietary fatty acids on the cuticular hydrocarbon phenotype of an herbivorous insect and consequences for mate recognition. *Journal of Chemical Ecology*, *41*, 32-43. doi:10.1007/s10886-014-0535-9
- Pechal, J. L., Crippen, T. L., Benbow, M. E., Tarone, A. M., Dowd, S., & Tomberlin, J. K. (2014). The potential use of bacterial community succession in forensics as described by high throughput metagenomic sequencing. *International Journal of Legal Medicine*, *128*, 193-205.
- Pechal, J. L., Crippen, T. L., Tarone, A. M., Lewis, A. J., Tomberlin, J. K., & Benbow, M. E. (2013). Microbial community functional change during vertebrate carrion decomposition. *PlosONE*, *8*(11), 1-11 e79035.
- Pechal, J. L., Moore, H. E., Drijfhout, F., & Benbow, M. E. (2014). Hydrocarbon profiles throughout adult Calliphoridae aging: A promising tool for forensic entomology. *Forensic Science International*, *245*, 65-71.
- Ramsay, J. O., & Silverman, B. W. (2005). *Functional Data Analysis*. New York: Springer.
- Richards, C. S., Rowlinson, C. C., Cuttiford, L., Grimsley, R., & Hall, M. J. R. (2013). Decomposed liver has a significantly adverse affect on the development rate of the blowfly *Calliphora vicina*. *International Journal of Legal Medicine*, *127*, 259-262.
- Richards, C. S., Simonsen, T. J., Abel, R. L., Hall, M. J. R., Schwyn, D. A., & Wicklein, M. (2012). Virtual forensic entomology: Improving estimates of minimum post-mortem interval with 3D micro-computed tomography. *Forensic Science International*, *220*, 251-264.
- Rivers, D. B., & Dahlem, G. A. (2014). *The Science of Forensic Entomology*. Oxford: Wiley Blackwell.

- Tarone, A. M., & Foran, D. R. (2008). Generalized additive models and *Lucilia sericata* growth: Assessing Confidence intervals and error rates in forensic entomology. *Journal of Forensic Science*, 53(4), 942-948.
- Tarone, A. M., & Foran, D. R. (2011). Gene expression during blow fly development: Improving the precision of age estimates in forensic entomology. *Journal of Forensic Science*, 56(S1), S112-S122.
- Tarone, A. M., Jennings, K. C., & Foran, D. R. (2007). Aging blow fly eggs using gene expression: A feasibility study. *Journal of Forensic Science*, 52(6), 1350-1354.
- Tarone, A. M., Picard, C. J., Spiegelman, C., & Foran, D. R. (2011). Population and temperature effects on *Lucilia sericata* (Diptera: Calliphoridae) body size and minimum development time. *Journal of Medical Entomology*, 48(5), 1062-1068. doi:10.1603/me11004
- Thyssen, P. J., de Souza, C. M., Shimamoto, P. M., Salewski, T. d. B., & Moretti, T. C. (2014). Rates of development of immatures of three species of *Chrysomya* (Diptera: Calliphoridae) reared in different types of animal tissues: implications for estimating the postmortem interval. *Parasitology Research*, 113, 3373-3380.
- Tomberlin, J. K., Benbow, M. E., Tarone, A. M., & Mohr, R. M. (2011). Basic research in evolution and ecology enhances forensics. *Trends in Ecology and Evolution*, 26(2), 53-55.
- Tomberlin, J. K., Crippen, T. L., Tarone, A. M., Singh, B., Adams, K., Rezenom, Y. H., . . . Wood, T. K. (2012). Interkingdom responses of flies to bacteria mediated by fly physiology and bacterial quorum sensing. *Animal Behaviour*, 84, 1449-1456.
- Tomberlin, J. K., Mohr, R., Benbow, M. E., Tarone, A. M., & VanLaerhoven, S. (2011). A Roadmap for bridging basic and applied research in forensic entomology. *Annual Review of Entomology*, 56, 401-421.
- Warren, J.-A., Ratnasekera, T. D. P., Campbell, D. A., & Anderson, G. S. (2017a). Initial investigations of spectral measurements to estimate the time within stages of *Protophormia terraenovae* (Robineau-Desvoidy) (Diptera: Calliphoridae). *Forensic Science International*, 278, 205-216. doi:10.1016/j.forsciint.2017.06.027
- Warren, J.-A., Ratnasekera, T. D. P., Campbell, D. A., & Anderson, G. S. (2017b). Spectral Signature of Immature *Lucilia sericata* (Meigen) (Diptera: Calliphoridae). *Insects*, 8(2). doi:10.3390/insects8020034

- Warren, J. A., & Anderson, G. S. (2009). A comparison of development times for *Protophormia terraenovae* (R-D) reared on different food substrates. *Canadian Society of Forensic Science Journal*, 42(3), 161-171.
- Wells, J. D., & Lamotte, L. R. (2010). *Estimating the postmortem interval* (second ed.). Ch 9 of *The Utility of Arthropods in Legal investigations* edited by Byrd, J.H. and Castner, J.L: CRC Press.
- Wilson, J. M., Lafon, N. W., Kreitlow, K. L., Brewster, C. C., & Fell, R. D. (2014). Comparing growth of pork- and venison-reared *Phormia regina* (Diptera: Calliphoridae) for the application of forensic entomology to wildlife poaching. *Journal of Medical Entomology*, 51(5), 1067-1072.
- Wood, J. D., Enser, M., Fisher, A. V., Nute, G. R., Sheard, P. R., Richardson, R. I., . . . Whittington, F. M. (2008). Fat deposition, fatty acid composition and meat quality: A review. *Meat science*, 78, 343-358.

Chapter 7. Hyperspectral measurements of the larval cuticular hydrocarbons of *Lucilia sericata* (Meigen) (Diptera: Calliphoridae)

WARREN J.-A., RATNASEKERA, T.D.P., CAMPBELL, D.A., and ANDERSON, G.S.

To be submitted to Journal of Forensic Entomology once they begin accepting submissions

7.1 Preface

Since daily delineations have been identified within the lengthier post feeding stage of *Protophormia terraenovae* and the post feeding and intra-puparial period of *Lucilia sericata* and the effect of food source on the spectral measurements has been examined, the next step is to postulate what is contributing to the spectral measurements. The most probable contributors are the cuticular hydrocarbons since they change day to day similarly to the reflectance spectral signature of the larval stages. The changes to the fat body and brain within the intra-puparial period are the probable contributors to the spectral signatures and light reflectance is most probably possible through the modified pore canals of the puparium. To determine precisely what is causing the spectral changes would be beyond the scope of this dissertation and so this chapter compares the changes in daily cuticular hydrocarbons to the daily spectral changes.

7.2 Abstract

Hyperspectral measurements of washed *Lucilia sericata* (Meigen) larvae raised at 25°C were collected each day from second instar to the intra-puparial period from three replicate colonies. Measurements were of the anterior end/midsection/posterior end of the larvae. Each day a sample weighing ~130mg from each of these measured insects, which

ranged from third instar until intra-puparial development, was collected from each replicate and then the cuticular hydrocarbons were extracted using hexane. Gas chromatography/mass spectrometry was then performed on the eluted sample to examine the cuticular hydrocarbons (C₂₂ to C₃₁) and their changes. The cuticular hydrocarbon findings were compared with the leading findings of Moore et al. (2013) and showed similar trends. Cuticular hydrocarbons changed daily as did the hyperspectral reflectance measurements. Some differences were observed between replicates, which suggest that they were not absolute replicates and so the functional regression model examined all three replicates individually. Further supporting that cuticular hydrocarbons are the foremost contributor to spectral reflectance measurements, prediction of day was best from the posterior measurements and inferior the further away the measurements were taken from the posterior integument where the oenocytes are often located.

7.3 Introduction

Among many other uses, forensic entomology is applied to death investigations to estimate the minimum elapsed time since death occurred, and this allows death investigators to focus their investigation into the correct time frame (Amendt et al., 2011; Gennard, 2012; Rivers & Dahlem, 2014). In order to add further precision to this estimate, forensic entomologists are combining forensic entomology with other sciences such as gene expression (Tarone et al., 2007; Tarone et al., 2011), cuticular hydrocarbon and volatile organic compound chemistry (Butcher et al., 2013; Frederickx et al., 2012; Moore, 2013; Moore et al., 2013, 2014; Pechal, Moore, et al., 2014; Xu et al., 2014; Zhu et al., 2007) and now hyperspectral remote sensing (Voss et al., 2016; Warren et al., 2017a, 2017b) to improve age estimates within lengthier stadia. Most estimates are of the minimum time it takes early arriving necrophagous insects to reach the oldest stage of development on the body. Although an accurate estimate, this method lacks precision in the lengthier immature stages. Depending on temperature, third instar, post feeding and intra-puparial period (combining the prepupal, pupal and pharate adult stages (Martin-Vega et al., 2016)), can take weeks. Providing a minimum time that the oldest insects take

to reach a stage offers a wide investigative time frame and can result in wasted resources used to investigate unnecessary time frames instead of the period of interest.

There are many drawbacks to trying to improve the precision with many of these methods, which require expensive equipment, trained personnel and are destructive to the sample. By definition, however, hyperspectral remote sensing, is non-destructive (G. Payne, Wallace, et al., 2005) and is not invasive so does not affect insect development. An incident light source is radiated on the insect for a short time, and the light reflecting from the insect surface is measured using a fibre optic cable held approximately 2 mm from the insect surface and attached to a spectrometer.

Reflectance spectral signatures are being applied to identify changes over time in many forensic fields such as aging bloodstains (Bremmer, de Bruin, et al., 2011; Bremmer, Nadort, et al., 2011; Edelman, Manti, et al., 2012; Edelman, van Leeuwen, et al., 2012; B. Li et al., 2011; Li et al., 2013, 2014), bruises (Hughes & Langlois, 2011; Langlois, 2007; Mimasaka et al., 2010; G. Payne, Langlois, Lennard, & Roux, 2007; Stam et al., 2011), ink in historical documents (Padoan et al., 2008), human dentin (Tramini, Bonnet, Sabatier, & Maury, 2001) and most recently in forensic entomology to assist with delineating lengthier stages in forensic entomology. This technique allows more precision in the estimated minimum post mortem interval ($_{\min}PMI$). Reflectance signatures are indicative of the insect's surface to a minimal light penetrating depth (Nansen et al., 2015). The reflectance signature is probably based on physical characteristics such as cuticle colour or opaqueness, shape, and texture (Nansen et al., 2014) as well as biochemical characteristics such as cuticular hydrocarbons (Blomquist, 2010b; Foley et al., 1998; Nansen et al., 2014). When day-to-day measurements are taken then day-to-day changes can be assessed (Schowengerdt, 2007).

There are three major classes of cuticular hydrocarbons in insects, the n-alkanes, methyl-branched alkanes and the alkenes (Blomquist, 2010b). Cuticular hydrocarbons are long chains of carbon atoms with hydrogen bonds that are found in the cuticle. They can be used as pheromones, and as a means for inter-specific cues (Blomquist & Bagneres, 2010). A key role of hydrocarbons in insects is chemical communication, but their primary

role is to prevent desiccation (Blomquist, 2010b). Cuticular hydrocarbons change throughout the larval stages (Butcher et al., 2013; Moore, 2013; Moore et al., 2013, 2014), and regularly with weathering in the puparial casing (Zhu et al., 2007). Cuticular hydrocarbons change through the immature stages for communication cues and recognition but also as certain stages require more waterproofing than others (Blomquist & Bagnères, 2010). Feeding blow fly larvae are moving through the moist food source and are less likely to suffer from desiccation than the wandering larvae that have moved away from the food source.

Hydrocarbons and their carbon-hydrogen bond patterns can be recognized using hyperspectral remote sensing in the near infrared in a non-destructive and rapid form, meanwhile keeping the insects alive, but this is not chemically specific and does not identify the precise hydrocarbon that GC/MS does (Blomquist, 2010b; Foley et al., 1998).

The objective of this research was to see if cuticular hydrocarbons are a convincing and probable contributor to the reflectance signature by demonstrating that the cuticular hydrocarbons change along with the daily reflectance signature of *Lucilia sericata* (Meigen) larvae.

7.4 Materials and Methods

Insect Rearing

Lucilia sericata colonies were established from blow flies provided by the Biological Sciences Insectary at Simon Fraser University and were maintained on sugar, water and milk powder, *ad libitum*. The insectary flies were collected from Burnaby, Langley, and Vancouver, British Columbia. Beef liver was added to the two colony cages regularly and was used as an oviposition medium. Once sufficient numbers of eggs were laid (an estimated 200/colony), the egg masses from each colony were divided among three replicates.

Beef liver was added frequently to each replicate to ensure that there was never a shortage of rearing substrate. Each replicate consisted of a 4 L glass jar containing

dampened sawdust to a depth of approximately 5 cm. Approximately 200 g of beef liver positioned on a folded industrial paper towel was placed on the sawdust. Each replicate jar was closed with two industrial paper towels and elastic bands to prevent larval escape.

The immature *L. sericata* were raised to pupariation in an environment chamber set for a 14:10 (L:D) photoperiod, 75% relative humidity and maintained at a mean temperature of 25°C. An ACR smart button[®] data logger recorded the temperature.

Hyperspectral Remote Sensing

Once the larvae had reached second instar, hyperspectral point source measurements were completed daily from the sample of insects until pupariation (seven days). An ASD (Analytical Spectral Devices[™], Boulder CO) LabSpec 4 Spectrometer was used to take the spectral measurements. Each day, 10 insects from each of the three replicates were washed in deionized water and gently patted with filter paper to remove surface contaminants. They were then patted dry with clean dry filter paper. Point source measurements were completed at anterior/mid and posterior regions of each larva excluding day 1 (second instar). Only a single point source measurement was completed for each second instar larva because of their small size. This ensured that the measurement was of the insect and not the surrounding background. As there was only a single measurement for second instar from the midsection and second instar can already easily be distinguished from the other days of development based on morphological characteristics, day one was excluded from the spectral analysis.

Hyperspectral measurements were completed in a blackened room to ensure that reflectance was of the insect specimens. All surfaces and equipment were painted matte black or draped with black fabric as a means to prevent contamination to the point source measurements. The ASD plant probe light source (necessary for heat sensitive targets) was the only light source in the room except for the negligible light from the turned away computer screen and light entering from under the door on the opposite side of some bookcases.

Data files were collected by RS3[™] software, the program that is specific to ASD spectrometers. Viewspec pro[™] was then used to convert the files to text files. Mathworks[™]

Matlab and fdaM (functional data analysis Matlab) tools were used to statistically analyse the data (<http://www.psych.mcgill.ca/misc/fda/downloads/FDAfuns/>).

Functional Regression Model

An analysis was completed to examine prediction of day within six days of development, from third instar to the beginning of intra-puparial period for the hyperspectral measurements for each of three replicates. The raw spectral reflectance observations, $X(w)$ across wavelength (w) were smoothed using a 6th order B-spline basis (with evenly spaced knots) while controlling roughness through a 3rd derivative penalty to reduce the noise associated with the raw spectra (Ramsay & Silverman, 2005). Before this, however, some minor but abrupt vertical shift artefacts that appeared in a few of the measurements at the 1100 and 1800nm wavelengths required adjusting. These few vertical shifts were identified as artefacts in the measurements because spectral measurements have a refined gradual change from one wavelength to the next (Foley et al., 1998). The jump points were identified and then they were redefined by shifting everything after that point by a constant amount to make the function continuous at the jump.

Data were scaled to have an average reflectance value of zero between 400 and 550 nm wavelengths and the maximum spectral reflectance scale for each observation was set to one.

The functional regression equations where $\beta(w)$ is the contributing β coefficient for the spectral measurements from each of the three replicates was examined. The simple linear regression model $Y=X\beta$ was expanded to manage the covariates X spanning continuously across a wide range of wavelengths, w . The resulting functional linear regression model with functional covariates $X(w)$ and coefficient $\beta(w)$ was:

$$Y_i = \int_{350}^{2500} X_{i,smooth}(w)\beta(w)dw.$$

In order to determine whether there was a repetition/jar effect between the three jars of insects, an overall model was created that takes into consideration all three replicates individually:

$$Y_i = \int_{350}^{2500} X_i(w)\beta_{jar3}(w)dw + \int_{350}^{2500} I_{jar1or2}X_i(w)\beta_{jar1or2}(w)dw$$

$$+ \int_{350}^{2500} I_{jar1}X_i(w)\beta_{jar1}(w)dw$$

Where I is a binary indicator function taking a value of one if the observation comes from the event listed in its subscript. Jar represents one of three different replicates.

Based on this model, five possible scenarios were tested:

If,

$\beta_{jar1or2}(w)=\beta_{jar1}(w)=0$ then all replicates are equivalent,

$\beta_{jar1}(w)=0$ then replicate one is equivalent to two and neither is equivalent to three,

$\beta_{jar1or2}(w)=0$ then replicate two equals three and neither is equivalent to one. One does not equal replicate two but replicate two is equivalent to three,

$\beta_{jar1or2}(w)=-\beta_{jar1}(w)$ then replicate one is equivalent to three and neither is equivalent to two, or

$\beta_{jar1or2}(w)\neq-\beta_{jar1}(w)$ and $\beta_{jar}(w)\neq 0$ then all replicates differ

Gas Chromatography/Mass Spectrometry

Once reflectance measurements of the live insects had been completed, a sample of the larvae from each replicate was frozen and killed to extract their cuticular hydrocarbons. Due to the size differences throughout development, the sample size of insects from each replicate that was used for extraction was based on weight (approximately 130mg). The three post feeding larvae on day 3 of measuring were slightly above the 130mg, but two post feeding larvae were well under weight so we opted for very slightly heavier rather than considerably lighter. The larvae were submerged in 500 μ L of hexane for 20 minutes and then the eluted hexane was collected with a pipette and transferred to a clean glass vial for gas chromatography/mass spectrometry (GC/MS). A Teflon seal was placed on the top of each vial to prevent evaporation of the hexane. It was unnecessary to run the eluted

hexane through a column to separate contaminants from the hydrocarbon mixture as the contaminants would probably not distort the hydrocarbon findings.

Twenty-one eluted hexane samples containing cuticular hydrocarbons from *L. sericata* larvae and two hexane extract samples from fresh thawed and spoiled beef liver (sampled from a jar containing developing third instar *L. sericata*), were run through a Varian Saturn 2000 ion trap GC/MS (Walnut Creek, Ca. 94598). The software that was used with the system was Varian MS Workstation system control version 6.9.1 and the elution column was DB5-MS (30m x 0.25mm internal diameter) (Folsom, Ca. 95630). A splitless injection was used and the oven was programmed so that it held at 50°C for five minutes and then it increased 10°C per minute until it reached 280°C.

For each sample, cuticular hydrocarbon findings were analysed to identify the alkane and the amounts of hydrocarbons were compared to an internal standard. Triacontane (C30) was selected as the internal standard because it was found in all the samples and is of a similar nature to the remaining sample and finally because it is an even numbered hydrocarbon. Finally, the results were compared with the findings of Moore et al., (2013) as this is the leading research of cuticular hydrocarbons in immature *L. sericata*.

7.5 Results and Discussion

Hyperspectral Remote Sensing

The posterior end spectral measurements provided daily predictions with the best precision for *Lucilia sericata* larvae raised at 25°C, compared with the midsection and anterior spectral measurements, in all three replicates (Figures 7-1, 7-2, & 7-3). The functional regressions demonstrate that the actual day of development falls well within the 95% prediction interval for the posterior measurements. There is much less precision in the prediction of day the further away from the abdominal integument that the measurements were completed. The probable reason for the loss of precision with distance is that the cuticular hydrocarbons are formed by the ectodermal oenocytes, which in many species are located in the abdominal integument (Martins & Ramalho-Ortigão, 2012). The 95%

confidence interval for the functional coefficients differs from zero over some wavelength regions, which indicates a significant effect at those wavelengths (Figures 7-4, 7-5, & 7-6; where the dotted red line is visible).

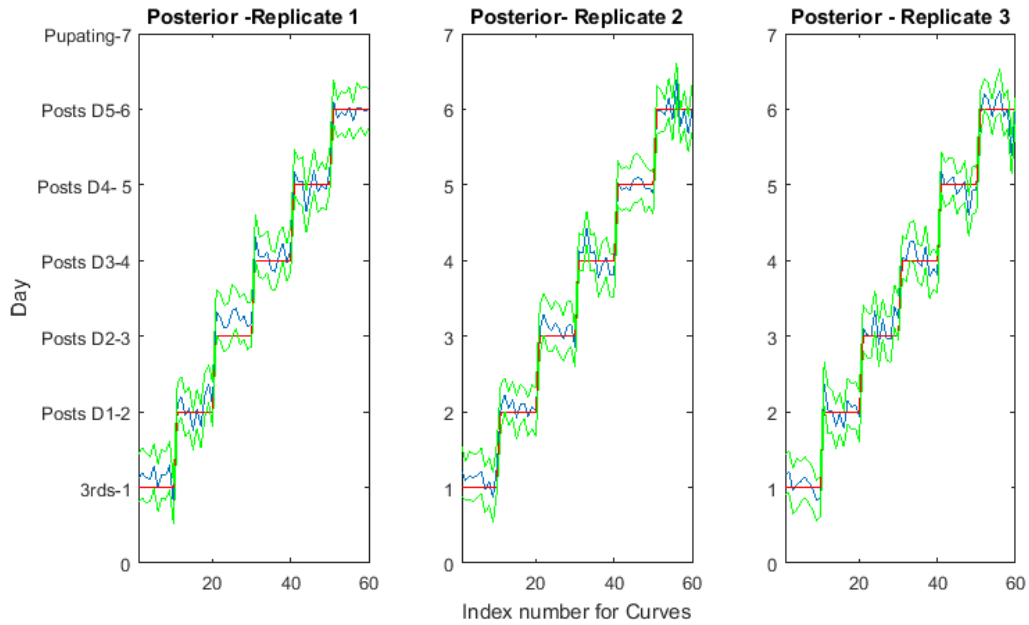


Figure 7-1 Functional regression of prediction of day of development from three replicates of posterior end spectral reflectance measurements of *Lucilia sericata* larvae raised at 25°C. The red line is the actual day of development and the blue represents the predicted day. The pointwise 95% prediction interval upper and lower limits are presented in green.

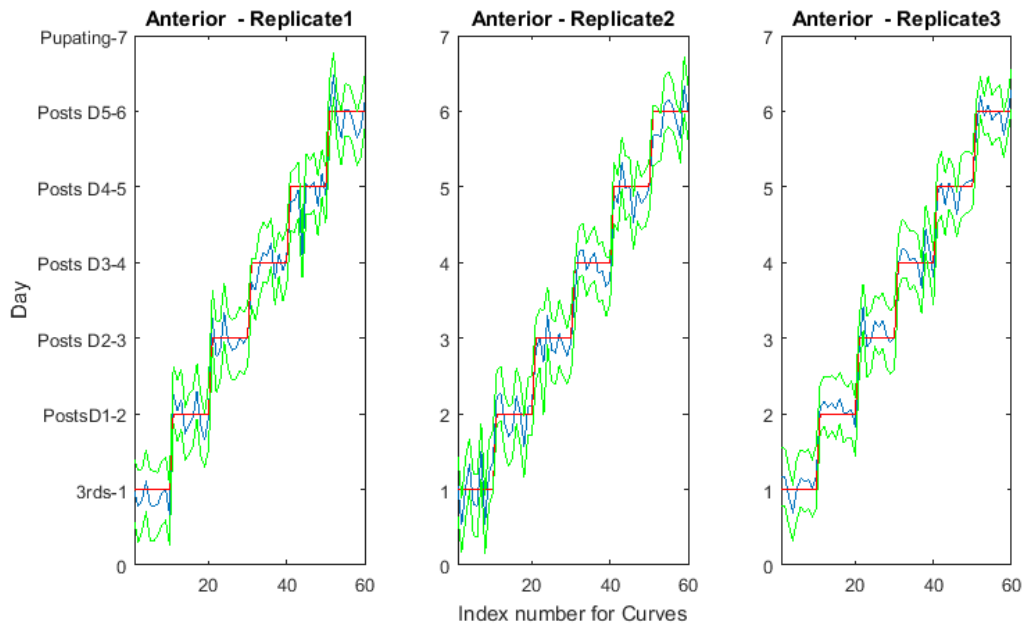


Figure 7-2 Functional regression of prediction of day of development from three replicates of anterior end spectral reflectance measurements of *Lucilia sericata* larvae raised at 25°C. The red line is the actual day of development and the blue represents the predicted day. The pointwise 95% prediction interval upper and lower limits are presented in green.

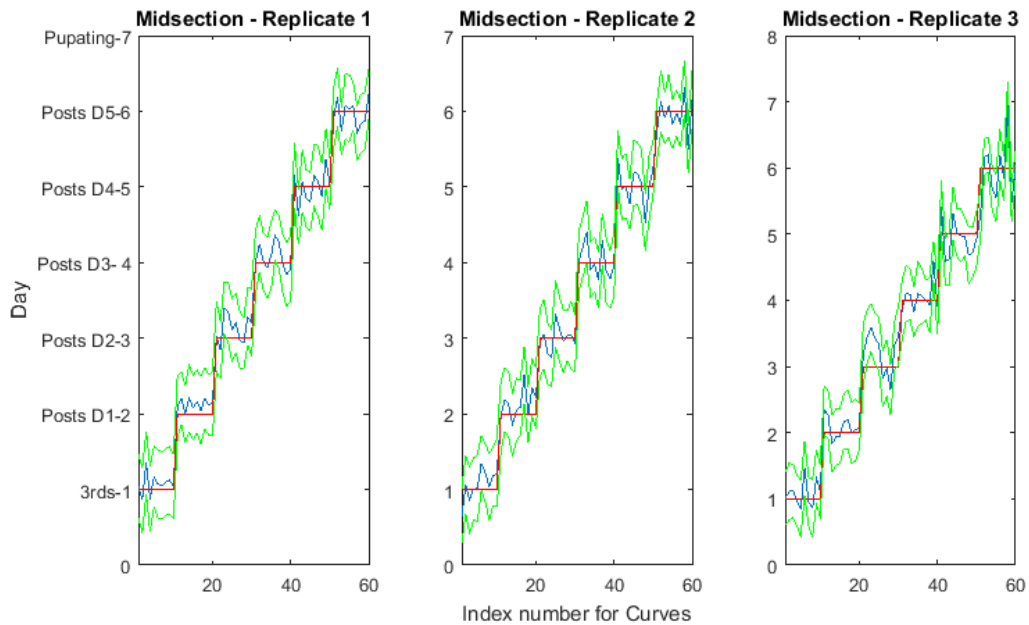


Figure 7-3 Functional regression of prediction of day of development from three replicates of midsection spectral reflectance measurements of *Lucilia sericata* larvae raised at 25°C. The red line is the actual day of development and the blue represents the predicted day. The pointwise 95% prediction interval upper and lower limits are presented in green.

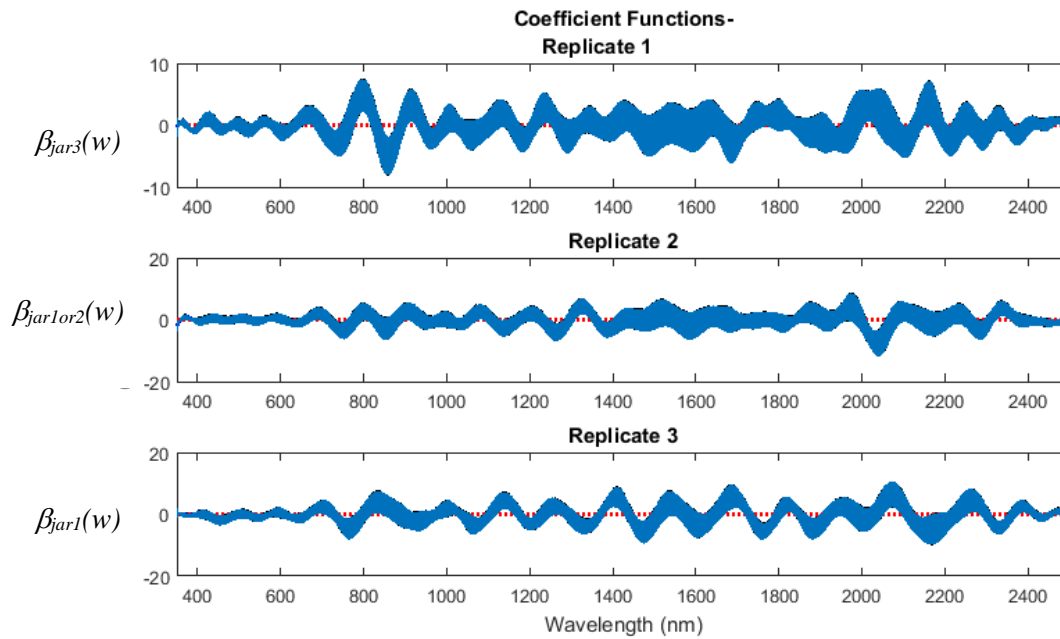


Figure 7-4 The coefficient functions of posterior end spectral measurements for each of three replicates of developing *Lucilia sericata* larvae at 25°C indicate that the functional regressions are significant. The $\beta(w)$ coefficients are not zero at the wavelengths where the zero line is visible and it is these wavelengths that are contributing to the model.

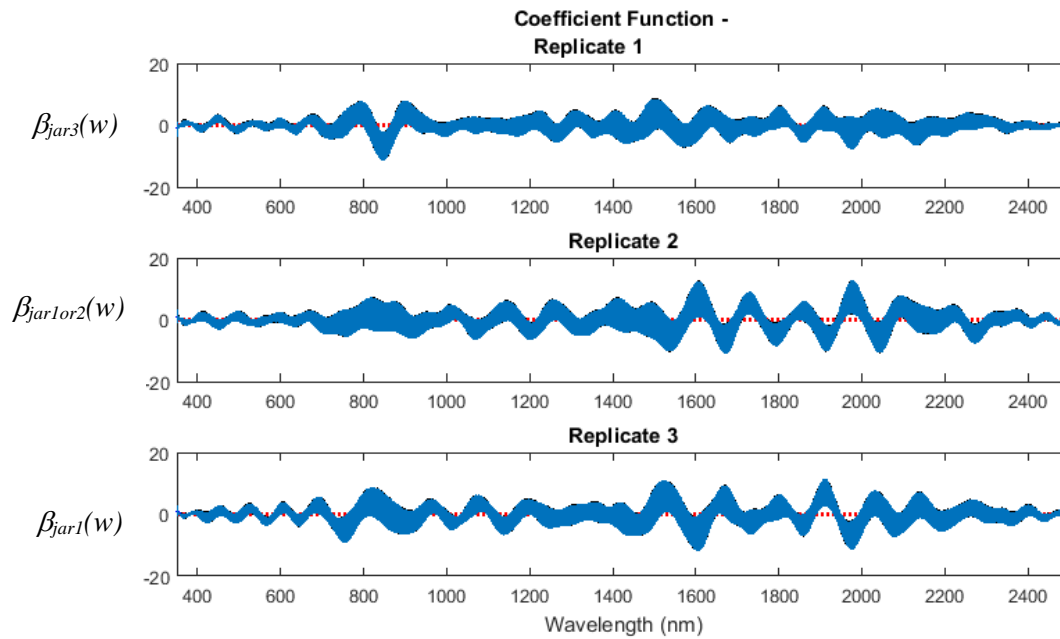


Figure 7-5 The coefficient functions of anterior end spectral measurements for each of three replicates of developing *Lucilia sericata* larvae at 25°C indicate that the functional regressions are significant. The $\beta(w)$ coefficients are not zero at the wavelengths where the zero line is visible and it is these wavelengths that are contributing to the model.

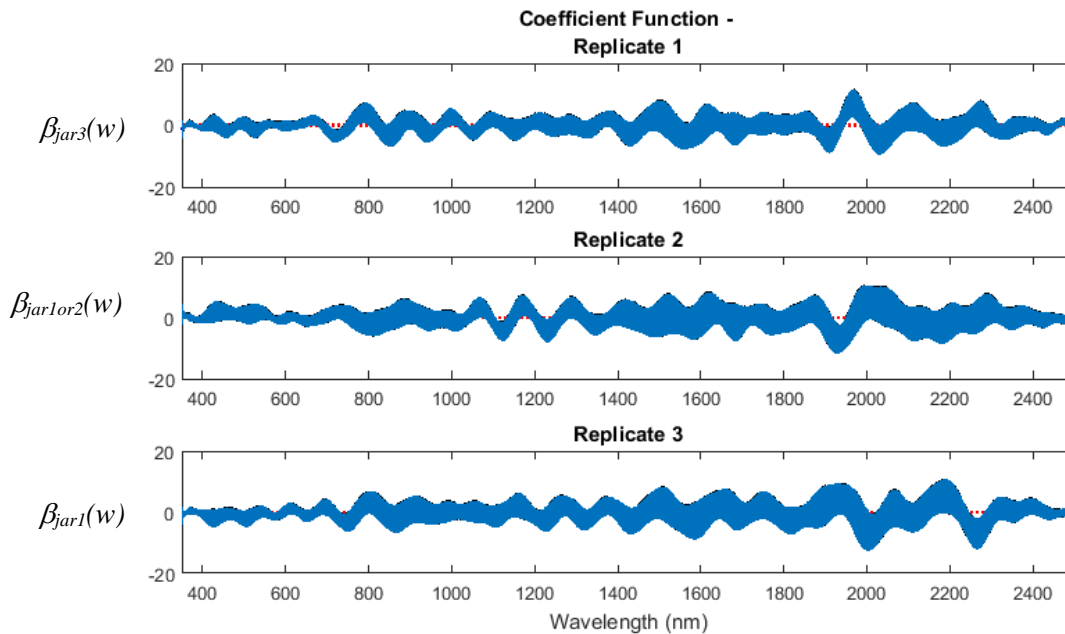


Figure 7-6 The coefficient functions of midsection spectral measurements for each of three replicates of developing *Lucilia sericata* larvae at 25°C indicate that the functional regressions are significant. The $\beta(w)$ coefficients are not zero at the wavelengths where the zero line is visible and it is these wavelengths that are contributing to the model.

The functional regression model was modified to take into consideration the slight differences between developing replicates. The five scenarios were tested and $\beta_{jar1or2}(w) \neq -\beta_{jar1}(w)$ and all $\beta_{jar}(w) \neq 0$, therefore, all replicates differed at a few wavelengths but otherwise were almost identical. The scenario test results can be seen in Figures 7-7, 7-8, & 7-9, which indicate that there are minimal differences between replicates at a few of the 2151 wavelengths examined and yet they all indicate the same predicted days as seen in Figures 7-1, 7-2 & 7-3.

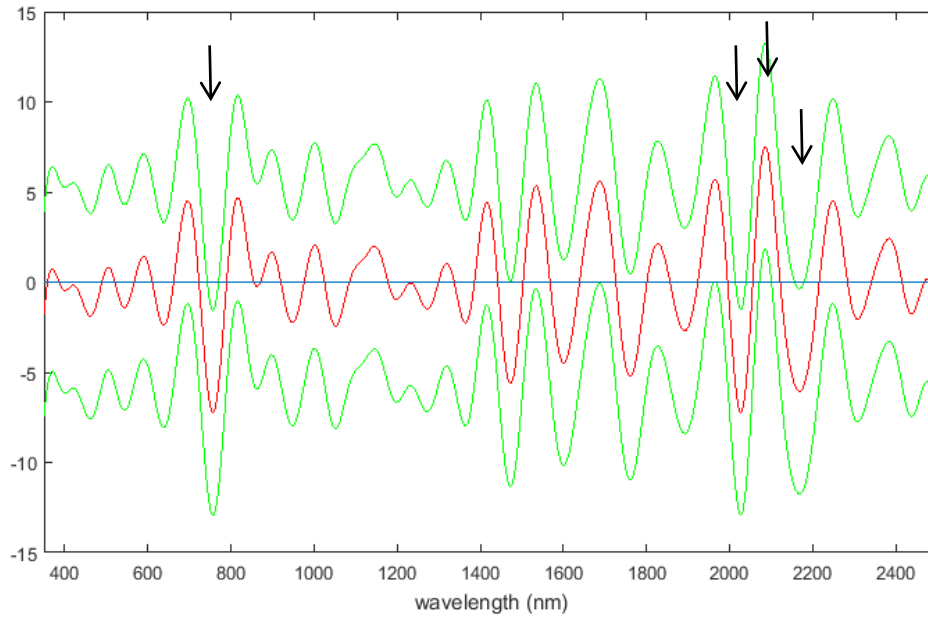


Figure 7-7 An examination of scenario #5 that $\beta_{jar1or2}(w) \neq -\beta_{jar1}(w)$ and $\beta_{jar}(w) \neq 0$ from the posterior end spectral measurements of *Lucilia sericata*. At four separate wavelength regions the mean (blue line) falls outside of the 95% prediction interval. The red line is the prediction and the green lines are the upper and lower limits.

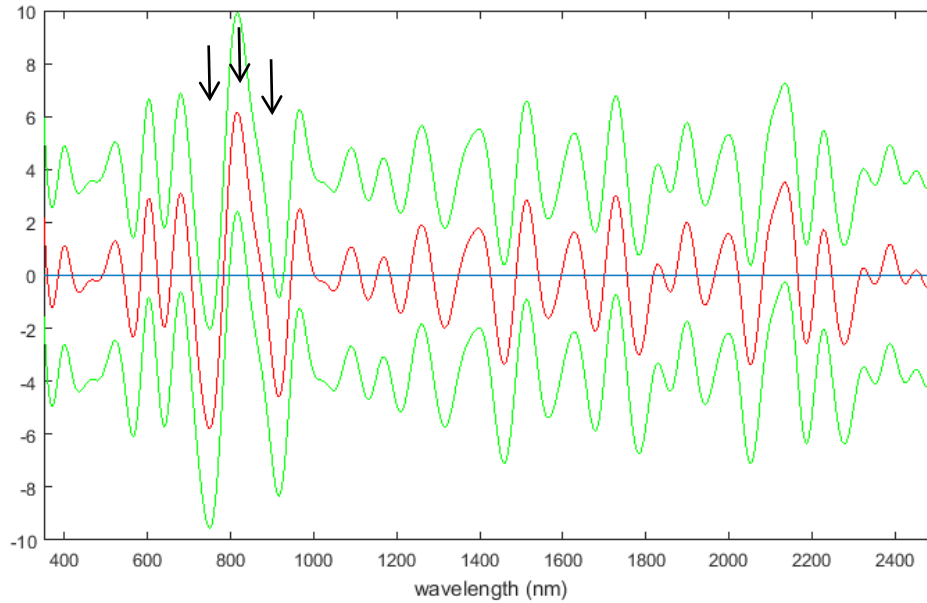


Figure 7-8 An examination of scenario #5 that $\beta_{jar1or\ 2}(w) \neq -\beta_{jar1}(w)$ and $\beta_{jar}(w) \neq 0$ from the anterior end spectral measurements of *Lucilia sericata*. At three separate wavelength regions the mean (blue line) falls outside of the 95% prediction interval. The red line is the prediction and the green lines are the upper and lower limits.

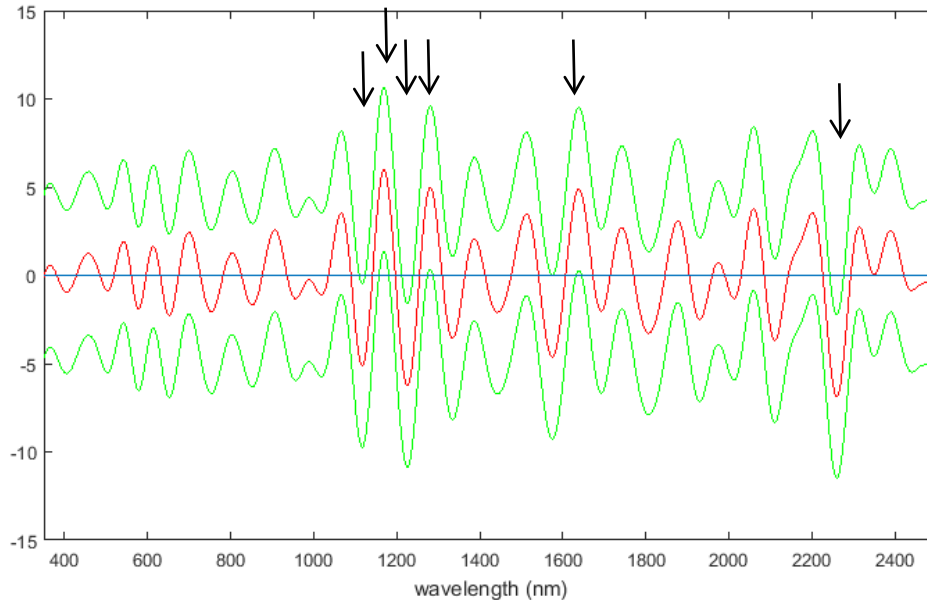


Figure 7-9 An examination of scenario #5 that $\beta_{jar1or\ 2}(w) \neq -\beta_{jar1}(w)$ and $\beta_{jar}(w) \neq 0$ from the midsection spectral measurements of *Lucilia sericata*. At six separate wavelength regions the mean (blue line) falls outside of the 95% prediction interval. The red line is the prediction and the green lines are the upper and lower limits.

Contributing factors to the spectral measurements are those detected to light penetrating depths (Nansen et al., 2015) and so probably include colour, opaqueness (fat body formation in the post feeding larvae), surface shape and texture, and spiracular and mouth part changes, as well as the main contributor, cuticular hydrocarbons. Oenocytes change with insect development, particularly with moult, in size, shape and distribution (Makki et al., 2014). They are probably not a direct contributor to the spectral measurements because they are located deep within the epidermis (Klowden, 2007) where the light probably cannot penetrate. Nevertheless, as oenocytes do produce cuticular hydrocarbons, they do contribute indirectly.

Gas Chromatography/Mass Spectrometry

The chromatograms of the cuticular hydrocarbons that were extracted in hexane for each replicate of insects over six days of measuring from third instar until entering intrapuparial development are presented in Figures 7-10, 7-11, & 7-12. Only cuticular hydrocarbons consisting of 22 to 31 carbon chains are presented because cuticular waxes

are combinations of 25 to 31 carbons, alcohols of 24 to 34 carbons and include the presence of fatty acid esters (Klowden, 2007). Also, the Varian Saturn 2000 ion trap GC/MS did not identify any alkanes above 31 carbons when searching to 43 carbons and there are several peroxides that obscure some of the shorter alkanes.

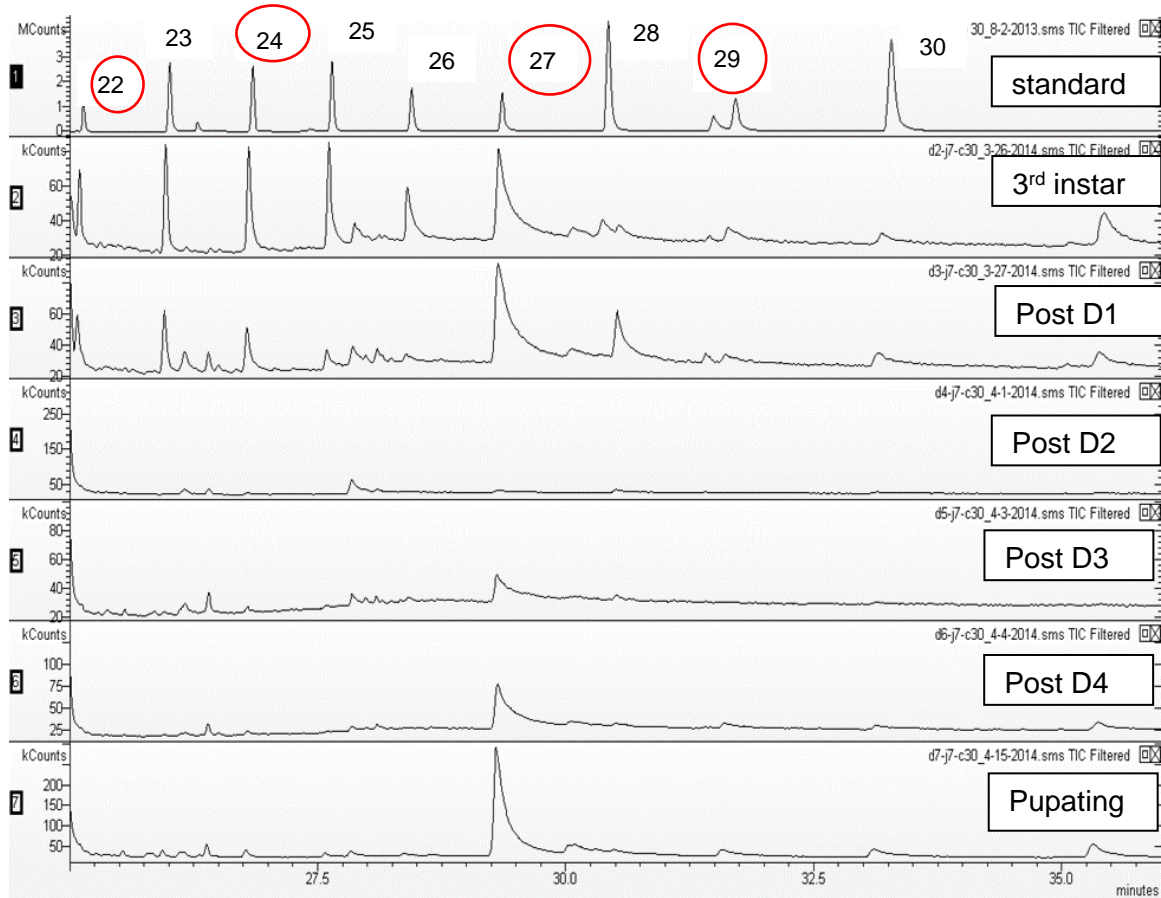


Figure 7-10 Replicate #1 GC chromatograms of six consecutive days (ranging from 3rd instar to the first day of the intra-pupal period) from the cuticular hydrocarbons of *L. sericata* raised at 25°C. The numbers at the top of the chromatogram represent the number of carbons and the red circles indicate similar trends to Moore et al. (2013)

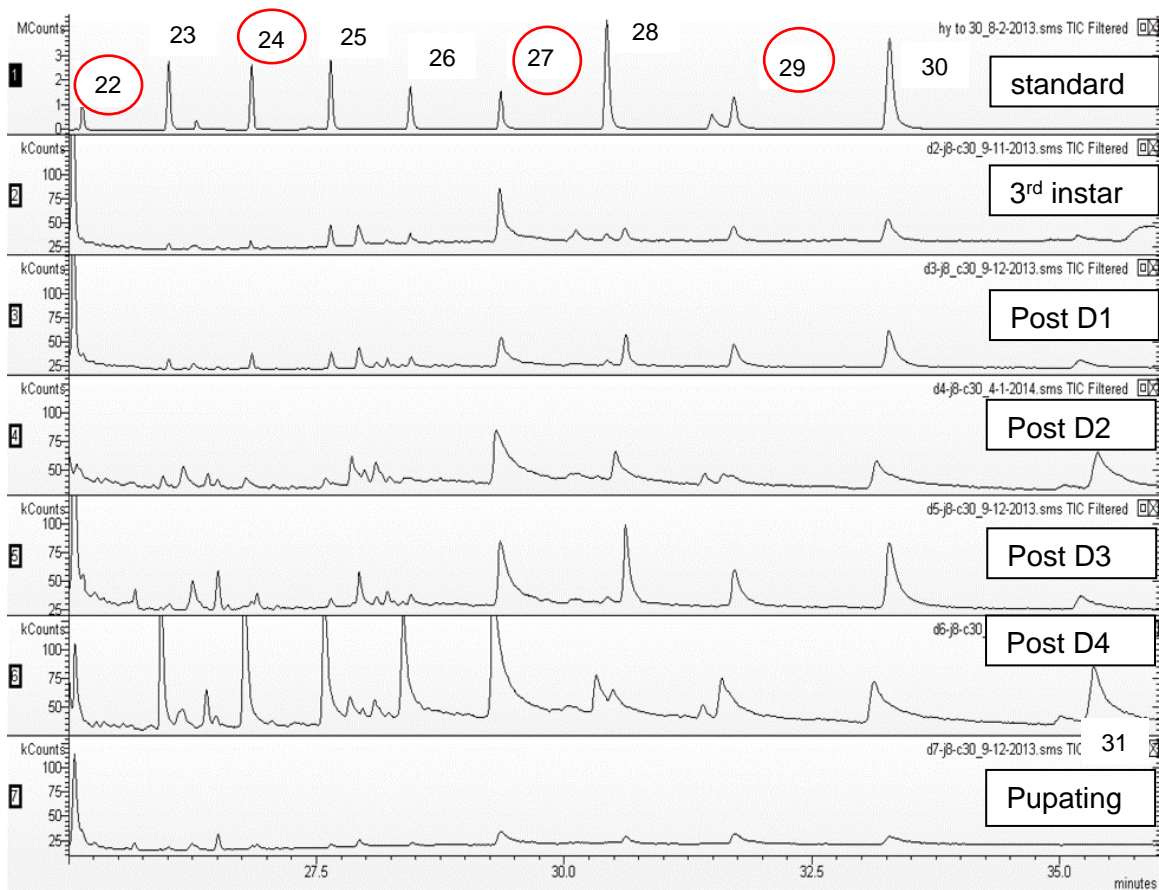


Figure 7-11 Replicate #2 GC chromatograms of six consecutive days (ranging from 3rd instar to the first day of the intra-pupal period) from the cuticular hydrocarbons of *L. sericata* raised at 25°C. The numbers at the top of the chromatogram represent the number of carbons and the red circles indicate similar trends to Moore et al. (2013)

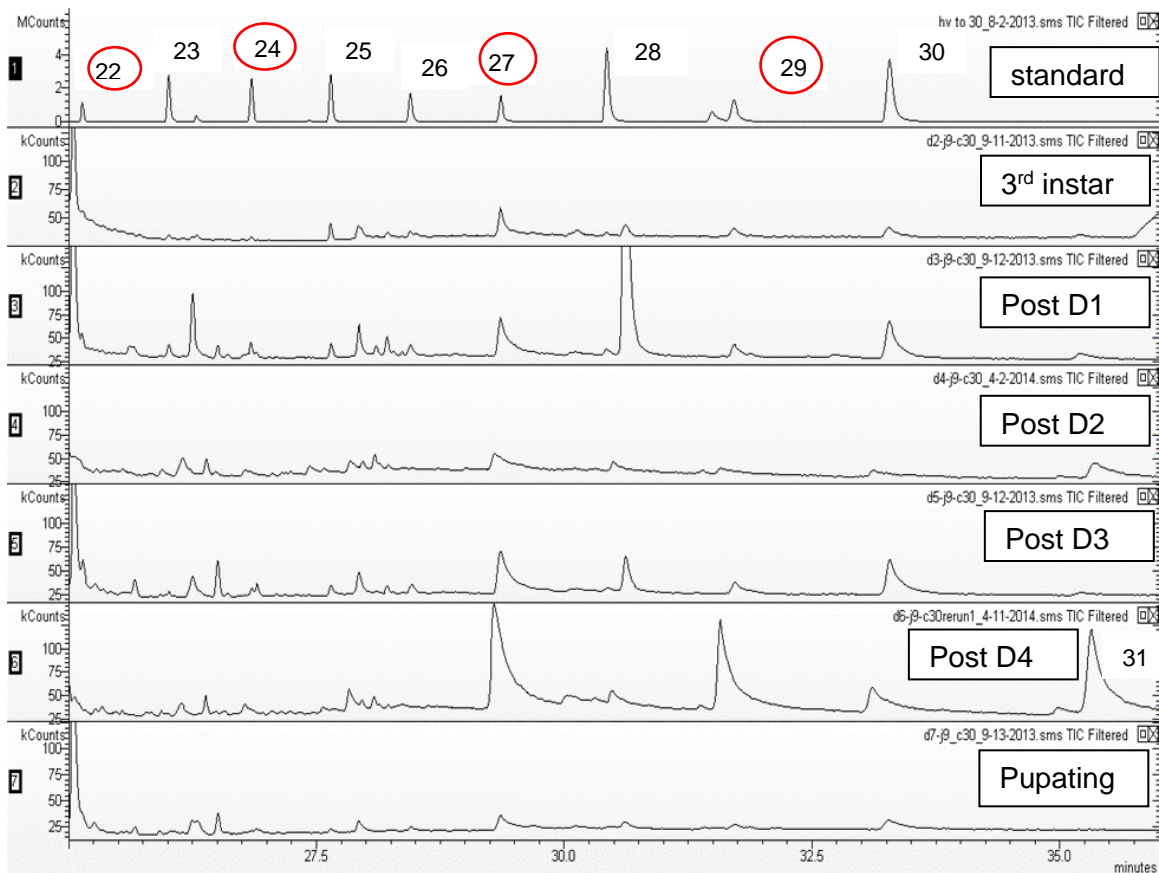


Figure 7-12 Replicate #3 GC chromatograms of six consecutive days (ranging from 3rd instar to the first day of the intra-puparial period) from the cuticular hydrocarbons of *L. sericata* raised at 25°C. The numbers at the top of the chromatogram represent the number of carbons and the red circles indicate similar trends to Moore et al. (2013)

Docosane (C₂₂) disappeared or was found in trace amounts by the time the larvae were entering the intra-puparial period (Table 7-1). Tri-,tetra- and pentacosane (C₂₃, C₂₄, and C₂₅) were always present even in trace amounts on some days (Figures 7-10, 7-11, & 7-12). Also, as seen in the chromatograms, hexacosane (C₂₆) was reduced to nil/trace amounts at post feeding day two and three. Heptacosane (C₂₇) and octacosane (C₂₈) were reduced to nil/trace at post feeding day two and then increase again before entering the intra-puparial period. Nonacosane (C₂₉) was always present in trace amounts but then increased substantially to enter intra-puparial period. Finally, hentriacontane (C₃₁) appeared during the postfeeding stage and then disappeared when the larvae were entering intra-puparial period. The increase in higher boiling point alkanes, such as C₂₇ to C₂₉, in

the post feeding stage indicates an increase in waterproofing (Chung & Carroll, 2015; Moore et al., 2013) which is strongly needed in the late post feeding stage to prevent desiccation.

Table 7-1 An examination of the alkane cuticular hydrocarbons from three replicates of *Lucilia sericata* raised at 25°C over seven days and of the fresh thawed and spoilt beef liver substrate. Each √ or X represents presence or absence, respectively, in each replicate. Only a single replicate of each of the fresh thawed and spoilt beef liver was examined for hydrocarbons and the findings were similar.

alkanes	retention time (mins)	Day 1	Day 2	Day 3	Day 4	Day 5	Day 6	Day 7	b. liver	trend
		2nd instar	3rd instar	post day 1	post day 2	post day 3	post day 4	Entering intra-puparial	Fresh thaw/spoil	
C22	25.13	√√√	√√√	√√√	X √√	X √√	√√√	X√X	√	Disappears by the intrapuparial period
C23	25.99	√√√	√√√	√√√	√√√	√√√	√√√	√√√	√	Always there
C24	26.84	√√√	√√√	√√√	√√√	√√√	√√√	√√√	X	Always there
C25	27.63	√√√	√√√	√√√	√√√	√√√	√√√	√√√	X	Always there
C26	28.45	√√√	√√√	√√√	√√X	X √√	√√√	√√√	X	Disappears and reappears
C27	29.35	√√√	√√√	X √√	√X X	√√√	X √√	X √√	X	Disappears and reappears
C28	30.44	√√√	√√√	X √√	X√X	√√√	√√√	√√√	X	Disappears and reappears
C29	31.72	√√√	√√√	√√√	√√√	X √√	√√√	√√√	X	Always there, low quant
C30	33.31	standard	none	Standard						
*C31	35.2	XXX	XX√	X √√	X √√	X √√	X√X	XXX	X	Appears in post and disapp by intrapuparial

*C31 was probably in replicate one but in trace amounts and so it was not identified as it was in replicates two and three.

Table 7-1 compares the cuticular hydrocarbon findings between replicates for each of the days ranging from second instar to the beginning of intra-pupal period. Instead of focussing on the amounts of hydrocarbons as the chromatograms indicate, the presence or absence is noted in the table. Second instar cuticular hydrocarbon alkanes are not included in the chromatograms but are included in Table 7-1 because firstly, distinguishing second instar is already easily accomplished through morphological characteristics and secondly, only midsection spectral measurements were possible from the second instar larvae. Past findings of *L. sericata* cuticular hydrocarbons may differ from the current research since the previous research does not include washing surface contaminants from the insects before analysis (Moore, 2013; Moore et al., 2013, 2014) and differences may also be due to analytical methods (Akino, 2006; Moore, 2013). The column oven temperature programs differed between the current research and previous research and this can be a contributor to different findings (Akino, 2006; Moore, 2013).

In Moore et al. (2013), the *L. sericata* were raised at 24°C instead of 25°C and the insects were raised on minced beef instead of beef liver. Also, the oven temperature followed a different program and was set for 50°C for two minutes and then increased by 25°C per minute to 200°C. It then followed increases from 200 to 260°C with increases of 3°C every minute. Finally, from 260 to 320°C, it increased 20°C per minute and remained there for two minutes. This was completed with an Agilent 6890N Network gas chromatography split/splitless injector and Agilent Chemstation software (Moore et al., 2013). Another difference from Moore et al. (2013) was that the current samples were not run through a silica gel column to remove contaminants as they were by Moore and colleagues (Moore et al., 2013) and as a result, by-products such as aldehydes were present and this was seen as a drift in some of the chromatogram peaks.

Many similarities in the current research were found with Moore and colleagues (Moore et al., 2013) in the changing trends of some of the alkanes. This was despite the differences in chemical analysis and origin of insect colonies. Due to the key differences mentioned above, day-to-day comparisons cannot be made, but trends over the larval stages can be compared. Both datasets found a drop in percentage of docosane (C₂₂) and

tetracosane (C₂₄). Tricosane (C₂₃) was present fairly consistently. In both datasets, heptacosane (C₂₇) disappeared and then reappeared towards the end of post feeding. Nonacosane (C₂₉) was consistently present but amounts increased greatly towards the end of the post feeding stage. Differences between datasets were found with octacosane (C₂₈) and hentriacontane (C₃₁). Moore et al. (2013) found that octacosane remained relatively constant with a minor drop towards the end of the postfeeding stage (Moore et al., 2013) and in the current research the trend was to decrease in amount at day two of post feeding and then remain at trace amounts. Moore et al. (2013) also found that hentriacontane increased substantially during the last days of the post feeding stage (Moore et al., 2013), whereas in the current experiment trace amounts of hentriacontane appeared in third instar and the early post feeding stage but disappeared before entering the intra-puparial period.

Cuticular hydrocarbons change through the immature stages because there are stages that require more waterproofing to prevent desiccation and some stages where the larvae are moving through the food source and have less of an issue with desiccation. Also cuticular hydrocarbons are used for chemical communication such as **kairomones** (Blomquist & Bagnères, 2010), to potentially communicate with *Proteus mirabilis* or other bacteria, or chemical cues for interspecific or intraspecific communication to attract conspecifics for larval aggregate formation to break down the food source (Greenberg & Kunich, 2002; Rivers & Dahlem, 2014).

Differences in presence or absence of a particular alkane between replicates can be due to the GC/MS not being sensitive enough to identify trace amounts, or because there was lag or acceleration between development in the different replicates. Replicate differences, although minor, were found in both the daily cuticular hydrocarbon alkanes and the daily spectral signatures. Ideally, the replicates should have the same alkane amounts for each of the examined samples of cuticular hydrocarbons and the same contributing β coefficients for the spectral measurements. With the addition of more precision to the findings, the slightest of differences will contribute to the measurements and will be observed between replicates. Individual flies ovipositing at slightly different times may factor in and so developing *L. sericata* may be at slightly different ages in the

replicates. Also, removal of the oviposition substrate from the cages one after the other and not at the same time may contribute to slight age differences in developing larvae and removing and placing the replicates into the environment chambers one after the other may influence temperature differences between replicates. Although the replicates were rotated in the temperature chambers, slight differences in exposure time to the minimal temperature differences can also impact the research. There may be a lag or acceleration of development of insects in some jars making them imperfect replicates. Nonetheless, measurements from all three replicates predict the same day within the 95% confidence interval.

Surprisingly, even numbered hydrocarbons were found in some days in moderate amounts. Often even numbered chain alkanes indicate contamination if found in similar amounts to the odd numbered chain alkanes and not in trace amounts (Blomquist, 2010b). Based on the way that hydrocarbons are formed, a decarboxylation of two even numbered fatty acid chains, even numbered alkanes are rare (Blomquist, 2010b; Park, 2005). Few things in nature have even numbered chain alkanes (Park, 2005) but Gram negative bacteria such as *Escherichia coli*, *Pseudomonas spp.* and *Proteus mirabilis* do have even numbered alkanes in their cell walls. It is most probable that in this situation the even numbered alkanes are not contamination but present instead as a result of *Proteus mirabilis* bacteria which have a symbiotic relationship with *Lucilia sericata* (Ma et al., 2012). *Proteus mirabilis* is located in the salivary glands of *L. sericata* and as the insect feeds through a majority of the larval stages and releases digestive enzymes (Rivers & Dahlem, 2014), the bacteria are bound to be spread to the insect surface.

7.6 Conclusion

The extracted hydrocarbons are most probably what is being measured in the spectral reflectance measurements because they too are changing daily and they are on the insect surface and so are at a light penetrating depth. Also, the further away the spectral measurements are from the posterior end of the larvae, the less accurate the age estimate.

This suggests that the hydrocarbons produced by the oenocytes in the abdominal integument have a larger effect on the spectral measures and prediction.

The more refined the prediction, the more factors that influence replicate similarity. Replicate differences are observed when the precision is increased. Since the prediction was refined to day within the stage and not to stage, more variables such as slight temperature differences or insect age differences will become evident in the prediction. Although in this dataset the prediction was still the same for all replicates, it might not be quite so accurate if precision is increased further.

The higher boiling point odd alkanes increase in the later post feeding when desiccation is most problematic. These changes in alkanes are consistent with the spectral measurement changes and can be used to estimate insect age to a day within the lengthy immature blow fly stage. Even numbered alkanes from *P. mirabilis* contributed to the hydrocarbon profile of the *L. sericata* larvae.

7.7 Acknowledgements

The authors would like to thank Regine Gries, for all of her hard work with the GC/MS and for her profound knowledge of cuticular hydrocarbons. We would also like to thank the volunteers that assisted with the daily hyperspectral measurements, Billi-Jo Cavanaugh, Alexis Ohman, Kelsey Dubiel, Robert Wilburn, Elaine Rasmussen, and Saadia Uraizee. And finally, we would like to thank ASD Inc, a Panalytical company for awarding J. Warren the Alexander Goetz prize so that this research could be conducted.

7.8 Reference List

Akino, T. (2006). Cuticular hydrocarbons of *Formica truncorum* (Hymenoptera: Formicidae): Description of new very long chained hydrocarbon components *Applied Entomology and Zoology*, 41(4), 667-677.

- Amendt, J., Richards, C. S., Campobasso, C. P., Zehner, R., & Hall, M. J. R. (2011). Forensic Entomology: applications and limitations. *Forensic Science Medical Pathology*, 7, 379-392.
- Blomquist, G. J. (2010). Structure and analysis of insect hydrocarbons. In G. J. Blomquist & A.-G. Bagnères (Eds.), *Insect Hydrocarbons Biology, Biochemistry and Chemical Ecology* (pp. 19-34). New York: Cambridge University Press.
- Blomquist, G. J., & Bagnères, A.-G. (2010). Introduction: history and overview of insect hydrocarbons. In G. J. Blomquist & A.-G. Bagnères (Eds.), *Insect Hydrocarbons Biology Biochemistry and Chemical Ecology* (pp. 3-18). New York: Cambridge University Press.
- Bremmer, R. H., de Bruin, D. M., de Joode, M., Buma, W. J., Van Leeuwen, T. G., & Aalders, M. C. G. (2011). Biphasic oxidation of oxy-hemoglobin in blood stains. *PLoS ONE*, 6(7), 1-6. doi:doi:10.1371/journal.pone.0021845
- Bremmer, R. H., Nadort, A., van Leeuwen, T. G., van Gemert, M. J. C., & Aalders, M. C. G. (2011). Age estimation of blood stains by hemoglobin derivative determination using reflectance spectroscopy. *Forensic Science International*, 206, 166-171. doi:doi:10.1016/j.forsciint.2010.07.034
- Butcher, J. B., Moore, H. E., Day, C. R., Adam, C. D., & Drijfhout, F. P. (2013). Artificial neural network analysis of hydrocarbon profiles for the ageing of *Lucilia sericata* for post mortem interval estimation. *Forensic Science International*, 232, 25-31.
- Chung, H., & Carroll, S. B. (2015). Wax, sex and the origin of species: Dual roles of insect cuticular hydrocarbons in adaptation and mating. *Bioessays Prospects and Overviews*, 37, 822-830. doi:DOI 10.1002/bies.201500014
- Edelman, G., Manti, V., van Ruth, S. M., van Leeuwen, T. G., & Aalders, M. (2012). Identification and age estimation of blood stains on colored backgrounds by near infrared spectroscopy. *Forensic Science International*, 220, 239-244. doi:doi:10.1016/j.forsciint.2012.03.009
- Edelman, G., van Leeuwen, T. G., & Aalders, M. C. G. (2012). Hyperspectral imaging for the age estimation of blood stains at the crime scene. *Forensic Science International*, 223, 72-77.
- Foley, W. J., McIlwee, A., Lawler, I., Aragonés, L., Woolnough, A. P., & Berding, N. (1998). Ecological applications of near infrared reflectance spectroscopy - a tool for rapid, cost-effective prediction of the composition of plant and animal tissues and aspects of animal performance. *Oecologia*, 116, 293-305.

- Frederickx, C., Dekeirsschieter, J., Brostaux, Y., Wathelet, J.-P., Verheggen, F. J., & Haubruge, E. (2012). Volatile organic compounds released by blowfly larvae and pupae: New perspectives in forensic entomology. *Forensic Science International*, *219*, 215-220.
- Gennard, D. E. (2012). *Forensic Entomology an introduction* (2nd ed.). Chichester, West Sussex: Wiley Blackwell.
- Greenberg, B., & Kunich, J. C. (2002). *Entomology and the Law, Flies as Forensic Indicators*. United Kingdom: Cambridge University Press.
- Hughes, V. K., & Langlois, N. E. I. (2011). Visual and spectrophotometric observations related to histology in a small sample of bruises from cadavers. *Forensic Science Medical Pathology*, *7*, 253-256.
- Klowden, M. J. (2007). *Physiological Systems in Insects*. Burlington MA: Elsevier Inc.
- Langlois, N. E. I. (2007). The science behind the quest to determine the age of bruises-- a review of the English language literature. *Forensic Science Medical Pathology*, *3*, 241-251.
- Li, B., Beveridge, P., O'Hare, W. T., & Islam, M. (2011). The estimation of the age of a blood stain using reflectance spectroscopy with a microspectrophotometer, spectral pre-processing and linear discriminant analysis. *Forensic Science International*, *212*, 198-204.
- Li, B., Beveridge, P., O'Hare, W. T., & Islam, M. (2013). The age estimation of blood stains up to 30 days old using visible wavelength hyperspectral image analysis and linear discriminant analysis. *Science and Justice*, *53*, 270-277.
- Li, B., Beveridge, P., O'Hare, W. T., & Islam, M. (2014). The application of visible wavelength reflectance hyperspectral imaging for the detection and identification of blood stains. *Science and Justice*, *54*, 432-438.
- Ma, Q., Fonseca, A., Liu, W., Fields, A. T., Pimsler, M. L., Spindola, A. F., . . . Wood, T. K. (2012). *Proteus mirabilis* interkingdom swarming signals attract blow flies. *International Society for Microbial Ecology*, *6*, 1356-1366.
- Makki, R., Cinnamon, E., & Gould, A. P. (2014). The development and functions of oenocytes. *Annual Review of entomology*, *59*, 405-425. doi:10.1146/annurev-ento-011613-162056

- Martin-Vega, D., Hall, M. J. R., & Simonsen, T. J. (2016). Resolving confusion in the use of concepts and terminology in intrapuparial development studies of cyclorrhaphous diptera *Journal of Medical Entomology*, 53(6), 1249-1251. doi:doi:10.1093/jme/tjw081
- Martins, G. F., & Ramalho-Ortigão, J. M. (2012). Oenocytes in insects. *Invertebrate Survival Journal*, 9(2).
- Mimasaka, S., Ohtani, M., Kuroda, N., & Tsunenari, S. (2010). Spectrophotometric Evaluation of the age of bruises in children: Measuring Changes in bruise color as an indicator of child physical abuse. *Tohoku Journal of Experimental Medicine*, 220, 171-175.
- Moore, H. E. (2013). *Analysis of cuticular hydrocarbons in forensically important blowflies using mass spectrometry and its application in Post Mortem Interval estimations*. (Doctor of Philosophy), Keele University, Keele Staffordshire University.
- Moore, H. E., Adam, C. D., & Drijfhout, F. P. (2013). Potential Use of Hydrocarbons for Aging *Lucilia sericata* Blowfly Larvae to Establish the Postmortem Interval. *Journal of Forensic Science*, 58(2), 404-412.
- Moore, H. E., Adam, C. D., & Drijfhout, F. P. (2014). Identifying 1st instar larvae for three forensically important blowfly species using “fingerprint” cuticular hydrocarbon analysis. *Forensic Science International*, 240, 48-53.
- Nansen, C., Coelho Jr, A., Viera, J. M., & Parra, J. R. P. (2014). Reflectance-based identification of parasitized host eggs and adult *Trichogramma* specimens. *Journal of Experimental Biology*, 217, 1187-1192. doi:10.1242/jeb.095661
- Nansen, C., Ribeiro, L. P., Dadour, I., & Roberts, J. D. (2015). Detection of temporal changes in insect body reflectance in response to killing agents. *PlosONE*, 10(4), 1-15. doi:10.1371/journal.pone.0124866
- Padoan, R., Steemers, T. A. G., Klein, M. E., Aalderink, B. J., & de Bruin, G. (2008). *Quantitative hyperspectral imaging of historical documents: Techniques and applications*. Paper presented at the 9th International Conference on NDT of Art, Jerusalem, Israel.
- Park, M.-O. (2005). New Pathway for Long-Chain n-Alkane Synthesis via 1-Alcohol in *Vibrio furnissii* M1. *Journal of Bacteriology*, 187(4), 1426-1429.

- Payne, G., Langlois, N., Lennard, C., & Roux, C. (2007). Applying visible hyperspectral (chemical) imaging to estimate the age of bruises. *Medicine, Science and the Law*, 47(3), 225-232.
- Payne, G., Wallace, C., Reedy, B., Lennard, C., Schuler, R., Exline, D., & Roux, C. (2005). Visible and near-infrared chemical imaging methods for the analysis of selected forensic samples. *Talanta*, 67, 334-344.
- Pechal, J. L., Moore, H. E., Drijfhout, F., & Benbow, M. E. (2014). Hydrocarbon profiles throughout adult Calliphoridae aging: A promising tool for forensic entomology. *Forensic Science International*, 245, 65-71.
- Ramsay, J. O., & Silverman, B. W. (2005). *Functional Data Analysis*. New York: Springer.
- Rivers, D. B., & Dahlem, G. A. (2014). *The Science of Forensic Entomology*. Oxford: Wiley Blackwell.
- Schowengerdt, R. A. (2007). *Remote Sensing Models and Methods for Image Processing*. London: Elsevier.
- Stam, B., van Gemert, M. J. C., van Leeuwen, T. G., Teeuw, A. H., van der Wal, A., & Aalders, M. C. G. (2011). Can color inhomogeneity of bruises be used to establish their age? *Journal of Biophotonics*, 4(10), 759-767. doi:10.1002/jbio.201100021
- Tarone, A. M., Jennings, K. C., & Foran, D. R. (2007). Aging blow fly eggs using gene expression: A feasibility study. *Journal of Forensic Science*, 52(6), 1350-1354.
- Tarone, A. M., Picard, C. J., Spiegelman, C., & Foran, D. R. (2011). Population and temperature effects on *Lucilia sericata* (Diptera: Calliphoridae) body size and minimum development time. *Journal of Medical Entomology*, 48(5), 1062-1068. doi:10.1603/me11004
- Tramini, P., Bonnet, B., Sabatier, R., & Maury, L. (2001). A method of age estimation using Raman microspectrometry imaging of the human dentin. *Forensic Science International*, 118, 1-9.
- Voss, S. C., Magni, P., Dadour, I., & Nansen, C. (2016). Reflectance-based determination of age and species of blowfly puparia. *International Journal of Legal Medicine*. doi:doi:10.1007/s00414-016-1458-5
- Warren, J.-A., Ratnasekera, T. D. P., Campbell, D. A., & Anderson, G. S. (2017a). Initial investigations of spectral measurements to estimate the time within stages of *Protophormia terraenovae* (Robineau-Desvoidy) (Diptera: Calliphoridae). *Forensic Science International*, 278, 205-216. doi:10.1016/j.forsciint.2017.06.027

- Warren, J.-A., Ratnasekera, T. D. P., Campbell, D. A., & Anderson, G. S. (2017b). Spectral Signature of Immature *Lucilia sericata* (Meigen) (Diptera: Calliphoridae). *Insects*, 8(2). doi:10.3390/insects8020034
- Xu, H., Ye, G.-Y., Xu, Y., Hu, C., & Zhu, G.-H. (2014). Age-dependent changes in cuticular hydrocarbons of larvae in *Aldrichina grahami* (Aldrich) (Diptera: Calliphoridae). *Forensic Science International*, 242, 236-241.
- Zhu, G. H., Xu, X. H., Yu, X. J., Zhang, Y., & Wang, J. F. (2007). Puparial case hydrocarbons of *Chrysomya megacephala* as an indicator of the postmortem interval. *Forensic Science International*, 169, 1-5.

Chapter 8. Overall Discussion

8.1 Preface

This chapter ties all of the current research together and proposes future research.

8.2 Overview

This research has shown that prediction of day within stage of development is achievable using hyperspectral remote sensing. Spectral measurements from the posterior of *Lucilia sericata* (Meigen) and *Protophormia terraenovae* (R-D) provide the best prediction for the larval stages as compared with anterior and midsection measurements. Measurements from the anterior of the puparium were most promising for aging within the intra-puparial period including prepupal, pupal and pharate adult (Martin-Vega et al., 2016), at wavelengths that extend from 350-2500 nm for *L. sericata* and this range is most probably the same for *P. terraenovae*, although *P. terraenovae* was only examined from 400-1000 nm. When examining *P. terraenovae* pupae from 400-1000 nm, the only distinction that could be made was the last day of the intra-puparial period from the earlier days of the intra-puparial period and this was best done by examining the midsection spectral measurements (Figure 3-9). The last day of the intra-puparial period was probably able to be separated from the previous days of the intra-puparial period because the outline of the adult fly was visible under the light source to the human eye and, therefore, at wavelengths in the visible spectrum (400-700nm).

The cuticular hydrocarbons contributed to the daily larval spectral measurements but so would any other light reflective feature from the cuticular surface to minimal light penetrating depth. Surface changes, colour or opaqueness, bacterial surface organisms, spiracle and mouthpart changes and moulting are also probably key contributors to the spectral measurements. Near infrared spectroscopy identifies the C-H bonds of the cuticular hydrocarbons (Blomquist, 2010b; Foley et al., 1998). The cuticular hydrocarbons

main function is to waterproof the insect cuticle. The changing needs of the larvae through the stages, as expressed in the cuticular hydrocarbons, allow scientists to identify consistent demarcations to estimate day within stages. The cuticular hydrocarbons are formed by the ectodermal oenocytes which are often located in the abdominal integument (Martins & Ramalho-Ortigão, 2012). The location of the oenocytes explain why the posterior region spectral measurements are much more valuable for predicting age as lipophorin is needed to transport the hydrocarbons to the more distant anterior and midsection regions of the insect by means of the haemolymph. The longer travel distance of the hydrocarbons to these areas may decrease the concentrations of the hydrocarbons in those areas compared with the nearby posterior region. As the oenocytes themselves are located deep in the epidermis (Klowden, 2007) and not found in any of the layers of the cuticle, their changing structure is unlikely to contribute directly to the spectral reflectance measures but does contribute indirectly through the production of the hydrocarbons.

The intra-puparial spectral measurements are most probably affected by cuticular hydrocarbons, the brain, ommatidia, fat body and colour changes. As shown in the southern army worm, *Spodoptera eridania* (Stoll) and the cabbage looper *Trichoplusia ni* (Hübner), the synthesized cuticular hydrocarbons are probably not being transported to the blow fly puparium but are instead being delivered to the pharate adult where they are now needed (Blomquist, 2010a). It is most probable that the light is able to permeate the puparium through the upright striations of the exocuticle which were once represented by the pore canals of the larva (Dennell, 1947). The spectrometer is identifying significant reflectance changes between 1000 and 2500 nm, which can be interpreted as changes during the intra-puparial period to the metamorphosing blow fly. Penetration depth is greater in the NIR than it is in the visible spectrum (Voss et al., 2016). The anterior measurements of the puparium provided the most reliable day prediction in the intra-puparial period. This is probably due to the changes that occur to the brain and blow fly ommatidia. These changes are much more immediate in metamorphosis than those changes that occur in the other parts of the insect body, which remain obscured longer by the fat body (Davies & Harvey, 2013). The *P. terraenovae* spectral measurements could not be used to distinguish between

days of the intra-puparial period since the spectrometer that was used ranged only from 400-1000 nm.

An unusual artefact was present in some of the spectral measurements which appeared as a vertical jump point in the measurement. This was obviously an accidental characteristic as spectra are smooth and change gradually over wavelengths (Foley et al., 1998). Because of their gradual change these anomalies could be corrected and these shifts were redefined by first scanning for their existence and then rescaling everything after that point by a constant amount to make the function continuous across the jump. These vertical jumps tended to be found at 1000 and 1800nm suggesting that there is a potential crimp within the PVC fibre optic cable affecting these wavelengths and causing a loss of signal only at these wavelengths.

In the first experiments using *P. terraenovae*, the larvae were taken directly from the food substrate and measured without washing. Feeding instars were probably coated with bacteria and food substrate so, in order to determine whether the presence of such contaminants could have impacted the hyperspectral measurements, the subsequent experiments with *L. sericata* involved measuring the insects, then washing and measuring them a second time. There were no significant differences seen between the measurements made of the unwashed and washed post feeding *L. sericata* larvae. This is to be expected as the larvae have moved away from the food source so are less likely to be coated in contaminants. Washing the larvae did result in a significant difference in the spectral measurements of second instar and feeding third instar *L. sericata*, which is not surprising as these instars are still actively feeding within the food substrate. However, despite this, the predicted age was still within the 95% prediction interval, whether or not the larvae were washed.

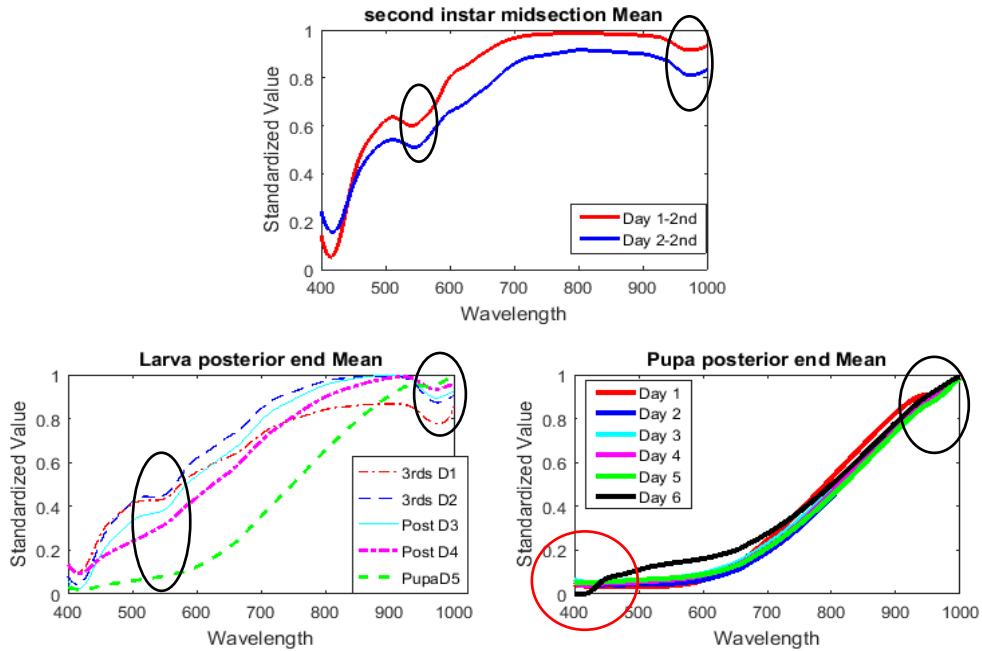
Laboratory experiments on blow flies regularly involve raising colonies on beef liver and this has been shown to be a good substitute for whole animal remains (Warren & Anderson, 2009). However, food substrate does affect the development rates of blow flies (Beuter & Mendes, 2013; Boatright & Tomberlin, 2010; Clark et al., 2006; Day & Wallman, 2006a; El-Moaty & Kheirallah, 2013; Flores et al., 2014; Niederegger et al.,

2013; Richards et al., 2013; Thyssen et al., 2014; Warren & Anderson, 2009; J. M. Wilson et al., 2014) and my research has shown that meat type also affects the spectral measurements of blow flies. There were significant effects when examining the interactional effect of pork heart with beef liver on *L. sericata* as well as significant effects from the different organ types and meat types alone. Fatty acid profiles differ between the food substrates and also have been shown to have an effect on the formation of the cuticular hydrocarbons of the mustard leaf beetle when investigating the effects of artificial diets on fatty acids (Otte et al., 2015). Food substrate may affect the spectral measurements directly but also contribute indirectly as food substrate and development coincide. It is probable that the food substrate affects development rate and the development rate is then affecting the spectral measurements. Before spectral measurements are applied to case work, research should be completed on insects developing on whole animals that were fed different diets to see if the fatty acid composition contributes directly or if diet indirectly affects the spectral measurements by affecting immature development. This is particularly necessary in animal neglect and abuse cases where the animal may not be fed adequately and a balanced diet is improbable. The spectral measurements of the insects developing on the neglected animal may then differ from those collected from insects developing on a healthy animal.

A visual analysis of the spectra for both *P. terraenovae* and *L. sericata* from second instar until adult emergence indicates that two separate troughs in the spectra are lost from second instar until adult emergence (Figure 8.1). The first trough, at 550 nm, is visible through second and third instar but disappeared once intra-puparial period was reached. The second trough (~975 nm), which is also visible in all stages, disappears just before adult emergence and is a good indicator that adult emergence is about to occur. The loss of the second trough was noticed in the posterior spectral measurements before either of the midsection or anterior measurements. The loss of these troughs is a result of water absorption. Early in the intra-puparial period, water is absorbed from the cuticle in order to reinforce the puparium (Zdarek & Fraenkel, 1972) and the disappearance of the trough at 550 nm would reflect this. Troughs in reflectance indicate strong absorption of energy by water at the coinciding wavelength (Lillesand, Kiefer, & Chipman, 2007) and due to

the disappearance of the trough, water must have been removed from the cuticle. Also noted was the difference between the spectra in the last day of the intra-puparial period of *P. terraenovae*. *P. terraenovae* day of development is easily distinguished at wavelengths between 400 and 500nm but is not so for *L. sericata*. This distinctive difference (Figure 8.1 (red circles)) found in *P. terraenovae* and not *L. sericata* was probably identified through the modified pore canals.

a) *Protophormia terraenovae* raised at 24.6°C (mean) (taken from chapter 3)



b) *Lucilia sericata* raised at 23.9°C (mean) (taken from chapter 4)

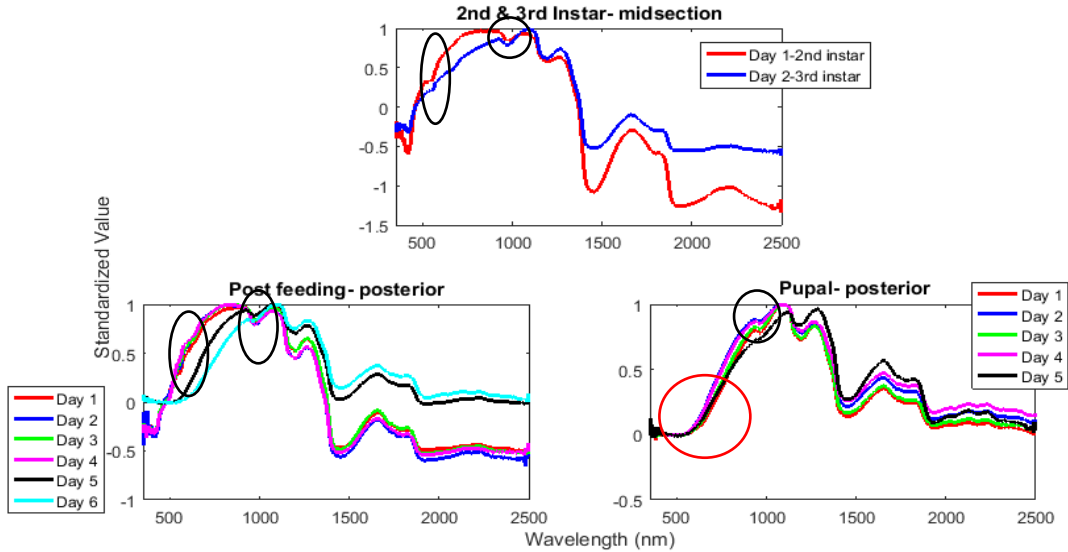


Figure 8-1 Mean daily posterior end and midsection spectral measurements separated into stages from *Protophormia terraenovae* and *Lucilia sericata*. Similar troughs are observed at 550 and 975nm (black circles). The 550nm trough was gone once the intra-puparial period was reached and the 975nm trough was no longer visible just before adult emergence. The red circle indicates the difference observed on the last day of intra-puparial period between *P. terraenovae* and *L. sericata*.

In general, it was also noticed that the last day of one stage had a similar spectral signature to the first day of the next. This suggests that changes are not immediate but more gradual and supports cuticular hydrocarbons being the main contributor since they also do not change instantaneously but instead gradually.

At this time, narrowing to a single or fewer wavelengths was not completed to avoid losing distinguishing details or features and to maintain high confidence; this could be considered in the future. By combining all of the beta coefficients and all contributing wavelengths, more detail was included in distinguishing days within stages from each other. In the future, the wavelengths can be narrowed to the top contributing wavelengths and not include all wavelengths. A spectrometer with only those specific wavelengths can be used which would reduce the cost of equipment.

The findings are all presented with potential error rates of 95% pointwise confidence and prediction intervals including the upper and lower limits. Providing accuracy and error rates is important as they are required by *Daubert v. Merrell Dow Pharmaceuticals Ltd.* The Daubert standard dictates the admissibility of evidence in court and replaced the less flexible Frye standard. Evidence is admissible if the theory or technique (1) can be tested, (2) has been peer reviewed, (3) has known error rates, (4) has existing standards controlling its operation by the relevant scientific community, and (5) has widespread acceptance by the relevant scientific community (*Daubert v. Merrell Dow Pharmaceuticals Ltd.*(92-102), 509 U.S. 579 1993). The National Research Council for the National Academy of Sciences (NAS) reviewed forensic sciences in the US in 2009 and criticized many sciences for not including error rates (Council, 2009). While forensic entomology was not mentioned specifically in the NAS report as having any serious concerns, it is agreed by forensic entomologists that forensic entomology should move towards standardization of terminology (Tomberlin, Mohr, et al., 2011), blind validation (VanLaerhoven, 2008) and determining error rates (Tarone & Foran, 2008).

Although this research narrows current estimates to within stage of development and is persuasive with its 95% point wise intervals to apply in the field of forensic entomology and death investigations, we still need to address its robustness among the

forensic community. Ideally, spectral measurements to age insects should first be included in blind validation studies before the technique is ever applied to criminal proceedings. All new applications of forensic science should address the requirements of the NAS report.

Furthermore, the findings in this dissertation are based on replenished colonies of wild caught *P. terraenovae* and *L. sericata* and although they were regularly replenished, applying these findings to forensic entomology cases or wild populations should be done with caution. There is always the potential that isolated insects will express genetic differences that are not seen in wild populations (Howe, 1967). Not only are there wild population differences, but wild insects also experience daily fluctuations (**thermoperiods**) and unpredictable fluctuating temperatures, which can affect day and rate of development (Howe, 1967). These temperature fluctuations are bound to affect spectral measurement prediction.

8.3 Future Work and Considerations

The next steps will be to expand the research to identify exactly where the oenocytes are in the developing immature blow fly so that the best region to measure can be stated conclusively. Further work needs to be completed on specific carrion types with different diets controlled for fatty acids so that the results can be carried over to case work without food substrate affecting the spectral measurements directly and only through development. This would be particularly important in neglect cases since the neglected may be lacking in balanced nutrients. This difference may affect the spectral measurements of the insects developing on the neglected animal/person.

Further work should be done to compare the measurements between the entire puparium and the developing pharate adult to confirm that the developing adult is, in fact, a strong contributor to the intra-puparial measurements from 1000- 2500 nm.

In the intra-puparial spectral measurements, there is the potential that there are sexually dimorphic differences in the forming pharate adults. These must be taken into consideration as there could be cuticular hydrocarbon differences as well as the

physiological differences between sexes. Spectral measurements should be performed, and each pupa maintained separately to determine sex once emerged. Cuticular hydrocarbon differences exist between sexes in blow flies (Braga, Pinto, de Carvalho Queiroz, & Blomquist, 2016; Pechal, Moore, et al., 2014; Trabalon, Campan, Clement, Lange, & Miquel, 1992). Not only do the cuticular hydrocarbons differ between sexes at different ages but genome size differences between sexes have been found in several blow fly species including *P. terraenovae* and *L. sericata* (Picard, Johnston, & Tarone, 2012).

Further blow fly species should have spectral measurements taken, and the current species should be examined at different temperatures and then a comparison can be made to see if the spectral measurements are consistent across temperature regimes. This approach would probably confirm that measurements are related to development changes rather than species and food substrates. It can also be expanded over more wavelengths to see if more detail is identified. As well as testing more data sets, blind validation of these experiments also needs to be explored.

Spectral measurements of adult flies can also be compared between adult teneral flies, post-teneral flies and those that have received their first protein meal to see if differences exist and distinctions between adult flies can be made. Being able to distinguish between teneral flies, post teneral flies and those that have received their first protein meal could allow aging newly emerged adult flies or distinguishing them from the adult flies that are newly arriving to the remains.

Development on whole human/wild life/SPCA remains compared with beef liver and other meat types for different blow fly species should be completed to see if beef liver is the best tissue for lab research to be completed on for other forensically important species as it is for *P. terraenovae* (Warren & Anderson, 2009). If development of other forensically important blow fly species on beef liver is not comparable with that of whole remains then another meat type must be identified for those species and research should continue with that meat type.

Laboratory measurements should be compared with field measurements from the same insects and the same spectrometer. The blackened laboratory minimized contributing

reflectance from surrounding objects. This is not an option in the field and not in many laboratories. It is unlikely that surrounding objects will contribute considerably to the measurements as hyperspectral remote sensing is frequently completed in the field. Ideally these measurements will be taken at the death scene or in the morgue at the time of collection with a field spectrometer to collect the spectral measurements at the nearest time to discovery without introducing more changes in development rate. Also, species will be determined immediately using hyperspectral remote sensing (Pickering et al., 2015). Temperature data could be collected as soon as possible and then forensic entomology report turn-around time would be faster and estimated times more precise.

8.4 Conclusions

The benefits of remote sensing in the forensic sciences far outweigh the limitation of costly science by offering a non-invasive, non-destructive contaminant-free means of completing current techniques, which often involve sacrificing the insect specimens. In addition, hyperspectral remote sensing offers new opportunities for established sciences. Forensic entomology is one of many sciences that can benefit from hyperspectral remote sensing. Methods already exist that can be used to age insects based on cuticular hydrocarbons, volatile organic compounds, gene expression and computed tomography but these methods cannot be completed in the field in a timely manner. One of the main benefits to hyperspectral remote sensing is the portability of the instrument. Remote sensing will not identify the exact molecules that are causing differences in the spectral signatures as GC/MS does but it does identify that there is a difference. Due to the ability to complete this immediately in the field, this may offer a much faster analysis of the specimens in the not so distant future.

This proof of concept research has indicated that differences in spectral measurements exist between days within stages. The hyperspectral analyses were presented as day within stages at each of the measured temperatures which is specific to those temperatures. A comparison at all temperatures can be made by converting the

findings to thermal units, ADD. A base temperature or lower temperature threshold for *L. sericata* from the Lower Mainland of British Columbia is needed to convert to ADD. As all findings would be in the same units, this would allow for a comparison over an array of temperatures.

Reference List

- Akbari, H., Uto, K., Kosugi, Y., Kojima, K., & Tanaka, N. (2010). Cancer detection using infrared hyperspectral imaging. *Journal of the Japanese Cancer Association*, 102(4), 852-857.
- Akino, T. (2006). Cuticular hydrocarbons of *Formica truncorum* (Hymenoptera: Formicidae): Description of new very long chained hydrocarbon components. *Applied Entomology and Zoology*, 41(4), 667-677.
- Amendt, J., Krettek, R., & Zehner, R. (2004). Forensic Entomology. *Naturwissenschaften*, 91, 51-65.
- Amendt, J., Richards, C. S., Campobasso, C. P., Zehner, R., & Hall, M. J. R. (2011). Forensic Entomology: applications and limitations. *Forensic Science Medical Pathology*, 7, 379-392.
- Anderson, G. S. (2000). Minimum and maximum development rates of some forensically important Calliphoridae (Diptera). *Journal of Forensic Science*, 45(4), 824-832.
- Anderson, G. S. (2001). Forensic entomology in British Columbia: A brief history. *Journal of the Entomological Society of British Columbia*, 98, 127-135.
- Anderson, G. S. (2010). Factors that influence insect succession on carrion. In J. H. a. C. Byrd, J.L. (Ed.), *Forensic entomology The utility of arthropods in legal investigations* (pp. 201-250). Boca Raton: CRC Press.
- Anderson, G. S., & VanLaerhoven, S. L. (1996). Initial studies on insect succession on carrion in southwestern British Columbia. *Journal of Forensic sciences*, 41(4), 613-621.
- Ash, N., & Greenberg, B. (1974). Developmental temperature responses of the sibling species *Phaenicia sericata* and *Phaenicia pallescens*. *Annals of the Entomological Society of America*, 68(2).
- Baer, I., Gurny, R., & Margot, P. (2007). NIR analysis of cellulose and lactose-application to ecstasy tablet analysis. *Forensic Science International*, 167, 234-241.
- Baker, B. (2002). The use of radar gun technology in the physics classroom/laboratory. *The Physics Teacher*, 40, 94-95.

- Bartick, E., Schwartz, R., Bhargava, R., Schaeberle, M., Fernandez, D., & Levin, I. (2002, September 2-7th 2002). *Spectrochemical Analysis and Hyperspectral Imaging of Latent Fingerprints*. Paper presented at the 16th Meeting of the International Association of Forensic Sciences, Montpellier, France.
- Beck, L. R., Lobitz, B. M., & Wood, B. L. (2000). Remote Sensing and Human Health: New sensors and new opportunities. *Emerging Infectious Diseases*, 6(3), 217-226.
- Beck, S. D. (1983). Insect thermoperiodism. *Annual Review of entomology*, 28, 91-108.
- Benbow, M. E., Lewis, A. J., Tomberlin, J. K., & Pechal, J. L. (2013). Seasonal necrophagous insect community assembly during vertebrate carrion decomposition. *Journal of Medical Entomology*, 50(2), 440-450.
- Bernhardt, V., Schomerus, C., Verhoff, M. A., & Amendt, J. (2016). Of pigs and men-comparing the development of *Calliphora vicina* (Diptera:Calliphoridae) on human and porcine tissue. *International Journal of Legal Medicine*. doi:10.1007/s00414-016-1487-0
- Beuter, L., & Mendes, J. (2013). Development of *Chrysomya albiceps* (Wiedemann) (Diptera: Calliphoridae) in different pig tissues. *Neotropical Entomology*, 42, 426-430.
- Blackburn, G. A. (1998). Quantifying Chlorophylls and Carotenoids at Leaf and Canopy Scales: An Evaluation of Some Hyperspectral Approaches. *Remote Sensing Environment*, 66, 273-285.
- Blomquist, G. J. (2010a). Biosynthesis of cuticular hydrocarbons. In G. J. Blomquist & A.-G. Bagnères (Eds.), *Insect Hydrocarbons Biology, Biochemistry and Chemical Ecology* (pp. 35-52). New York: Cambridge University Press.
- Blomquist, G. J. (2010b). Structure and analysis of insect hydrocarbons. In G. J. Blomquist & A.-G. Bagnères (Eds.), *Insect Hydrocarbons Biology, Biochemistry and Chemical Ecology* (pp. 19-34). New York: Cambridge University Press.
- Blomquist, G. J., & Bagnères, A.-G. (2010). Introduction: history and overview of insect hydrocarbons. In G. J. Blomquist & A.-G. Bagnères (Eds.), *Insect Hydrocarbons Biology Biochemistry and Chemical Ecology* (pp. 3-18). New York: Cambridge University Press.
- Boatright, S. A., & Tomberlin, J. K. (2010). Effects of temperature and tissue type on the development of *Cochliomyia macellaria* (Diptera: Calliphoridae). *Journal of Medical Entomology*, 47(5), 917-923.

- Boehme, P., Amendt, J., & Zehner, R. (2009). *Using real-time PCR approaches to determine a blowfly pupa's age*. Paper presented at the North American Forensic Entomology Association (NAFEA), Miami, Florida.
- Boehme, P., Spahn, P., Amendt, J., & Zehner, R. (2013). Differential gene expression during metamorphosis: a promising approach for age estimation of forensically important *Calliphora vicina* pupae (Diptera: Calliphoridae). *International Journal of Legal Medicine*, *127*, 243-249.
- Borengasser, M., Hungate, W. S., & Watkins, R. (2008). *Hyperspectral Remote Sensing: Principles and Applications* (First ed.). Boca Raton: Taylor and Francis Group.
- Bourel, B., Tournel, G., Hedouin, V., Deveaux, M., Goff, M. L., & Gosset, D. (2001). Morphine extraction in necrophagous insects remains for determining ante-mortem opiate intoxication. *Forensic Science International*, *120*, 127-131.
- Braga, M. V., Pinto, Z. T., de Carvalho Queiroz, M. M., & Blomquist, G. J. (2016). Effect of age on cuticular hydrocarbon profiles in adult *Chrysomya putoria* (Diptera: Calliphoridae). *Forensic Science International*, *259*, e37-e47.
- Brauns, E. B., & Dyer, R. B. (2006). Fourier Transform Hyperspectral Visible Imaging and the Nondestructive Analysis of Potentially Fraudulent Documents. *Applied Spectroscopy*, *60*(8), 833-840.
- Bremmer, R. H., de Bruin, D. M., de Joode, M., Buma, W. J., Van Leeuwen, T. G., & Aalders, M. C. G. (2011). Biphasic oxidation of oxy-hemoglobin in blood stains. *PLoS ONE*, *6*(7), 1-6. doi:doi:10.1371/journal.pone.0021845
- Bremmer, R. H., Nadort, A., van Leeuwen, T. G., van Gemert, M. J. C., & Aalders, M. C. G. (2011). Age estimation of blood stains by hemoglobin derivative determination using reflectance spectroscopy. *Forensic Science International*, *206*, 166-171. doi:doi:10.1016/j.forsciint.2010.07.034
- Brewer, L. N., Ohlhausen, J. A., Kotula, P. G., & Michael, J. R. (2008). Forensic analysis of bioagents by X-ray and TOF-SIMS hyperspectral imaging. *Forensic Science International*, *179*, 98-106.
- Brown, H. E., Diuk-Wasser, M. A., Guan, Y., Caskey, S., & Fish, D. (2008). Comparison of three satellite sensors at three spatial scales to predict larval mosquito presence in connecticut wetlands. *Remote Sensing of Environment*, *112*, 2301-2308.
- Brown, K., Thorne, A., & Harvey, M. (2015). *Calliphora vicina* (Diptera: Calliphoridae) pupae: a timeline of external morphological development and a new age and PMI estimation tool. *International Journal of Legal Medicine*, *129*, 835-850.

- Buchanan, M. V., Asano, K., & Bohanon, A. (1997). Characterization of fingerprints from adults and children. *Proceedings of SPIE*, 2941, 89-92. doi:doi: 10.1117/12.266300
- Bumbrah, G. S., & Sharma, R. M. (2015). Raman spectroscopy – Basic principle, instrumentation and selected applications for the characterization of drugs of abuse. *Egyptian Journal of Forensic Science*, article in press. doi:http://dx.doi.org/10.1016/j.ejfs.2015.06.001
- Butcher, J. B., Moore, H. E., Day, C. R., Adam, C. D., & Drijfhout, F. P. (2013). Artificial neural network analysis of hydrocarbon profiles for the ageing of *Lucilia sericata* for post mortem interval estimation. *Forensic Science International*, 232, 25-31.
- Byrd, J. H. (2016). [Department of Pathology, Immunology and Laboratory Medicine, University of Florida College of Medicine].
- Campbell, J. B. (2007). *Introduction to Remote Sensing* (Fourth ed.). New York: The Guilford Press.
- Campobasso, C. P., Linville, J. G., Wells, J. D., & Introna, F. (2005). Forensic Genetic Analysis of Insect Gut Contents. *The American Journal of Forensic Medicine and Pathology*, 26(2), 161-165.
- Canada, N. R. (2001). Fundamentals of Remote sensing, A Canada Centre for Remote Sensing Remote Sensing Tutorial. Retrieved from http://ccrs.nrcan.gc.ca/resource/tutor/fundam/pdf/fundamentals_e.pdf
- Carroll, M. W., Glaser, J. A., Hellmich, R. L., Hunt, T. E., Sappington, T. W., Calvin, D., . . . Fridgen, J. (2008). Use of spectral vegetation indices derived from airborne hyperspectral imagery for detection of European corn borer infestation in Iowa corn plots. *Journal of Economic Entomology*, 101(5), 1614-1623.
- Catts, E. P. (1992). Problems in estimating the postmortem interval in death investigations. *Journal of Agricultural Entomology*, 9(4), 245-255.
- Catts, E. P., & Goff, M. L. (1992). Forensic entomology in criminal investigations. *Annual Review of entomology*, 37, 253-272.
- Chapman, R. F. (1980). *The Insects, Structure and Function*. London, Hodder and Stoughton.
- Chung, H., & Carroll, S. B. (2015). Wax, sex and the origin of species: Dual roles of insect cuticular hydrocarbons in adaptation and mating. *Bioessays Prospects and Overviews*, 37, 822-830. doi:DOI 10.1002/bies.201500014

- Clark, K., Evans, L., & Wall, R. (2006). Growth rates of the blowfly, *Lucilia sericata*, on different body tissues. *Forensic Science International*, 156, 145-149.
- Claybourn, M., & Ansell, M. (2000). Using Raman Spectroscopy to solve crime: inks, questioned documents and fraud. *Scientific and Technical, The Forensic Science Society*, 40(4), 261-271.
- Council, N. R. (2009). *Strengthening Forensic Science in the United States: A Path Forward*. Washington, D.C.: The National Academies Press.
- Cracknell, A. P., & Hayes, L. (2007). *Introduction to remote sensing*. Boca Raton: CRC Press.
- Crane, N. J., Bartick, E. G., Perlman, R. S., . , & Huffman, S. (2007). Infrared Spectroscopic Imaging for Noninvasive Detection of Latent Fingerprints. *Journal of Forensic sciences*, 52(1), 48-53.
- Davies, K., & Harvey, M. L. (2013). Internal Morphological Analysis for Age Estimation of Blow Fly Pupae (Diptera: Calliphoridae) in Postmortem Interval Estimation. *Journal of Forensic Science*, 58(1), 79-84. doi:doi: 10.1111/j.1556-4029.2012.02196.x
- Day, D. M., & Wallman, J. F. (2006a). Influence of substrate tissue type on larval growth in *Calliphora augur* and *Lucilia cuprina* (Diptera: Calliphoridae). *Journal of Forensic Science*, 51(3), 657-663.
- Day, D. M., & Wallman, J. F. (2006b). Width as an alternative measurement to length for post-mortem interval estimations using *Calliphora augur* (Diptera: Calliphoridae) larvae. *Forensic Science International*, 159, 158-167.
- de Lourdes Chávez-Briones, M., Hernández-Cortés, R., Díaz-Torres, P., Niderhauser-García, A., Ancer-Rodríguez, J., Jaramillo-Rangel, G., & Ortega-Martínez, M. (2013). Identification of Human Remains by DNA Analysis of the Gastrointestinal Contents of Fly Larvae. *Journal of Forensic sciences*, 58(1), 248-250.
- Defilippo, F., Bonilauri, P., & Dottori, M. (2013). Effect of Temperature on Six Different Developmental Landmarks within the Pupal Stage of the Forensically Important Blowfly *Calliphora vicina* (Robineau-Desvoidy) (Diptera: Calliphoridae). *Journal of Forensic sciences*, 58(6), 1554-1557.
- Dennell, R. (1946). *A Study of an Insect Cuticle: The Larval Cuticle of Sarcophaga ferculata Pand. (Diptera)*. Paper presented at the Proceedings of the Royal Society of London. Series B, Biological Sciences.

- Dennell, R. (1947). A Study of an Insect Cuticle: The Formation of the Puparium of *Sarcophaga falculata* Pand.(Diptera). *Proceedings of the Royal Society of London. Series B, Biological Sciences*, 134(874), 79-110.
- Early, M., & Goff, M. L. (1986). Arthropod succession patterns in exposed carrion on the island of Oahu, Hawaii. *Journal of Medical Entomology*, 23(5), 520-531.
- Edelman, G., Manti, V., van Ruth, S. M., van Leeuwen, T. G., & Aalders, M. (2012). Identification and age estimation of blood stains on colored backgrounds by near infrared spectroscopy. *Forensic Science International*, 220, 239-244. doi:doi:10.1016/j.forsciint.2012.03.009
- Edelman, G., van Leeuwen, T. G., & Aalders, M. C. G. (2012). Hyperspectral imaging for the age estimation of blood stains at the crime scene. *Forensic Science International*, 223, 72-77.
- El-Moaty, Z. A., & Kheirallah, A. E. M. (2013). Developmental variation of the blow fly *Lucilia sericata* (Meigen, 1826) (Diptera: Calliphoridae) by different substrate tissue types. *Journal of Asia-Pacific Entomology*, 16, 297-300.
- Erzinçlioğlu, Y. Z. (1996). *Blowflies. Naturalists Handbook 23*. Slough, Great Britain: Richmond Publishing Co. Ltd.
- Exline, D., Schuler, R., Treado, P. J., & Corporation, C. I. (2003). Improved fingerprint visualization using luminescence and visible reflectance chemical imaging. *Forensic Science Communications*, 5(3), unknown.
- Fan, Y., Zurek, L., Dykstra, M. J., & Schal, C. (2003). Hydrocarbon synthesis by enzymatically dissociated oenocytes of the abdominal integument of the German Cockroach, *Blattella germanica*. *Naturwissenschaften*, 90, 121-126.
- Finell, N., & Järvilehto, M. (1983). Development of the compound eyes of the blow fly *Calliphora erythrocephala*: changes in morphology and function during metamorphosis. *Annales Zoologici Fennici*, 20, 223-234.
- Fleming, R. W., Torralba, A., & Adelson, E. H. (2004). Specular reflections and the perception of shape. *Journal of Vision*, 4, 798-820.
- Flores, M., Longnecker, M., & Tomberlin, J. K. (2014). Effects of temperature and tissue type on *Chrysomya rufifacies* (Diptera: Calliphoridae) (Macquart) development. *Forensic Science International*, 245, 24-29.

- Flynn, K., O'Leary, R., Lennard, C., Roux, C., & Reedy, B. J. (2005). Forensic applications of infrared chemical imaging: Multilayered paint chips. *Journal of Forensic Science*, 50(4), 832-841.
- Flynn, K., O'Leary, R., Roux, C., & Reedy, B. J. (2006). Forensic analysis of bicomponent fibers using infrared chemical imaging. *Journal of Forensic Science*, 51(3), 586-596.
- Foley, W. J., McIlwee, A., Lawler, I., Aragonés, L., Woolnough, A. P., & Berding, N. (1998). Ecological applications of near infrared reflectance spectroscopy - a tool for rapid, cost-effective prediction of the composition of plant and animal tissues and aspects of animal performance. *Oecologia*, 116, 293-305.
- Frederickx, C., Dekeirsschieter, J., Brostaux, Y., Wathélet, J.-P., Verheggen, F. J., & Haubruge, E. (2012). Volatile organic compounds released by blowfly larvae and pupae: New perspectives in forensic entomology. *Forensic Science International*, 219, 215-220.
- Fuller, T., Thomasson, H. A., Mulembakani, P. M., Johnston, S. C., Lloyd-Smith, J. O., Kivalu, N. K., . . . Rimoin, A. W. (2011). Using remote sensing to map the risk of human Monkeypox virus in the Congo Basin. *EcoHealth*, 8, 14-25. doi:DOI: 10.1007/s10393-010-0355-5
- Gallagher, M. B., Sandhu, S., & Kimsey, R. (2010). Variation in developmental time for geographically distinct populations of the common Green Bottle Fly, *Lucilia sericata* (Meigen). *Journal of Forensic Science*, 55(2), 438-442. doi:10.1111/j.1556-4029.2009.01285.x
- Gennard, D. E. (2012). *Forensic Entomology an introduction* (2nd ed.). Chichester, West Sussex: Wiley Blackwell.
- Goff, M. L. (2000). *A fly for the prosecution, How Insect Evidence Helps Solve Crimes*. Cambridge Massachusetts: Harvard University Press
- Gosselin, M., Wille, S. M. R., del Mar Ramirez Fernandez, M., Di Fazio, V., Samyn, N., De Boeck, G., & Bourel, B. (2011). Entomotoxicology, experimental set-up and interpretation for forensic toxicologists. *Forensic Science International*, 208, 1-9.
- Govender, M., Chetty, K. and H. Bulcock. (2007). A review of hyperspectral remote sensing and its application in vegetation and water resource studies. *Water SA (online)*, 33(2), 145-151.

- Grassberger, M., & Reiter, C. (2001). Effects of temperature on *Lucilia sericata* (Diptera: Calliphoridae) development with special reference to the Isomegalen- and Isomorphen -Diagram. *Forensic Science International*, 120, 32-36.
- Grassberger, M., & Reiter, C. (2002). Effect of temperature on development of the forensically important holarctic blow fly *Protophormia terraenovae* (Robineau-Desvoidy) (Diptera:Calliphoridae). *Forensic Science International*, 128, 177-182.
- Greenberg, B. (1991). Flies as forensic indicators. *Journal of Medical Entomology*, 28, 565-577.
- Greenberg, B., & Kunich, J. C. (2002). *Entomology and the Law, Flies as Forensic Indicators*. United Kingdom: Cambridge University Press.
- Hais, M., Wild, J., Berec, L., Br °una, J., Kennedy, R., Braaten, J., & Brož, Z. (2016). Landsat imagery spectral trajectories—Important variables for spatially predicting the risks of Bark Beetle disturbance. *Remote Sensing*, 8(687), 1-22. doi:doi:10.3390/rs8080687
- Hall, M. J. R., & Brandt, A. P. (2006a). Forensic entomology. *Science in School The European journal for science teachers*. Retrieved from www.scienceinschool.org
- Hall, M. J. R., & Brandt, A. P. (2006b, 26-29th April). *The use of thermal imaging to study the effect of larval masses on the development of blow fly larvae*. Paper presented at the Page 33 in Programs and Abstracts of European Association of Forensic Entomology, Bari, Italy.
- Harnden, L. M., & Tomberlin, J. K. (2016). Effects of temperature and diet on black soldier fly, *Hermetia illucens* (L.) (Diptera: Stratiomyidae), development. *Forensic Science International*, 266, 109-116.
- Hart, W. G., Ingle, S. J., Davis, M. R., Mangum, C., Higgins, A., & Boling, J. C. (1971, 2-4 March). *Some uses of infrared aerial color photography in entomology*. Paper presented at the Proceedings of the third Biennial workshop on Aerial Color in the Plant Sciences.
- Hendricks, D. E. (1980). Low frequency sodar device that counts flying insects attracted to sex pheremone dispensers. *Environmental Entomology*, 9, 452-457.
- Henssge, C., Madea, B., Knight, B., Nokes, L., & Krompecher, T. (1995). *The estimation of the time since death in the early postmortem interval* (2nd ed. ed.): Arnold.
- Hobson, R. P. (1932). Studies on the nutrition of blow fly larvae. III. The liquefaction of muscle. *Journal of Experimental Biology*, 9, 359-365.

- Holz, R. K. (1985). *The Surveillant Science: The Remote Sensing of the Environment* (Second ed.): John Wiley and Sons.
- Howe, R. W. (1967). Temperature effects on embryonic development in insects. *Annual Review of entomology*, *12*, 15-42.
- Hughes, V. K., & Langlois, N. E. I. (2011). Visual and spectrophotometric observations related to histology in a small sample of bruises from cadavers. *Forensic Science Medical Pathology*, *7*, 253-256.
- Ireland, S., & Turner, B. (2006). The effects of larval crowding and food type on the size and development of the blowfly, *Calliphora vomitoria*. *Forensic Science International*, *159*, 175-181.
- Järvilehto, M., & Finell, N. (1983). Development of the function of visual receptor cells during the pupal life of the fly *Calliphora*. *Journal of Comparative Physiology*, *150*, 529-536.
- Johnson, A. P., & Wallman, J. F. (2014). Infrared imaging as a non-invasive tool for documenting maggot mass temperatures. *Australian Journal of Forensic Science*, *46*(1), 73-79.
- Kalacska, M., & Bell, L. S. (2006). Remote sensing as a tool for the detection of clandestine mass graves. *Canadian Society of Forensic Science*, *39*(1), 1-13.
- Kalacska, M., Bell, L. S., Sanchez-Azofeifa, G. A., & Caelli, T. (2009). The application of remote sensing for detecting mass graves: An experimental animal case study from Costa Rica. *Journal of Forensic Science*, *54*(1), 159-166.
- Kalacska, M., Bell, L. S., & Thiessen, B. (2007). Remote detection of clandestine graves. *Blue Line Magazine*, 8-10.
- Kalacska, M., Sanchez-Azofeifa, G. A., Rivard, B., Caelli, T., White, H. P., & Calvo-Alvarado, J. C. (2007). Ecological fingerprinting of ecosystem succession: Estimating secondary tropical dry forest structure and diversity using imaging spectroscopy. *Remote Sensing of Environment*, *108*, 82-96.
- Kamal, A. S. (1958). Comparative study of thirteen species of sarcosaprophagous Calliphoridae and Sarcophagidae (Diptera) I. Bionomics. *Annals of the Entomological Society of America*, *51*, 261-270.
- Kaneshrajah, G., & Turner, B. (2004). *Calliphora vicina* larvae grow at different rates on different body tissues. *International Journal of Legal Medicine*, *118*, 242-244. doi:DOI 10.1007/s00414-004-0444-5

- Kashyap, V. K., & Pillai, V. V. (1989). Efficacy of entomological method in estimation of post-mortem interval: a comparative analysis. *Forensic Science International*, *40*, 245-250.
- Khan, Z., Shafait, F., & Mian, A. (2015). Automatic ink mismatch detection for forensic document analysis. *Pattern Recognition*, *48*, 3615-3626.
- Kharbouche, H., Augsburger, M., Cherix, D., Sporkert, F., Giroud, D., Wyss, C., . . . Mangin, P. (2008). Codeine accumulation and elimination in larvae, pupae, and imago of the blowfly *Lucilia sericata* and effects on its development. *International Journal of Legal Medicine*, *122*, 205-211. doi:DOI 10.1007/s00414-007-0217-z
- Klowden, M. J. (2007). *Physiological Systems in Insects*. Burlington MA: Elsevier Inc.
- Langlois, N. E. I. (2007). The science behind the quest to determine the age of bruises-- a review of the English language literature. *Forensic Science Medical Pathology*, *3*, 241-251.
- Lawrence, R., & Labus, M. (2003). Early detection of Douglas -fir beetle infestation with subcanopy resolution hyperspectral imagery. *Western Journal of Applied Forestry*, *18*(3), 1-5.
- Leblanc, G., Kalacska, M., & Soffer, R. (2014). Detection of single graves by airborne hyperspectral imaging. *Forensic Science International*, *245*, 17-23.
- Lega, M., Ferrara, C., Persechino, G., & Bishop, P. (2014). Remote sensing in environmental police investigations: aerial platforms and an innovative application of thermography to detect several illegal activities. *Environmental Monitoring Assessment*, *186*, 8291-8301. doi:DOI 10.1007/s10661-014-4003-3
- Li, B., Beveridge, P., O'Hare, W. T., & Islam, M. (2011). The estimation of the age of a blood stain using reflectance spectroscopy with a microspectrophotometer, spectral pre-processing and linear discriminant analysis. *Forensic Science International*, *212*, 198-204.
- Li, B., Beveridge, P., O'Hare, W. T., & Islam, M. (2013). The age estimation of blood stains up to 30 days old using visible wavelength hyperspectral image analysis and linear discriminant analysis. *Science and Justice*, *53*, 270-277.
- Li, B., Beveridge, P., O'Hare, W. T., & Islam, M. (2014). The application of visible wavelength reflectance hyperspectral imaging for the detection and identification of blood stains. *Science and Justice*, *54*, 432-438.

- Li, X., Cai, J. F., Guo, Y. D., Xiong, F., Zhang, L., Feng, H., . . . Chen, Y. Q. (2011). Mitochondrial DNA and STR analyses for human DNA from maggots crop contents: A forensic entomology case from central-southern China. *Tropical Biomedicine*, 28(2), 333-338.
- Lillesand, T. M., Kiefer, R. W., & Chipman, J. W. (2007). *Remote Sensing and Image Interpretation* (6th ed.). Hoboken New Jersey: John Wiley and Sons.
- Ma, Q., Fonseca, A., Liu, W., Fields, A. T., Pimsler, M. L., Spindola, A. F., . . . Wood, T. K. (2012). *Proteus mirabilis* interkingdom swarming signals attract blow flies. *International Society for Microbial Ecology*, 6, 1356-1366.
- MacLeod, N. A., & Matousek, P. (2008). Emerging non-invasive raman methods in process control and forensic application. *Pharmaceutical Research*, 25(10), 2205-2215.
- Makki, R., Cinnamon, E., & Gould, A. P. (2014). The development and functions of oenocytes. *Annual Review of entomology*, 59, 405-425. doi:10.1146/annurev-ento-011613-162056
- Malkoff, D. B., & Oliver, W. R. (2000). *Hyperspectral imaging applied to forensic medicine*. Paper presented at the Proceedings of SPIE.
- Mandeville, D. J. (1988). as cited in Byrd J.H. Laboratory Rearing of Forensic Insects. In J. H. Byrd & J. L. Castner (Eds.), *Forensic Entomology: The Utility of Arthropods in Legal Investigations 2001*. Boca Raton: CRC Press Ltd.
- Martin-Vega, D., Hall, M. J. R., & Simonsen, T. J. (2016). Resolving confusion in the use of concepts and terminology in intrapuparial development studies of cyclorrhaphous diptera *Journal of Medical Entomology*, 53(6), 1249-1251. doi:doi:10.1093/jme/tjw081
- Martin-Vega, D., Simonsen, T. J., & Hall, M. J. R. (2017). Looking into the puparium: Micro-CT visualization of the internal morphological changes during metamorphosis of the blow fly, *Calliphora vicina*, with the first quantitative analysis of organ development in cyclorrhaphous dipterans. *Journal of Morphology*, 278, 629-651. doi:10.1002/jmor.20660
- Martin-Vega, D., Simonsen, T. J., Wicklein, M., & Hall, M. J. R. (2017). Age estimation during the blow fly intra-puparial period: a qualitative and quantitative approach using micro-computed tomography. *International Journal of Legal Medicine*. doi:10.1007/s00414-017-1598-2

- Martin, J. E. H. (1977). *The Insect and Arachnids of Canada. Part 1. Collecting, preparing and preserving insects, mites and spiders*, Biosystematics Research Institute. Ottawa, Ontario, Research Branch, Canada Department of Agriculture.
- Martins, G. F., & Ramalho-Ortigão, J. M. (2012). Oenocytes in insects. *Invertebrate Survival Journal*, 9(2).
- Maynard, P., Jenkins, J., Edey, C., Payne, G., Lennard, C., McDonagh, A., & Roux, C. (2009). Near infrared imaging for the improved detection of fingermarks on difficult surfaces. *Australian Journal of Forensic Sciences*, 41(1), 43-62.
- Mazella, W. D., & Buzzini, P. (2005). Raman spectroscopy of blue gel pen inks. *Forensic Science International*, 152, 241-247.
- McKnight, B. E. (1981). *The Washing Away of Wrongs: Forensic Medicine in Thirteenth Century China by Sung T'zu*. Ann Arbor, Center for Chinese Studies, Univ. Mich.
- Mégnin, P. (1894). La Faune des Cadavres *Encyclopedie Scientifique des Aide-Memoire* (pp. 28). Paris: Masson Gauthier-Villars et Fils.
- Meng, J., Li, S., Wang, W., Liu, Q., Xie, S., & Ma, W. (2016). Mapping forest health using spectral and textural information extracted from SPOT-5 satellite images. *Remote Sensing*, 8(719), 1-20. doi:doi:10.3390/rs8090719
- Mimasaka, S., Ohtani, M., Kuroda, N., & Tsunenari, S. (2010). Spectrophotometric Evaluation of the age of bruises in children: Measuring Changes in bruise color as an indicator of child physical abuse. *Tohoku Journal of Experimental Medicine*, 220, 171-175.
- Mirik, M., Ansley, R. J., Steddom, K., Rush, C. M., Michels, G. J., Workneh, F., . . . Elliott, N. C. (2014). High spectral and spatial resolution hyperspectral imagery for quantifying Russian wheat aphid infestation in wheat using the constrained energy minimization classifier. *Journal of Applied Remote Sensing*, 8, 083661-083661-083661-083614.
- Mirik, M., Michels jr., G. J., Kassymzhanova-Mirik, S., Elliot, N. C., & Bowling, R. (2006). Hyperspectral spectrometry as a means to differentiate uninfested and infested winter wheat by greenbug (Hemiptera: Aphididae). *Journal of Economic Entomology*, 99(5), 1682-1690.
- Mirik, M., Michels jr., G. J., Kassymzhanova-Mirik, S., Elliot, N. C., Catana, V., Jones, D. B., & Bowling, R. (2006). Using digital image analysis and spectral reflectance data to quantify damage by greenbug (Hemiptera: Aphididae) in winter wheat. *Computers and Electronics in Agriculture*, 51, 86-98.

- Moore, H. E. (2013). *Analysis of cuticular hydrocarbons in forensically important blowflies using mass spectrometry and its application in Post Mortem Interval estimations*. (Doctor of Philosophy), Keele University, Keele Staffordshire University.
- Moore, H. E., Adam, C. D., & Drijfhout, F. P. (2013). Potential Use of Hydrocarbons for Aging *Lucilia sericata* Blowfly Larvae to Establish the Postmortem Interval. *Journal of Forensic Science*, 58(2), 404-412.
- Moore, H. E., Adam, C. D., & Drijfhout, F. P. (2014). Identifying 1st instar larvae for three forensically important blowfly species using “fingerprint” cuticular hydrocarbon analysis. *Forensic Science International*, 240, 48-53.
- Moran, M. S., Inoue, Y., & Barnes, E. M. (1997). Opportunities and limitations for image-based remote sensing in precision crop management. *Remote Sensing Environment*, 61, 319-346.
- Nansen, C., Coelho Jr, A., Viera, J. M., & Parra, J. R. P. (2014). Reflectance-based identification of parasitized host eggs and adult *Trichogramma* specimens. *Journal of Experimental Biology*, 217, 1187-1192. doi:10.1242/jeb.095661
- Nansen, C., Ribeiro, L. P., Dadour, I., & Roberts, J. D. (2015). Detection of temporal changes in insect body reflectance in response to killing agents. *PlosONE*, 10(4), 1-15. doi:10.1371/journal.pone.0124866
- Neigh, C. S. R., Bolton, D. K., Diabate, M., Williams, J. J., & Carvalhais, N. (2014). An Automated Approach to Map the History of Forest Disturbance from Insect Mortality and Harvest with Landsat Time-Series Data. *Remote Sensing*, 6, 2782-2808.
- Ng, P. H. R., Walker, S., Tahtouh, M., & Reedy, B. (2009). Detection of illicit substances in fingerprints by infrared spectral imaging. *Analytical and Bioanalytical Chemistry*, 394, 2039-2048.
- Niederegger, S., Wartenberg, N., Spiess, R., & Mall, G. (2013). Influence of food substrates on the development of the blowflies *Calliphora vicina* and *Calliphora vomitoria* (Diptera, Calliphoridae). *Parasitology Research*, 112, 2847-2853.
- Nuorteva, P. (1977). Sarcosaprophagous insects as forensic indicators. In C. G. Tedeschi, W. G. Eckert, & L. G. Tedeschi (Eds.), *Forensic Medicine: A study in trauma and environmental hazards* (pp. 1-680). Philadelphia: WB Saunders Co.

- Otte, T., Hilker, M., & Geiselhardt, S. (2015). The effect of dietary fatty acids on the cuticular hydrocarbon phenotype of an herbivorous insect and consequences for mate recognition. *Journal of Chemical Ecology*, *41*, 32-43. doi:10.1007/s10886-014-0535-9
- Padoan, R., Steemers, T. A. G., Klein, M. E., Aalderink, B. J., & de Bruin, G. (2008). *Quantitative hyperspectral imaging of historical documents: Techniques and applications*. Paper presented at the 9th International Conference on NDT of Art, Jerusalem, Israel.
- Park, M.-O. (2005). New Pathway for Long-Chain n-Alkane Synthesis via 1-Alcohol in *Vibrio furnissii* M1. *Journal of Bacteriology*, *187*(4), 1426-1429.
- Payne, G., Langlois, N., Lennard, C., & Roux, C. (2007). Applying visible hyperspectral (chemical) imaging to estimate the age of bruises. *Medicine, Science and the Law*, *47*(3), 225-232.
- Payne, G., Reedy, B., Lennard, C., Comber, B., Exline, D., & Roux, C. (2005). A further study to investigate the detection and enhancement of latent fingerprints using visible absorption and luminescence chemical imaging. *Forensic Science International*, *150*, 33-51.
- Payne, G., Wallace, C., Reedy, B., Lennard, C., Schuler, R., Exline, D., & Roux, C. (2005). Visible and near-infrared chemical imaging methods for the analysis of selected forensic samples. *Talanta*, *67*, 334-344.
- Payne, J. A. (1965). A summer carrion study of the baby pig *Sus scrofa* Linnaeus. *Ecology*, *46*, 592-602.
- Pechal, J. L., Benbow, M. E., Crippen, T. L., Tarone, A. M., & Tomberlin, J. K. (2014). Delayed insect access alters carrion decomposition and necrophagous insect community assembly. *Ecosphere*, *5*(4), 1-21. doi:http://dx.doi.org/10.1890/ES14-00022.1
- Pechal, J. L., Crippen, T. L., Benbow, M. E., Tarone, A. M., Dowd, S., & Tomberlin, J. K. (2014). The potential use of bacterial community succession in forensics as described by high throughput metagenomic sequencing. *International Journal of Legal Medicine*, *128*, 193-205.
- Pechal, J. L., Crippen, T. L., Tarone, A. M., Lewis, A. J., Tomberlin, J. K., & Benbow, M. E. (2013). Microbial community functional change during vertebrate carrion decomposition. *PlosONE*, *8*(11), 1-11 e79035.

- Pechal, J. L., Moore, H. E., Drijfhout, F., & Benbow, M. E. (2014). Hydrocarbon profiles throughout adult Calliphoridae aging: A promising tool for forensic entomology. *Forensic Science International*, *245*, 65-71.
- Picard, C. J., Johnston, J. S., & Tarone, A. M. (2012). Genome sizes of forensically relevant diptera. *Journal of Medical Entomology*, *49*(1), 192-197.
- Pickering, C. L., Hands, J. R., Fullwood, L. M., Smith, J. A., & Baker, M. J. (2015). Rapid discrimination of maggots utilising ATR-FTIR spectroscopy. *Forensic Science International*, *249*, 189-196.
- Ramsay, J. O., & Silverman, B. W. (2005). *Functional Data Analysis*. New York: Springer.
- Randeberg, L. L., Baarstad, I., Loke, T., Kaspersen, P., & Svaasand, L. O. (2006). *Hyperspectral Imaging of Bruised Skin*. Paper presented at the Proceedings of SPIE.
- Reed, G., Savage, K., Edwards, D., & Daeid, N. N. (2014). Hyperspectral imaging of gel pen inks: An emerging tool in document analysis. *Science and Justice*, *54*, 71-80.
- Reibe, S., Doetinchem, P. v., & Madea, B. (2010). A new simulation-based model for calculating post-mortem intervals using developmental data for *Lucilia sericata* (Dipt.: Calliphoridae). *Parasitology Research*, *107*, 9-16.
- Reiter, C., & Grassberger, M. (2002). *Post-mortem interval estimation using insect development data*. Paper presented at the Proceedings of the First European Forensic Entomology Seminar Rosny sous Bois, France.
- Reynolds, D. R., & Riley, J. R. (2002). Remote-sensing, telemetric and computer-based technologies for investigating insect movement: A survey of existing and potential techniques. *Computers and Electronics in Agriculture*, *35*, 271-307.
- Richards, C. S., Rowlinson, C. C., Cuttiford, L., Grimsley, R., & Hall, M. J. R. (2013). Decomposed liver has a significantly adverse affect on the development rate of the blowfly *Calliphora vicina*. *International Journal of Legal Medicine*, *127*, 259-262.
- Richards, C. S., Simonsen, T. J., Abel, R. L., Hall, M. J. R., Schwyn, D. A., & Wicklein, M. (2012). Virtual forensic entomology: Improving estimates of minimum post-mortem interval with 3D micro-computed tomography. *Forensic Science International*, *220*, 251-264.
- Riley, J. R. (1989). Remote Sensing in Entomology. *Annual Review of entomology*, *34*, 247-271.

- Rivers, D. B., & Dahlem, G. A. (2014). *The Science of Forensic Entomology*. Oxford: Wiley Blackwell.
- Rogers, D. J., & Randolph, S. E. (1991). Mortality rates and population density of tsetse flies correlated with satellite imagery. *Nature*, *351*, 739-741.
- Ruiz-Moreno, D. (2016). Assessing Chikungunya risk in a metropolitan area of Argentina through satellite images and mathematical models. *BMC Infectious diseases*, *16*(49), 1-12. doi:DOI 10.1186/s12879-016-1348-y
- Sadler, D. W., Fuke, C., Court, F., & Pounder, D. J. (1995). Drug accumulation and elimination in *Calliphora vicina* larvae. *Forensic Science International*, *71*, 191-197.
- Schneider, R. C., & Kovar, K.-A. (2003). Analysis of ecstasy tablets: Comparison of reflectance and transmittance near infrared spectroscopy. *Forensic Science International*, *134*, 187-195.
- Schowengerdt, R. A. (2007). *Remote Sensing Models and Methods for Image Processing*. London: Elsevier.
- Schultz, J. J. (2008). Sequential monitoring of burials containing small pig cadavers using ground penetrating radar. *Journal of Forensic Science*, *53*(279-287).
- Schultz, R. A., Nielsen, T., Zavaleta, J. R., Ruch, R., Wyatt, R., & Garner, H. R. (2001). Hyperspectral Imaging: A Novel Approach For Microscopic Analysis. *Bioimaging*, *43*, 239-247.
- Servakaranpalayam, S. S. (2006). *Potential applications of hyperspectral imaging for the determination of total soluble solids, water content and firmness in mango*. (Master of Science), MacDonald Campus, McGill University, Montreal.
- Shean, B. S., Messinger, L., & Papworth, M. (1993). Observations of differential decomposition on sun exposed v. shaded pig carrion in coastal Washington State. *Journal of Forensic Science*, *38*(4), 938-949.
- Silva, C. S., Pimental, M. F., Honorato, R. S., Pasquini, C., Prats-Montalban, J. M., & Ferrer, A. (2014). Near infrared hyperspectral imaging for forensic analysis of document forgery. *Analyst*, *139*, 5176-5184.
- Singh, C. B., Jayas, D. S., Paliwal, J., & White, N. D. G. (2009). Detection of insect-damaged wheat kernels using near-infrared hyperspectral imaging. *Journal of Stored Products Research*, *45*, 151-158.

- Smith, K. G. V. (1986). *A Manual of Forensic Entomology*. London: British Museum (Natural History).
- Snirer, E. (2013). *Hyperspectral Remote Sensing of Individual Gravesites –Exploring the effects of Cadaver Decomposition on Vegetation and Soil Spectra*. (Masters of Science), McGill University, Montreal, Quebec.
- Socolinsky, D. A., Selinger, A., & Neuheisel, J. D. (2003). Face recognition with visible and thermal infrared imagery. *Computer Vision and Image Understanding*, 91, 72-114.
- Solberg, S., Eklundh, L., Gjertsen, A. K., Johansson, T., Joyce, S., Lange, H., . . . Solberg, A. (2007). Testing remote sensing techniques for monitoring large scale insect defoliation. *Remote Sensing of Environment*, 99(3), 295-303.
- Sondermann, N., & Kovar, K.-A. (1999). Screening experiments of ecstasy street samples using near infrared spectroscopy. *Forensic Science International*, 106, 147-156.
- Stam, B., van Gemert, M. J. C., van Leeuwen, T. G., Teeuw, A. H., van der Wal, A., & Aalders, M. C. G. (2011). Can color inhomogeneity of bruises be used to establish their age? *Journal of Biophotonics*, 4(10), 759-767. doi:10.1002/jbio.201100021
- Sumriddetchkajorn, S., & Intaravanne, Y. (2008). Hyperspectral imaging-based credit card verifier structure with adaptive learning. *Applied Optics*, 47(35), 6594-6600.
- Tabor Kreitlow, K. L. (2010). Insect succession in a natural environment. In J. H. Byrd & J. L. Castner (Eds.), *Forensic Entomology The Utility of Arthropods in legal investigations* (pp. 251-270). Boca Raton: CRC Press.
- Tahtouh, M., Despland, P., Shimmon, R., Kalman, J. R., & Reedy, B. J. (2007). The application of infrared chemical imaging to the detection and enhancement of latent fingerprints: Method optimization and further findings. *Journal of Forensic Science*, 52(5), 1089-1096.
- Tantawi, T. I., & Greenberg, B. (1993). The effect of killing and preservative solutions on estimates of maggot age in forensic cases. *Journal of Forensic Science*, 38(3), 702-707.
- Tarone, A. M., & Foran, D. R. (2008). Generalized additive models and *Lucilia sericata* growth: Assessing Confidence intervals and error rates in forensic entomology. *Journal of Forensic Science*, 53(4), 942-948.

- Tarone, A. M., & Foran, D. R. (2011). Gene expression during blow fly development: Improving the precision of age estimates in forensic entomology. *Journal of Forensic Science*, 56(S1), S112-S122.
- Tarone, A. M., Jennings, K. C., & Foran, D. R. (2007). Aging blow fly eggs using gene expression: A feasibility study. *Journal of Forensic Science*, 52(6), 1350-1354.
- Tarone, A. M., Picard, C. J., Spiegelman, C., & Foran, D. R. (2011). Population and temperature effects on *Lucilia sericata* (Diptera: Calliphoridae) body size and minimum development time. *Journal of Medical Entomology*, 48(5), 1062-1068. doi:10.1603/me11004
- Thomas, J., Buzzini, P., Massonnet, G., Reedy, B., & Roux, C. (2005). Raman spectroscopy and the forensic analysis of black/grey and blue cotton fibres. Part 1. Investigation of the effects of varying laser wavelength. *Forensic Science International*, 152, 189-197.
- Thyssen, P. J., de Souza, C. M., Shimamoto, P. M., Salewski, T. d. B., & Moretti, T. C. (2014). Rates of development of immatures of three species of *Chrysomya* (Diptera: Calliphoridae) reared in different types of animal tissues: implications for estimating the postmortem interval. *Parasitology Research*, 113, 3373-3380.
- Tomberlin, J. K., Benbow, M. E., Tarone, A. M., & Mohr, R. M. (2011). Basic research in evolution and ecology enhances forensics. *Trends in Ecology and Evolution*, 26(2), 53-55.
- Tomberlin, J. K., Crippen, T. L., Tarone, A. M., Singh, B., Adams, K., Rezenom, Y. H., . . . Wood, T. K. (2012). Interkingdom responses of flies to bacteria mediated by fly physiology and bacterial quorum sensing. *Animal Behaviour*, 84, 1449-1456.
- Tomberlin, J. K., Mohr, R., Benbow, M. E., Tarone, A. M., & VanLaerhoven, S. (2011). A Roadmap for bridging basic and applied research in forensic entomology. *Annual Review of entomology*, 56, 401-421.
- Trabalon, M., Campan, M., Clement, J.-L., Lange, C., & Miquel, M.-T. (1992). Cuticular hydrocarbons of *Calliphora vomitoria* (Diptera): Relation to age and sex. *General and Comparative Endocrinology*, 85(2), 208-216. doi:http://dx.doi.org/10.1016/0016-6480(92)90004-4
- Tramini, P., Bonnet, B., Sabatier, R., & Maury, L. (2001). A method of age estimation using Raman microspectrometry imaging of the human dentin. *Forensic Science International*, 118, 1-9.

- Udristioiu, E. G., Bunaciu, A. A., Aboul-Enein, H. Y., & Tanase, I. G. (2009). Forensic analysis of color toners by raman spectroscopy. *Instrumentation Science and Technology*, 37, 23-29.
- Ustin, S. L., Smith, M. O., & Adams, J. B. (1993). Remote Sensing of Ecological Processes: A Strategy for Developing and Testing Ecological Models Using Spectral Mixture Analysis. <http://cstars.ucdavis.edu/papers/pdf/ustinetal1993d.pdf>, 1-22.
- VanLaerhoven, S. L. (2008). Blind validation of postmortem interval estimates using developmental rates of blow flies. *Forensic Science International*, 180, 76-80.
- Verhoeven, G. (2008). Imaging the invisible using modified digital still cameras for straightforward and low-cost archaeological near-infrared photography. *Journal of Archaeological Science*, 35, 3087-3100.
- Voss, S. C., Magni, P., Dadour, I., & Nansen, C. (2016). Reflectance-based determination of age and species of blowfly puparia. *International Journal of Legal Medicine*. doi:doi:10.1007/s00414-016-1458-5
- Wallace, J. R., Byrd, J. H., LeBlanc, H. N., & Cervenka, V. J. (2015). North America. In J. K. Tomberlin & M. E. Benbow (Eds.), *Forensic Entomology International Dimensions and Frontiers* (pp. 433). Boca Raton, Fl.: CRC Press.
- Warbrick-Smith, J., Raubenheimer, D., Simpson, S. J., & Behmer, S. T. (2009). Three hundred and fifty generations of extreme food specialisation: testing predictions of nutritional ecology. *Entomologia Experimentalis et Applicata*, 132, 65-75.
- Warren, J.-A. (2006). *The development of Protophormia terraenovae (Robineau-Desvoidy) (Diptera: Calliphoridae) at constant and fluctuating temperatures*. (Master of Arts), Simon Fraser University, Burnaby.
- Warren, J.-A., & Anderson, G. S. (2009). A comparison of development times for *Protophormia terraenovae* (R-D) reared on different food substrates. *Canadian Society of Forensic Science Journal*, 42(3), 161-171.
- Warren, J.-A., & Anderson, G. S. (2013a). The development of *Protophormia terraenovae* (R-D) at constant temperatures and its minimum temperature threshold *Forensic Science International*, 233, 374-379.
- Warren, J.-A., & Anderson, G. S. (2013b). Effect of fluctuating temperatures on the development of a forensically important blow fly, *Protophormia terraenovae* (Diptera: Calliphoridae). *Environmental Entomology*, 42(1), 167-172.

- Warren, J.-A., Ratnasekera, T. D. P., Campbell, D. A., & Anderson, G. S. (2017a). Initial investigations of spectral measurements to estimate the time within stages of *Protophormia terraenovae* (Robineau-Desvoidy) (Diptera: Calliphoridae). *Forensic Science International*, 278, 205-216. doi:10.1016/j.forsciint.2017.06.027
- Warren, J.-A., Ratnasekera, T. D. P., Campbell, D. A., & Anderson, G. S. (2017b). Spectral Signature of Immature *Lucilia sericata* (Meigen) (Diptera: Calliphoridae). *Insects*, 8(2). doi:10.3390/insects8020034
- Wells, J. D., & Lamotte, L. R. (1995). Estimating maggot age from weight using inverse prediction. *Journal of Forensic Science*, 40(4), 585-590.
- Wells, J. D., & Lamotte, L. R. (2001). Estimating the postmortem interval. In J. H. Byrd & J. L. Castner (Eds.), *Forensic Entomology: The Utility of Arthropods in Legal Investigations* (1st edition ed., pp. 263-286). Boca Raton: CRC Press.
- Wells, J. D., & Lamotte, L. R. (2010). *Estimating the postmortem interval* (second ed.). Ch 9 of *The Utility of Arthropods in Legal investigations* edited by Byrd, J.H. and Castner, J.L: CRC Press.
- West, M. J., & Went, M. J. (2009). The spectroscopic detection of drugs of abuse on textile fibres after recovery with adhesive lifters. *Forensic Science International*, 189, 100-103.
- Westbrook, J. K., Eyster, R. S., & Wolf, W. W. (2014). WSR-88D doppler radar detection of corn earworm moth migration. *International Journal of Biometeorology*, 58, 931-940.
- Whitworth, T. L. (2006). Keys to the genera and species of blow flies (Diptera: Calliphoridae) of America north of Mexico. *Proceedings of the Entomological Society of Washington*, pp. 689-725.
- Wilder, J., Philips, P. J., Jiang, C., & Wiener, S. (1996). Comparison of Visible and Infra-Red Imagery for Face Recognition. *IEEE*, 0-8186-7713-9/96, 182-187.
- Williams, D. W., Bartels, D. W., Sawyer, A. J., & Mastro, V. (2004). *Application of hyperspectral imaging to survey for emerald ash borer* Paper presented at the Proceedings of XV U.S. Department of Agriculture Interagency Research Forum on Gypsy Moth and other invasive species Annapolis Maryland.
- Wilson, B. C., & Jacques, S. L. (1990). Optical Reflectance and Transmittance of Tissues: Principles and Applications. *IEEE Journal of Quantum Electronics*, 26(12), 2186-2199.

- Wilson, J. M., Lafon, N. W., Kreitlow, K. L., Brewster, C. C., & Fell, R. D. (2014). Comparing growth of pork- and venison-reared *Phormia regina* (Diptera: Calliphoridae) for the application of forensic entomology to wildlife poaching. *Journal of Medical Entomology*, *51*(5), 1067-1072.
- Wolfe, J., & Exline, D. L. (2003). Characterization of condom lubricant components using Raman spectroscopy and Raman chemical imaging. *Journal of Forensic sciences*, *48*(5), 1065-1074.
- Wood, J. D., Enser, M., Fisher, A. V., Nute, G. R., Sheard, P. R., Richardson, R. I., . . . Whittington, F. M. (2008). Fat deposition, fatty acid composition and meat quality: A review. *Meat science*, *78*, 343-358.
- Xing, J., Guyer, D., Ariana, D., & Lu, R. (2008). Determining optimal wavebands using genetic algorithm for detection of internal insect infestation in tart cherry. *Sensing and Instrumentation for food quality*, *2*, 161-167.
- Xu, H., Ye, G.-Y., Xu, Y., Hu, C., & Zhu, G.-H. (2014). Age-dependent changes in cuticular hydrocarbons of larvae in *Aldrichina grahami* (Aldrich) (Diptera: Calliphoridae). *Forensic Science International*, *242*, 236-241.
- Zajac, B. K., Amendt, J., Horres, R., Verhoff, M. A., & Zehner, R. (2015). De novo transcriptome analysis and highly sensitive digital gene expression profiling of *Calliphora vicina* (Diptera: Calliphoridae) pupae using MACE (Massive Analysis of cDNA Ends). *Forensic Science International: Genetics*, *15*, 137-146.
- Zdarek, J., & Fraenkel, G. (1972). The mechanism of puparium formation in flies. *Journal of Experimental Zoology*, *179*, 315-324.
- Zehner, R., Amendt, J., Schütt, S., Sauer, J., Krettek, R., & Povolný, D. (2004). Genetic identification of forensically important flesh flies (Diptera: Sarcophagidae). *International Journal of Legal Medicine*, *118*, 245-247.
- Zhu, G. H., Xu, X. H., Yu, X. J., Zhang, Y., & Wang, J. F. (2007). Puparial case hydrocarbons of *Chrysomya megacephala* as an indicator of the postmortem interval. *Forensic Science International*, *169*, 1-5.